High Resolution Stratigraphy of Ordovician Carbonates, Kentucky: Evidence for a Greenhouse to Glacial Transition

by

Michael C. Pope

Dissertation submitted to the Faculty of the
Virginia Polytechnic Institute and State University
in partial fulfillment of the requirements for the degree of

DOCTOR OF PHILOSOPHY

in

Geological Sciences

APPROVED:

J. Fred Read, Chairman

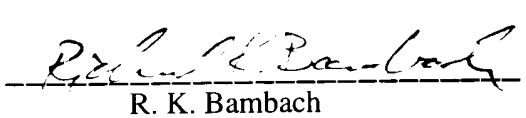

R. K. Bambach

C. Coruh

K. A. Eriksson

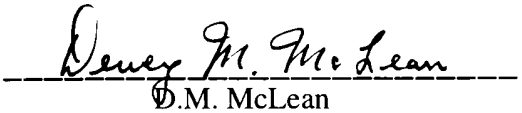

D.M. McLean

December, 1995
Blacksburg, Virginia

High Resolution Stratigraphy of Ordovician Carbonates, Kentucky: Evidence for a Greenhouse to Glacial Transition

by

Michael C. Pope

Dissertation submitted to the Faculty of the
Virginia Polytechnic Institute and State University
in partial fulfillment of the requirements for the degree of

DOCTOR OF PHILOSOPHY

in

Geological Sciences

APPROVED:

J. Fred Read, Chairman

R. K. Bambach

C. Coruh

K. A. Eriksson

D.M. McLean

December, 1995
Blacksburg, Virginia

HIGH RESOLUTION STRATIGRAPHY OF ORDOVICIAN CARBONATES, KENTUCKY: EVIDENCE FOR A GREENHOUSE TO GLACIAL TRANSITION

by

Michael C. Pope

J. Fred Read, Chairman

Geological Sciences

(ABSTRACT)

Early Ordovician Knox Group carbonates consist of meter-scale dolomite cycles deposited on a passive margin. The meter-scale cycles were deposited under warm, semi-arid conditions, under low amplitude sea level fluctuations on a relatively ice-free earth. The overlying Knox unconformity (~ 10 m.y. duration), formed by global eustatic sea level fall and tectonic uplift of the subducting margin at the onset of Taconic orogenesis.

Middle Ordovician carbonates were deposited on a ramp peripheral to a foredeep in Tennessee. The Middle Ordovician High Bridge Group consists of a 2nd-order supersequence with three 3rd-order sequences (each 30 to 100 m thick), which record a long term change from humid conditions in TST's into more arid conditions during HST's. Peritidal cycles formed under low-amplitude eustatic fluctuations.

The late Middle to Late Ordovician carbonates and clastics comprise a 2nd-order supersequence deposited on a ramp peripheral to the Taconic foredeep. The supersequence is composed of four 3rd-order sequences (each 40 to 80 m thick), which contain 11 parasequence sets (2 to 20 m thick). The small sequences are composed of stacked, predominantly subtidal meter-scale cycles (parasequences). Meter-scale subtidal cycles contain facies that suggest they formed under moderate amplitude (20 to 40 m) sea level fluctuations, likely produced by glacio-eustasy. However, peritidal cycles in the HST's indicate they formed under low-amplitude sea level fluctuations, thus suggesting the amplitude of sea level fluctuations decreased during 3rd-order sea level falls. The facies in the supersequence indicate they formed under cool, humid conditions during the 2nd-order TST and became more arid during the 2nd-order HST. The unconformity at the top of the supersequence formed during eustatic sea level drawdown associated with extensive Latest Ordovician glaciation.

The long term climatic shifts from semi-arid to more humid climates during the Ordovician probably reflects the uplift of orogenic highlands to the east during orogenesis, which altered the regional climatic conditions as well as plate motion to cooler latitudes. The change from humid to arid climate during the 3rd-order sequences may be due to marine inundation inducing humid conditions, whereas more arid climates during the HST's may reflect emergence of the ramp. The shift from low amplitude fluctuations in the Early Ordovician to moderate sea level fluctuations during the Late Ordovician suggests that glaciation began during this time.

TABLE OF CONTENTS

LIST OF FIGURES

LIST OF TABLES

ACKNOWLEDGMENTS

I thank the Kentucky Geological Survey, especially Garland Dever, Patrick Gooding, Ray Daniel, Martin Noger and Brandon Nuttall for providing me with abundant data and helping me clarify some points of Ordovician stratigraphy in Kentucky. Similarly, I thank Steve Holland, Mark Patzkowsky, Mark Kulp, and Frank Ettensohn for helping me understand the finer points of the Ordovician stratigraphy in Kentucky.

I thank Mildred Memitt, Bob Montgomery, Sam Peavy and Cahit Coruh for helping me through the Sun workstations in geophysics so I could use the wireline logs in this study. I thank all my committe members Ken Eriksson, Richard Bambach, Dewey McLean and Cahit Coruh for all the helpful advice and support throughout this project. I thank Art Snoke for keeping me current on the local running scene and letting me loose in meteorology.

I thank all my fellow graduate students for their support, encouragement and stimulating ideas and discussions during my tenure at Virginia Tech. In particular I'd like to thank Cole Davisson, Chris Fedo, Sven Morgan, Jane Parks, Eric Gardner, Sam Peavy, Bill Domoracki, Rich Whitmarsh, and Debbie Hopkins.

I thank my labmates Aus Al-Tawil, Anna Balog and Taury Smith for making the carbonate lab such an interesting place to work, without their encouragement, support and friendship it would've been just another place to work rather than a fantastically fun experiernce.

I thank Fred Read for teaching me to be a better geologist, allowing me to explore many of my own ideas in my research but guiding me all the way; how to write better and to never give up when trying to get research funding. This was a much better place than Stanford could possibly have been!!

I thank my wife Pauline, my family and my friends for their unflagging support and encouragement throughout my graduate studies, especially when they didn't understand what it was that I was doing most of the time, because without their support I would not have finished this project.

Chapter 1: Introduction

This dissertation presents the results of a study of Ordovician carbonate and clastic stratigraphy in Kentucky and Virginia, which formed during the Early Ordovician greenhouse to Late Ordovician glacial transition. This study is based on 10 large outcrops (> 60 m high), 18 diamond drill cores (~ 250 m thick), and over 80 gamma ray logs. The outcrops and cores in the study area were located in central Kentucky along the Cincinnati Arch, whereas the wireline logs covered the arch and the Appalachian Basin to the east.

Chapter 2 presents the high-resolution sequence stratigraphy of the Late Mohawkian to Cincinnatian 2nd-order supersequence in Kentucky. This sequence stratigraphy integrates outcrops, cores and gamma-ray logs and thus provides more detail than previous studies. It also allows for subsurface correlations of the sequence stratigraphy into the Appalachian Basin, away from the outcrop belts along the Cincinnati Arch downramp into Virginia.

Chapter 3 presents more details of the Lexington Limestone, the basal, transgressive unit of the Late Mohawkian to Cincinnatian supersequence. This unit is unique because it appears to be a cool water carbonate, with evidence for moderate amplitude (20 to 40 m) high-frequency eustatic fluctuations, which likely reflect the onset of Gondwana glaciation during this time.

Chapter 4 presents a detailed analysis of seismites (seismically-induced sedimentary structures) in the Late Mohawkian to Cincinnatian supersequence. These structures are sedimentary recorders of large earthquakes in the Taconic foreland basin, primarily along the Cincinnati Arch and in the proximal foredeep of Virginia. The areal distribution and correlability of the seismites can be used to determine the Moment Magnitude of the earthquakes that produced these features.

Chapter 5 presents a summary of the climatic conditions and eustatic fluctuations recorded in the central Appalachians during the Ordovician, and places these into a regional and global framework related to the transition from an Early Ordovician global greenhouse period to a Late Ordovician glacial period.

Chapter 2: High-Resolution Surface and Subsurface Sequence Stratigraphy of Middle to Late Ordovician (Late Mohawkian to Cincinnatian) Carbonate Rocks, Kentucky, U.S. A.

ABSTRACT

The late Middle to Late Ordovician (Late Mohawkian to Cincinnatian) supersequence in Kentucky and Virginia is 250 to 500 m thick, approximately 12 m.y. in duration and contains four large 3rd-order sequences (each 40 to 150 m thick) that are regionally correlative in outcrops, cores and gamma ray logs. Parasequence sets (up to 20 m thick) and component parasequences (1 to 8 m thick) make up the larger sequences, and are only locally correlative. Subtidal-dominated parasequences comprise the basal part of each sequence whereas shallower subtidal or peritidal parasequences compose upper parts of sequences.

Each large 3rd-order sequence is asymmetric and marked by lowstand, transgressive and highstand systems tracts with unique lithologic and gamma-ray log response characteristics. LST's are poorly developed, and consist of marine siltstone or grainstone/packstone sheets extending into deep ramp settings. LST's have high-gamma ray values in their base and lower, blockier gamma-ray responses in their tops. TST's are thin, composed of high-energy, locally phosphatic grainstone and deeper ramp, interbedded skeletal packstone and shale, and become shalier upsection, with a corresponding increase in gamma-ray values to maximum flooding surfaces. MFS's are cryptic in outcrop and cores but are evident on gamma ray logs as a turnaround, between increasing gamma-ray values below and decreasing gamma-ray values above. HST's are thick and composed of aggraded skeletal grainstone or prograded peritidal facies (restricted skeletal wackestone/packstone and fenestral lime mudstone or silty dolomite). Sequence boundaries that developed on peritidal facies are low-relief surfaces below which underlying facies are diagenetically mottled by meteoric fluids. Sequence boundaries on subtidal facies are cryptic and marked by basinward shift in overlying facies.

Parasequences in all systems tracts except late HST are predominantly subtidal. Parasequences in the LST and early HST show a shallowing-upward trend, but in the TST parasequences progressively deepen upward to the MFS. Late HST parasequences are shallow subtidal or peritidal carbonates that progressively shallow upward. Juxtaposition of facies within the subtidal cycles of the TST's suggest moderate

amplitude (up to 30 m or more) relative high-frequency sea level fluctuations, but facies in peritidal parasequences of late HST's indicate lower amplitude relative high-frequency sea level fluctuations.

The stratigraphic packaging was likely caused by thrust-induced tectonics, interacting with 2nd to 5th order eustasy and autocyclic processes whose fingerprint is difficult to decipher for each depositional scale.

INTRODUCTION

The late Middle Ordovician (Late Mohawkian) Lexington Limestone and overlying Late Ordovician (Cinncinnatian) units (~250 m thick) of central Kentucky and their downdip equivalents in Virginia (~500 m thick), form a 2nd-order supersequence (~12 m.y. duration) of mixed carbonates and shale that formed on a shallow ramp bordering the Appalachian foreland basin (Cressman, 1973; Weir et al., 1984). This interval spans the time from earlier ice-free, greenhouse conditions (Early Ordovician) to Gondwana glaciation at the end of the Ordovician (Caputo and Crowell, 1985; Hambrey, 1985; Frakes et al., 1992) during high CO_2 conditions (Crowley and Baum, 1991; Berner, 1990, 1992). It also marks a regional change from earlier Ordovician tropical carbonate deposition to temperate carbonate conditions (Patzkowsky and Holland, 1993; Lavoie, 1995), suggested by paleomagnetic and paleoclimatic indicators (Van der Voo, 1988; Scotese and McKerrow, 1990; Witzke, 1990), oxygen isotopes (Railsback et al., 1990), bryomol (bryozoan-brachiopod-echinoderm) fauna assemblage (Nelson, 1988), abundance of phosphate (Cressman, 1973; Patzkowsky and Holland, 1993) and low sedimentation rate (2 to 3 cm/kyr; Pope and Read, in press). Furthermore, the succession records the development of a large ramp in a tectonically active foreland basin.

In view of this, we examined the succession to determine how the sequence stratigraphy was affected by tectonics, climate, glacio-eustasy and Gondwana ice buildup on this large ramp. Previous sedimentological studies of the ramp concentrated on outcrops, which sample only small stratigraphic intervals. We incorporated outcrop data, continuous diamond drill cores (up to 250 m), and over 60 wireline logs to better understand the depositional controls on sequence development.

STRUCTURAL AND STRATIGRAPHIC FRAMEWORK

Cambrian-Early Ordovician passive margin sedimentation (Knox-Beekmantown Group) terminated with the collision of a magmatic arc that produced a foreland basin and associated unconformity from Alabama to Newfoundland (Rodgers, 1971; Jacobi, 1981; Mussman and Read, 1986; Lash, 1988). The basin was bordered on the east by tectonic highlands, and on the west by a shallow carbonate ramp. Major stuctural elements on this ramp were the Nashville and Jessamine domes over the Cincinnati Arch, the Sebree Trough west of the Cincinnati Arch and border faults of the Rome Trough, which were reactivated during the Middle and Late Ordovician (Figure 1)(Borella and Osborne, 1978; Weir et al., 1984).

The foreland basin developed in two phases (Rodgers, 1971). The first was the "Blountian phase" (Llanvirn to Early Caradoc) when a rapidly subsiding foredeep, the "Sevier Basin" developed in Alabama, Tennessee and Virginia (Shanmugam and Walker, 1983). The "Middle Ordovician Limestone" supersequence was deposited on the ramp bordering the foredeep in Virginia, along with its updip equivalent, the High Bridge Group in Kentucky. The second orogenic phase was the "Taconic phase" (Late Caradoc to Ashgill), when a foredeep in the central Appalachians northeast of the earlier Sevier Basin developed (Read, 1989; Lash, 1988). This basin was the site of Martinsburg turbidite deposition in northern Virginia, Maryland, and Pennsylvania. The Late Mohawkian to Cincinnatian carbonates and clastics described in this paper developed on a shallow ramp in Kentucky and Virginia which sloped gently northeastward from the Cincinnati Arch into the Martinsburg Basin, and passed west of the arch into the narrow and deep Sebree Trough (Cressman, 1973; Keith, 1988).

Stratigraphic Framework of the Late Mohawkian to Cincinnatian Sequence: The late Middle Ordovician (Late Mowhawkian) Lexington Limestone (80 to 100 m thick) consists of thin- to medium-bedded, skeletal limestone and shale which rests disconformably on the Early Mohawkian High Bridge Group in Kentucky (Cressman, 1973) (Figure 2). The basal, Curdsville Member of the Lexington Limestone is a skeletal grainstone/packstone with thin shale interbeds, with multiple pyritic and phosphate encrusted hardgrounds. This is overlain by Logana Member (3 to 10 m thick) of interbedded calcisiltite and shale. In the subsurface in the south, this is overlain by faunally restricted, nodular skeletal wackestone/packstone ("Faulconer Bed" of the Perryville Member) that passes up into a thin fenestral lime mudstone with a karstic

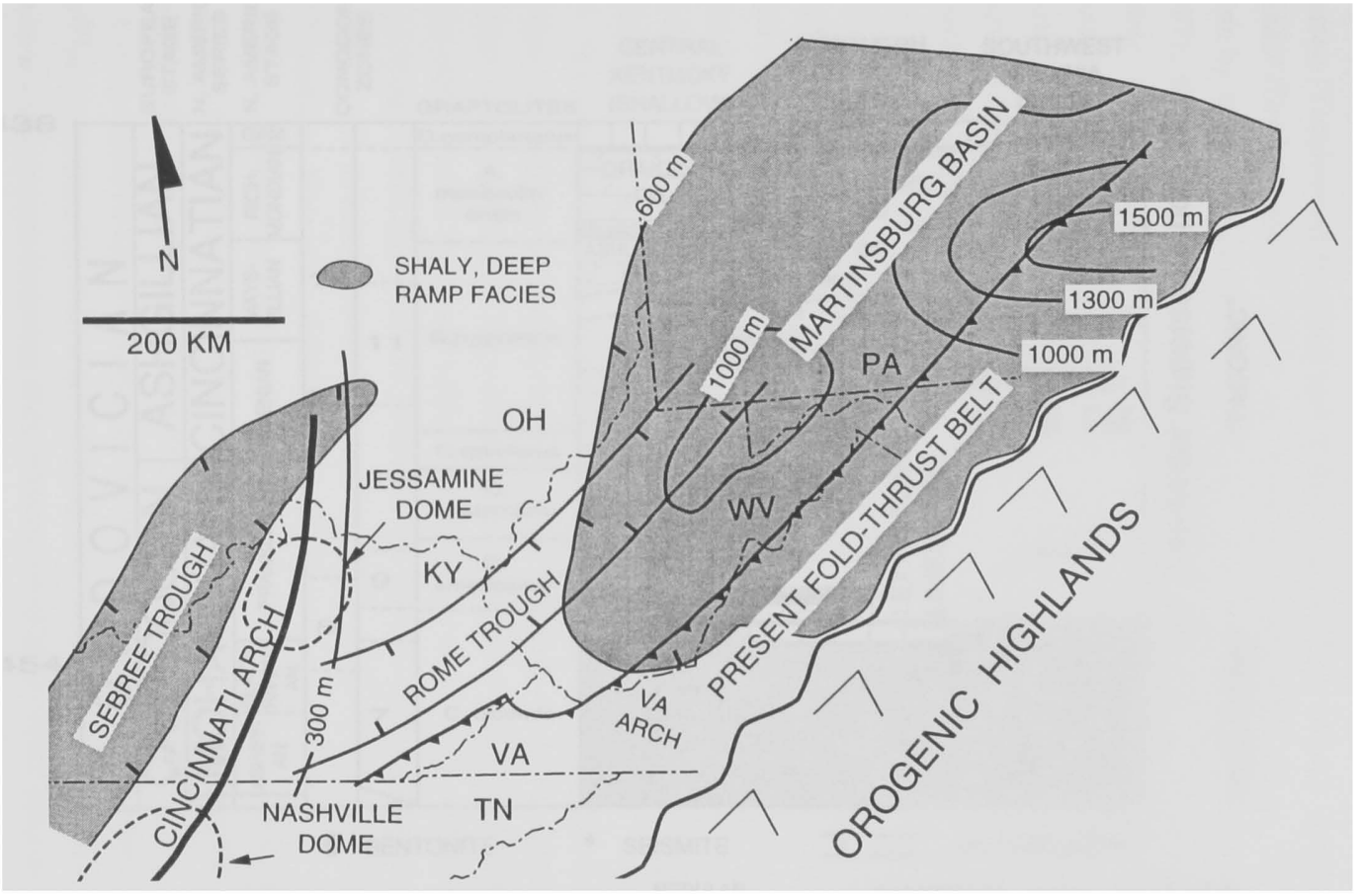

Figure 1. Map of the central Appalachian Basin, eastern U.S., showing prominent structural features active during deposition of the Late Mohawkian to Cincinnatian supersequence.

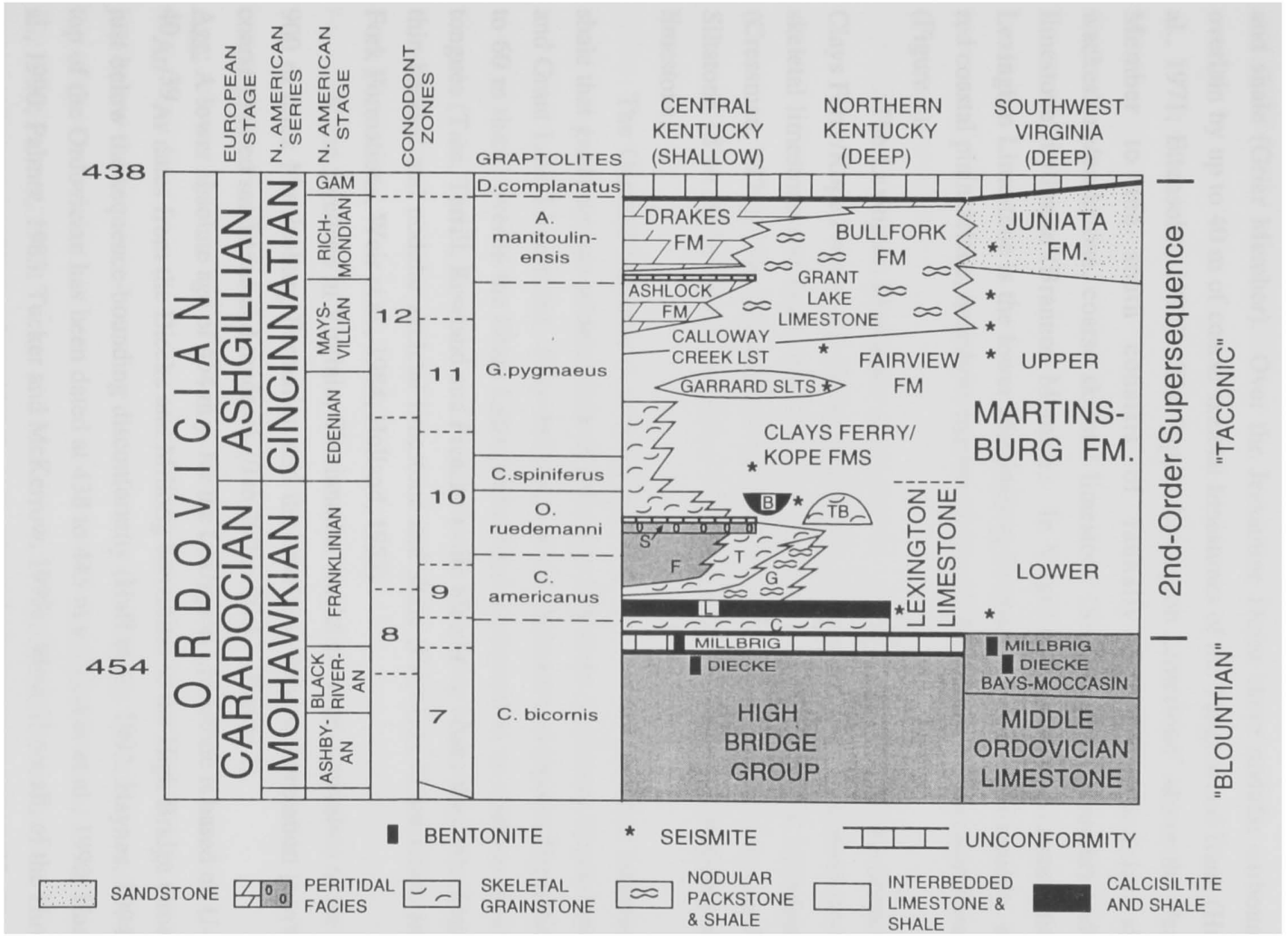

Figure 2. Chronostratigraphic chart of Mohawkian to Cincinnatian rocks in Kentucky and Virginia. Member and bed names in the Lexington Limestone are from Cressman (1973), whereas foramation names in the Cincinnatian are from Weir et al. (1984).

upper surface ("Salvisa Bed" of the Perryville Member; 1 to 5 m thick) that caps the "lower Lexington Limestone". To the north, this passes into cross-bedded skeletal grainstone (Tanglewood Member) that grades downramp into nodular skeletal limestone and shale (Grier Member). Over the Jessamine Dome these nodular carbonates are overlain by up to 40 m of coarse skeletal limestones of the Tanglewood Bank (Hrabar et al., 1971; Ettensohn, 1992). The "upper Lexington Limestone" above the Perryville Member to the south consists of faunally restricted, nodular skeletal wackestone/packstone, coarse skeletal limestone (Sulphur Well Member) and shale-limestone rhythmite (Brannon Member). In Virginia, the time-equivalent unit to the Lexington Limestone is the lower Martinsburg Formation, which conformably overlies red coastal plain/deltaic, nearshore marine clastics of the Bays and Moccasin Formations (Figure 2).

The Lexington Limestone is overlain by and interfingers with the deeper water Clays Ferry/Kope Formations (50 to 80 m thick), composed of thin- and medium-bedded skeletal limestone and shale, which to the south contain coarse skeletal limestone units (Cressman, 1973). The Clays Ferry Formation is conformably overlain by the Garrard Siltstone (8 to 30 m thick) composed of quartz siltstone and interfingering skeletal limestone.

The Garrard Siltstone is overlain by 30 to 40 m of thin-bedded limestone and shale that grade up into nodular skeletal limestone and shale (Calloway Creek Limestone and Grant Lake Limestone). Silty dolomites of the Ashlock and Drakes Formations (10 to 60 m thick) overlie the Grant Lake, and extend northward as as a series of dolomite tongues (Tate, Terrill, Rowland and Preachersville Members) where they interfinger with thin-bedded and nodular skeletal limestone and shale (Fairview, Grant Lake, and Bull Fork Formations; Weir et al., 1984; Holland, 1983)

In the foredeep in Virginia, Cincinnatian rocks are time-equivalent to the 250 to 900 m thick Martinsburg Formation and the overlying Juniata Formation grayish-red, coarse grained sandstone and mudrock (0 to 200 m thick) (Figure 2).

Age: A lower absolute age of 454 m.y. for the Lexington Limestone is based on U-Pb and $^{40}Ar/^{39}Ar$ dates from the Diecke and Millbrig bentonites in the High Bridge Group at or just below the sequence-bounding disconformity (Huff et al., 1992; Haynes, 1994). The top of the Ordovician has been dated at 438 to 443 m.y. (Tucker et al., 1990; Harland et al., 1990; Palmer, 1983; Tucker and McKerrow, 1995). Most, if not all, of the Hirnantian (Gamachian) stage (Figure 2), which is approximately 2 m.y. in duration (Harland et al.,

1990) is missing in Kentucky (Brenchley et al., 1994), thus the Late Mohawkian to Cincinnatian interval is between 9 to 14 m.y. long.

SEQUENCE STRATIGRAPHY

Several scales of depositional sequences characterized by updip bounding unconformities and major landward and basinward shifts in facies belts, occur in the Ordovician succession in the region. The sequence stratigraphic terms are adapted from Posamentier et al. (1988), Posamentier and Vail (1988), Jervey (1988), Vail et al. (1991) and Weber et al. (1995). Systems tracts within depositional sequences are abbreviated as: lowstand (LST), transgressive (TST), highstand (HST) and ramp-margin (RMW) which overlies a conformable sequence boundary downdip (Vail et al., 1991). The transgressive and highstand systems tracts are separated by a maximum flooding surface (MFS).

The location of the cores, outcrops and gamma-ray logs used in this study are shown in Figure 3. Gross facies belts along the Late Mohawkian to Cincinnatian ramp profile are summarized in Tables 1 and 2 and Figure 4 (Cressman, 1973; Weir et al., 1984; Holland, 1993; Jennette and Pryor, 1993; Pope and Read, in press). These are peritidal facies of fenestral lime mudstone, silty dolomite, both with low gamma ray values, and faunally restricted (lagoonal?) nodular skeletal wackestone/packstone (low to moderate gamma-ray values); subtidal shoal bryozoan and grainstone banks and sheets (very low gamma-ray values); deeper subtidal, nodular skeletal wackestone/packstone and shale, and thin-bedded skeletal packstone, calcisiltite and shale, and evenly bedded rhythmites of calcisiltite and shale all have moderate to high values on the gamma ray logs due to their relatively high shale content which is highest in the rhythmite facies. High gamma-ray values also are associated with the Diecke and Millbrig bentonites near the unconformity at the base of the Lexington Limestone.

Late Mohawkian to Cincinnatian Supersequence:

In Kentucky, the Late Mohawkian to Cincinnatian interval is a 250 to 300 m thick, second-order supersequence (after Weber et al., 1995; Figure 3). The basal sequence boundary is an unconformity between the High Bridge Group and Lexington Limestone,with up to 5 m erosional relief over the Jessamine Dome (Cressman, 1973). The Diecke bentonite occurs just below the unconformity, which commonly is overlain by the Millbrig bentonite throughout southern and central Kentucky, except over the

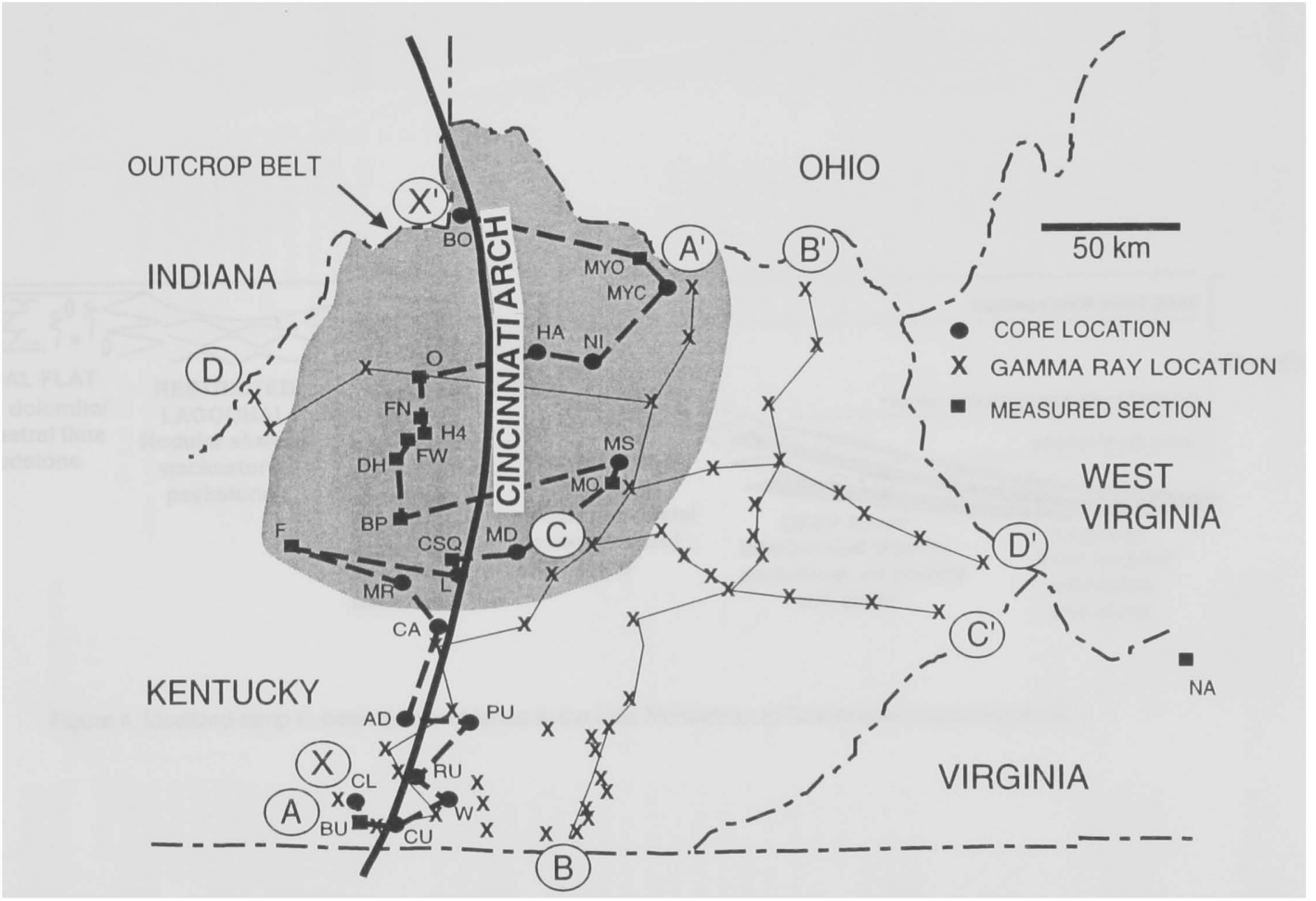

Figure 3. Detailed location map of Kentucky and Virginia showing outcrops, cores and gamma ray log used in this study. Shaded area is the approximate limit of Late Ordovician outcrops in Kentucky. The lithologic cross-section in Figure 5 is marked X-X'. The gamma ray correlation diagrams of Figure 6 are marked A-A', B-B', C-C', and D-D'.

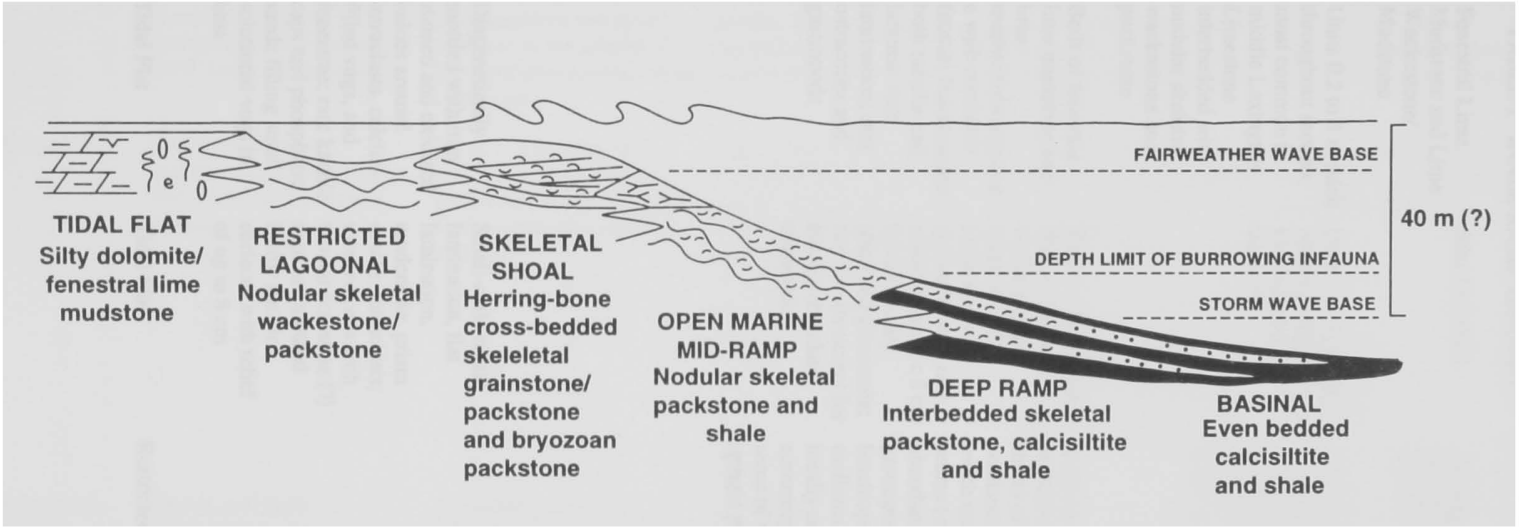

Figure 4. Idealized ramp-to-basin profile of facies in the Late Mohawkian to Cincinnatian supersequence.

TABLE 1 INNER RAMP SEDIMENTS (<10 m Water Depth)

Rock Type	Fenestral Lime Mudstone and Lime Wackestone/ Mudstone	Silty Dolomite	Nodular Bedded Skeletal Wackestone/ Packstone	Cross-bedded Skeletal Grainstone
Occurrence	Units 0.2 to 3 m thick throughout section, most common in middle Lexington Limestone interbedded with nodular skeletal wackestone and packstone	Units 2 to 30 m thick, occurs in upper Cincinnatian, thins to the north	Units 0.5 to 8 m thick, occur in Lexington Limestone but most abundant along southern Cincinnati Arch	Units from 0.5 to 8 m thick, occurs in basal and upper Lexington Limestone
Lithologic Description	Beds of fenestral lime mudstone and lime mudstone/wackestone with restricted faunas; fenestrae are both tubular and laminar; rare lamination; rare ostracodes and gastropods	Two to 15 cm thick beds of fine and coarse grained massive and laminated silty dolomite, with rare shaley seams (< 5 cm thick); locally abundant glauconite; few fossils except for locally abundant ostracodes	Irregular beds and nodules (10 to 20 cm thick) of skeltal wackestone/packstone ewith thin shaley seams (<25%); abundant ostracodes, gastropods, brachiopods, molluscs, and corals; locally common stromatoporoids some of which are in upright position	10 to 50 cm thick beds of fine to very coarse skeletal grainstone, commonly with fine skeletal grainstone and shale partings (1 to 10 cm thick); cross-beds draped by shale; bryozoan gravels at toes of cross-bed sets; sets are wedge, irregular, or tabular shaped; some channels preserved; some overturned stromatoporoids; flanked laterally by small bryozoan banks or mounds (< 5 m thick)
Sedimentary Structures	Diagenetically mottled with iron stained and oxidized haloes around intraclasts, calcite-filled vugs, and fenestrae; rare karstic caps and phosphatic sands filling small solutional vugs in host	Small-scale ripple lamination, flat lamination, mudcracks, prism cracks, intraclasts; mottled caps with tubular fenestrae (?) caps are mottled below karstic surfaces with relief of up to 8 cm		Fine planar laminations, or alternating coarse layers with fine drapes; common bipolar cross-bedding; abundant pyritic and phosphatic hardgrounds cap grainstones; locally massive
Environment	Tidal Flat	Tidal Flat	Restricted Lagoon	Tidal Influenced Skeletal Shoals

TABLE 2 MID- AND DEEP RAMP SEDIMENTS

Rock Type	Siltstone (Garrard Siltstone)	Thin Skeletal Grainstone	Nodular shaly skeletal wackestone/ packstone	Thin, irregularly bedded skeletal packstone, calcisiltite and shale	Even bedded calcisiltite and shale
Occurrence	Units 3 to 10 m thick, occurs in LST of Sequence 3, restricted to the southeast side of Cincinnati Arch south of Lexington	Units up to 1.5 m thick, occurs throughout the supersequence but most common in the middle of the Lexington Limestone as cycle caps	Units from 0.5 to 7 m thick; occurs throughout section, most common in the middle of the supersequence	Units 0.3 to 80 m thick; occur throughout the supersequence and is most abundant in northern Kentucky and downramp in Virginia	Units from 1 to 7 m thick; occur above basal grainstone and in topographic depressions south of Jessamine Dome
Lithology	5 to 50 cm beds of calcareous siltstone; many bryozoans in thin shaley partings (< 5 cm thick)	0.2 to 1. 5 m beds of skeletal grainstone and packstone with thin (<1cm thick) calcareous shale partings	3 to 20 cm thick irregular layers and nodules of whole skeletal wackestone, packstone and calcareous shale (up to 40 %); abundant bryozoans, brachiopods, gastropods, trilobites, some echinoderms in limestone; thin-shelled brachiopods and bryozoans in shales; bedding is burrow homogenized	2 to 20 cm beds of skeletal packstone, calcisiltite, and limy shale; packstone beds have flat bases and irregular tops some with calcisiltite caps; interbedded with limy shales (30-50%); abundant gastropods, brachiopods and bryozoans in packstone; many thin brachiopods in shales;	5 to 10 cm beds of fine calcisiltite and calcareous shale; rare trilobites
Sedimentary Structures	Planar and ripple laminations, some hummocky cross-stratification; alternating fine to coarse grain size define laminations in cores; abundant seismites	Abundant horizontal laminations, and rare cross-laminations, many beds have flat bases with rippled tops; rarely capped by pyritic and phosphatic hardgrounds	Abundant burrows; rare preserved laminations; rare skeletal packstone grading up into calcareous shale; pyritic and phospatic hardgrounds occur throughout this unit	Normal and reverse grading in skeletal packstones; planar and hummocky cross-laminations, local scouring, and preserved ripples in calcisiltites, abundant thin horizontal burrows	Fine planar laminations in calcisiltite; abundant framboidal pyrite; no bioturbation evident
Environment	Storm dominated mid-ramp, between fairweather and storm wave base	Mid-ramp thin grainstone storm sheets and sand waves, open oarine	Mid-ramp, open marine sub fairweather wave base	Storm dominated deep ramp, between fairweather and storm wave base	Deep ramp, dominantly below storm wave base, anoxic
Water Depths	10 to 30 m	< 30 m	10 to 30 m	20 to 40 m	> 40 m

Jessamine Dome where it has been eroded (Haynes, 1994). The unconformity is underlain by light-colored, diagenetically mottled High Bridge Group lime mudstone and overlain with a sharp contact by darker colored, coarse skeletal limestone of the Lexington Limestone. Iron stained clasts (up to 10 cm diameter) of the High Bridge limestone occur in the basal units of the Lexington Limestone (Cressman, 1973). On the gamma ray logs, the boundary between the High Bridge Group and Lexington Limestone is near the extremely high gamma ray spike of the Millbrig bentonite, or at the top of a thin unit of low gamma-ray values (clean limestone of the High Bridge Group) above which the gamma ray values increase upsection into the Lexington Limestone.

The LST to the supersequence is developed in the southern part of the foreland basin, where nearshore coarse deltaic clastics (Bays Formation; 60 to 135 m thick) pass out into coastal plain and tidal flat red, limy mudrocks with thin paleosols (Moccasin Formation; 0 to 166 m thick) (Read, 1980; Kreisa, 1980; McHugh, 1985). A possible sequence boundary within the Moccasin redbeds may occur at the base of the Walker Mountain Sandstone, a regionally traceable lowstand conglomeratic quartz sandstone that thins to the west and northeast (Goggin and Haynes, 1995).

The TST of this supersequence consists of Lexington Limestone skeletal limestones and the lower third of the Clays Ferry-Kope shaly skeletal limestone. The upper part of the TST has some buildup formation over the Jessamine Dome, and southward backstepping of skeletal limestone units (Figure 5). The TST is an overall, blocky, low gamma-ray interval throughout the Lexington Limestone interval, with some higher gamma-ray values associated with rhythmite tongues (Logana Member) near the base (Figures 5 and 6). Gamma ray values gradually increase above the blocky signatures Lexington Limestone up to the 2nd-order MFS within the Kope/Clays Ferry Formations (Figure 6).

The maximum flooding surface (MFS) occurs in the Clays Ferry-Kope Formations, where deeper water, interbedded skeletal limestone and shale extend far back onto the ramp, and thick skeletal grainstone/packstone and fenestral beds are in their maximum backstepped position. To the north, the MFS probably lies above the local drowning surface on the Tanglewood Bank, and is difficult to trace downdip into the deeper water shaly limestone (Kope/Clays Ferry). It is difficult to determine the position of the 2nd-order MFS on the gamma ray logs, because many smaller-scale flooding events have approximately the same response (Figure 6).

Figure 5. Regional lithologic cross-section (X-X') of the Late Mohawkian to Cincinnatian supersequence. Location of all sections are shown on Figure 3. The datum is the top of the silty peritidal dolomite capping Sequence 3.

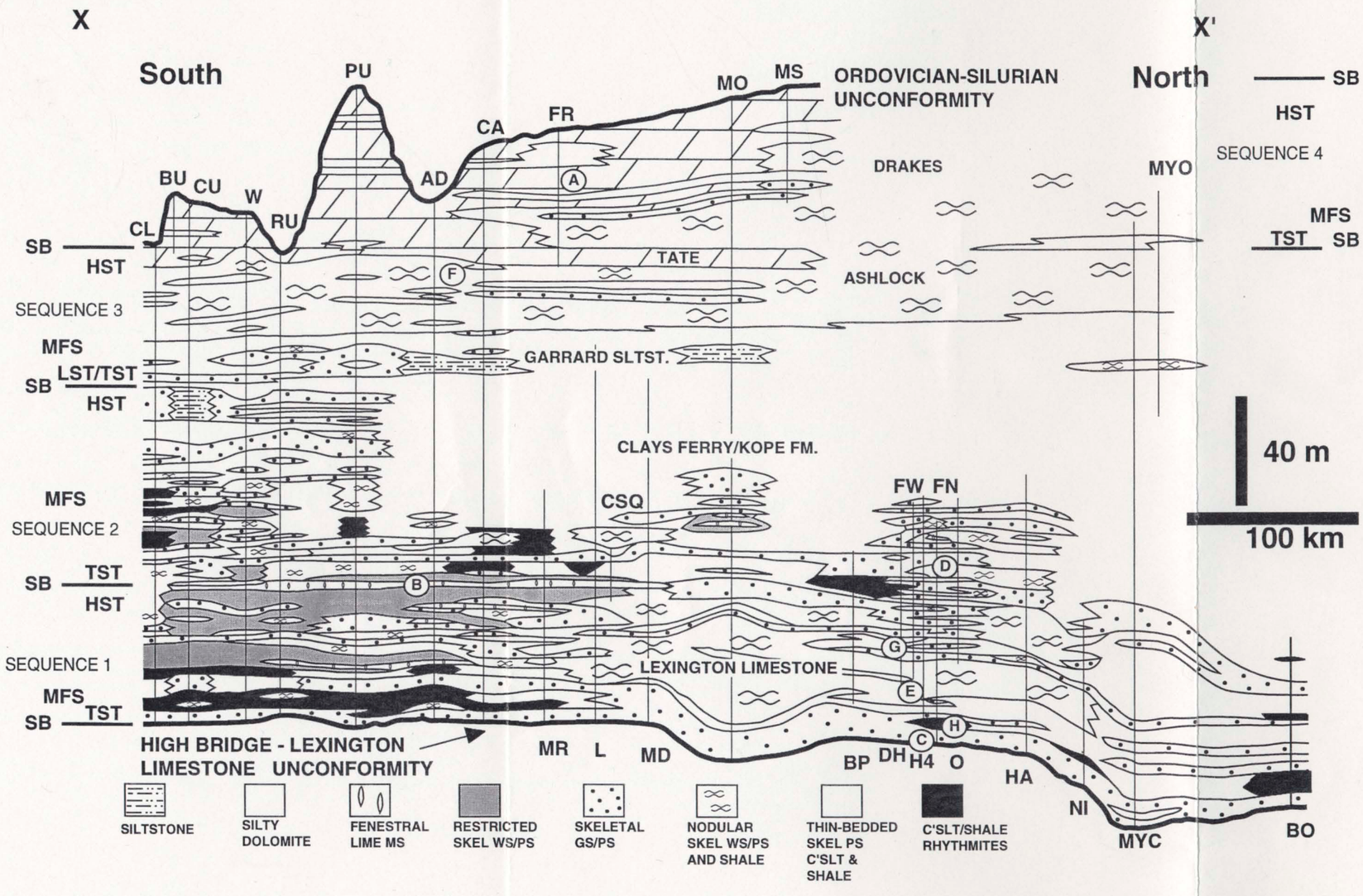
X
South
X'
North
PU
MO
MS
ORDOVICIAN-SILURIAN
UNCONFORMITY
CA
FR
BU
CU
W
RU
CL
AD
A
DRAKES
MYO
SB
HST
SEQUENCE 4
MFS
TST
SB
SB
HST
F
TATE
ASHLOCK
SEQUENCE 3
MFS
GARRARD SLTST.
SB
LST/TST
HST
CLAYS FERRY/KOPE FM.
40 m
MFS
CSQ
FW FN
SEQUENCE 2
SB
TST
HST
B
D
G
LEXINGTON LIMESTONE
SEQUENCE 1
E
MFS
SB
TST
H
C
HIGH BRIDGE - LEXINGTON
LIMESTONE UNCONFORMITY
MR
L
MD
BP
DH
H4
O
HA
NI
MYC
BO
100 km
SILTSTONE
SILTY
DOLOMITE
FENESTRAL
LIME MS
RESTRICTED
SKEL WS/PS
SKELETAL
GS/PS
NODULAR
SKEL WS/PS
AND SHALE
THIN-BEDDED
SKEL PS
C'SLT &
SHALE
C'SLT/SHALE
RHYTHMITES

Figure 6. Wireline correlation Diagrams.

A. Line A-A' approximately parallel to the crest of the Cincinnati Arch and the lithologic cross-section (X-X') of Figure 5.

B. Line B-B' parallel to the Cincinnati Arch, but downramp in the Appalachian Basin. Note thickening in the central area over the Rome trough.

C. Line C-C' west to east line from near the crest of the Cincinnati Arch into the Appalachian Basin.

D. Line D-D' west to east line from the Sebree Trough across the crest of the Cincinnati Arch into the Appalachian Basin.

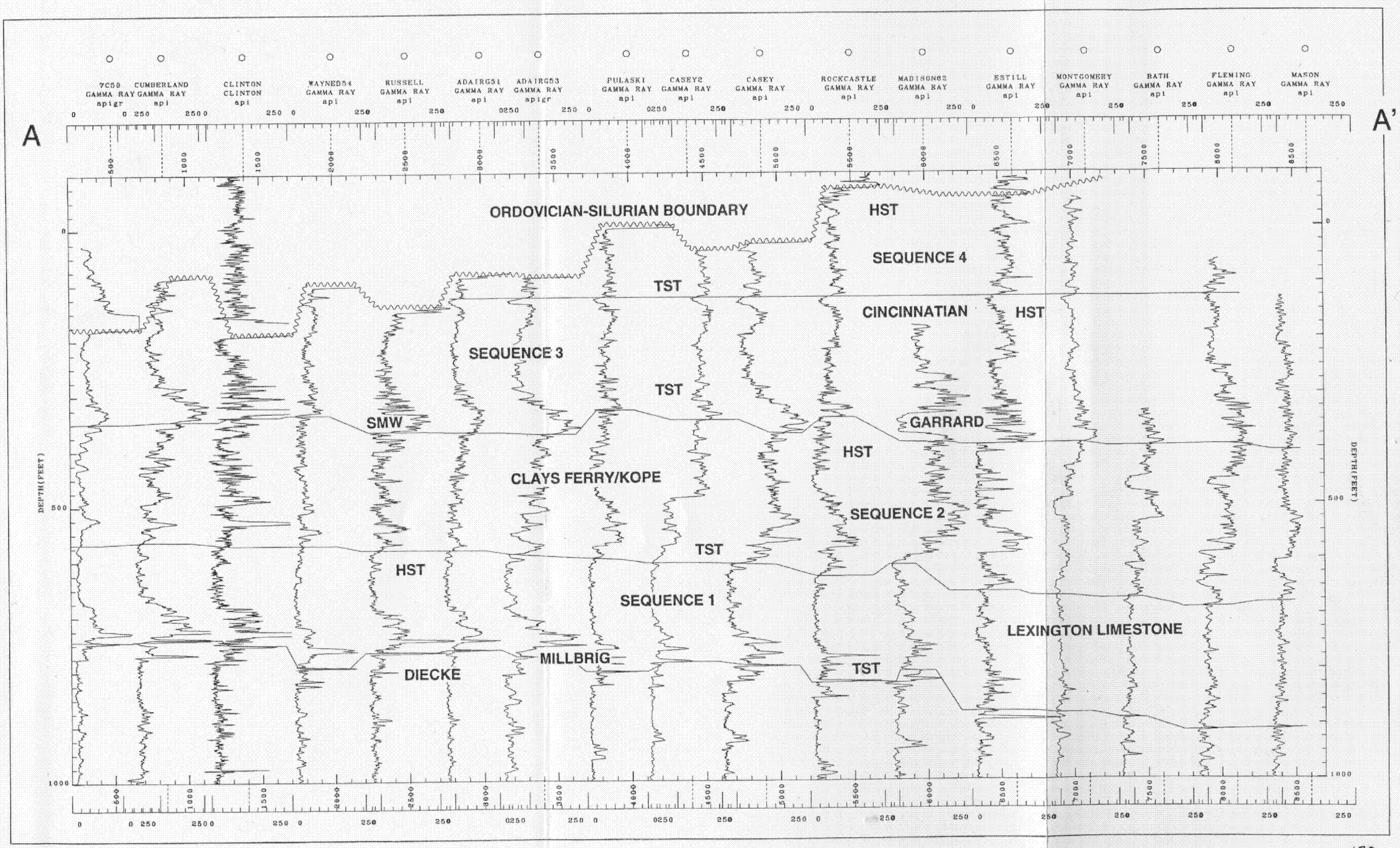
A
A'
7C50 GAMMA RAY api gr
CUMBERLAND GAMMA RAY api
CLINTON CLINTON api
WAYNED54 GAMMA RAY api
RUSSELL GAMMA RAY api
ADAIRG51 GAMMA RAY api
ADAIRG53 GAMMA RAY api gr
PULASKI GAMMA RAY api
CASEY2 GAMMA RAY api
CASEY GAMMA RAY api
ROCKCASTLE GAMMA RAY api
MADISONG2 GAMMA RAY api
ESTILL GAMMA RAY api
MONTGOMERY GAMMA RAY api
BATH GAMMA RAY api
FLEMING GAMMA RAY api
MASON GAMMA RAY api
ORDOVICIAN-SILURIAN BOUNDARY
HST
SEQUENCE 4
TST
CINCINNATIAN
HST
SEQUENCE 3
TST
SMW
GARRARD
HST
CLAYS FERRY/KOPE
SEQUENCE 2
TST
HST
SEQUENCE 1
LEXINGTON LIMESTONE
MILLBRIG
TST
DIECKE
DEPTH(FEET)

170

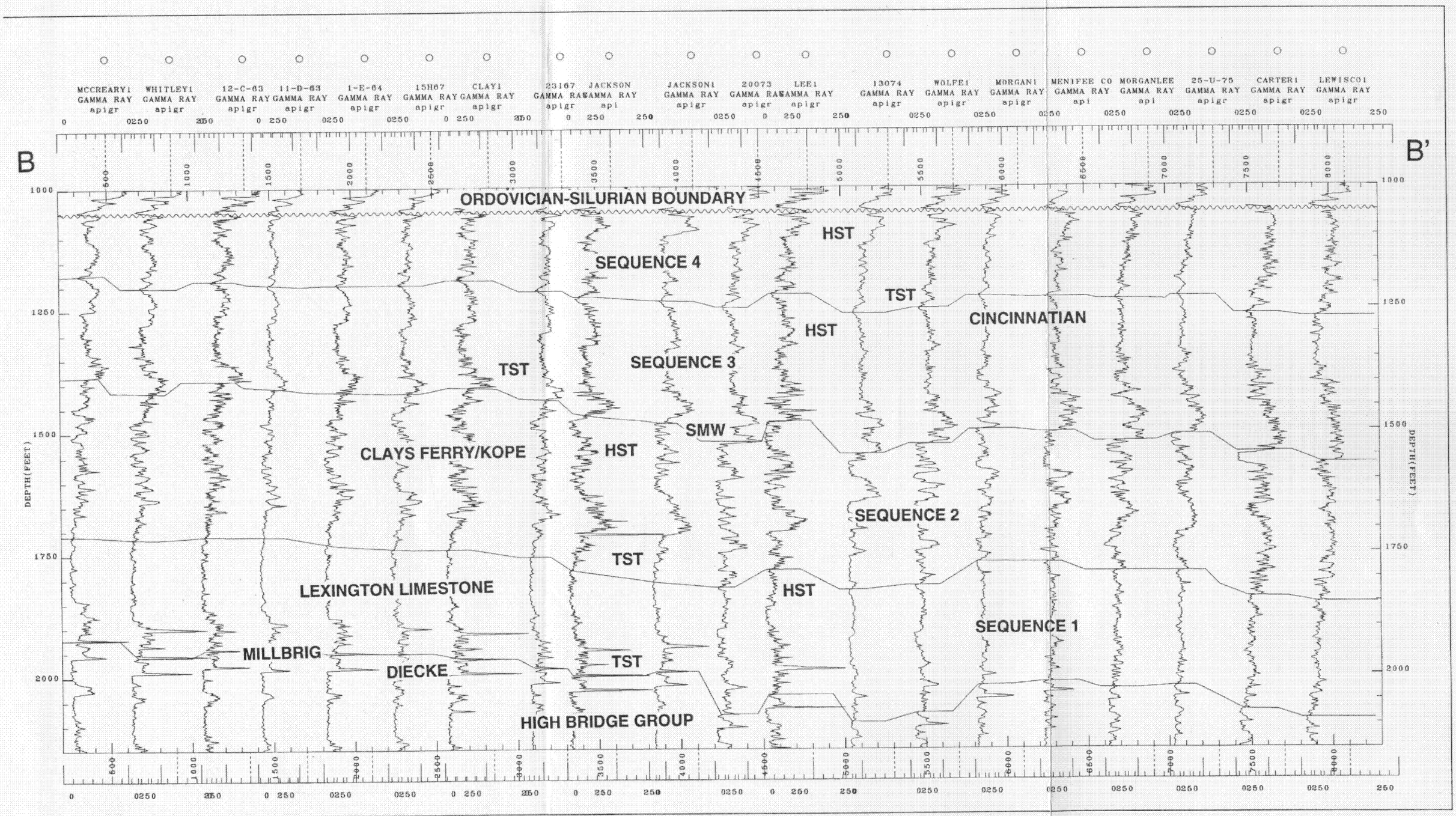
B
B'
MCCREARY1 GAMMA RAY apigr
WHITLEY1 GAMMA RAY apigr
12-C-63 GAMMA RAY apigr
11-D-63 GAMMA RAY apigr
1-E-64 GAMMA RAY apigr
15H67 GAMMA RAY apigr
CLAY1 GAMMA RAY apigr
23167 JACKSON GAMMA RAY apigr
JACKSON1 GAMMA RAY apigr
20073 LEE1 GAMMA RAY apigr
13074 GAMMA RAY apigr
WOLFE1 GAMMA RAY apigr
MORGAN1 GAMMA RAY apigr
MENIFEE CO GAMMA RAY api
MORGANLEE GAMMA RAY api
25-U-75 GAMMA RAY apigr
CARTER1 GAMMA RAY apigr
LEWISCO1 GAMMA RAY apigr
ORDOVICIAN-SILURIAN BOUNDARY
HST
SEQUENCE 4
TST
CINCINNATIAN
HST
TST
SEQUENCE 3
SMW
CLAYS FERRY/KOPE
HST
SEQUENCE 2
TST
LEXINGTON LIMESTONE
HST
SEQUENCE 1
MILLBRIG
TST
DIECKE
HIGH BRIDGE GROUP
DEPTH(FEET)
1000
1250
1500
1750
2000

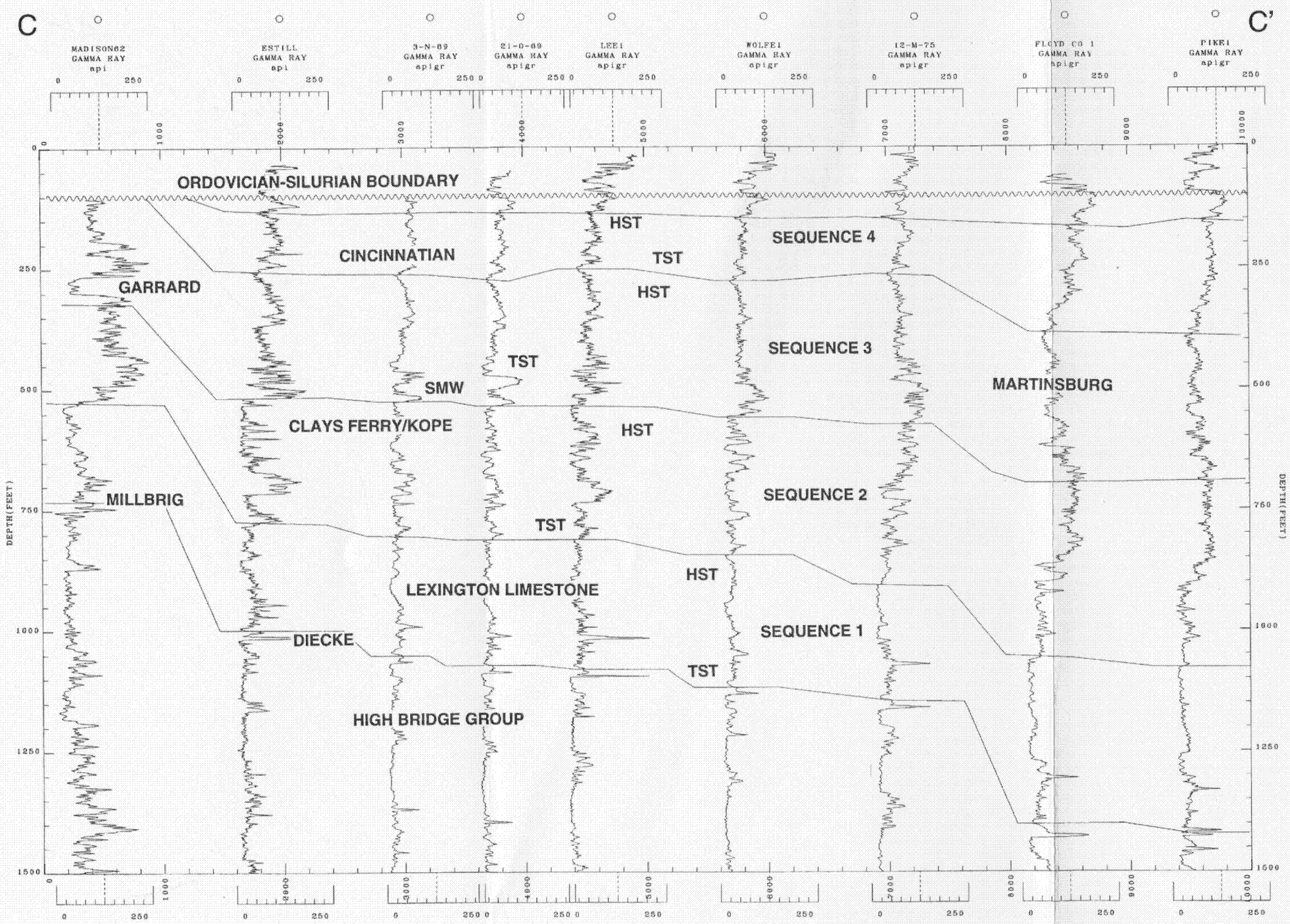
C
C'
MADISON02 GAMMA RAY api
ESTILL GAMMA RAY api
3-N-69 GAMMA RAY apigr
21-0-69 GAMMA RAY apigr
LEE1 GAMMA RAY apigr
WOLFE1 GAMMA RAY apigr
12-M-75 GAMMA RAY apigr
FLOYD CO 1 GAMMA RAY apigr
PIKE1 GAMMA RAY apigr
ORDOVICIAN-SILURIAN BOUNDARY
CINCINNATIAN
GARRARD
SMW
CLAYS FERRY/KOPE
MILLBRIG
DIECKE
LEXINGTON LIMESTONE
HIGH BRIDGE GROUP
MARTINSBURG
HST
TST
HST
TST
HST
TST
HST
TST
SEQUENCE 4
SEQUENCE 3
SEQUENCE 2
SEQUENCE 1
DEPTH(FEET)
DEPTH (FEET)

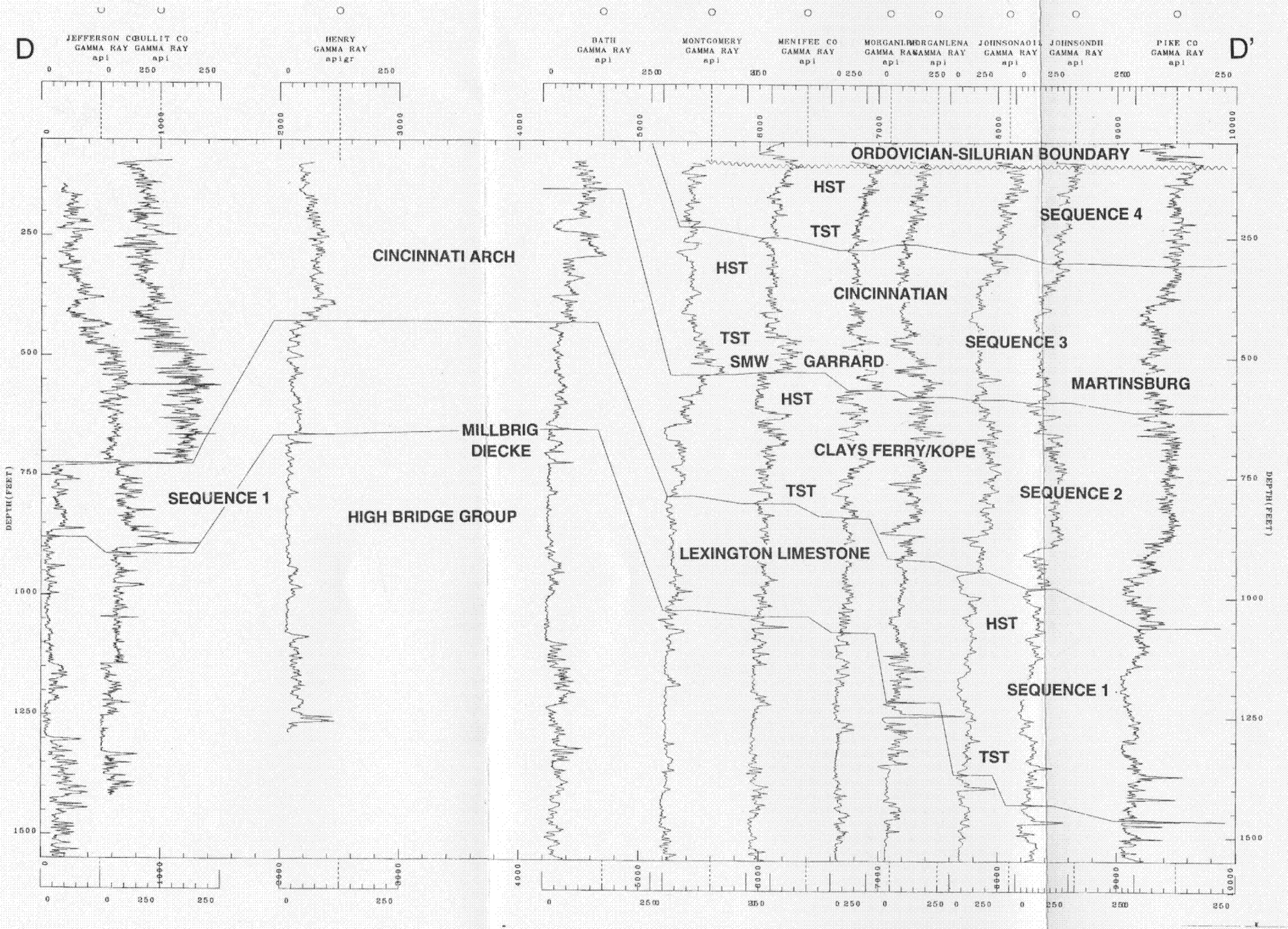
D
D'
JEFFERSON CO GAMMA RAY api
ULLIT CO GAMMA RAY api
HENRY GAMMA RAY apigr
BATH GAMMA RAY api
MONTGOMERY GAMMA RAY api
MENIFEE CO GAMMA RAY api
MORGANLENA GAMMA RAY api
MORGANLENA GAMMA RAY api
JOHNSONAOIL GAMMA RAY api
JOHNSONOIL GAMMA RAY api
PIKE CO GAMMA RAY api
DEPTH(FEET)
ORDOVICIAN-SILURIAN BOUNDARY
HST
TST
SEQUENCE 4
CINCINNATI ARCH
HST
CINCINNATIAN
TST
SEQUENCE 3
SMW
GARRARD
MARTINSBURG
HST
MILLBRIG
DIECKE
CLAYS FERRY/KOPE
SEQUENCE 1
TST
SEQUENCE 2
HIGH BRIDGE GROUP
LEXINGTON LIMESTONE
HST
SEQUENCE 1
TST

The supersequence HST is marked by shallowing from the skeletal limestone and shale of the Clays Ferry and Kope Formations, up into Grant Lake nodular limestone and shale, and then into peritidal silty dolomites (Ashlock and Drakes Formations) that thin to the north. (Weir et al., 1984) (Figure 5). There is a gradual decrease in the gamma ray values throughout the HST toward the sequence boundary.

The Late Ordovician/Silurian unconformity capping this supersequence varies regionally. The unconformity cuts out the Hirnantian (Gamachian) stage in Kentucky (Brenchley et al., 1994) and was probably caused by the sea level drawdown associated with glaciation during the latest Ordovician (Hambrey, 1985; Caputo and Crowell, 1985). In the central Kentucky outcrop belt, the Late Ordovician silty dolomites capping the section are unconformably overlain by Early Silurian Brassfield Dolomite, an open marine, dolomitized, cherty skeletal wackestone/packstone. Locally, the Silurian rocks contain re-worked Ordovician clasts and have dips up to 4^{o} discordant relative to the Ordovician and Silurian beds (Weir et al., 1984). Further south along the Cincinnati Arch, Devonian black shales rest unconformably on the Late Ordovician rocks (Figure 5). On gamma ray logs, the unconformity at the top of the supersequence is seen along the Cincinnati Arch as a sharp decrease in gamma values associated with overlying Silurian Brassfield dolomites, or a sharp increase in gamma values associated with overlying Devonian shales southward along the Arch (Figure 6). In the subsurface east of the Cincinnati Arch, the Ordovician-Silurian boundary is generally marked by decreasing gamma ray values, with numerous well defined peaks associated with tongues of Silurian dolomite or sandstone, the unconformity being placed on the gamma ray logs at the base of the lowest tongue of low gamma ray values.

Third Order Sequences

The Late Mohawkian to Cincinnatian supersequence contains four 3rd-order depositional sequences, each 40 to 80 m thick along the Cincinnati Arch, and 60 to 110 m thick in the basin. Each 3rd-order depositional sequence is asymmetric with a thin TST capped by a thicker HST. The approximate average duration of these sequences is 2 to 4 m.y.

Depositional Sequence 1:

The lowest 3rd-order depositional sequence consists of the informal "lower Lexington Limestone" and is from the disconformable base of the Lexington Limestone to the top of

the Perryville Member of the Lexington Limestone (Figure 5). The Curdsville Member forms the TST, which consists of skeletal packstone/grainstone containing a few percent rounded quartz sand grains, and many pyritic and phosphatic hardgrounds. The TST has upward increasing gamma ray values which reflect the change from low shale content of the Curdsville Member to the more shaly Logana Member (Figure 6). The many, very high gamma ray spikes in the TST may be bentonites.

The MFS occurs within the black, organic-rich (?) deeper water rhythmites of the Logana Member (Figure 5) approximately 5 to 10 m above the sequence boundary, and is marked by a strong gamma ray spike at the turnaround between upward increasing to upward decreasing gamma-ray values (Figure 6).

The HST contains an upward increase in nodular, faunally restricted skeletal wackestone/ packstone that pass basinward into tidally-influenced skeletal grainstone, that pinches out northward and passes into noduar, open marine skeletal packstone and shale with tongues of interbedded skeletal packstone and shale. On the Cincinnati Arch the HST is capped by fenestral lime mudstone of the Perryville Member (Figure 5) , and skeletal grainstone elsewhere. Gamma ray values rapidly decrease upward in the HST, into a blocky signature reflecting the decreased shale content of the HST. Downramp, the gamma ray response of lower part of the HST has pronounced alternations of high and low values (defining smaller-scale sequences), and a blocky low gamma-ray response limited to the limestone-rich upper HST (Figure 6).

The 3rd-order sequence boundary above the Perryville Member is a karsted surface beneath which the tidal flat facies are diagenetically color-mottled and iron stained. It has small vugs (up to 5 cm diameter) that penetrate down to 1.5 m below the unconformity surface that are filled with quartz-poor, phosphatic sand infiltrated from above during the subsequent transgressive event. This sequence boundary, a karstic surface in the south, becomes conformable over the Jessamine Dome, where it probably underlies a tongue of skeletal grainstone low in the Tanglewood Bank. The position of the unconformity surface is not evident on the gamma ray logs, but the blocky, low gamma ray character of the Perryville tidal flat facies or downdip skeletal grainstone is consistently overlain by a higher gamma ray unit that corresponds with initial flooding above the sequence boundary (Figure 6).

Depositional Sequence 2: This extends from the top of the Perryville Member to the base of the Garrard Siltstone. A Ramp Margin Wedge (RMW) of tidally-influenced skeletal grainstone, nodular skeletal packstone and shale occurs in outcrops around the Jessamine

Dome (Figure 7). The base of the TST is a thin (< 10 cm thick) phosphatic sand that infiltrates the karstic surface on the Perryville Member. This is overlain by units that are phosphatic, with multiple hardgrounds, and composed of faunally restricted, light gray, skeletal wackestone/packstone, nodular skeletal packstone/ grainstone and shale, and skeletal grainstone units of the "upper Lexington Limestone" which backstep to the south. The TST also contains a locally restricted unit of thin-bedded calcisiltite and shale rhythmite (Brannon Member, Lexington Limestone) in a structurally controlled trough across the Cincinnati Arch (Kulp, 1995). Over the Jessamine Dome, the skeletal grainstone and nodular, shaly skeletal packstone form an aggrading bank ("Tanglewood Bank"; Hrabar et al., 1971; Cressman, 1973; "Tanglewood Buildup" of Ettensohn, 1992) that contains very minor, fenestral lime mudstone, gastropod wackestone/packstone and interbedded skeletal packstone and shale. On gamma ray logs, the TST is marked by generally increasing gamma ray values up to the MFS (Figure 6).

The Tanglewood Bank developed on a fault-bounded uplift on the Jessamine Dome (Borella and Osborne, 1978; Ettensohn, 1992). The bank developed during the LST and TST of depositional sequence 2 and is over 50 m thick and covers up to 5000 km^2. Tanglewood Bank is composed of 1 to 8 m thick, asymmetric shallowing-upward cycles (Figure 7). The cycles consist of nodular skeletal wackestone/packstone and shale with rare thin-bedded skeletal packstone, calcisiltite and shale, and these pass up into tidally cross-bedded skeletal grainstone (Hrabar et al., 1971) (Figure 8). The grainstone facies interfinger with bryozoan banks and nodular skeletal wackestone/packstone and shale.

The MFS of Sequence 2 corresponds to the 2nd-order MFS in the deeper water Clays Ferry/Kope Formations; downdip, the MFS probably occurs occurs above the Tanglewood Bank (Figure 3). However, even using both lithologic logs and gamma ray logs, it is difficult to pick an actual surface for the sequence 2 MFS, as opposed to a broad zone of maximum flooding. On gamma ray logs, the actual position of the MFS appears to occupy different stratigraphic positions in sections along the Cincinnati Arch. Downramp, the MFS occupies a more constant position low in the sequence. The high gamma ray signal marking the MFS on the arch can be followed to the east where it is generally the largest of the gamma ray spikes, near the middle of Sequence 2 (Figure 6 C, D). It is underlain and overlain by a pronounced low gamma ray interval; note that the MFS does not occur at the highest gamma ray values, which occur in the east in the middle of the HST. To the east, the MFS on gamma ray logs is marked by pronounced

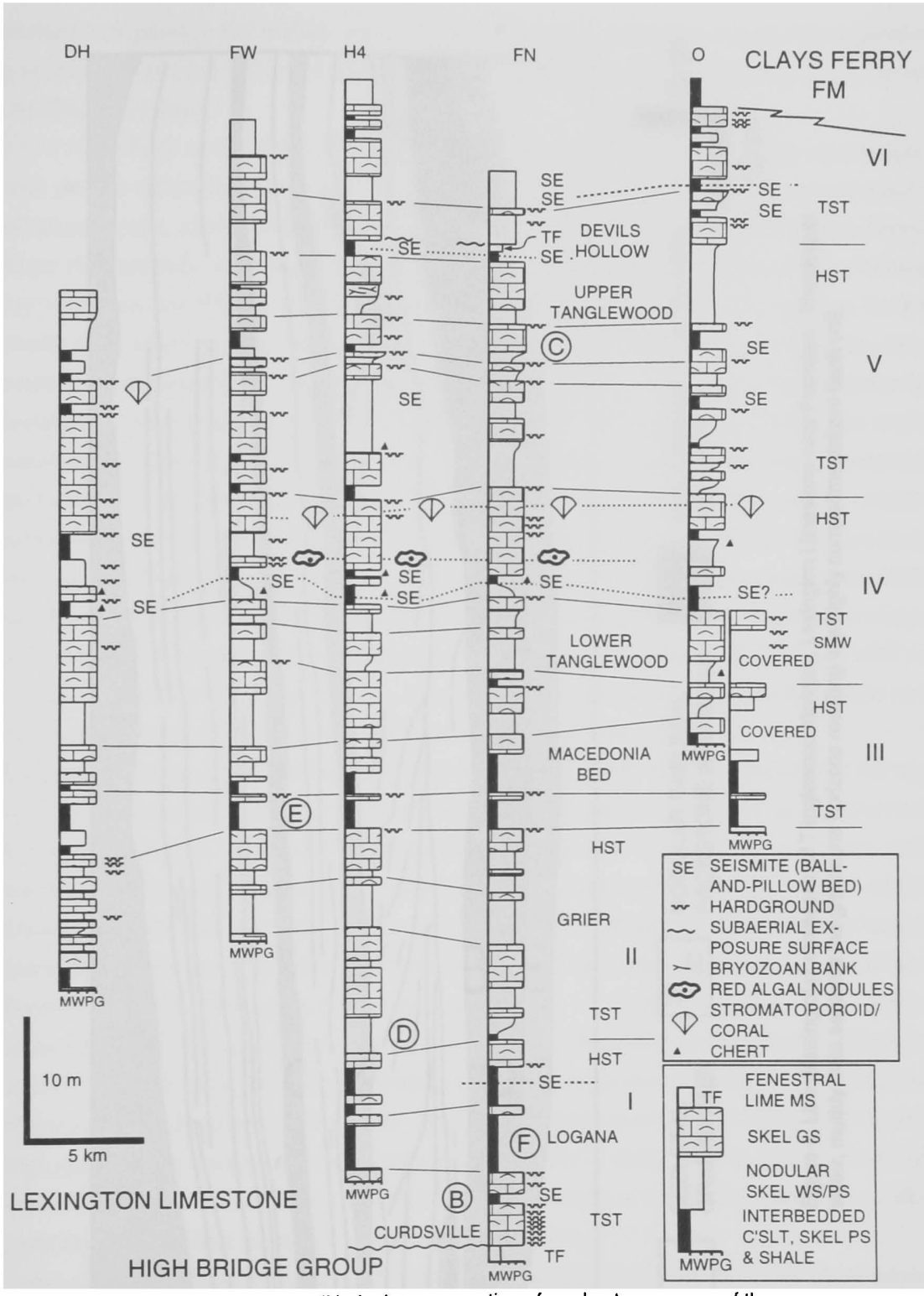

Figure 7. Southwest to northeast lithologic cross-section of road-cut exposures of the Lexington Limestone near Frankfort, Kentucky.

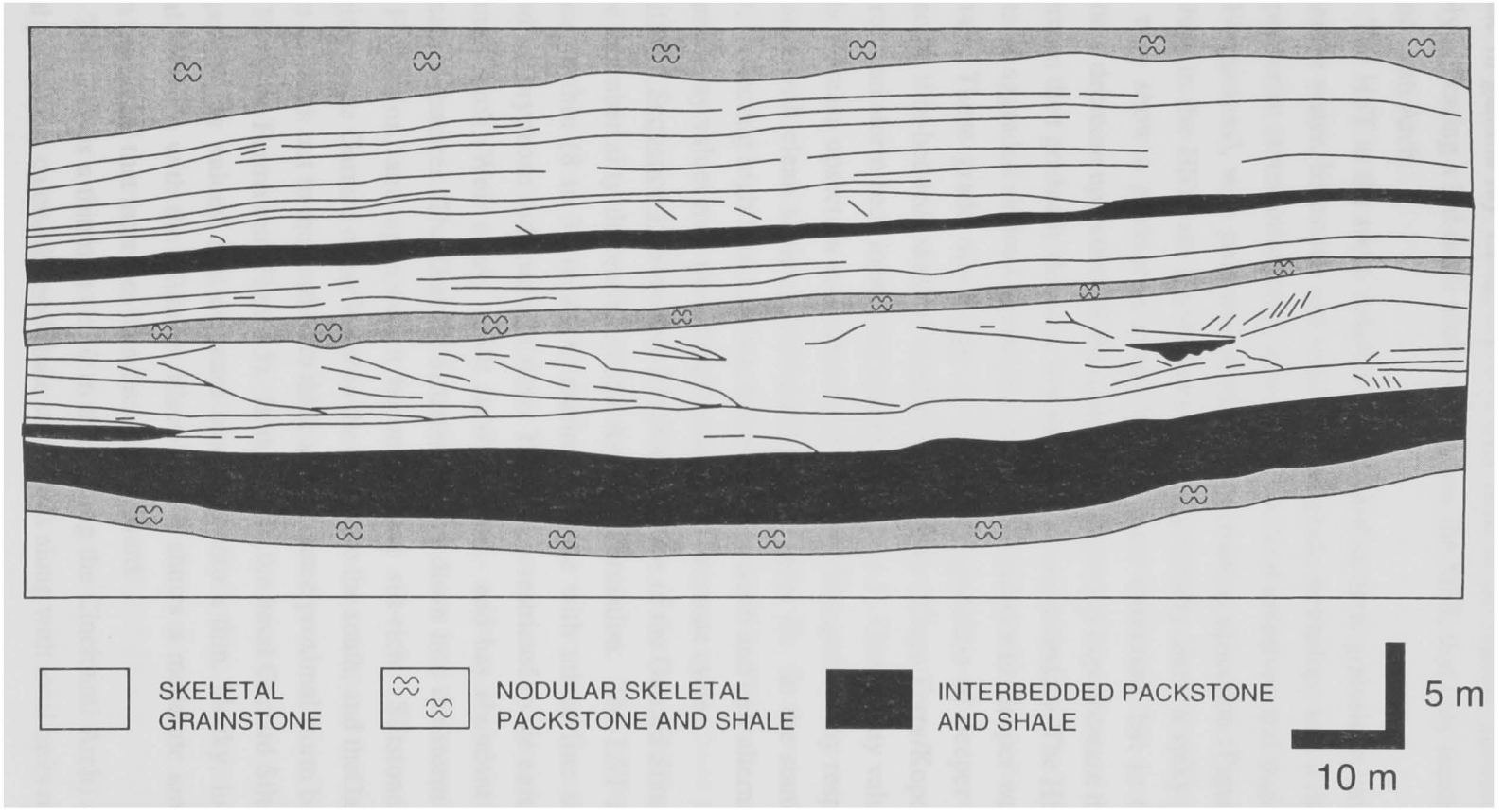

Figure 8. Line drawing of photomosaic of Tanglewood Member, Lexington Limestone near Frankfort. The deeper water, muddy units separate the grainstone horizons resulting in a highly compartmentalized bank unit.

decrease in gamma ray values above a thin zone of decreasing gamma ray response, possibly indicating a 3rd-order shallowing below the MFS, that only locally shows up on the Cincinnati Arch.

The HST in the south consists of aggraded skeletal grainstone units interbedded with deeper water, limestone and shale. These grade downslope into a thick succession of deeper water, storm-influenced, thin-bedded skeletal limestone and shale (Clays Ferry/ Kope Formations), with proximal storm-beds increasing upsection (Figure 3). Gamma ray values in the HST are highly variable, but generally show a spiky pattern; in the south, they show a gradual decrease then increase upsection, but in the north they commonly decrease upsection. In the east, HST gamma ray logs decrease then increase to a maximum then gradually decrease toward the sequence boundary. The HST in the south consists of aggraded skeletal grainstone units interbedded with deeper water, limestone and shale. These grade downslope into a thick succession of deeper water, storm-influenced, thin-bedded, skeletal limestone and shale (Clays Ferry/Kope Formations), with proximal storm beds increasing upsection (Figure 3). Gamma ray values in the HST steadily increase upsection and some show a blocky low gamma ray response, perhaps associated with clean skeletal grainstone units (Figure 6). In the south, the HST is blocky, reflecting high lime content, whereas to the north and east alternating high and low gamma ray values may mark small-scale shale-limestone cycles.

Depositional Sequence 3: Sequence 3 is from the base of the Garrard Siltstone to the top of Tate Member silty dolomites of the Ashlock Formation. The LST is the Garrard Siltstone, a thin (8 to 30 m thick) marine siltstone with minor fine sandstone, and interbedded bryozoan rudstone and shale. This unit is restricted to the eastern side of the Cincinnati Arch (Weir et al., 1984; Jacobs, 1986), and has abundant soft-sediment deformation features. The Garrard Siltstone grades down into the storm bedded Clays Ferry Formation, and upsection it becomes more silt-rich. Siltstones presumably belonging to the Garrard occur lower in the section to the south, and theGarrard Siltstone appears to pinch out to the north into thick amalgamated proximal storm beds at the base of the Fairview Formation (Figure 5). In the south, the basal Garrard Siltstone has very high gamma-ray values, that decrease upsection into a thin, blocky, low gamma-ray interval in areas with the siltstone. Elsewhere, it shows a moderate amplitude, spiky gamma ray signal that increases then decreases upward.

The TST is a thin unit (< 10 m thick along the Cincinnati Arch) of interbedded skeletal packstone, calcisiltite and shale storm beds along with local units of cross-bedded

skeletal grainstone (~2 m thick). On gamma ray logs, the TST generally shows gradually increasing values which reach a maximum at the MFS. The MFS lies within an interval of deeper water, interbedded limestone and shale and is marked on the logs by a turnaround in gamma ray values (Figure 6).

The HST is an upward-shallowing sequence of nodular skeletal wackestone/packstone with some deeper water shale intervals (Calloway Creek/Grant Lake Limestones), capped by the thin Tate silty dolomite (Figure 5). The silty, fenestral dolomite cap contains many small irregular exposure surfaces (paleosols?) near Fredericktown, Kentucky. The gamma-ray logs of the HST decrease gradually to a thin, relatively regional low corresponding to a smaller scale shoaling, about midway in sequence 3, gamma ray values increase and then decrease into a regional gamma ray low marking the Tate dolomiteat the top of sequence 3. Downdip, the HST gamma-ray log shows slight gradually decreasing average values up to the sequence boundary. Superimposed on this trend is up to 5 cycles marked by high gamma ray values at their bases (Figure 6).

Depositional Sequence 4: Sequence 4 extends from the top of the Tate dolomite tongue up to the Ordovician-Silurian unconformity capping the 2nd-order supersequence (Figure 3). The TST is marked by a southward backstep of the silty dolomites units which are onlapped by nodular argillaceous skeletal wackestones/ packstone. These pass basinward into a thin unit of thin-bedded, skeletal packstone, calcisiltite and shale overlain by a thick unit of nodular skeletal wackestone/ packstone (Grant Lake Limestone/Bullfork Formation). On the wireline logs, the TST shows gradually increasing gamma ray values that reach a maximum 10 to 15 m above the underlying sequence boundary. The MFS cannot be picked lithologically to the south on the Arch, but in the north it may occur in the landward extent of the nodular skeletal packstone and shale which onlaps the underlying dolomite.

The HST consists of thin, nodular skeletal limestone, and minor grainstone, overlain by thick peritidal silty dolomites that grade north, east and west into open ramp, thinly interbedded, skeletal wackestone/packstone and abundant shale. Along the western maring of the Cincinnati Arch the HST locally contains shaly skeletal wackestone/packstone with abundant corals in thin (< 3 m thick) biostromes. The peritidal silty dolomites commonly are well-laminated and shale-poor in south, but are more shaly and are bioturbated to the north. On gamma-ray logs, the HST is marked by overall gradually decreasing gamma-ray values associated with low gamma ray dolomites

in the HST of Sequence 4; however, superimposed are higher frequency flooding events marked by gamma ray spikes signalling small-scale flooding events associated with nodular shaly skeletal limestone.

Parasequence Sets

Approximately 11 small-scale, 3rd-order parasequence sets, each up to 20 m thick, and with possible durations of 800 k.y. to 1.3 m.y, occur in the Late Mohawkian to Cincinnatian 2nd-order supersequence (Figure 5). These parasequence sets contain regionally correlative flooding events, overlain by regionally offlapping shallower water facies. In turn, they consist of bundles of meter-scale cycles (or parasequences). Most parasequence sets are asymmetric and have only thin transgressive units. Where better developed, these transgressive units are thin hardground bearing skeletal packstone/grainstone, or restricted nodular wackestone/packstone. Where the TST is thin or absent most of these parasequence sets consist of a flooding surface overlain by thin bedded skeletal packstone-, calcisiltite - shale, that shallows into nodular bedded, shaly skeletal packstone, capped by skeletal grainstone-, silty dolomite or fenestral lime mudstone (rare).

Parasequence Sets-Sequence 1: Three parasequence sets occur in the Lexington interval (Sequence 1) (Figure 5). The first has a thin transgressive grainstone overlain by rhythmite marking the MFS. The HST is capped by a regional skeletal grainstone. The next two parasequence sets are characterized by successively shallower and less extensive flooding events, along with late HST peritidal faunally restricted wackestone/lime mudstone or fenestral lime mudstone that offlap progressively further into the basin. These three parasequence sets also can be seen in the north as 3 upward shallowing nodular or interbedded limestone and shale that grade up into nodular or skeletal grainstone. The flooding surfaces to these small sequences can be seen on some of the gamma ray logs as high gamma ray values.

Parasequence Sets-Sequence 2: Parasequence sets are less clear in Sequence 2, perhaps because it is dominated by relatively deeper water facies and many of the shallow water facies form mosaics or local shoals. On some logs (Carter 1, Jackson, Figure 6B; Ice and Estill, Figure 6A), two relatively large gamma ray kicks appear to mark dominant flooding events in Sequence 2, the lower one coinciding with the supersequence

maximum flooding surface. Superimposed on these are 6 to 7 local 4th-order cycles marked by flooding events.

Parasequence Sets-Sequence 3: Two parasequence sets are evident in Sequence 3 on the gamma ray logs (i.e., 1-E-64, Clay 1, Figure 6 B; Estill, Figure 6 D) and each of these is marked by gradually decreasing gamma ray values above each MFS. On the lithologic cross-section (Figure 5) these correspond to the thin-bedded shaly limestone and shale near the Sequence 3 MFS, and a subordinate flooding event in the upper half of Sequence 3. To the north and east, only the lower MFS is evident on the gamma ray logs (Figure 6B), which show several (up to 5) gamma kicks marking local 4th-order cycles (Pike and Floyd logs; Figure 6D)

Parasequence Setss-Sequence 4: Three parasequence sets developed in Sequence 4 and are marked by either thin-bedded shaly limestone, or nodular shaly limestone in TST's and early HST's with silty dolomitic tongues comprising the late HST's (Figure 5). On gamma ray logs these parasequence sets are less clear; however, three large, positive gamma ray kicks are small MFS's that may correspond to the MFS of these parasequence sets (Figure 6).

Meter-Scale Cycles (Parasequences)

Systems tracts making up the Ordovician sequences consist of stacked meter-scale cycles (1 to 8 m thick) (Table 3, Figure 9), most of which are subtidal, asymmetric, and upward-shallowing, or less common symmetrical transgressive-regressive units. These meter-scale cycles, are arranged from shallowest to deepest in Figure 9, their characteristics are given in Table 3. The component facies are shown in Figure 4 and Tables 1 & 2. Many cycles are capped by marine hardgrounds. Subaerial exposure surfaces on cycle caps are rare. Cycles are tabular, and traceable over several hundred meters of outcrop exposure, and some may be traced up to 20 km or more between measured sections and cores (Figure 7). However, the meter-scale cycles cannot be correlated over the 300 km extent of outcrops and cores.

Peritidal Cycles: These are common in HST of Sequences 1, 3 and 4 and associated with local "islands" in Sequences 1 and 2 (Figure 5). In the Late Mohawkian Lexington Limestone the peritidal cycles consist of restricted lime wackestone/mudstone, overlain by fenestral limestone (Figure 9, A). Overall, these inner ramp facies are only poorly cyclic, the cycles ranging from a meter to several meters thick. Most peritidal cycles are

TABLE 3. CHARACTERISTICS OF METER-SCALE CYCLES

1. PERITIDAL CYCLES: In the Lexington Limestone (Fig. 9, B) they consist of (in descending order):

3. Cap of fenestral limestone, whose upper surface may be karstic
2. Nodular skeletal wackestone/lime mudstone, with a shallow water fauna (coral, brachiopods, stromatoporoids, gastropods, ostracodes) and carbonate mud matrix, along with thin interlayered shale (<25%)
1. Thin basal shale parting.

Peritidal cycles in the Cincinnatian consist of (Fig. 9, A):

3. Cap of well-laminated silty dolomite with mudcracks and rare burrows; upper surface may be diagenetically mottled and stained
2. Light-colored units of massive to laminated silty dolomite, couplets of dolomitic silt/mud with planar and ripple laminations and abundant glauconite
1. Thin bed (<15 cm) of skeletal wackestone/packstone

2. PACKSTONE/GRAINSTONE CYCLES: These are common in the transgressive portions of the two basal 3rd-order sequences. They consist of (Figure XX):

3. Hardground on dark colored, cherty skeletal packstone grading down into
2. Light colored, coarse skeletal grainstone, rests on irregular surface of
1. Basal hardground on darker colored skeletal packstone, highly burrowed.

3. THICK-GRAINSTONE SHOAL CYCLES: These are common in the bank facies of the Upper Lexington Limestone (Tanglewood Member) over the Jessamine Dome, and in upper parts of smaller 3rd-order cycles. They consist of (Fig. 9, D):

4. Hardground cap commonly on
3. Decimeter to meter thick units of herring-bone cross-bedded coarse skeletal grainstone. Cross strata consist of alternating centimeter thick beds of coarse grainstone and fine dolomitic shale with abundant ramose bryozoans
2. Nodular bedded, dark argillaceous skeletal wackestone/mudstone, with a diverse fossil assemblage
1. Thin-bedded rhythmite of shale and dark laminated calcisiltite (rare)

4. NODULAR CARBONATE CYCLES: In the Lexington Limestone they consist of (Fig. 9, E):

3. Thin coarse skeletal grainstone that is rarely cross-bedded, but may show a rippled top or hardground cap
2. Nodular-bedded units of shaly skeletal packstone/wackestone with open marine biotas; some storm beds are present, but typically burrowed
1. Evenly bedded calcisiltite and shale (rare).

In the Cincinnatian the nodular cycles consist of (Fig. 9,F):

2. Thick units of nodular bedded skeletal packstone with open marine biota
1. Nodular calcisiltite and shale with few fossils.

5. THIN-BEDDED SHALE-LIMESTONE CYCLES: These occur in deeper ramp positions in shale-rich sections and near the base of the large-scale cycles. They consist of (Fig. 9, G):

3. Thin skeletal grainstone or packstone that is rarely tidally cross-bedded
2. Interlayered storm-deposits of graded skeletal packstone/wackestone and up to 50% shale beds. Limestones tend to thin and fine downward with increasing shale content into
1. Evenly bedded calcisiltite and shale (rare). May grade down in symmetrical cycles into shaly wackestone that rests on an underlying thin grainstone cap.

6. RHYTHMITE CYCLES: Rhythmites commonly occur in the bases of the small sequences, rare cyclic units (Fig. 9, F) consist of:

3. Thin grainstone/packstone that varies from massive to laminated grading down into
2. Thick (up to 8 m) units of evenly bedded calcisiltite and shale
1. Interlayered limestone and shale storm beds

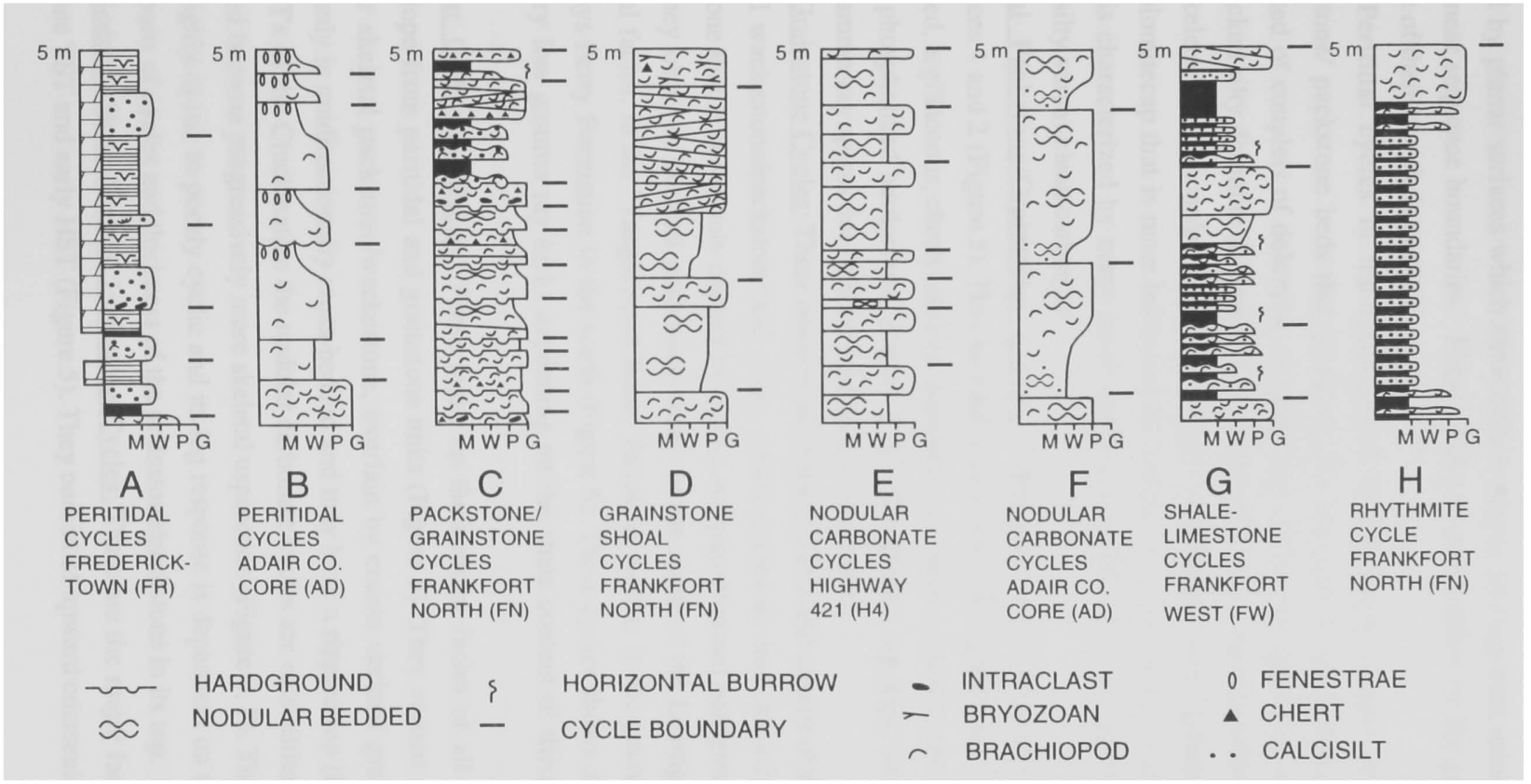

Figure 9. Portions of stratigraphic columns showing representative meter-scale cyclic sections in the Late Mohawkian to Cincinnnatian supersequence. Letters A-H correspond to circled letters on the regional lithologic cross-section (Figure 5) and on the local lithologic cross-section near Frankfort (Figure 7).

capped by planar surfaces which show little evidence of long-term subaerial exposure, except near sequence boundaries. These cycles are not evident on the gamma ray logs because of their low shale content.

Peritidal cycles in the Cincinnatian in the south consist of thin skeletal wackestone/ packstone beds that grade up into massive or laminated silty dolomite, composed of couplets of dolomitic silt and mud, which are capped by well-laminated, mudcracked silty dolomite (Figure 9, B). To the north, Cincinnatian peritidal cycles have shaly skeletal wackestone/packstone lower parts that grade up into sparsely fossiliferous silty dolomitecap that is more burrowed toward the top. Gamma-ray response of these cycles is characterized by many small spikes that reflect the rapid alternation of shaly versus silty versus clean carbonate.

Skeletal Packstone/Grainstone Cycles: These are very common in the TST's of Sequences 1 and 2 (Figure 5). They consist of coarse skeletal grainstone grading up into burrowed, argillaceous, cherty, skeletal packstone and shale capped by an irregular pyritic and/or phosphatized hardground (Figure 9, C). On gamma ray logs, these cycles have large gamma-ray spikes due to shaly interbeds or bentonites.

Thick Grainstone Cycles: These occur in all systems tracts and consist of nodular-bedded skeletal wackestone/packstone and shale, which grades up into cross-bedded skeletal grainstone that is commonly capped by pyritic and phosphatized hardgrounds (Figure 9, D). They occur in skeletal grainstone sheets to the north of the Lexington Limestone peritidal facies, in the "Tanglewood Bank" facies, as well as in the grainstone sheets in the Clays Ferry Formation in the south (Figure 5). These cycles shows alternating high and very low gamma ray kicks depending on the shale content of their muddy lower parts.

Nodular Carbonate Cycles: These make up the nodular facies of all systems tracts downslope from peritidal and grainstone units (Figure 5). They consist of argillaceous nodular skeletal packstone/wackestone, overlain by coarse skeletal grainstone, which commonly is unidirectionally cross-bedded and may have a rippled top (Figure 9, E). In the TST's of the Cincinnatian the nodular carbonate cycles are calcisiltite-rich near their base and become progressively more skeletal uspsection (Figure 9, F). This facies ranges from highly cyclic to poorly cyclic and its log response is dependent on shale content in lower parts of cycles and thickness of the grainstone/packstone in its top.

Thin-Bedded, Shale-Skeletal Limestone Cycles: These are the major facies of the 2nd-order late TST and early HST (Figure 5). They consist of upward coarsening units of thin,

evenly bedded limestone with gray to black shale-partings and interbeds (up to 20 cm thick). Lower parts of cycles are fine grained calcisiltite/minor skeletal packstone/wackestone and interlayered shale; limestone beds thicken-and coarsen upward and "clean-up" into thin skeletal grainstone/packstone caps (Figure 9, G). This facies ranges from highly cyclic to almost non-cyclic, and its gamma-ray signature is highly variable and commonly "spiky" due to subtle changes in shale content.

Rhythmite Cycles: Cycles in the rhythmite facies are rare. These facies are a relatively rare but distinctive component associated with maximum flooding units, and also occurs in deeper protected areas between shoals (Figure 5). They are characterized by thinly, very evenly bedded, alternating layers of calcisiltite and laminated and micrograded black shale; layers within rhythmites commonly are a few centimeters thick. Where cycles are developed, they include relatively large, several meter thick, symmetric cycles of thin grainstone to thin-bedded skeletal limestone to rhythmite to thin-bedded skeletal limestone to skeletal grainstone (Figure 9, H), and also include asymmetric cycles of rhythmite to skeletal wackestone/packstone to grainstone. Burrows are rare, except in the skeletal limestones, and laminations in the rhythmites are well preserved. The gamma-ray log shows very pronounced spikes associated with these cycles, due to abundant calcareous shale, alternating with limestone layers.

INTERPRETATION

Depositional Environments

Water depths for the facies (Figure 4) are conservative estimates modified from the Persian Gulf, a shallow sea in a relatively small, modern-day foreland basin (Purser and Seibold, 1973). These water depth estimates also are compatible with previous water estimates in these and correlative units in the Appalachian Basin (Cressman, 1973; Weir et al., 1984; Kreisa, 1980; Brookfield, 1988; Holland, 1993; Jennette and Pryor, 1993) and are more conservative than proposed water depths for similar facies in Ordovician rocks of New York (Cisne and Hay, Brett, Baird, etc.).

The peritidal limestones and silty dolomites formed in supratidal, intertidal and shallow subtidal conditions based on presence of mudcracks, microbial laminitions, fenestrae, and very restricted ostracodal faunas. The faunally "restricted" wackestone/packstone, with its less diverse biota than more seaward facies; formed in protected lagoons behind banks which became sites for production and accumulation of

lime mud, perhaps from weakly calcified algae, by settling of mud carried in from the surrounding banks and possibly by precipitation, although this is less likely given the non-tropical setting (Matthews, 1966?; Stockman and Ginsburg, 1965?; Read, 1974). Possibly analogous lagoons in Shark Bay are from 2 to 10 m deep (Read, 1974). The abundant limestone in the Lexington peritidal facies, and the dominance of silty dolomites in the Ashlock-Drakes Formations (Figure 2) suggests that the climate changed from relatively humid in the Late Mohawkian to more arid in the Late Cincinnatian (Patzkowsky and Holland, 1993).

Thin to thick skeletal grainstone units which commonly contain tidal and wave formed sedimentary structures, were formed on shallow banks and offbank areas which were re-worked by waves and tidal currents. Local red algae on the banks suggest photic zone water depths of less than 30 m (c.f. Purser and Siebold, 1973), although the bulk of the biota could live below the photic zone. Shallower, tidally-influenced grainstones likely were re-worked in depths of 10 m or less by fairweather waves (Hrabar et al., 1971; Cressman 1973). Given the non-tropical setting for the Lexington Limestone and Clays Ferry-Kope Formations (Holland and Patzkowsky, 1993), the thick grainstone banks and thin grainstone units capping many nodular and shaly limestone cycles could have formed in water depths to 20 m or more, in areas subjected to frequent winter gales in mid-latitudes, or less frequent hurricanes (Logan and Cebulski, 1970; Purser and Siebold, 1973; Brookfield, 1988; Jennette and Pryor, 1993; Lavoie, 1995).

Nodular bedded skeletal wackestone/packstone contain evidence of storm-deposition in the form of graded skeletal beds, storm laminated calcisiltites, and mud caps (Kreisa, 1981; Jennette and Pryor, 1993). Open marine, diverse biotas and abundant mud suggest they formed seaward or in deeper water than grainstone facies, probably between fairweather and storm wave base, but in shallower water than the deep ramp, thin-bedded limestones and shale which occur seaward (downdip). Abundant burrowing, coupled with incipient cementation in nodules, formed the characteristic layering (Mullins and Neumann, 1980). Although swell wave base on temperate shelves can be many tens of meters (Collins, 1988; James et al., 1992), the Ordovician epeiric sea setting would suggest storm wave base of perhaps 30 to 40 meters (Logan and Cebulski, 1974; Purser and Siebold, 1973). The fine sediment may have been produced in place, or carried in from shallower updip areas, to accumulatealong with shells from the resident benthos.

Thin, irregularly bedded skeletal packstone, calcisiltite and shale formed in open ramp settings subject to frequent storm re-working possibly to depths of 30 to 40 m,

below the threshold level for abundant burrowing organisms. In protected areas behind skeletal banks, these facies may have formed at shallower depths (possibly below 10 m). In these storm dominated deep ramp settings, whole and fragmental skeletal debris from the resident benthos, plus fine carbonate from upslope was re-worked by frequent storms to generate the abundant shelly storm beds, and with waning conditions the laminated calcisiltite. Shale interbeds could represent background sedimentation during periods of limited carbonate production or accumulation, or could be related to more humid, millenial-scale climate phases when abundant fine clastics entered the basin from the orogenic highlands to the east and northeast (c.f. Elrick et al., 1991).

Thin evenly-bedded calcisiltite and shale formed at depths below storm wave base, in which numerous distal, storm induced turbidity flows transported calcisilt from the shallow storm influenced ramp to deposit it in anoxic bottom waters on the deep ramp which lacked burrowers (Kreisa, 1981; Aigner, 1985; Jennette and Pryor, 1993). Calcareous silt deposition may have interrupted deposition of background fine siliciclastic shale to form the rhythmically interbedded carbonate-shale beds. However, the rhythmic interlayering of calcareous silt and shale in beds a few centimeters thick appears too regular to be due to random storm events. Instead the storm influx of calcareous silt may have ceased for considerable periods, perhaps during cooler, wetter phases allowing deposition of shale carried in from the orogenic highlands, perhaps in a similar manner to that proposed by Elrick et al. (1991). These alternating calcisiltite and shale beds may represent millenial-scale climate changes. The high gamma ray response of these facies may be due to high uranium content in in the black calcareous shales, which alternate with limestone layers.

The marine Garrard Siltstone formed on the storm re-worked ramp in depths of less than 30 m, where it interfingered with high-energy grainstone shoals. Periodically mobile silty substrates were colonized by bryozoans which were re-worked during storms.

Development of High-Frequency Cycles on the Ordovician Ramp

The meter-scale cycles reflect variable high-frequency relative rise and fall in sea level that repeatedly caused landward and basinward shifts of facies tracts. Separating out whether individual high-frequency cycles are eustatic, tectonic or autocyclic is difficult if not impossible for these rocks.

Ginsburg's (1971) autocyclic model involves tidal flat progradation on a rimmed shelf shutting down the carbonate factory as accomodation space is filled and the subtidal factory narrows. This if followed by startup of the factory as the platform subsides and becomes submerged. Such autocyclic processes could have occurred during deposition of the Perryville Member, Ashlock and Drakes peritidal facies, and perhaps during migration of skeletal shoals over the Jessamine Dome. However, autocyclic processes triggered by tidal flat progradation could not have been the main cause of the cycle formation on the Ordovician ramp because most of the cycles are subtidal (cf. Osleger, 1991). Furthermore, it is difficult to shut down the carbonate factory on ramps, as opposed to Ginsburg's rimmed shelf model, because the carbonate factory moves seaward down the ramp, and thus does not decrease in area (Tucker and Wright, Book 1992). However, each time the ramp shallowed above wave base, wave abrasion or wave sweeping could have been important in keeping the shallow water facies from aggrading into intertidal supratidal environments (c.f. Osleger, 1991). The mosaic-like facies pattern evident in parts of the section, expecially in Sequence 2, strongly suggests that localized shallowing of banks and islands were an important control on cycle development. Such a process suggests a strong autocyclic component.

Thrust-related tectonics has been important in generating long-term accommodation on the ramp, as well as causing uplift along the Cincinnati Arch (Borella and Osborne, 1978; Quinlan and Beaumont, 1984; Tankard, 1989; Ettensohn, 1991). Seismites througout the Late Mohawkian to Cincinnatian succession indicate that the platform was subjected to earthquakes, which may have been associated with jerky subsidence (Pope et al., in press). However, the frequency and occurrence of the seismites shed little light on whether the high-frequency cycles were due to tectonic pulses of subsidence because the seismites are only generated by rare, large events (Obermeier et al., 1991). Given the tectonic setting, it is likely that at least some cycles could record rapid deepening due to pulses of subsidence.

High-frequency eustasy also may have played an important role in cycle formation but this is difficult to prove. The correlatability of these cycles suggest a eustatic origin (Jennette and Pryor, 1993). For example, Kope/Fairview deep ramp cycles in northern Kentucky and Ohio were correlated over a 32 x 35 km area by Jennette and Pryor (1993). Similarly, meter-scale cyles of the Lexington Limestone near Frankfort, Kentucky can be correlated over 10 to 15 km (Figure 7) implying synchronous water depth changes at least over this distance. Average duration of the Late Mohawkian to

Cincinnatian cycles range from 50 to 200 k.y., based on the 9 to 14 m.y. duration for the supersequence, divided by the number of cycles in each section. The estimated average cycle duration of 57 k.y. for Cincinnatian strata (Tobin, 1982) falls within this range. Spectral analysis of the Kentucky Ordovician lithologic logs (in which each facies was assigned a water depth rank; Olsen, 1985) and the gamma ray logs (which mainly are sensitive to shale content) was done to define any dominant cycle thicknesses. These thicknesses can then be converted to duration, by using a calculated accumulation rate for each section. The spectra contain numerous peaks. Some of these cycles appear to fall on Milankovitch frequencies, but many do not (Pope et al., in prep). In almost all sections, a precessional signal is not evident, the dominant peaks being in the long and short term eccentricity range (100 to 400 k.y), and longer term (1 to 4 m.y.) peaks probably marking the depositional sequences. Only in the Martinsburg Formation downdip in Virginia were periods in the range of precession. The relatively poor preservation of a higher frequency precessional signal in these rocks may be partly due to interplay of autocyclic and allogenic processes (Golhammer et al., 1993).

Cycles that formed in distal portions on the ramp are critical to understanding the origin of the high-frequency cycles. Here cycles are of calcisiltite-shale rhythmite (probable water depths of 20 to 40 m or more) up into thin-bedded shaly skeletal limestone beds up into thin caps of shallow water, high-energy, grainstone and rare fenestral lime mudstone; the shoaling transformation occurring in 1 to 5 m of stratigraphic thickness. Little of this shallowing could have been due to sedimentation which would only have filled a few meters of accommodation space because of the low sedimentation rates (2 to 3 cm/k.y.). Water depths of rhythmites in protected interbank depressions could be as little as 20 m, but could be below 40 m in open marine settings below storm-wave base (Read, 1980 ; Purser and Siebold, 1973). Thus, these cycles imply a probable sea-level induced lowering of wave-base of 15 to 40 m or so. Given the common 10^4 to 10^5 year duration of the cycles, this implies high-frequency 4th-order eustatic changes of moderate-magnitude (10 to 30 m) formed of some of the meter-scale cycles.

Thick grainstone capped cycles over the Tanglewood Bank were formed by rapid deepening to sub-fair weather wave base to form nodular skeletal wackestone/packstone and shale, followed by shallowing during relative sea level fall to form the thick cross-bedded grainstone cycle caps. Although some of these cycles may be autocyclic and due to shifting of the locus of shallow bank deposition, most require rapid relative sea level

rise (induced by rapid subsidence or high-frequency sea level rise), but they also require subequent sea level fall, because an individual cycle is too thin to bring the seafloor from below wave base into the zone of high-energy tidal and wave agitation, and would appear to require 10 m or more of relative sea level fall. The inferred 4th-order relative sea level changes of 10 to 40 m caused considerable compartmentalization of the Tanglewood Bank grainstone facies, which are separated vertically by interbedded muddy units. This stacking contrasts with buildups in the earlier Ordovician which show little intercalation of deep water facies once the banks were established (Read, 1980, 1982; Ross et al., 1991).

Grainstone/packstone cycles of the transgressive Curdsville Member and post-Perryville "upper" Lexington Limestone also require high-frequency sea level change. These thin grainstone sheets were laid down as transgressive high-energy, skeletal sheets on the wave-or-tide swept inner ramp (c.f. Osleger, 1991) during overall 3rd-order transgression. Superimposed high-frequency relative sea level rises drowned the grainstones, covering them beneath thin skeletal wackestone/packstone capped by phosphate-pyrite hardgrounds as water depths increased leading to sediment starvation. These cycles could not be due just to jerky subsidence, because many of these cycles are less than a meter thick, and this would be insufficient to bring the seafloor from a deep-water, sediment-starved surfaces up to shallow, wave-agitated depths of a few meters. These hardground-bounded cycles resemble Cenozoic high-energy, inner-shelf cool water carbonate cycles of southwestern and southern Australia (Collins, 1988; James and Bone, 1994).

Since high-frequency, large sea level oscillations (>20 m) cannot be driven solely by changes in global groundwater or lake volumes, or heating/cooling of global sea temperatures (Jacobs and Sahagian, 1993), it is suggested that many of the Late Mohawkian to Cincinnatian meter-scale cycles formed by a glacio-eustasy. If so, then incipient Gondwana glaciation in the Ordovician may have begun by 454 Ma and lasted up to 14 m.y. as postulated by Frakes et al. (1992), peaking in the Hirnantian for less than 2 m.y. (Brenchley et al., 1994).

The peritidal facies on the Ordovician ramp commonly are poorly cyclic. The relatively poor cyclicity in the restricted wackestone/packstone and fenestral/laminated carbonates could be due to presence of considerable topography (either tectonic or depositional) on the Cincinnati Arch and between the skeletal shoals, coupled with moderate amplitude eustasy. This would be analogous to Shark Bay, western Australia

where toward the end of the last glacial rise marine flooding of interdune depressions formed locally deep lagoons, which were filled by a single Holocene marine cycle up to 6 m thick, dominated by thick lime wackestone/mudstone capped by thin lime sands and capping fenestral limestone (Read, 1974). Filling in of any pre-existing topography on the Ordovician inner ramp may have formed an aggraded top lying at or near the position of the 4th-order highstands. Consequently, subsequent marine flooding formed only shallow water depths on the inner ramp, even if absolute changes of sea level were tens of meters, ans son only restricted facies were deposited in lower parts of cycles. Such aggraded inner ramp conditions may account for the meter-scale cycles in the "upper" Lexington and in the Ashlock and Drakes Formations (Figures 5 and 9). However, if 4th-order sea level changes of a few tens of meters were involved in cycle formation, then updip peritidal settings should have felt the full effect of eustatic sea level fall. Limited evidence of such pronounced sea level falls and prolonged emergence in the peritidal units suggests that sea level fluctuations during 3rd-order late highstands were relatively small compared with 3rd-order transgressive phases. Alternately, peritidal successions such as the Perryville Member of the Lexington Limestone, which is capped by a karst surface, may have formed by offlap of tidal flat cycles, to form a composite karst surface due to updip pinchout of offlapping peritidal cycles. Nevertheless, high-frequency sea level changes would have to be small, in order to not expose peritidal cycles downdip.

Development of the Lowstand Systems Tracts

The lowstand clastics at the base of the supersequence in the foreland basin in Virginia and Tennessee developed during emergence of the High Bridge Group on the Cincinnati Arch in Kentucky. In the foreland basin, high clastic sediment influx from the tectonic highlands to the south and east, coupled with relative sea level fall caused filling of the subsiding foredeep, and allowed deposition of deltaic and coastal plain redbeds over earlier basinal and shallow marine limestones. The thickness of the redbeds may have been influenced by the underlying Tazewell Arch (Read, 1980), which was active during deposition of the underying supersequence. This arch localized strike parallel transport of clastics to the northeast once the foredeep had filled to the south in Tennessee. Correlation of bentonites near the basal unconformity on the Cincinnati Arch and above the sequence boundary beneath the Walker Mountain conglomerate in Virginia indicate that the development of the unconformity was not synchronous (Goggin and Haynes, 1995), suggesting tectonic warping during eustatic fall.

In Kentucky, lowstand systems tracts make up a small portion of the sequences. In the basin, the lowstand units have a well defined blocky, low gamma ray response above much higher gamma ray values which reflects "cleaning" upsection within the LST.

The Sequence 2 LST formed during subaerial exposure and karsting on top of the Perryville Member updip, meanwhile lowstand skeletal sheets developed downdip over what were originally deep ramp facies to form the foundation for the Tanglewood Bank.

The Garrard Siltstone, the lowstand to sequence 3, is underlain by a conformable sequence boundary in outcrops and cores; any updip unconformity probably lies far to the south or east outside the study area. The restriction of the Garrard Siltstone to the southeastern side of the Cincinnati Arch, suggests its distribution is structurally controlled (Weir et al., 1984; Jacobs, 1986). It prograded from south to north but its source is not known. During widespread lowstand storm- and current- deposition of fine marine siliciclastic silts limited shallow water carbonate deposition to local skeletal sand banks and small bryozoan mounds.

Transgressive Systems Tract Development

TST's within the Ordovician succession commonly make up less than 25 % of a sequence. This reflects rapid flooding of the ramp during relative sea level rise, perhaps coupled with low sedimentation rate due to high turbidity and cool water. Coarse grainstone units in the TST's backstep because accomodation rate exceeded sedimentation rate. The TST of the grainstone-dominated Curdsville Member in Sequence 1, and the TST at the base of Sequence 2 strongly resemble wave swept, shallow inner-shelf units in cool water temperature settings (Collins, 1988; James et al., 1992; Boreen and James, 1994). Superimposed high-frequency relative sea level changes generated the grainy, each cycle becomes muddy upward, and was capped by hardgrounds formed during high-frequency drowning events which lead to sediment starvation. Sedimentation only resumed when sea level fell during the next high-frequency lowstand.

The Tanglewood bank lies in the TST of the 2nd-order Ordovician supersequence. Buildups are absent from the 3rd-order HST's, which have only thin, grainstone or biohermal (coral/stromatoporoid) development. The location of carbonate buildups within 2nd-order TST's (Greenlee and Lehman, 1993) reflect high rates of accomodation relative

to regional shelf sedimentation versus local high sedimentation rates by buildup assemblages.

The upward increase in shale content and increasing deposition of fine siliciclastics along with carbonates on the deep ramp in the 3rd-order TST's is due to upward deepening. The upward increase in gamma-ray values in the TST's reflects this upward increase in shale. Parasequences in TST's include both shallowing-upward or deepening-upward types. They show both increasing gamma-ray values as shale content increases, and decreasing gamma-ray values where the parasequences are limier upsection.

The lack of tidal flat facies in the TST's could be due the development of high-energy grainy shorelines, rather than tidal flat-lagoon complexes during transgression. However, unequivocal beach facies have not been identified, suggesting that relatively open shelf water depths were quickly established early in the transgression, which limited the shallowest facies in the TST's to open shelf grainstone sheets.

Maximum Flooding Surfaces Development

Maximum flooding of the 2nd- and 3rd-order sequences clearly lies within the tongues of shaly, nodular or thin-bedded deep ramp facies that extend farthest onto the shallow ramp. However, picking a discrete MFS is difficult in outcrops or cores, but commonly is more evident on the gamma ray logs because of the high values produced by high shale or organic content. The MFS was produced by highest accomodation rate, due to high rate of sea level rise, coupled with maximum load-induced subsidence. The maximum flooding surfaces show little evidence of condensed intervals, or being surfaces onto which HST strata downlap, because the relatively constant sedimentation rates across ramps inhibits development of a starved ramp slope. These uniform sedimentation rates across the ramp are due to input of sediment from the shallow ramp, as well as input of fine siliciclastics from the basinward margin toward it's orogenic highlands. The most clearly defined flooding surface in the Cincinnati Arch area is the 3rd-order MFS in Sequence 1 (the Logana Member of the Lexington Limestone) (Figure 5). This flooding event is traceable within the entire outcrop area, except for a small area near Madison County where the skeletal-rich facies of the Grier Member directly overlie Curdsville Member. The other flooding zones, whether defined on the basis of lithology or gamma ray logs do not appear to be confined to a single clearly recognizable stratigraphic horizon. This may be due to the presence of depositional topography along the arch, as a

reult of localized depositional upbuilding and tectonic warping. Maximum flooding events probably decreased sedimentation rate by increasing water depths, which brought the ramp into cooler, deeper more turbid waters, reducing carbonate production.

Highstand Systems Tract Development

HST's are well developed on the Ordovician ramp. Early HST's over much of the ramp were characterized by thin-bedded, shaly skeletal limestone and nodular limestones and shale, which reflect incipient drowning of the ramp. The shallowing-upward trend in the HST's from thin-bedded or nodular shaly limestone, up into skeletal grainstone/packstone, restricted skeletal wackestone/packstone, and peritidal limestone or silty dolomite, reflects decreasing accomodation and relative high sedimentation rates. The presence of corals, abundant dolomite, and more abundant fenestral lime mud in the HST's, suggest these may have developed under slightly warmer conditions than the TST's. Climatic warming might also have increased sedimentation rate, further promoting rapid progradation of the ramp.

Skeletal grainstone units in the HST's, are mainly skeletal grainstone sheets a few meters thick and from 50 to 150 km wide. These reflect limited accomodation, and frequent incipient drowning of sheet banks by deeper water limestone and shale. Peritidal facies of the HST's formed belts over 300 km wide. These highly aggraded ramps passed updip into sequence- bounding unconformities, (top of the Perryville, Sequence 1, and the Ordovician-Silurian unconformity, top of sequence 4). Sequence 2 developed during relatively greater accomodation, thus the study area only sampled the relatively downdip parts of the ramp at this time.

Sequence Boundary Development

The supersequence boundary on the High Bridge Group in Kentucky is a small-scale karst surface on top of iron-stained, muddy peritidal facies, suggesting that it formed under meteoric diagenetic conditions in a humid climate. Further to the east, in Virginia, the supersequence boundary was an erosional surface below quartz sandstone and conglomerate facies (Goggin and Haynes, 1995). Similarly, the sequence boundary on top of the Perryville Member (top of Sequence 1) also is an irregular karstic surface with small (< 10 cm diameter) vugs formed under a wet climate. The vugs were infiltrated by phosphatic sand during the subsequent transgression.

The sequence boundary below the Garrard Siltstone (top of Sequence 2) is a conformable contact above which marine siltstone were deposited in their most basinward position (Figure 5). The updip part of the the ramp is not exposed in the study area, but probably lies far to the south or east.

The sequence boundary on top of the Tate Member dolomite (top of Sequence 3) is a highly irregular, low-relief surface capped by a shaly residuum. The silty dolomite below the sequence boundary contains abundant sub-vertical, spar filled fenestrae that show intense diagenetic color-mottling, that may have been produced by meteoric diagenesis.

The Ordovician-Silurian unconformity, which caps the supersequence, has large scale erosion with up to 60 m of erosional truncation. Updip bevelling of dolomites of Sequence 4, and angular discordance between Ordovician and Silurian strata reflect slower subsidence and deeper erosion to the south, possibly coupled with angular down-to-basin rotation of the Ordovician ramp prior to Silurian transgression. The lack of karsting along this unconformity suggests it formed under a more arid climate.

Tectonic Controls on Sequence Development

Tectonics, particularly thrust-induced subsidence/uplift exerted a strong control on thicknesses, facies and sequence development of the Middle to Late Ordovician units in the Appalachian foreland.

Flemings and Jordan (1989, 1991) and Jordan and Flemings (1992) used modelling studies to examine the effects of thrust-loading, subsidence and eustasy in foreland basin settings. Incremental loading of continental lithosphere, which probably occurs at rates of up to 10's of mm's/year for durations of many millions of years, will not produce instantaneous massive subsidence (Jordan and Flemings, 1991; Flemings and Jordan, 1990), but will cause gradual increase in thrust-induced subsidence, that will slowly decrease as thrusting slows or halts. After thrusting stops, nearshore clastics that were previously ponded along the active margin during thrusting, should prograde and fill the foredeep. Progradation might be further enhanced by erosional removal of a part of the load which will cause istostatic uplift of the thrust belt, and the proximal part of the basin (Quinlan and Beaumont, 1984; Ettensohn, 1991).

The Knox unconformity, which marks the change from Cambrian to Early Ordovician passive margin to later Ordovician foreland basin sedimentation was produced by thrust-loading in conjunction with a global drop in sea level (Mussman and

Read, 1986; Lash, 1985; Jacobi, 1981). Initial collision and subsidence of the leading edge of the plate produced broad uplift along the previously passive margin, which allowed falling sea level to expose much of the Cambro-Ordovician Knox platform, except in areas such as the Pennsylvania depocenter where subsidence was relatively high (Read, 1980; 1989). Onset of major Blountian thrusting then caused rapid downwarping of the margin to form a narrow, deep foreland basin in which Chazyan to Blackriveran Middle Ordovician limestone (the supersequence beneath the Mohawkian to Cincinnatian supersequence described here) were deposited. Throughout Kentucky and westernmost Virginia, carbonate depostion during this phase was mainly peritidal facies in Kentucky, while more open marine facies developed peripheral to the foreland basin in Virginia.

As thrusting halted, the southern basin filled and lowstand clastics of Sequence 1 (Bays-Moccasin Formations) were deposited along the eastern margin of the southern basin. The unconformity below the Walker Mountain Sandstone of the Bays and Moccasin Formations in southwest Virginia (lowstand of Sequence 1) is a local unit that dies out westward into the basin, and likely was produced by local deformation along the eastern basin margin (Goggin and Haynes, 1995). If Hayne's (1994) and Goggin and Hayne's (1995) correlation of the Diecke and Millbrig bentonites are correct, the Walker Mountain Sandstone unconformity occurs slightly earlier than the post-High Bridge unconformity on the Arch, as the unconformities in the two areas appear to cross the bentonitic markers.

The Late Mohawkian to Cincinnatian supersequence described here formed during the second (Taconic) phase of thrusting. This caused major subsidence in the northern foreland basin (Martinsburg Basin) in the Franklinian-Edenian. Thrust- and sediment-induced loading extended far out into the foreland from the earlier basin, causing widespread subsidence throughout Kentucky, culminating in maximum flooding by Edenian time (Clays Ferry/Kope deposition). Slowing or cessation of Taconic thrusting decreased subsidence, allowing the basin and adjacent foreland to fill, resulting in sweeping progradation of Juniata and Tuscarora clastics across the foredeep and onto the foreland. This was followed by widespread development of the Late Ordovician-Silurian unconformity during Late Ordovician glacial draw down and possible uplift (Diecchio, 1991; Dorsch et al., 1994; Dorsch and Driese, 1995).

Several features suggest the Cincinnatian Arch was a positive feature that resisted subsidence during Late Mohawkian to Cincinnatian time (Cressman, 1973; Borella and Osborne, 1978; Ettensohn, 1992). The erosional relief of the post-High Bridge

unconformity appears to be localized over the Cincinnati Arch (Cressman, 1973). The regional Millbrig bentonite is eroded over much of the Jessamine Dome on the Arch, being preserved only in small structural lows (Haynes, 1994). Also, the subsequent Lexington Limestone shallow water facies are localized over the Arch passing west, north and east into deeper water facies (Hrabar et al., 1971; Mackey, 1972; Cressman, 1973; Ettensohn, 1992). During "upper" Lexington Limestone deposition, structurally-controlled troughs across the arch localized shaly, deep water facies (e.g., Brannon Member; Cressman, 1973; Kulp, 1995).

The Cincinnati Arch appears to have persisted as a positive feature into the Cincinnatian because it appears to have localized deposition of the Garrard Siltstone along its southeast side (Weir et al., 1984; Jacobs, 1986). Furthermore, seismically-induced liquefaction features or seismites (Pope et al, in press) occur in several horizons over the arch in several horizons from the Lexington Limestone up through the Fairview Formation, indicating periodic large quakes in the region of the arch.

It has been suggested that the Cincinnati Arch/Jessamine Dome was a peripheral bulge resulting from Taconic thrusting, coupled with subsidence in the Appalachian and Illinois Basins (Sebree Trough) (Quinlan and Beaumont, 1984). However, other bulges appear to have been active at this time and were localized further east; they include the Tazewell Arch (Read, 1980), the more westerly "Tazewell-Adirondack" axis (Diecchio, 1993). The complex regional development of arches suggests that a simple flexural beam model is too simplistic to explain the foreland tectonics in this basin. Nevertheless, the evidence for the the arch resisting subsidence during the Mohawkian to Cincinnatian and the drowning of the arch during Clays Ferry-Kope (Edenian) time suggests that thrusting may have been active until the Edenian but gradually slowed into the latest Ordovician.

Eustatic Controls on Sequence Development

A third-order relative sea level curve (Figure 10) was constructed from the sequence stratigraphy, the chronostratigraphic position of sequence boundaries and maximum flooding surfaces, relative water depths and landward versus basinward shift in facies. Biostratigraphic control is from conodont-based studies of Sweet and Bergstrom (1966) and Sweet (1979).

The Kentucky curve shows a long term 2nd-order relative sea level rise and fall from the disconformity at the base of the Lexington Limestone to the top of the Cincinnatian with 11 smaller rise and falls, corresponding to the parasequence sets,

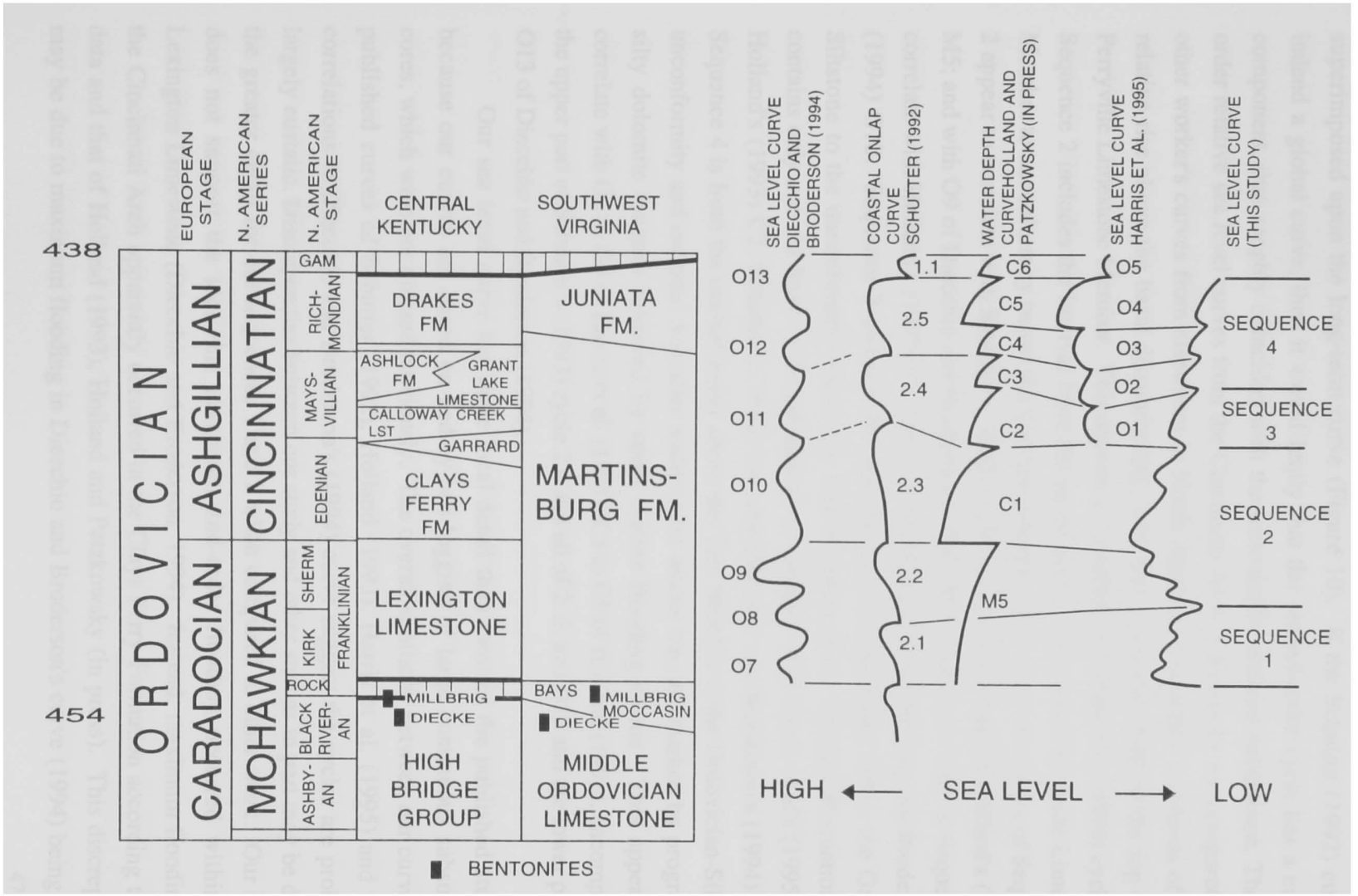

Figure 10. Relative sea level curves from the Late Mohawkian to Cincinnatian supersequence around the United States.

superimposed upon the long-term curve (Figure 10). If the Schutter (1992) curve is indeed a global curve, then it would imply that the second-order cycle has a eustatic component, that roughly coincided with the tectonically induced subsidence. The 3rd-order relative sea level curves from the Cincinnati Arch in Kentucky are compared with other worker's curves from elsewhere in North America. Sequence 1 consists of rapid relative rise above the basal disconformity, with three step-wise falls to the top of the Perryville Limestone Member. This appears to correlate with Schutter's (1993) cycle 2.1. Sequence 2 includes the interval from the unconformity above the Perryville Limestone Member to unconformity below the Garrard Siltstone. The lower two cycles of Sequence 2 appear to correlate with Schutter's (1992) cycle 2.2, the upper half of Holland's (1993) M5; and with O9 of Diecchio and Broderson (1994). The upper two cycles in Sequence 2 correlate with Holland's (1993) C1, Schutter's (1992) 2.3, and Diecchio and Broderson's (1994) O10. Sequence 3 includes the interval from unconformity below the Garrard Siltstone to the unconformity above the Tate Member of the Ashlock Formation and contains only one sea level cycle and appears to correlate with Harris et al's (1995) O1, Holland's (1993) C2, Schutter's (1992) 2.4, and Diecchio and Broderson's (1994) O11. Sequence 4 is from the unconformity above the Tate Member to the Ordovician-Silurian unconformity and includes 3 smaller scale cycles whose tops are marked by prograding silty dolomite tongues followed by small marine flooding events. This appears to correlate with O2 to O4 of Harris et al. (1995), C3 to C5 of Holland (1993), encompasses the upper part of Schutter's (1993) cycle 2.4 and all of 2. 5, and O12 and the lower part of O13 of Diecchio and Broderson (1994).

Our sea level curve has more local detail than most of the published studies, because our curves are based on bed-by-bed logging of large continuous subsurface cores, which were not utilized previously. The overall similarity between our curve and published curves of Schutter (1992), Holland (1993), Harris et al. (1995) and some correlations to Diecchio and Broderson's (1994) curve suggest the cycles are probably largely eustatic. Discrepancies between our study and other studies in part may be due to the greater detail for our sequences 1 and 2 when compared to other work. Our study does not support the idea that maximum 2nd-order flooding occurred within the Lexington Limestone (Diecchio and Broderson, 1994). Instead, maximum flooding on the Cincinnati Arch apparently occurred in the Clays Ferry Formation according to our data and that of Holland (1993), Holland and Patzkowsky (in press). This discrepancy may be due to maximum flooding in Diecchio and Broderson's curve (1994) being from

the deep Martinsburg Basin to the north, where flooding probably occurred earlier than on the shallower Cincinnati Arch. Our data does not support the idea that the flooding event during C5, is of greater magnitude than similar events in C3 and C4 transgressions (Holland, 1993).

The similar character of the sea level curves, suggests that the 3rd-order cycles may be, at least in part eustatically driven. Again, the similarity of the 3rd-order curves to Schutter's (1993) curve, if this is indeed global, would strengthen the argument that the 3rd-order cycles are indeed eustatic.

Evidence for Climate and Seawater Temperature Changes During Sequence Development

The climate during deposition of the Late Mohawkian to Cincinnatian supersequence appears to have gone from humid to slightly more semi-arid. This is indicated by the presence of peritidal fenestral lime mudstone with karstic caps in the TST of the 2nd-order supersequence (indicating a relatively humid climate) in comparison to the silty dolomitic peritidal facies of the 2nd-order HST, which suggest slightly more arid conditions favorable for tidal flat dolomitization. However, there is little evidence that conditions ever were sufficiently arid for gypsum or anhydrite deposition.

The systems tracts suggest that seawater temperatures may have changed during deposition of each 3rd-order sequence. TST's are marked by coarse grained skeletal grainstones with abundant phosphatic and pyritic hardgrounds; these together with the lack of lime mud, and absence of warm water faunas, such as corals, green algae or stromatoporoids, all suggest waters during development of TST's were cool. Conversely, HST's show an increase in lime mud, and more abundant corals and stromatoporoids which suggest that surface waters were warmer during these times. It is not clear whether the apparent cooler waters of the TST's vs the HST's reflect a cool to warm change during 3rd-order sequence development, or merely reflect a stratified water mass with cooler bottom waters flooding the ramp during TST's, while updip warmer surface waters dominated shallow nearshore areas (Martindale and Boreen, 1995). To answer this would require a much larger transect of the ramp so that all the coeval facies of each systems tract were exposed.

There is some evidence that the magnitude of high-frequency sea level changes could have been influenced by warming into the HST's. This would allow LST's and TST's to form during times when sea level changes were large (perhaps due to more ice at

the poles), while during the HST, warmer conditions resulted in lower amplitude changes. This might help explain why there is only limited karsting of peritidal cycles in the HST's and intercalated deeper water facies are absent from downdip occurrences of peritidal facies.

CONCLUSIONS

1. Late Middle to Late Ordovician rocks of Kentucky and Virginia are a 2nd-order supersequence extending from the base of the Lexington Limestone to the Ordovician-Silurian unconformity. It ranges from 250 to 500 m thick, and has a duration of from 9 to 14 m.y.

2. Four well-defined 3rd-order sequences, 40 to 80 m thick, each ~3 to 6 m.y. duration, occur within the 2nd-order supersequence. Lowstands in the proximal parts of the foreland basin include redbeds and coarse clastics. On the foreland in Kentucky, lowstands are high-energy grainstone sheets or marine siltstones that extend into deep ramp settings. TST's are characterized by high-energy cyclic units of grainstone or nodular skeletal wackestone/ packstone. HST's are characterized by aggraded high-energy grainstone facies or prograded peritidal facies . The large 3rd-order sequences are composite sequences composed of smaller-scale parasequence sets made up of bundles of upward-shallowing meter-scale cycles. These are marked by regionally correlative flooding surfaces, and HST's dominated by shallow water facies.

3. High-frequency, 4th- and 5th-order cycles that are 1 to 8 m thick and perhaps 50 to 130 k.y. duration, are bundled into the smaller-scale 3rd-order cycles. The facies making up these cycles reflect their position on the ramp, the amount of accommodation available, and the amount of any high-frequency sea level fluctuations which may have been several tens of meters at times (possibly up to 40 m for some).

4. The Tanglewood Bank, a large buildup that developed during the 2nd-order TST, shows a great deal of compartmentalization of grain-rich units by muddy units. This may be indicative of moderate amplitude eustatic fluctuations which influenced parasequence development and clearly would control any potential reservoir characteristics of analogous facies in the geologic record.

5. The complex sequences and component meter-scale cycles, and rapid vertical and lateral facies changes resulted from deposition on a "cooler" water ramp under the

influence of foreland basin thrust-related tectonics, and 3rd- to 5th-order glacio-eustasy, possibly related to Gondwana glaciation during a time of high global CO_2.

6. Both climate and seawater temperatures appear to have varied during sequence development.

REFERENCES

Aigner, T., 1985, Storm Depositional Systems: Lecture notes in Earth Sciences, v. 3, Springer-Verlag, Berlin, 174 p.

Bergstrom, S.M., and Sweet, W.C., 1966, Conodonts from the Lexington Limestone (Middle Ordovician) of Kentucky and its lateral equivalents in Ohio and Indiana: Bulletin of American Paleontology, v. 50, p. 271-441.

Berner, R.A., 1990, Atmospheric carbon dioxide levels over Phaneozoic time: Science, v. 249, p. 1382-1386.

Berner, R.A., 1992, Palaeo-CO_2 and climate: Nature, v. 358, p. 114.

Boreen , T., James, N.P., Wilson, C., and Heggie, D.,.1993, Surficial cool-water carbonate sediments on the Otway continental margin, southeastern Australia: Marine Geology, v. 112, p. 35-56.

Boreen, T.D., and James, N.P., 1994, Stratigraphic sedimentology of Tertiary cool-water limestones, SE Australia: Journal of Sedimentary Reasearch, Section B, Stratigraphy and Global Studies, v. 65, p. 142-159.

Borella P.E., and Osborne, R.H., 1978, Late Middle and early Late Ordovician history of the Cincinnati arch Province, central Kentucky to central Tennessee: Geological Society of America Bulletin, v. 89, p. 1559-1573.

Brenchley, P.J., Marshall, J.D., Carden, G.A.F., Robertson, D.B.R., Meidla, T., Hints, L., and Anderson, T.F., 1994, Bathymetric and isotopic evidence for short-lived Late Ordovician glaciation in a greenhouse period: Geology, v. 22, p. 295-298.

Brookfield, M.E., 1988, A mid-Ordovician temperate carbonate shelf-The Black River and Trenton Limestone Groups of southern Ontario, Canada: Sedimentary Geology, v. 60, p. 137-154.

Caputo, M.V., and Crowell, J.C., 1985, Migration of glacial centers across Gondwana during Paleozoic Era: Geological Society of America Bulletin, v. 96, p. 1020-1036.

Cisne, J.L., Karig, D.E., Rabe, B.D., and Hay, B.J., 1982, Topography and tectonics of the Taconic outer trench shelf slope as revealed through gradient analysis of fossil assemblages: Lethaia, v. 15, p. 230-246.

Cressman, E.R., 1973, Lithostratigraphy and depositional environments of the Lexington Limestone (Ordovician) of central Kentucky: United States Geological Survey Professional Paper 768, 61 p.

Collins, L.B., 1988, Sediments and history of the Rottnest Shelf, southwest Australia: a swell-dominated, non-tropical carbonate margin: Sedimentary Geology, v. 60, p. 15-49.

Compston, W. and I.S. Williams, 1992, Ion probe ages for the British Ordovician and Silurian Stratotypes: *in* B.D. Webby, and J.R. Laurie, eds., Global Perspectives on Ordovician Geology: A.A. Balkema, Rotterdam, p. 59-68.

Crowley, T.J., and Baum, S.K., 1991, Toward reconciliation of Late Ordovician (~440 Ma) glaciation with very high CO_2 levels: Journal of Geophysical Research, v. 96, p. 22,597-22,610.

Diecchio, R.H., 1991, Taconian sedimentary basins in the Appalachians: *in* Barnes, C.R., and Williams, S.H., eds., Advances in Ordovician geology: Geological Survey of Canada, Paper 90-9, p. 225-234.

Diecchio, R.J., 1993, Stratigraphic interpretation of the Ordovician of the Appalachian Basin and implications for Taconian flexural modeling: Tectonics, v. 12, p. 1410-1419.

Diecchio, R. and Broderson, B.T., 1994, Recognition of regional (eustatic?) and local (tectonic) relative sea-level events in outcrop and gamma-ray logs, Ordovician, West Virginia: *in* Dennison, J., and Ettensohn, F. R., eds., Tectonic and eustatic controls on sedimentary cycles: SEPM Concepts in sedimentology and paleontology, v. 4, p. 170-180.

Dorsch, J., Bambach, R.K., and Driese, S.G., 1994, Basin-rebound origin for the "Tuscarora unconformity" in southwestern Virginia and its bearing on the nature of the Taconic orogeny: American Journal of Science, v. 294, p. 237-255.

Dorsch, J., and Driese, S.G., 1995, The Taconic foredeep as sediment sink and sediment exporter: Implications for the origin of the White quartzarenite blanket (Upper Ordovician-Silurian) of the central and southern Appalachians: American Journal of Science, v. 295, p. 201-243.

Elrick, M., Read, J.F., and Coruh, C., 1991, Short-term paleoclimatic fluctuations expressed in lower Mississippian ramp-slope deposits, southwestern Montana: Geology, v. 19, p. 799-802.

Ettensohn, F.R., 1991, Flexural interpretation of relationships between Ordovician tectonism and stratigraphic sequences, central and southern Appalachians, U.S.A.: *in* Barnes, C.R., and Williams, S.H., eds., Advances in Ordovician geology: Geological Survey of Canada Paper 90-9, p. 213-224.

Ettensohn, F.R. (ed.), 1992, Changing interpretations of Kentucky geology--layer-cake, facies, flexure, and eustacy: State of Ohio, Department of Natural Resources, Miscellaneous Report No. 5, 184 p.

Ettensohn, F.C., Pashin, J.C., and Jacobs, G.W., 1986, Characteristics of shallow-water, marine shelf silts and sands: Two Paleozoic examples from eastern Kentucky: Appalachian Basin Industrial Associates, v. 10, p. 197-211.

Flemings, P.B., and Jordan, T.E., 1990, Stratigraphic modeling of foreland basins: Interpreting thrust deformation and lithosphere rheology: Geology, v. 18, p. 430-434.

Flemings, P.B., and Jordan, T.E., 1989, A synthetic stratigraphic model of foreland basin development: Journal of Geophysical Research, v. 94, p. 3851-3866.

Frakes, L.A., Francis, J.E., and Syktus, J.I., 1992, Climatic modes of the Phanerozoic: Cambridge University Press, Cambridge, UK, 274 p.

Ginsburg, R.N., 1971, Landward movement of carbonate mud: a new model for regressive cycles in carbonates: American Association of Petroleum Geologists Bulletin, v. 55, p. 340.

Goggin, K.E., and Haynes, J.T., 1995, Mohawkian clastic wedges in the central and southern Appalachians: early signatures of the Taconic orogeny: Geological Society of America, Southeastern Section, Abstracts with Programs, v. 27, p. 56-57.

Goldhammer, R.K., Lehmann, P.J., and Dunn, P.A., 1993, The origin of high-frequency platform carbonate cycles and third-order sequences (Lower Ordovician El Paso Gp, west Texas): constraints from outcrop data and stratigraphic modeling: Journal of Sedimentary Petrology, v. 63, p. 318-359.

Greenlee, S.M., and Lehman, P.J., 1993, Stratigraphic framework of productive carbonate buildups: *in* Loucks, R.G., and Sarg, J.F., (eds), Carbonate Sequence Stratigraphy, American Association of Petroleum Geologists Memoir 57, Tulsa, p. 43-62.

Hambrey, M.J., 1985, The Late Ordovician-Early Silurian glacial period: Palaeogeography, Palaeoclimatology, Palaeoecology, v. 51, p. 273-289.

Harris, M.T., Sexton, L.A., and Sheehan, P.M., 1995, Depositional facies and sequences of Upper Ordovician shelf and shallow ramp carbonates of the eastern Great Basin (Utah and Nevada), U.S.A.: *in* Cooper, J.D., Droser, M.L., and Finney, S.C., (eds), Ordovician Odyssey, Short papers for the seventh international symposium on the Ordovician system, Pacific Section Society of Paleontologists and Mineralogists, Fullerton, p. 265-266.

Haq, B.U., Hardenbol, J., and Vail, P.R., 1987, Chronology of fluctuating sea level since the Triassic: Science, v. 235, p. 1156-1167.

Harland, W.B., Armstrong, R.L., Cox, A.V., Craig, L.E., Smith, A.G., and Smith, D.G1990, A geologic time scale, 1989: Cambridge University Press, Cambridge, UK, 261 p.

Hay, B.J., and Cisne, J.L., 1988, Deposition in the oxygen-deficient Taconic foreland basin, Late Ordovician: in B.D. Keith (ed.), The Trenton Group (Upper Ordovician Series) of eastern North America, American Association of Petroleum Geologists, Tulsa, OK, Studies in Geology #29, p. 113-134.

Haynes, J.T., 1994, The Ordovician Deicke and Millbrig K-Bentonite beds of the Cincinnati Arch and the southern Valley and Ridge Province: Geological Society of America Special Paper 290, 80 p.

Holland, S.M., 1993, Sequence stratigraphy of a carbonate-clastic ramp: The Cincinnatian Series (Upper Ordovician) in its type area: Geological Society of America Bulletin, v. 105, p. 306-322.

Hrabar, S.V., Cressman, E.R., and P.E. Potter, 1971, Crossbedding of the Tanglewood Limestone Member of the Lexington Limestone (Ordovician) of the Blue Grass region of Kentucky: Brigham Young University Geology Studies, v. 18, p. 99-114.

Huff, W.D., Bergstrom, S.M., and Kolata, D.R., 1992, Gigantic Ordovician volcanic ash fall in North America and Europe: Biological, tectonomagmatic, and event-stratigraphic significance: Geology, v. 20, p. 875-878., 1991

Jacobi, R.D., 1981, Peripheral bulge-a causal mechanism for the Lower/Middle Ordovician disconformity along the western margin of the northern Appalachians: Earth and Planetary Science Letters, v. 56, p. 245-251.

Jacobs, G.W., 1986, Mixed siliciclastic-carbonate storm deposits in the Upper Ordovician of central Kentucky: Geological Society of America Program with Abstracts, v. 18, p. 228.

Jacobs, D., and Sahagian, D., 1993, Climate induced fluctuations in sea level during non-glacial times: Nature, v. 361, p. 710-712.

James, N.P., Bone, Y., Von der Borch, C.C., and Gostin, V.A., 1992, Modern carbonate and terrigeneous clastic sediments on a cool-water, high-energy, mid-latitude shelf: Lacepede, southern Australia: Sedimentology, v. 39, p. 877-903.

James, N.P., and Bone, Y., 1994, Paleoecology of cool-water, subtidal cycles in Mid-Cenozoic limestones, Eucla Platform, southern Australia: Palaios, v. 9, p. 457-476.

Jennette, D.C., and Pryor, W.A, 1993, Cyclic alternation of proximal and distal storm facies: Kope and Fairview Formations (Upper Ordovician), Ohio and Kentucky: Journal of Sedimentary Petrology, v. 63, p. 183-203.

Jervey, M.T., 1988, Quantitative geological modeling of siliciclastic rock sequences and their seismic expression: *in* Wilgus, C.K., Hastings, B.S., Kendal, C. G. St. C., Posamentier, H.W., Ross, C. A., and Von Wagoner, J.C., (eds), Sea-Level Changes: An Integrated Approach, Society of Economic Paleontologists and Mineralogists Special Publication No. 42, p. 109-124.

Jordan, T.E., and Flemings, P.B., 1991, Large-scale stratigraphic architecture, eustatic variation, and unsteady tectonism: A theoretical evaluation: Journal of Geophysical Research, v. 96, p. 6681-6699.

Keith, B.D., 1989, Regional facies of Upper Ordovician Series of eastern North America: *in* B.D. Keith, ed., The Trenton Group (Upper Ordovician Series) of eastern North America: American Association of Petroleum Geologists, Tulsa, OK, Studies in Geology #29, p. 1-16.

Kreisa, R.D., 1980, The Martinsburg Formation (Middle and Upper Ordovician) and related facies in southwestern Virginia: unpublished Ph.D. dissertation, Virginia Polytechnic Institute and State University, Blacksburg, Virginia, 358 p.

Kreisa, R.D., 1981, Storm-generated sedimentary structures in subtidal marine facies with examples from the Middle and Upper Ordovician of southwestern Virginia: Journal of Sedimentary Petrology, v. 51, p. 823-848.

Kulp, M., 1995, Paleoenvironmental interpretation of the Brannon Member, Middle-Upper Ordovician Lexington Limestone, central Bluegrass region of Kentucky: Unpublished master's thesis, University of Kentucky, Lexington, Kentucky, 222 p.

Lash, G.G., 1988, Middle and Late Ordovician shelf activation and foredeep evolution, central Appalachian Orogen: *in* B.D. Keith, ed., The Trenton Group (Upper Ordovician Series) of eastern North America: American Association of Petroleum Geologists, Tulsa, OK, Studies in Geology #29, p. 37-53.

Lavoie, D., 1995, A Late Ordovician high-energy temperate-water carbonate ramp, southern Quebec, Canada: implications for Late Ordovician oceanography: Sedimentology, v. 42, p. 95-116.

Logan, B.W., and Cebulski, D.E., 1970, Sedimentary environments of Shark Bay, western Australia: *in* Carbonate sedimentation and environments of Shark Bay, western Australia, American Association of Petroleum Geologists Memoir 13, p. 1-37.

Mackey, R.T., 1972, Lithostratigraphy and depositional environment of the Perryville Limestone and related members of the Lower Lexington Limestone (Ordovician) of south-central Kentucky: (unpublished M.S. thesis) University of Kentucky, Lexington, KY, 76 p.

Martindale, B., and Boreen, T., 1995, Mississippian cool-water carbonate hydrocarbon reservoirs in the southern foothills of the Canadian Rocky Mountains: *in* Abstracts volume, Cool and cold-water carbonate conference, Geelong, Australia, p. 46-48.

Matthews, R., K., 1966, Genesis of Recent lime mud in southern British Honduras: Journal of Sedimentary Petrology, v. 36, p. 428-454.

McHugh, M.L., 1985, Reevaluation of the southwestern end of the Salem Synclinorium: Unpublished M.S. Thesis, Virginia Polytechnic Institute and State University, Blacksburg, Virginia, 111 p.

Mullins, H., Neumann, A.C., Wilber, R.J., and Boardman, M.R., 1980, Nodular carbonate sediment on Bahamian slopes: possible precursors to nodular limestones: Journal of Sedimentary Petrology, v. 50, p. 117-131.

Mussman, W.J., and Read, J.F., 1986, Sedimentology and development of a passive- to convergent-margin unconformity: Middle Ordovician Knox unconformity, Virginia Appalachians: Geological Society of America Bulletin, v. 97, p. 282-295.

Nelson, C.S., 1988, An introductory perspective on non-tropical shelf carbonates: Sedimentary Geology, v. 60, p. 3-12.

Obermeier, S.F., Bleuer, N.R., Munson, C.A., Munson, P.J., Martin, W.S., McWilliams, K.M., Tabaczynski, D.A., Odum, J.K., Rubin, M., and Eggert, D.L., 1991, Evidence of Strong Earthquake shaking in the Lower Wabash Valley from Prehistoric Liquefaction Features: Science, v. 251, p. 1061-1063.

Olsen, P.E., 1986, A 40-million year lake record of early Mesozoic orbital climate forcing: Science, v. 234, p. 842-848.

Osleger, D.S., 1991, Subtidal carbonate cycles: implications for allocyclic versus autocyclic controls: Geology, v. 19, p. 917-920.

Palmer, A.R., 1983, The decade of North American Geology, 1983 Geologic Time Scale: Geology, v. 11, p. 503-504.

Patzkowsky, M.E., and Holland, S.M., 1993, Biotic response to a Middle Ordovician paleoceanographic event in eastern North America: Geology, v. 21, p. 619-622.

Pope, M.C., and Read, J.F., 1994, Characteristics of depositional sequences, systems tracts and bounding surfaces in Early Ordovician greenhouse passive margin carbonates to Late Ordovician glacio-eustatic influenced foreland basin facies: Geological Society of America Abstract with Programs, Southeastern Section Meeting, Blacksburg, VA, p. 58.

Pope, M.C., and Read, J.F., (in press), High-frequency cyclicity of the Lexington Limestone (Middle Ordovician), a cool-water carbonate clastic ramp in an active foreland basin: Society of Economic Paleontologists and Mineralogists Special Publication.

Pope, M.C., Peavy, S., Read, J.F., and Coruh, C., (in prep) Spectral analysis of gamma ray logs in limestone/shale systems

Posamentier, H.W., Jervey, M.T., and Vail, P.R., 1988, Eustatic controls on clastic deposition I-conceptual framework: *in* Wilgus, C.K., Hastings, B.S., Kendal, C. G. St. C., Posamentier, H.W., Ross, C. A., and Von Wagoner, J.C., (eds), Sea-Level Changes: An Integrated Approach, Society of Economic Paleontologists and Mineralogists Special Publication No. 42, p. 109-124.

Posamentier, H.W., and Vail, P.R., 1988, Eustatic controls on clastic deposition II-sequence and systems tracts models: *in* Wilgus, C.K., Hastings, B.S., Kendal, C. G. St. C., Posamentier, H.W., Ross, C. A., and Von Wagoner, J.C., (eds), Sea-Level Changes: An Integrated Approach, Society of Economic Paleontologists and Mineralogists Special Publication No. 42, p. 109-124.

Pratt, B. R., 1994, Seismites in the Mesoproterozoic Altyn Formation (Belt Supergroup), Montana: A test for tectonic control of peritidal carbonate cyclicity: Geology, v. 22, p. 1091-1094.

Purser, B.H., and Siebold, E., 1973, The principal environmental factors influencing Holocene sedimentation and diagenesis in the Persian Gulf: *in* Purser, B.H., (ed), The Persian Gulf, Springer-Verlag, New York, p. 1-10.

Quinlan, G.M., and Beaumont, C., 1984, Appalachian thrusting, lithospheric flexure, and the Paleozoic stratigraphy of the eastern interior of North America: Canadian Journal of Earth Science, v. 21, p. 973-996.

Railsback, L.B., Ackerly, S.C., Anderson, T.F., and Cisne, J.L., 1990, Paleontological and isotope evidence for warm saline deep waters in Ordovician oceans: Nature, v. 343, p. 156- 159.

Read, J.F., 1974, Carbonate bank and wave-built platform sedimentation, Edel Province, Shark Bay, western Australia: *in* Logan, B.W., Read, J.F., Hagan, G.M., Hoffman, P., Brown, R.G., Woods, P.J., and Gebelein, C. D., (eds), Evolution an diagenesis of Quaternary carbonate sequences, Shark Bay, western Australia, Society of Economic Paleontologists and Mineralogists Memoir 22, Tulsa, p. 1-60.

Read, J.F., 1980, Carbonate ramp-to-basin transitions and foreland basin evolution, Middle Ordovician, Virginia Appalachians: American Association of Petroleum Geologists Bulletin, v. 64, p. 1575-1612.

Read, J.F., 1989, Controls on evolution of Cambrian-Ordovician passive margin, U.S. Appalachians:*in* Crevello, P.D., Wilson, J.L., Sarg, J.F., and Read, J.F., eds., Controls on carbonate platform and basin development: Society of Economic Paleontologists and Mineralogists Special Publication 44, p. 147-165.

Rodgers, J., 1971, The Taconic orogeny: Geological Society of America Bulletin, v. 82, p. 1141-1178.

Ross, R.J., James, N.P., Hintze, L.F., and Poole, F.G., 1989, Architecture and evolution of a Whiterockian (early Middle Ordovician) carbonate platform, Basin ranges of western U.S.A.: *in* Crevello, P.D., Wilson, J.L., Sarg, J.F., and Read, J.F., (eds), Controls on carbonate platform development, Society of Economic Paleontologists and Mineralogists Special Publication 44, p.163-

Schutter, S.R., 1992, Ordovician hydrocarbon distribution in North America and its relationship to eustatic cycles: *in* Webby, B.D., and Laurie, J.R., eds., Global Perspectives on Ordovician Geology: Balkema, Rotterdam, p. 421-432.

Scotese, C.R., and McKerrow, W.S., 1990, Revised world maps and introduction: *in* McKerrow, W.S., and Scotese, C.R., eds., Palaeozoic palaeogeography and biogeography: Geological Society of London Memoir 12, p. 1-21.

Shanmugam, G., and Walker, K., 1980, Sedimentation, subsidence and evolution of a foredeep basin in the Middle Ordovician, southern Appalachians: American Journal of Science, v. 280, p. 479-496.

Stockman, K.W., and Ginsburg, R.N., and Shinn, E.A., 1965, The production of lime mud by algae in south Florida: Journal of Sedimetary Petrology, v. 37, p. 633-648.

Sweet, W. D., 1979, Conodonts and conodont stratigraphy of post-Tyrone Ordovician rocks of the Cincinnati Region: United States Geological Survey Professional Paper 1066-G, 26 p.

Tankard, A.J., 1986, On the depositional response to thrusting and lithospheric flexure: examples from the Appalachian and Rocky Mountain basins: *in* Allen, P.A., and Homewood, P., (eds), Foreland Basins, International Association of Sedimentologists Special Publication #8, Blackwell Publications, Oxford, p. 369-392.

Tobin, R.C., 1982, An assessment of the lithostratigraphic and interpretive value of the traditional "biostratigraphy" of the type Upper Ordovician of North America: American Journal of Science, v. 286, p. 673-701.

Tucker, M.E., and Wright, P.V., 1990, Carbonate Sedimentology: Blackwell Scientific Publications, Oxford, 482 p.

Tucker, R.D., Krogh, T.E., Ross, R.J. Jr., and Williams, S.H., 1990, Time-scale calibration by high-precision U-Pb zircon dating of interstratified volcanic ashes in the Ordovician and Silurian stratotypes of Britain: Earth and Plantary Science Letters, v. 100, p. 51-58.

Tucker, R.D., and McKerrow, W.S., 1995, Early Paleozoic chronology: a review in light of new U-Pb zircon ages from New Foundland and Britain: Canadian Journal of Earth Sciences, v. 32, p. 368-379.

Vail, P.R., Audemard, F., Bowman, S.A., Eisner, P.N., and Perez-Cruz, C., 1991; The stratigraphic signatures of tectonics, eustacy, and sedimentology-an overview: *in* Einsele, G., Ricken, W., and Seilacher, A., (eds), Cycles and Events in Stratigraphy, Springer-Verlag, New York, p. 617-659.

Van der Voo, R., 1988, Paleozoic paleogeography of North America, Gondwana, and intervening displaced terranes: Comparison of paleomagnetism with paleoclimatology and biogeographical patterns: Geological Society of America Bulletin, v. 100, p. 311-324.

Weber, L.J., Sarg, J.F., and Wright, F.M., 1995, Part 3, Sequence stratigraphy and reservoir delineation of the Middle Pennsylvanian (Desmoinesian), Paradox Basin and Aneth Field, southwestern U.S.A: *in* Read, J.F., Kerans, C., Weber, L.J., Sarg, J.F., and Wright, F.M., (eds), Milankovitch sea-level changes, cycles, and reservoirs on carbonate platforms in Greenhouse and Ice-free worlds, Society of Economic Paleontologists and Mineralogists, Short Course Notes No. 35, Tulsa, p. 1-81.

Witzke, 1990, Palaeoclimatic constraints for Paleozoic palaeolatitudes of Laurentia and Euramerica: *in* McKerrow, W.S., and Scotese, C.R., eds., Palaeozoic palaeogeography and biogeography: Geological Society of London Memoir 12, p. 57-74.

Weir, G.W., Peterson, W.L., and Swadley, W.C., 1984, Lithostratigraphy of Upper Ordovician strata exposed in Kentucky:United States Geological Survey Professional Paper 1151-E, 121 p.

Chapter 3: High-Resolution Stratigraphy of the Lexington Limestone (late Middle Ordovician) Kentucky, U.S.A.: A Cool Water Carbonate-Clastic Unit in a Tectonically Active Foreland Basin

ABSTRACT

The late Middle Ordovician Lexington Limestone of Kentucky contains evidence of cool water deposition on a high-energy ramp in an active foreland basin. The ramp sloped gently northeastward from a forebulge (Cincinnati Arch) into the Appalachian foreland basin and passed westward into the narrow Sebree Trough. The Lexington Limestone is the Transgressive Systems Tract of the Late Mohawkian to Cincinnatian 2nd-order supersequence (~9 to 14 m.y. duration). It is predominantly subtidal limestone and shale with rare tidal flats and skeletal shoals developed on structurally controlled highs on the peripheral bulge. The Lexington Limestone consists of a large 3rd-order sequence (~ 60 m thick) and the transgressive part of another large sequence (~40 m thick). The Lexington Limestone contains 5 smaller (up to 25 m thick; ~1.8 to 2.8 m.y. duration) third-order depositional sequences, which are composed of meter-scale (1 to 8 m thick) cycles.

Brachiopods and bryozoans are the most abundant faunal elements in the Lexington Limestone. The bryomol faunal association, the abundance of phosphate (up to 2.4 wt. percent), the presence of low-Mg calcite cements, the abundance of marine-cemented and phosphatized hardgrounds, the low accumulation rates (2.1 to 3.3 cm/kyr) and the lack of warm-water features (i.e. chlorozoan fauna, ooids, evaporites) indicate cool water deposition. Stromatoporoid and corals in restricted lagoonal facies, especially in 3rd-order highstands may indicate warmer near-surface seawater temperatures in these periods.

Tidal flat facies are fenestral to irregularly laminated lime mudstones with evidence of early meteoric diagenesis in cycle caps. Lagoonal/restricted facies are nodular-irregularly bedded whole skeletal wackestone/packstone with a restricted fauna. Bipolar cross-bedded fine to coarse grainstone comprises the tidally-influenced skeletal shoal facies. The most common facies is the intermediate ramp nodular-irregularly bedded skeletal wackestone/packstone and shale. Thin-bedded shale and limestone storm beds are the deep ramp facies, wheras evenly bedded calcisiltite and shale rhythmites are

"basinal" facies. The water depths of each facies are uncertain but all facies probably were shallower than 60.

Subtidal meter-scale cycles, juxtaposing shallow and deep ramp facies, indicate moderate amplitude sea level fluctuations (a few tens of meters) probably related to the onset of glaciation on Gondwana. Tidal flat cycles in highstands show only minor evidence of emergence, except at sequence boundaries, suggesting that sea level fluctuations were smaller at these times. The available biostratigraphic and chronostratigraphic data indicate average cycle duration was ~ 40-65 k.y.

The similarities between the Lexington Limestone and the Trenton Group in the Appalachian Basin suggest that cool oceanic waters were present to paleolatitudes of 15-30° S during the Late Mohawkian. The abrupt change to cool water deposition following Early Mohawkian warm water carbonates may be related to regional volcanism, increasingly higher sea level (and deeper, cooler water) and global change in oceanic temperatures associated with the onset of Gondwana glaciation. However, the Taconic magmatic arc which produced increased subsidence in the northern Appalachians duduring this time may have also induced a change in oceanic circulation, blocking warm, equatorial waters from the foreland basin and allowing cool subpolar waters from the south to inundate the southern Laurentian epeiric sea.

INTRODUCTION

The late Middle Ordovician Lexington Limestone of central Kentucky, is a 100 M thick sequence of cyclic, subtidal skeletal limestones and shale that formed on a shallow ramp bordering the Appalachian foreland basin (Cressman, 1973) (Fig. 1). The Lexington Limestone is the basal transgressive portion of the Late Mohawkian to Cincinnatian 2nd-order supersequence (Fig. 2) and marks a change from tropical to temperate carbonate deposition (Patzkowsky and Holland, 1993). The late Middle Ordovician may mark the beginning of glaciation on Gondwana (Frakes et al., 1992) which reached a maximum at the end of the Ordovician (Caputo and Crowell, 1985; Hambrey, 1985; Brenchley et al., 1994) (Fig. 2) during global greenhouse conditions with high CO_2 values (Crowley and Baum, 1991; Berner, 1990, 1992). Thus, the stratigraphic record in Kentucky may record a change in amplitude of sea level oscillations associated with waxing and waning of continental ice sheets as the Gondwana ice sheet developed. This study, based on six large continuous road-cut

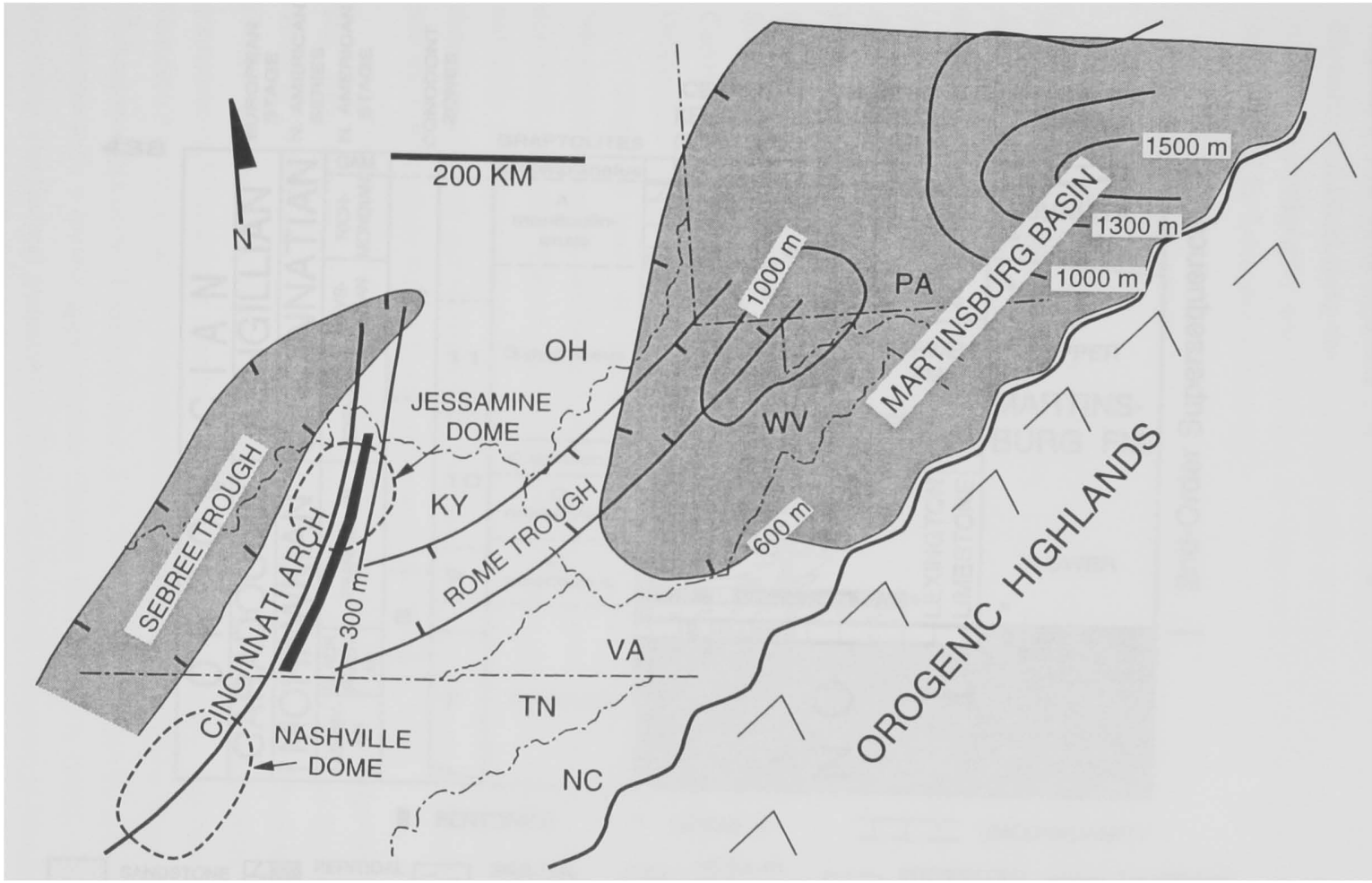

Figure 1. Location map of central Appalachians showing distribution of major structural elements active during the late Middle Ordovician. Thick line parallel to the Cincinnati Arch is the approximate location of lithologic cross-section in Figure 4. Isopach thicknesses are of late Middle to Late Ordovician strata.

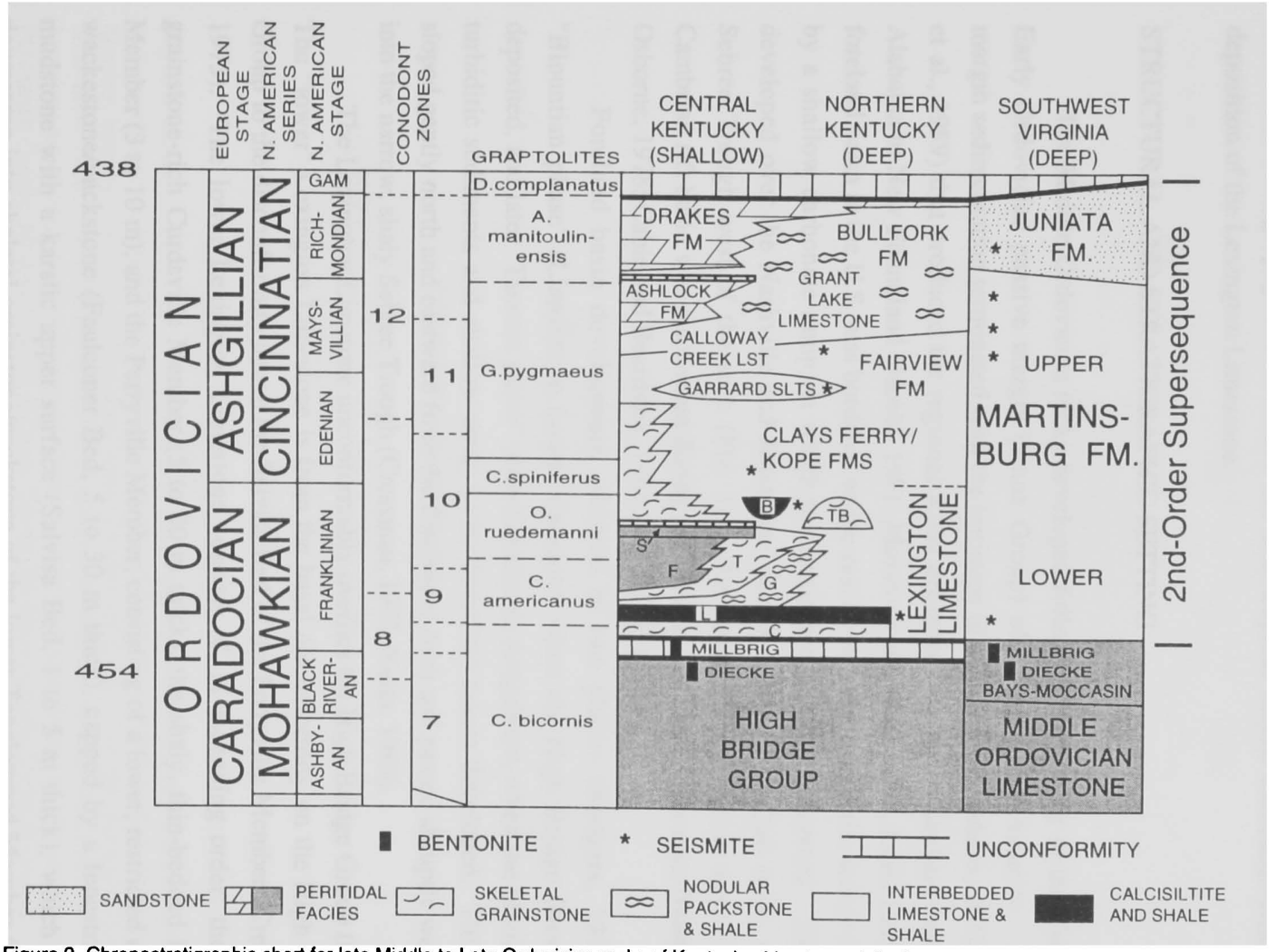

Figure 2. Chronostratigraphic chart for late Middle to Late Ordovician rocks of Kentucky. Members of the Lexington Limestone are from Cressman (1973): Curdsville (C), Logana (L), Salvisa Bed of Perryville (S), Faulconer Bed of Perryville (F), Tanglewood (lower-T), Grier (G), Tanglewood (upper-T), Brannon (B). Lexington Limestone is the basal (transgressive) part of the Late Mohawkian to Cincinnatian supersequence.

exposures over 60 m high near Frankfort and Lexington, Kentucky and 17 continuous diamond drill cores along the Cincinnati Arch, Kentucky (Fig. 3), documents the high-resolution stratigraphy and evidence for non-tropical mixed carbonate-siliciclastic deposition of the Lexington Limestone.

STRUCTURAL AND STRATIGRAPHIC SETTING

The Middle Ordovician rocks developed following foundering of the Cambrian-Early Ordovician passive margin (Knox Group) of easten North America. Passive margin sedimentation terminated with the initiation of subduction (Rodgers, 1971; Drake et al., 1989) that produced the regional Knox unconformity and a foreland basin from Alabama to New Foundland (Jacobi, 1981; Mussman and Read, 1986; Lash, 1989). The foreland basin in the U.S. was bordered on the east by tectonic highlands, and on the west by a shallow carbonate ramp on which the Lexington Limestone formed. The ramp developed over the Nashville and Jessamine domes on the Cincinnati Arch, and the Sebree Trough west of the arch (Fig. 1). The Rome Trough which was a Middle Cambrian rift basin was reactivated during the Middle and Late Ordovician (Borella and Osborne, 1978; Cable and Beardsley, 1984; Weir et al., 1984).

Foreland basin development occurred in two phases (Rodgers, 1971) the "Blountian phase" (Llanvirn to Lower Caradoc), when the High Bridge Group was deposited, and later "Taconic phase" (Late Caradoc to Ashgillian), when the Martinsburg turbiditic sediments and shallow ramp facies described herein developed. This ramp sloped gently north and eastward from the Cincinnati Arch and passed abruptly westward into the narrow, shaly Sebree Trough (Cressman, 1973; Keith, 1989).

The Lexington Limetone unconformably overlies the High Bridge Group (Fig. 4). The "lower" Lexington Limestone is from the basal disconformity on the High Bridge Group to the disconformity above the Salvisa Bed of the Perryville Member (Cressman, 1973). The lower Lexington Limestone consists of, in ascending order: the basal grainstone-rich Curdsville Member (5 to 20 m thick), the shaly, thin-bedded Logana Member (3 to 10 m), and the Perryville Member, consisting of a lower, restricted nodular wackestone/packstone (Faulconer Bed; 5 to 30 m thick), capped by a fenestral lime mudstone with a karstic upper surface (Salvisa Bed, 1 to 5 m thick), which passes downramp into skeletal grainstone/packstone of the lower Tanglewood Member (2 to 10 m thick), nodular skeletal wackestone/packstone and shale of the Grier Member (5 to 30

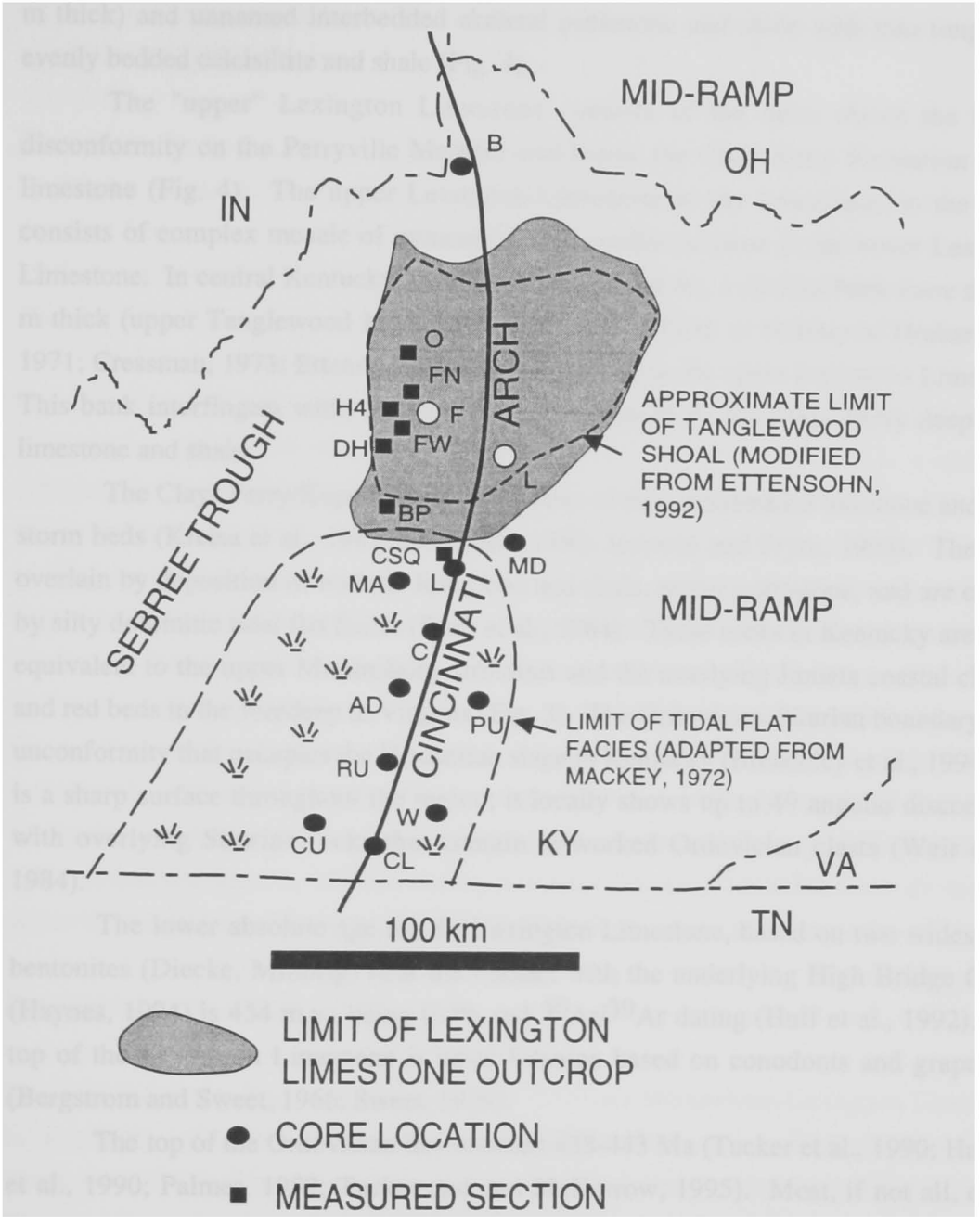

Figure 3. Detailed location map of Cincinnati Arch region showing location of cores and outcrops in the study area, as well as the generalized distribution of tidal flat facies (Salvisa Bed, Perryville Member; Mackey, 1972) and skeletal shoal facies (Tanglewood Buildup) over the Jessamine Dome (Ettensohn, 1992). The cities of Frankfort and Lexington are indicated by white filled circles. Locations are: CU-Cumberland County; CL-Clinton County; W-Wayne County; RU-Russell County; PU-Pulaski County; AD-Adair County; C-Casey County; MA-Marion County; L-Lincoln County; CSQ-Caldwell Stone Quarry; MD-MadisonCounty; BP-Bluegrass-Parkway; DH-Devils Hollow Road; FW-Frankfort West; H4-Highway 421; FN-Frankfort North; O-Owenton; and B-Boone County.

m thick) and unnamed interbedded skeletal packstone and shale with thin tongues of evenly bedded calcisiltite and shale (Fig. 4).

The "upper" Lexington Limestone consists of the units above the karstic disconformity on the Perryville Member and below the Clays Ferry Formation shaley limestone (Fig. 4). The upper Lexington Limestone in the subsurface, to the south, consists of complex mosaic of unnamed facies similar to those in the lower Lexington Limestone. In central Kentucky, over the Jessamine Dome, a skeletal bank more than 50 m thick (upper Tanglewood Member or Tanglewood Bank or buildup of Hrabar et al., 1971; Cressman, 1973; Ettensohn, 1992) is developed in the upper Lexington Limestone. This bank interfingers with, and is eventually drowned by the Clays Ferry deep water limestone and shale.

The Clays Ferry/Kope Formations consist of thin, interbedded limestone and shale storm beds (Kreisa et al., 1981; Ettensohn, 1992; Jennette and Pryor, 1993). These are overlain by deposition of nodular limestone and shale, minor grainstone, and are capped by silty dolomitic tidal flat facies (Weir et al., 1984). These rocks in Kentucky are time-equivalent to the upper Martinsburg turbidites and the overlying Juniata coastal clastics and red beds in the foredeep in Virginia (Fig. 3). The Ordovician-Silurian boundary is an unconformity that occupies the Hirnantian stage in Kentucky (Brenchley et al., 1994) and is a sharp surface throughout the region; it locally shows up to 4^{o} angular discordance with overlying Silurian rocks that contain re-worked Ordovician clasts (Weir et al., 1984).

The lower absolute age for the Lexington Limestone, based on two widespread bentonites (Diecke, Millbrig) near the contact with the underlying High Bridge Group (Haynes, 1994) is 454 m.y., using U-Pb and $^{40}Ar/^{39}Ar$ dating (Huff et al., 1992). The top of the Lexington Limestone is basal Edenian based on conodonts and graptolites (Bergstrom and Sweet, 1966; Sweet. 1979).

The top of the Ordovician lies between 438-443 Ma (Tucker et al., 1990; Harland et al., 1990; Palmer, 1982; Tucker and and McKerrow, 1995). Most, if not all, of the Hirnantian stage (~2 m.y.; Harland, 1990; Haq et al., 1987) is missing in Kentucky (Brenchley et al., 1994; Sweet, 1979) so the duration of the Late Mohawkian to Cincinnatian supersequence is between 9-14 m.y. Because, the Lexington Limestone is approximately the basal third of this supersequence (~300 m thick), and since the majority of this sequence is subtidal with little evidence of subaerial exposure, the Lexington Limestone is interpreted to represent approximately one-third the time

duration of this sequence. Thus, the duration of the Lexington Limestone is approximately 3 to 4.8 m.y.

Tectonism During Lexington Limestone Deposition: Rapid facies changes in the Lexington Limestone indicate the Nashville and Jessamine domes were fault-bounded positive features along the Cincinnati Arch during deposition (Borella and Osborne, 1978; Weir et al., 1984). The restriction of tidal flat facies in the Lexington Limestone (Salvisa Bed of Perryville Member) to a northerly extending tongue along the Cincinnati Arch indicate the arch was a topographic high during this time. A detailed study of this unit (Mackey, 1972) showed that tidal flats developed on topographic highs while deeper ramp facies formed in the topographic lows suggesting the Arch was a series of structurally-controlled alternating topographic highs and lows. Locally developed tidally-influenced grainstones in the upper Lexington Tanglewood Member are restricted to the Jessamine Dome which indicate this area was a positive feature during Lexington deposition (Hrabar et al., 1971)(Fig. 2). Rapid facies and thickness changes across the Kentucky River- and Irvine-Paint Creek Faults indicate they were active in the Ordovician (Black and Haney, 1975; Cressman, 1973; Borella and Osborne, 1978; Grossnickle, 1985; Ettensohn et al., 1986; Ettensohn, 1992; Cable and Beardsley, 1984). Seismically induced ball-and-pillow structures (seismites) (Pope and Read, 1992; Ettensohn and Rast, 1995), synsedimentary faults (Black and Haney, 1975) tectonically induced breccia beds in subtidal facies, and soft-sediment filled fractures all indicate active tectonism occurred during deposition of the Lexington Limestone.

SEQUENCE STRATIGRAPHY

2nd- and 3rd-Order Sequence Stratigraphy: The Late Mohawkian Lexington Limestone in Kentucky rests disconformably on the Early Mohawkian High Bridge Group (Cressman, 1973). Downdip in Virginia the time-equivalent lower Martinsburg rocks rest conformably on lowstand Bays deltaic/nearshore marine facies, and Moccasin red beds, a coastal plain/tidal flat complex (Pope and Read, 1994) (Fig. 3). These lowstand units are largely derived from the southwest and prograded longitudinally into the basin above the High Bridge equivalent, the "Middle Ordovician Limestone" (Read, 1980).

The Lexington Limestone is the lower, transgressive part of the Late Mohawkian to Cincinnatian 2nd-order supersequence (time equivalent to the basinal lower

Martinsburg Formation)(Fig. 3). The Lexington Limestone consists dominantly of subtidal skeletal limestone and shale (Cressman, 1973) and includes a transgressive-regressive 3rd-order depositional sequence (Sequence 1; ~60 m thick) capped by regional tidal flat facies with a sequence bounding karstic upper surface which is overlain by the transgressive portion of the next large 3rd-order sequence (Sequence 2; Fig. 4).

The Transgressive Systems Tract (TST) of Lexington Limestone depositional sequence (Fig. 4) consists of a thin skeletal grainstone (Curdsville Member) resting above the basal disconformity and a portion of the shaly Logana Member. The Maximum Flooding Surface (MFS) of sequence 1 occurs within the Logana Member, however it is not a single surface but rather a zone of monotonous deep water facies. The Highstand Systems Tract (HST) in this sequence consist of restricted skeletal wackestone/packstone capped by a regional fenestral lime mudstone/tidal flat in the south; these pass down ramp into nodular skeletal packstone and shale, with rare interbedded calcisiltite and shale tongues, both of which are capped by skeletal grainstone (Fig. 4). A sequence-bounding subaerial exposure surface developed on tidal facies to the south, and passes downramp to the north into a correlative conformity within skeletal grainstone, nodular skeletal packstone and shale (Fig. 4).

A lowstand Ramp Margin Wedge (RMW), consisting of skeletal grainstone and nodular skeletal packstone and shale, was deposited over the Jessamine Dome (Fig. 4). The TST of overlying sequence 2 in the south is a complex facies mosaic that generally deepens upward (Fig.4). Restricted skeletal wackestone facies at the base are overlain by phosphatic nodular skeletal packstone, shale and skeletal grainstone that backsteps southward. To the north, the TST of sequence 2 is marked by development of the Tanglewood Bank, a compartmentalized skeletal shoal complex surrounded by deeper ramp facies, over the Jessamine Dome (Fig. 4).

Small Scale Depositional Sequences:

Third-order depositional sequence of the Lexington Limestone are arranged in 3 small-scale sequences (5-25 m thick) composed of meter-scale cycles (Fig. 4). Some small-scale sequences are asymmetric upward-shallowing, whereas others are symmetrical transgressive-regressive units. The small-scale sequences are traceable for tens to up to a hundred kilometers or more, changing facies gradually downdip, and locally forming a complex mosaic facies pattern in cross-section (Fig. 4). These small sequences are marked by regionally developed flooding events within the study area (Fig. 4).

Sequence 1 (lower Lexington Limestone) contains 3 small scale sequences. The basal small sequence 1a (Fig. 4) consists of transgressive skeletal grainstone (Curdsville Member) with rare quartz grains and numerous hardgrounds developed above the basal unconformity; this grades up into a shale-dominated unit with interbedded calcisiltite and skeletal packstone (Logana Member), which is capped by a thin unit of skeletal grainstone and bryozoan packstone. The second small depositional sequence 1b (Fig. 4) has a transgressive shaly unit overlain by backstepping restricted wackestone and packstone in the south that passes basinward into skeletal grainstone, nodular wackestone/packstone and shaly limestone. This sequence is capped by a thin skeletal grainstone. The overlying third small sequence 1c (Fig. 4) has a shaly base with prograding restricted skeletal wackestone and packstone that passes basinward into thick skeletal grainstone, nodular wackestone and shaly limestone. The prograding tidal flat facies (Salvisa Bed, Perryville Member) cap this sequence to the south and pass northward into a skeletal grainstone unit.

The upper Lexington Limestone (lower part of sequence 2) includes two small-scale sequences and a portion of a third sequence. South of the Jessamine Dome, the lower depositional sequence (2a, Fig. 4) consists of a shaley limestone with many seismites, which progressively onlap restricted wackestone/packstone, nodular skeletal packstone and shale with abundant hardgrounds, phosphatic skeletal grainstone, and bryozoan packstone. On the Jessamine Dome, sequence 2a has a skeletal grainstone shoal lowstand unit. This lowstand is overlain by a transgressive, shaley unit with many seismites, grading up into nodular carbonate and capped by skeletal grainstone. Depositional sequence 2b (Fig. 4) is a complex mosaic of nodular skeletal wackestone/packstone, skeletal grainstone and isolated units of restricted skeletal wackestone/packstone and deep ramp units. The HST of sequence 2b is marked by a thick skeletal grainstone unit and thin fenestral limestone on the Jessamine Dome and the highest occurrence of restricted skeletal wackestone/packstone to the south. Sequence 2c (Fig. 4) consists of interbedded skeletal grainstone/packstone and nodular skeletal wackestone/ packstone on the Jessamine Dome and backstepped skeletal grainstone and nodular skeletal wackestone/packstone to the south. The upper part of sequence 2c includes the interbedded skeletal packstone and shale of the Clays Ferry Formation which interfinger with the shallower ramp facies. Regional drowning of the grainstone-rich facies by these Clays Ferry facies over the Jessamine Dome signal the end of Lexington Limestone deposition.

FACIES IN THE LEXINGTON LIMESTONE

The sedimentary facies in the Lexington Limestone are summarized in Tables 1 and 2. Major faunal characteristics of each facies are shown in Fig. 5. Typical meter-scale cycles on the ramp are shown in Figure 6. The water depth estimates for facies are based on conservative estimates from modern ramp analogs such as Purser and Kinsman, 1974, a smaller modern-day foreland basin, and Shark Bay (Logan and Cebulski, 1970). The water depth estimates of facies are poorly constrained and the facies distribution in Figure 4 is more easily understood if the water depths of facies overlap of shallower rather than deeper estimates. However, if the facies developed at the deeper, modern day analogue depths, then there are still problems reconciling nearly horizontal sequence boundaries and

Fenestral and Massive Lime Mudstone: This facies developed mainly over the Cincinnati Arch in the south (Mackey, 1972) and consists of light gray to cream colored fenestral lime mudstone with ostracodes, gastropods and rare algal laminations (Table 1). The lime mudstone is commonly diagenetically mottled with oxidized haloes around fenestrae. Micro-scalloped erosional surfaces usually mark the tops of these units and small sinkholes are common below the regionally developed disconformity capping the Salvisa Bed (Fig. 7A).

The restricted fauna (Fig. 6), abundant tubular and laminar fenestrae and rare algal laminations (Table 1) indicate deposition on humid tidal flats. Fe-stained oxidation haloes around fenestrae and diagenetic color mottling restricted to these sediments indicate early near-surface oxidative groundwaters percolated through these tidal flats when they shallowed to sea level. Micro-scalloped and planar erosional surfaces, and small sinkholes developed by karst processes during exposure of topographic highs, especially at the top of the major Lexington sequence (Salvisa Bed, Perryville Member). Phosphatic sands filling small sinkholes (Fig. 7A) are transgressive units which infiltrated the sediments during subsequent flooding of the tidal flat facies. The amount of time missing in these subaerial erosion surfaces is unknown.

Restricted Nodular Skeletal Wackestone/Packstone: The restricted nodular skeletal wackestone/packstone, which occur at the base of cycles in the subsurface to the south. This facies consists of faunally restricted nodular-bedded skeletal wackestone/packstone with rare shale partings (Table 1 and Fig. 7B).

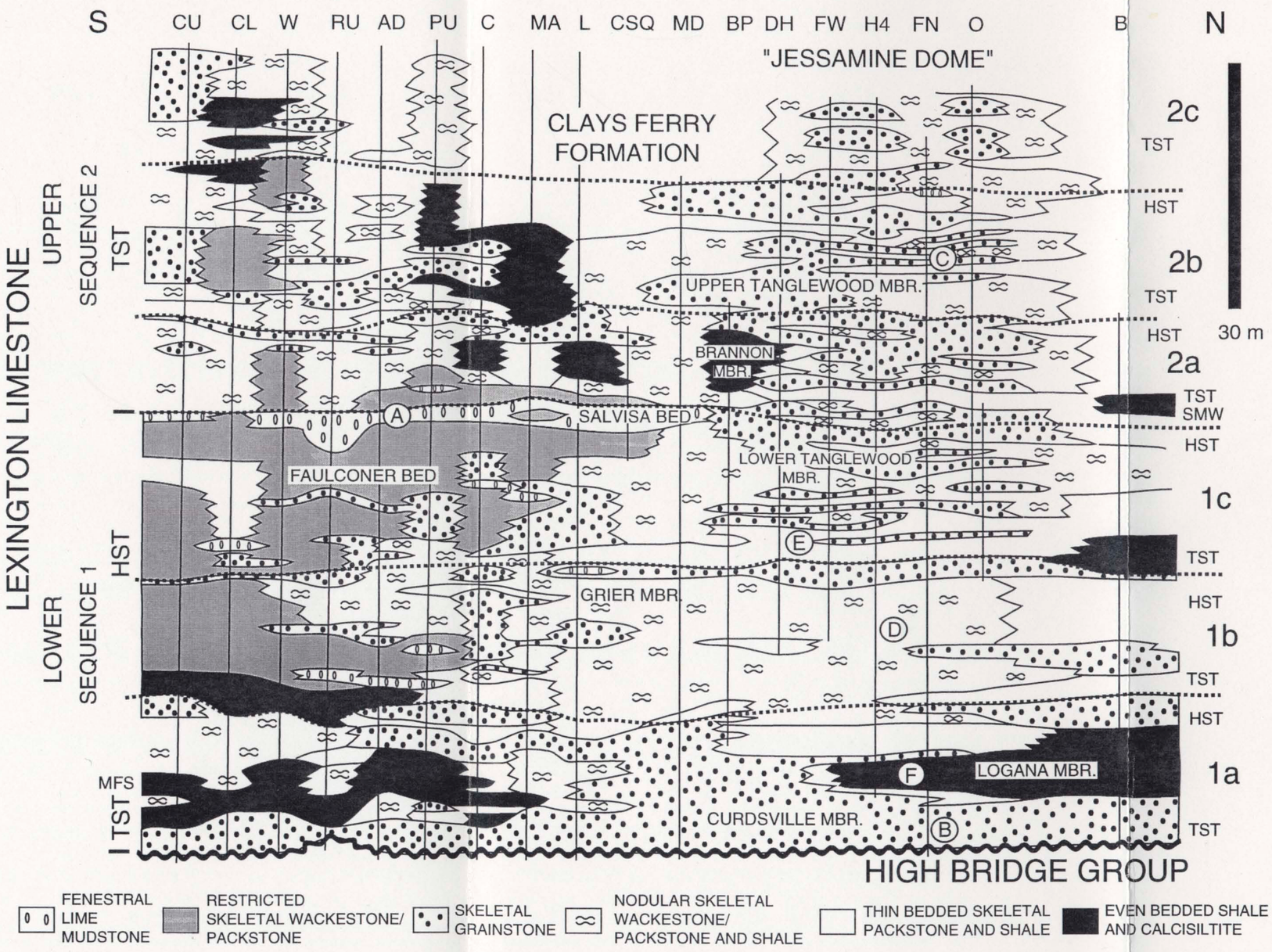

Figure 4. Stratigraphic cross-section showing major facies distribution within the Lexington Limestone. Informal units of Lexington Limestone and 3rd-order sequences and their component systems tracts are shown on left side of column. Dotted sub-horizontal lines mark small-scale sequence boundaries. Letters A-F indicate the location of portions of sections in Figure 6.

TABLE 1 SHALLOW WATER SEDIMENTS (<10 m Water Depth)

Rock Type	Fenestral Lime Mudstone	Nodular Bedded Skeletal Wackestone/ Packstone	Cross-bedded Skeletal Grainstone
Occurrence	Units 0.2 to 3 m thick throughout section, most common in upper Lexington interbedded with nodular skeletal wackestone and packstone	Units 0.5 to 8 m thick, occurs throughout section but is most abundant in southern part of Cincinnati Arch	Units from 0.5 to 8 m thick, occurs in basal and upper Lexington Limestone
Lithologic Description	Beds of fenestral lime mudstone; fenestrae are both tubular and laminar; rare laminations; rare ostracodes and gastropods	Irregular beds and nodules 10 to 20 cm thick with thin shaley seams (<25%); abundant ostracodes, gastropods, brachiopods, molluscs, and corals; locally common stromatoporoids; abundant lime mud	10 to 50 cm thick beds of fine to very coarse skeletal grainstone, commonly with fine skeletal grainstone and shale partings to 3 cm thick; bryozoan gravels at toes of cross-bed sets; beds are wedge, irregular, or tabular units; some channels and preserved small (3 m) skeletal mounds
Sedimentary Structures and Diagenetic Characteristics	Diagenetically mottled with iron stained and oxidized haloes around intraclasts and fenestrae; rarely shows karstic caps and phosphatic sands infilling sinkholes;	Whole fossils, including corals and stromatoporoids, some of which are in upright position	Fine planar laminations, or alternating coarse layers with fine drapes; common bipolar cross-bedding; abundant pyritic and phosphatic hardgrounds cap grainstones; locally massive; some overturned stromatoporoids; flanked laterally by bryozoan banks
Environment	Tidal Flat	Restricted Lagoon	Tidal Influenced Skeletal Shoals

TABLE 2 DEEP SUBTIDAL SEDIMENTS

Rock Type	Thin Skeletal Grainstone	Nodular bedded skeletal wackestone/ packstone	Irregularly bedded skeletal packstone, calcisiltite and shale	Even bedded calcisiltite and shale
Occurrence	Units up to 1.5 m thick, composed of skeletal grainstone and packstone with rare thin shale partings; occurs throughout section but most common in the middle of the Lexington Limestone as cycle caps	Units from 0.5 to 7 m thick, composed of skeletal wackestone, packstone and limy shale (up to 40 %); occurs throughout section most common in the middle of the section as cycle bases	Units 0.3 to 4 m thick; composed of skeletal packstone beds, some with calcisiltite caps; interbedded with limy shales (30-50%); most common in TST's	Units from 1 to 7 m thick; occur above basal grainstone and in topographic depression south of Jessamine Dome
Lithology	0.2 to 1. 5 m beds of skeletal grainstone and packstone with thin (<1cm thick) calcareous shale partings; occurs as sheets	3 to 20 cm thick irregular layers and nodules of whole skeletal wackestone, packstone and calcareous shale. Abundant bryozoans, brachiopods, gastropods in limestone; thin shelled brachiopods and bryozoans in shales; bedding is burrow homogenized	2 to 20 cm beds of skeletal packstone, calcisiltite, and limy shale. Abundant gastropods, brachiopods and bryozoans in packstone; many thin brachiopods in shales	5 to 10 cm beds of fine calcisiltite and calcareous shale; rare trilobites
Sedimentary Structures and Diagenetic Characteristics	Abundant horizontal laminations, and rare unidirectional cross-laminations, many beds have flat bases with rippled tops; rarely capped by pyritic and phosphatic hardrounds	Abundant burrows; rare preserved laminations; rare skeletal packstone grading up into calcareous shale; pyritic and phospatic hardgrounds occur throughout this unit	Normal and reverse grading in skeletal packstones; planar and hummocky cross-laminations, local scouring, and preserved ripples in calcisiltites, abundant thin horizontal laminations; rare vertical burrows; Packstone beds have flat bases and irregular tops	Fine planar laminations in calcisiltite; abundant synsedimentary framboidal pyrite; no bioturbation evident
Inferred Water Depth	10-20 m	10-30 m	30-50 m	>50 m
Facies interpretation	Mid-Ramp, Open Marine	Mid-Ramp, Open Marine	Storm Dominated Deep Ramp	Basinal-Deep Ramp

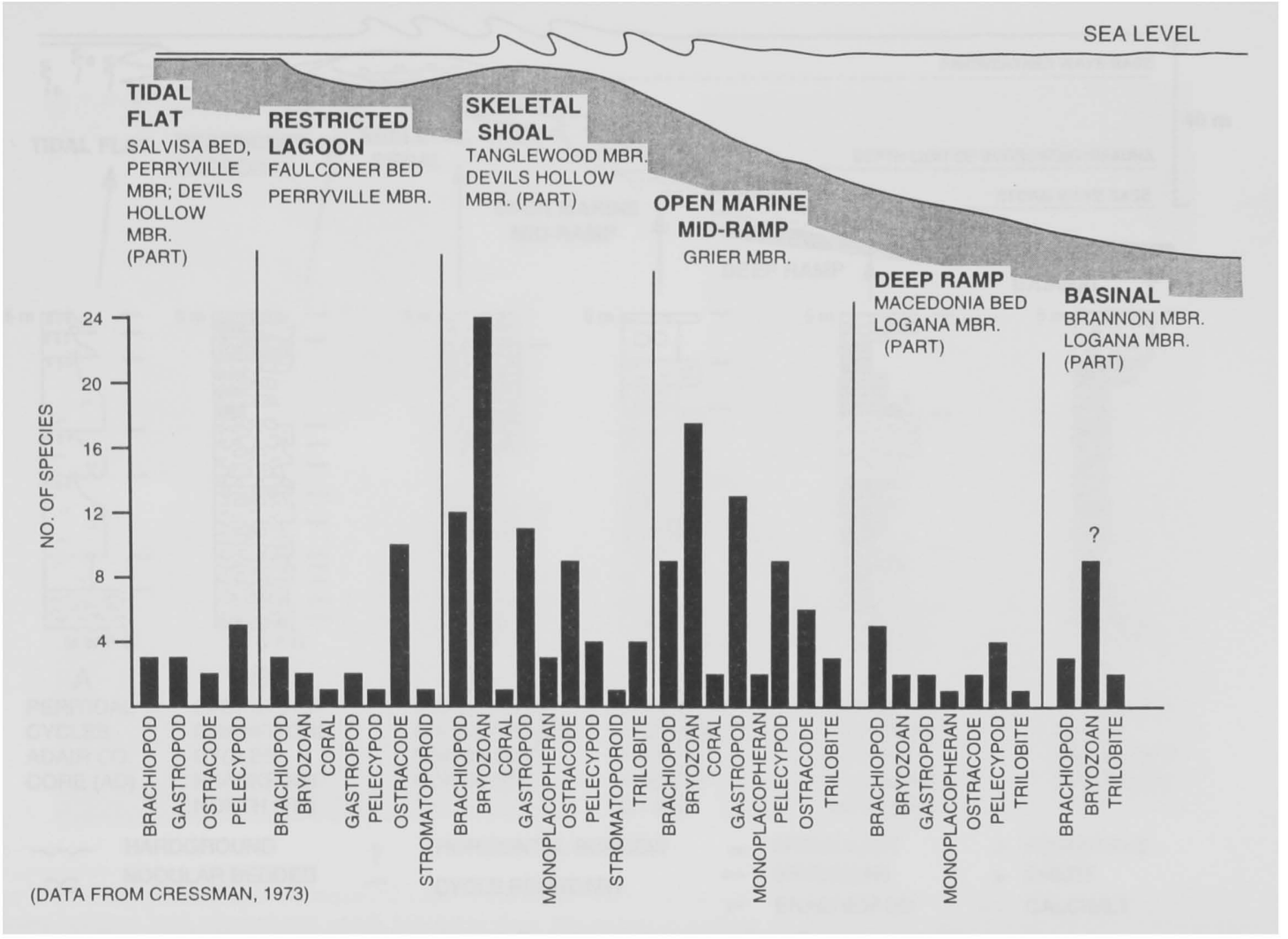

Figure 5. Frequency histogram showing number of species in each biotic group for facies along the proposed ramp-to-basin profile.

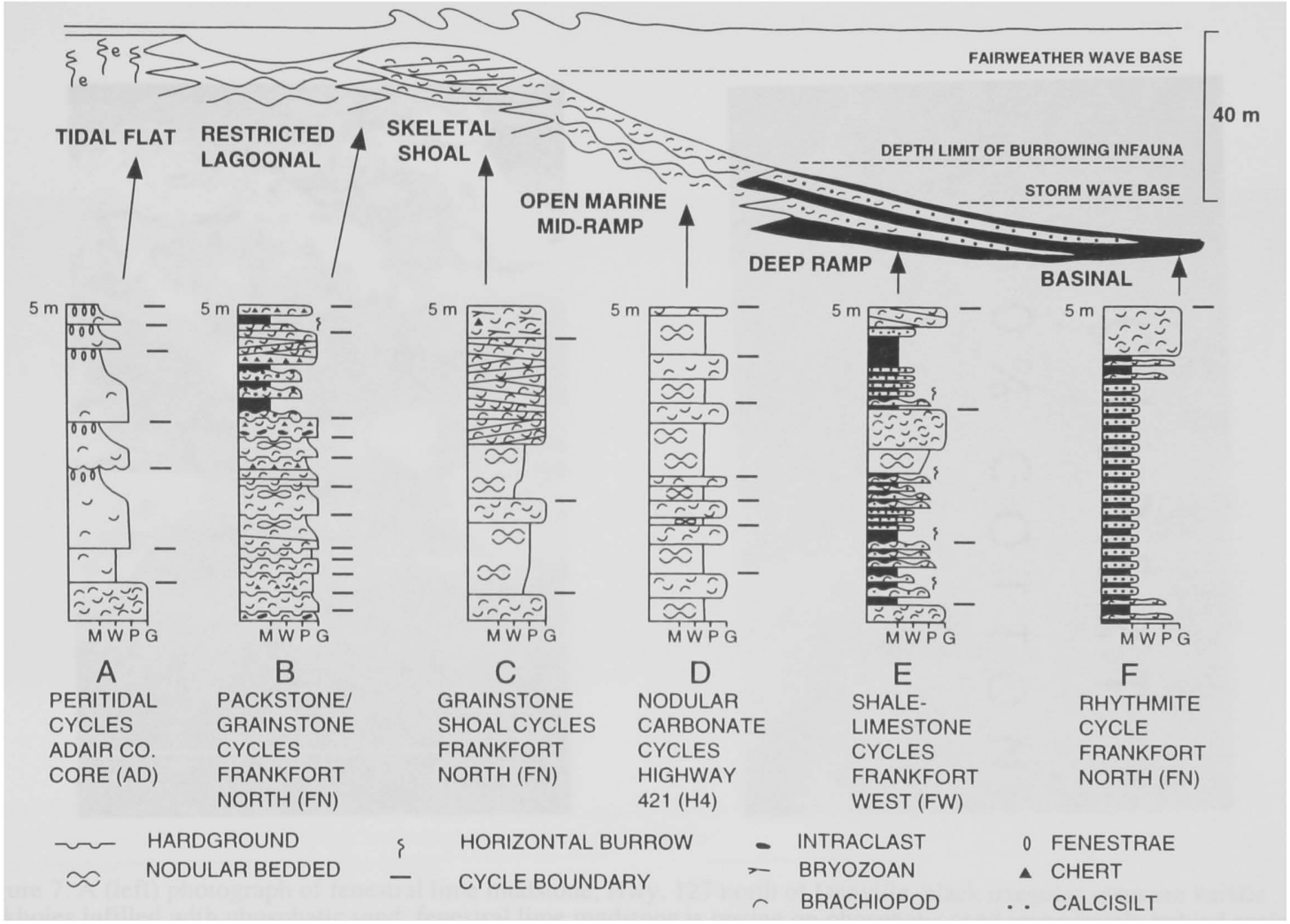

Figure 6. Portions of measured sections (A-F corresponding to locations Figures 4 and 10), showing typical meter-scale cycles of their corresponding facies along the ramp-to-basin profile.

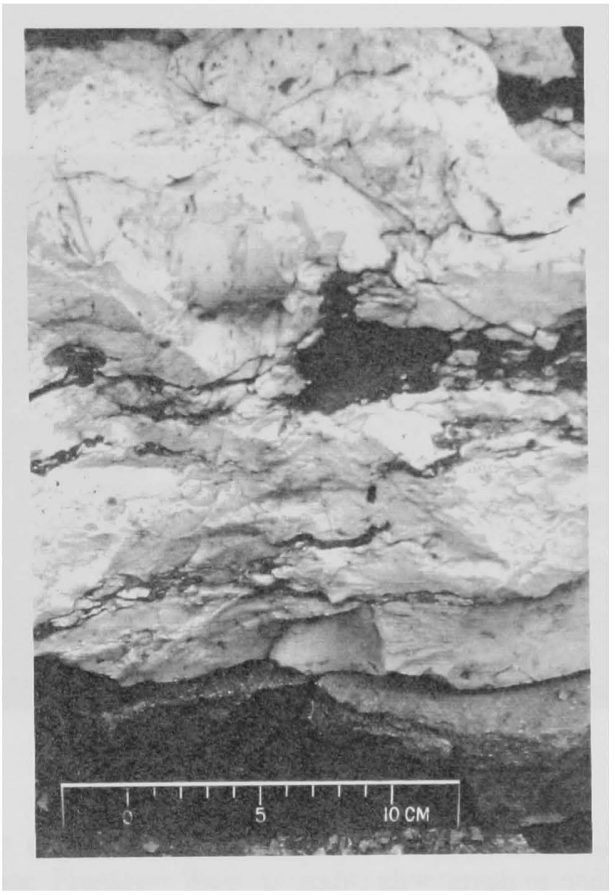

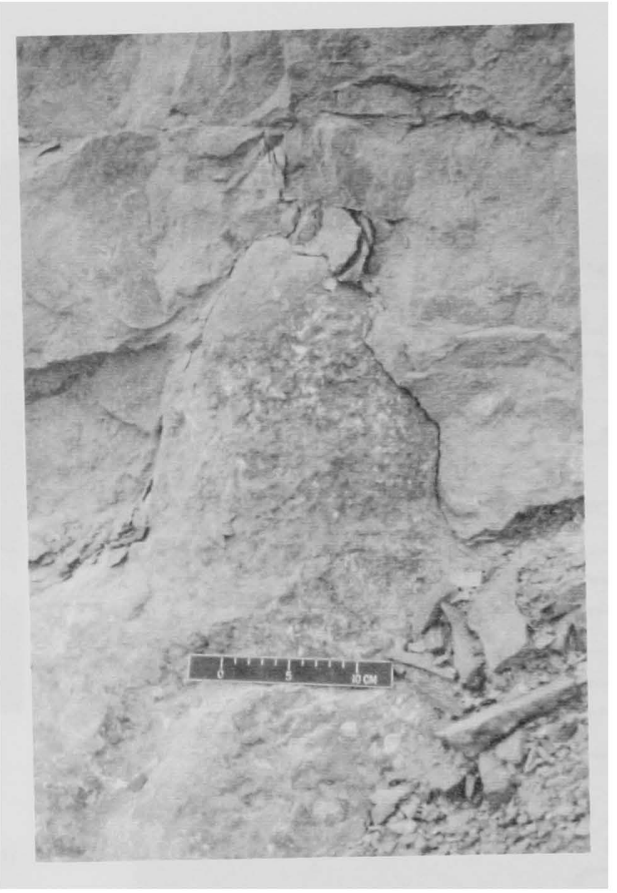

Figure 7. A (left) photograph of fenestral lime mudstone, Hwy. 127 north of Danville, black irregular areas are karstic sinkholes infilled with phosphatic sand; fenestral lime mudstone is resting on phosphatic sand immediately behind scale bar; B (right) photograph of faunally restricted, nodular wackestone with large upright stromatoporoid, Caldwell Stone Quarry.

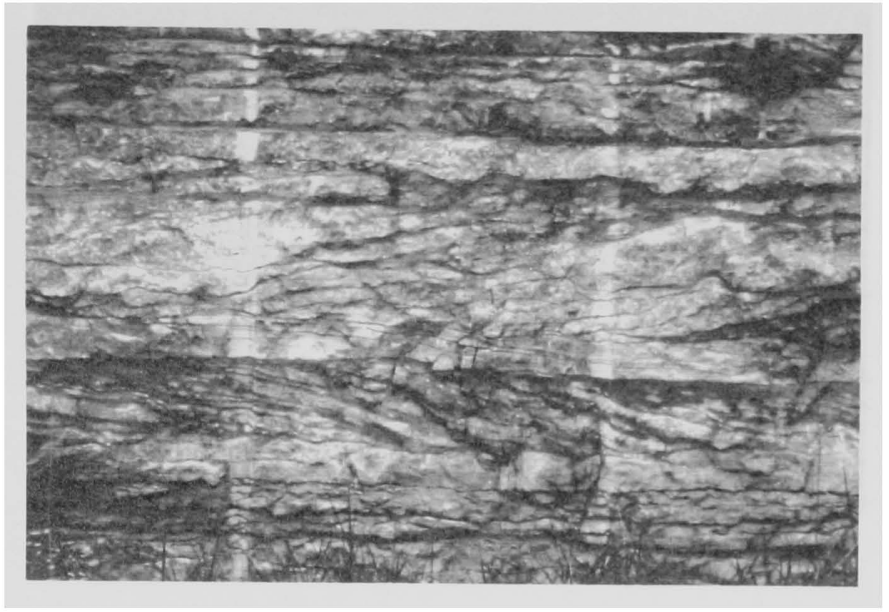

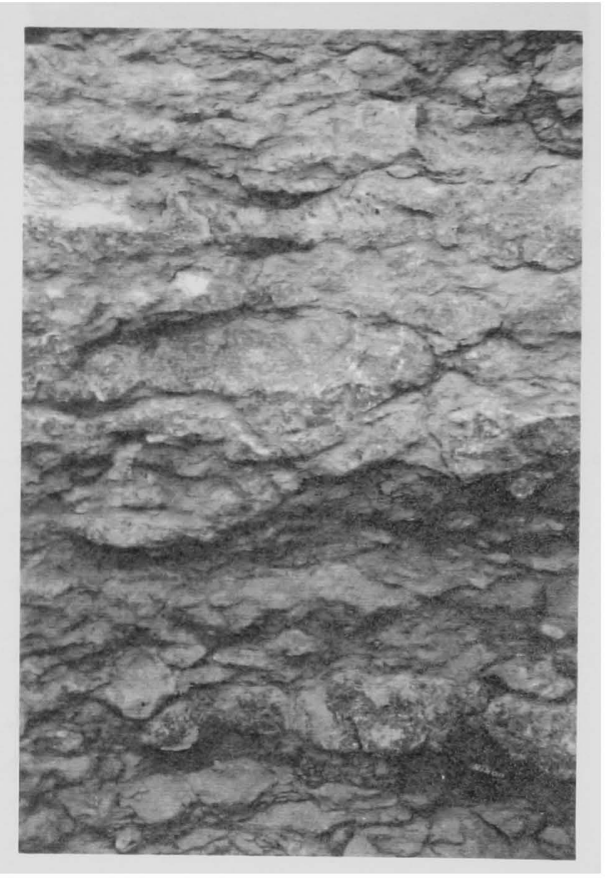

Figure 7. C (Left, above) photograph of bipolar cross-bedded skeletal grainstone, Frankfort West; D (right) photograph of nodular skeletal wackestone/packstone and shale, Owenton.

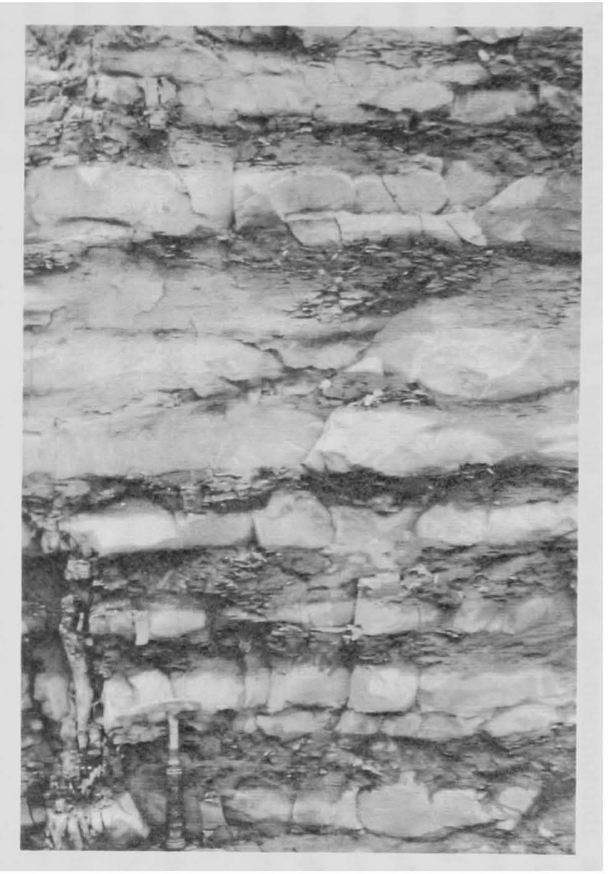

Figure 7. E (Left, above) photograph of interbedded skeletal packstone, calcisiltite and shale. F (right) photograph of evenly bedded calcisiltite and shale rhythmite.

The restricted fauna (Fig. 6), upright corals and stromatoporoids, and lack of current-induced sedimentary structures indicate deposition in a muddy, carbonate rich setting, protected from much wave reworking. These nodular skeletal wackestone/packstones differ from skeletal wackestone/packstone deposited in an open marine setting by their restricted faunas (Fig. 6), abundance of lime mudstone, and scarcity of shale. The nodular bedding is a result of burrowing infauna and the abundance of lime mudstone is the result of skeletal breakdown and pellets. The presence of corals, stromatoporoids and much lime mud in these sediments suggest warm, near-surface, sea water temperatures during deposition.

Bipolar Cross-Bedded Skeletal Grainstones: The herring-bone cross-bedded skeletal grainstone with shale drapes, and thin internal laminations are composed of brachiopod, bryozoan and echinoderm fragments (Figs. 6 and 7C; Table 1). They occur in the lower Lexington Limestone as thick units basinward of "restricted" nodular wackestone/packstone and as thinner continuous sheets which extend into the basin (Fig. 4). The grainstones in the upper Lexington Limestone are restricted to topographic highs (Hrabar et al., 1971; Cressman, 1973; Ettensohn, 1992) indicating they were deposited as shoals rather than widespread sheets. These shoals near Frankfort, Kentucky have lensoidal shapes with some channelization (Fig. 8). Nearly 600 paleocurrent measurements in these grainstone units indicate a bimodal distribution with dominant NE-SW (37^{o}, 197^{o}) current directions (Hrabar et al., 1971).

The excellent sorting, bi-polar cross-bedding and thin shale drapes indicate these units were deposited under the influence of strong tidal currents (Hrabar et al., 1971). The overturned stromatoporoids also may have toppled by tidal currents or storms. Massive coarse-grained bryozoan gravels at the base of some cross-bed sets are thalweg deposits filling channels or are the remnants of bryozoan thickets growing at the margins of the skeletal shoals which were destroyed and re-distributed during migration of grainstone shoals. Many of the bi-polar cross-bedded skeletal grainstones are capped by low-relief iron-stained hardgrounds. More massive grainstones above iron-stained hardgrounds cover burrowed firm-grounds and hardgrounds that had developed in quieter water settings, perhaps in topographic lows between shoals, or during small drowning events. Dolomite is present only at the top of one of the skeletal shoal units suggesting that most shoals did not shallow into tidal flats forlong, it at all.

Skeletal Grainstone/Packstone: Skeletal grainstone/packstones, brachiopod, bryozoan, and echinederm fragments commonly are laminated, rarely show bipolar cross-bedding,

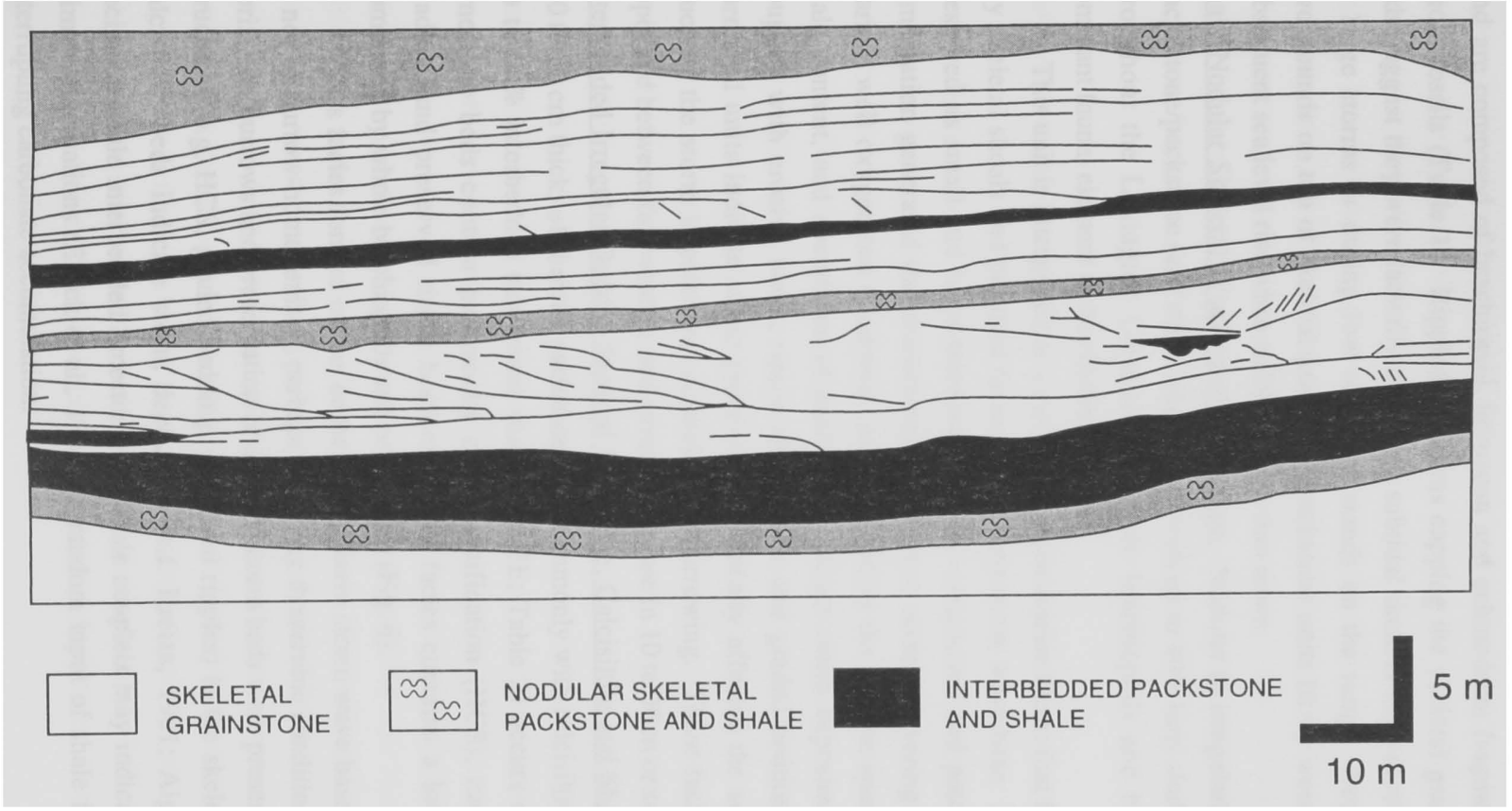

Figure 8. Line drawing of photomosaic of compartmentalized Tanglewood Member at Highway 127, south of Frankfort, Kentucky. The compartmentalization is tidally-influenced skeletal grainstone intercalated with open marine, nodular limestone and shale and deep ramp, interbedded skeletal packstone and shale. The skeletal grainstone shows lateral migration from left to right (north to south) and channel morphology. The irregularly shaped black unit encased in skeletal grainstone is a mud-filled channel plug.

and are composed of brachiopod, bryozoan and echinoderm fragments, but have few whole fossils (Table 1). Rippled bedforms capping the skeletal grainstone/packstone beds suggest they were laterally migrating subtidal skeletal sand sheets/dunes produced by large storms or during low sea level stands on the ramp. Iron-stained, pyritic, hardgrounds on top of skeletal grainstone/packstone units likely were produced during subsequent sea level rise when sedimentation shut down.

Shaly Nodular Skeletal Wackestone/Packstone: Nodular to irregularly bedded skeletal wackestone/packstone (and minor grainstone) with up to 40% limy shale (Table 2) occurs throughout the Lexington Limestone. Whole brachiopods and bryozoans are the dominant faunal element in this facies (Fig. 6).

This unit is interpreted as a mid-ramp, open-marine facies that formed seaward of any skeletal shoals and peritidal facies, and within storm wave base. Burrowing (rarely preserved as small and large burrows), uneven compaction and patchy early seafloor cementation generated the characteristic uneven to nodular layering (Fig. 7D). Open marine, well oxygenated conditions are indicated by the diverse species (Fig. 6), high shale content, and abundance of burrowing. Relict storm deposited limestone-shale couplets with erosive bases, ripple laminations and graded bedding in these highly burrowed units indicate storm processes periodically affected the sea floor, although much of the storm imprint was destroyed by burrowing. These facies probably were deposited between fair weather and strom wave base in 10 to 30 m or so water depth.

Interbedded Irregular Bedded Skeletal Packstone, Calcisiltite and Shale: Irregular beds (10 to 20 cm thick) of skeletal packstone, and commonly with calcisiltite caps, along with up to 50% interbedded calcareous shale (Fig. 7E; Table 2) occurs off the arch. The limestone beds contain hummocky cross-stratification (HCS), normal and reverse grading, and preserved ripple bedforms. This facies contains a low diversity fauna dominated by whole brachiopods and pelecypods (Fig. 6).

This facies formed on the deeper ramp above storm wave base, but deep enough to not be burrow-homogenized, perhaps reflecting dysaerobic conditions. Abundant fine horizontal burrows and preservation of discrete storm beds were preserved. Sedimentary structures (e.g. HCS, graded bedding, preserved ripples) in the skeletal packstone and calcisiltite beds indicate storm deposition (c.f. Kreisa, 1981; Aigner, 1985). The decimeter-scale interbedded limestone and shale couplets may indicate high-frequency climate fluctuations (Elrick et al., 1991) or random input of shale from land sources, interrupting carbonate accumulation.

Evenly Bedded Calcisiltite and Shale: Evenly-bedded calcisiltite layers (up to 10 cm thick) are interbedded with up to 60% limy shale (Fig. 7F) and both preserve fine planar laminations (Table 2). This unit was deposited under the influence of traction currents, and was little modified by a burrowing infauna or by storm re-working. The scarcity of burrowing and shelly fossils and abundance of synsedimentary pyrite suggests deposition in an oxygen- poor environment, possibly below the pycnocline, in water depths that may have been only 20 m or so in deep ares protected by banks, but in open ramp settings might have been many tens of meters.

MARINE HARDGROUNDS AND KARSTIC SURFACES

Marine Hardgrounds: Marine hardgrounds are common throughout the Lexington Limestone and are marked on outcrops by iron-staining due to oxidation of pyrite surfacing the hardgrounds. They are concentrated in the basal transgressive grainstone (Curdsville Member) and above many skeletal grainstones in the upper Lexington Limestone. The hardgrounds in the lower Lexington are pyritic, phosphate encrusted irregular surfaces, and have cm-scale borings penetrating up to 10 cm (Fig. 9). Nodular hardgrounds with many mm-scale Trypanites borings cap the transgressive grainstone beds in the Curdsville Member near Frankfort. Upper Lexington hardgrounds are well developed above, and locally within, cross-bedded skeletal grainstone caps. These hardgrounds usually have little relief, are pyritic, encrusted with phosphate, and generally are overlain by pyritic shale. Rip-ups of phosphatic and pyritic hardgrounds were re-worked into some bipolar cross-bedded skeletal grainstones.

The marine hardgrounds formed during deepening of former shallow water, high-energy settings during times when sediment accumulation was low. The pyritic and phosphatic rinds and overlying shaly sediments likely formed under deep water conditions when chemical precipitation occurred. The presence of borings into the hardgrounds and ripped-up hardground fragments in skeletal grainstones indicate the hardgrounds formed at the sediment/water interface and that occasional storms or tidal currents were sufficiently strong to rip up the early-cemented, pyrite-encrusted sea floor. The phosphatic rind associated with some of the hardgrounds indicates their formation was enhanced by phosphate-rich, probably oxygen-poor, bottom water, perhaps related to upwelling during the subsequent drowning.

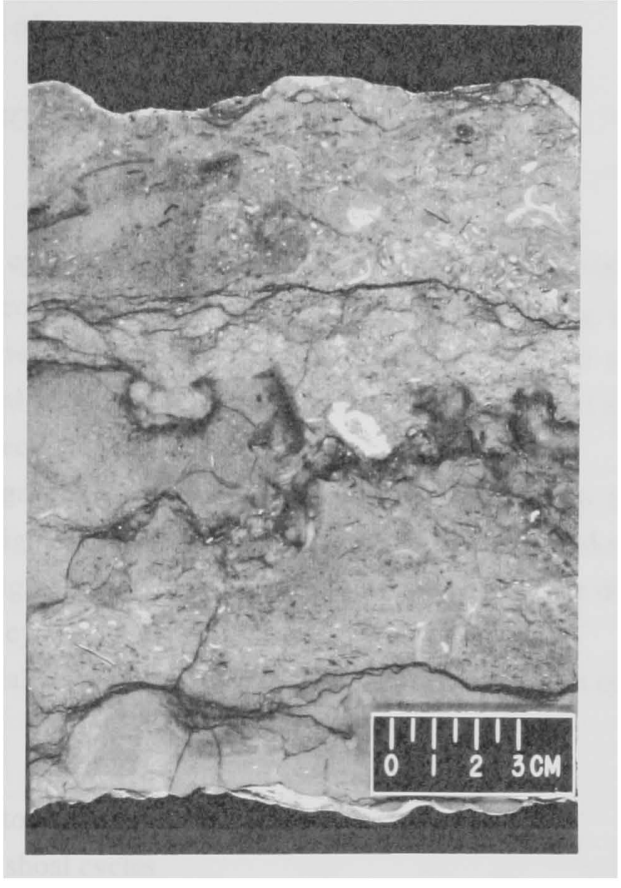

Figure 9. Photograph of marine hardground in a slab of Curdsville Member, Lexington Limestone. The hardground is the dark, irregular, phosphatic-stained surface near the center of the photo. The large white fragment directly above the hardground is chert replacing a brachiopod shell.

Karstic Surfaces: Planar and micro-scalloped surfaces, with relief up to a few centimeters, developed locally on tidal flat facies deposited on topographically high areas. Small sinkholes filled with phosphatic sands are found in the northernmost exposures of the regionally developed tidal flat facies (Salvisa Bed, Perryville Member) (Fig. 7A). The irregular surfaces and sinkholes formed by karstic processes when falling sea level exposed the tidal flats. The phosphatic sands infiltrated the sinkholes during subsequent flooding of the tidal flats.

CYCLIC STACKING OF FACIES

Meter-Scale Cycles:

Meter-scale cycles (1 to 8 m thick; Fig. 6) are evident within the small-scale sequences. These commonly are asymmetric upward shallowing units, but some are symmetrical transgressive-regressive units. These cycles tend to be tabular units traceable over several hundred meters in outcrop, and in some cases up to 30 km or more between measured sections (Fig.10).

Pyritic hardgrounds commonly cap some grainstone-rich meter-scale cycles, beneath overlying slightly deeper water units. Evidence of subaerial emergence is rare in the section, occurring only on some fenestral units and on a single dolomitic grainstone capping meter-scale cycles.

The meter-scale cycles, arranged from shallowest to deepest on the ramp (Fig. 6), are:

A) Peritidal cycles
B) Grainstone/packstone cycles
C) Thick-grainstone shoal cycles
D) Nodular carbonate cycles
E) Shale-limestone cycles
F) Rhythmite cycles

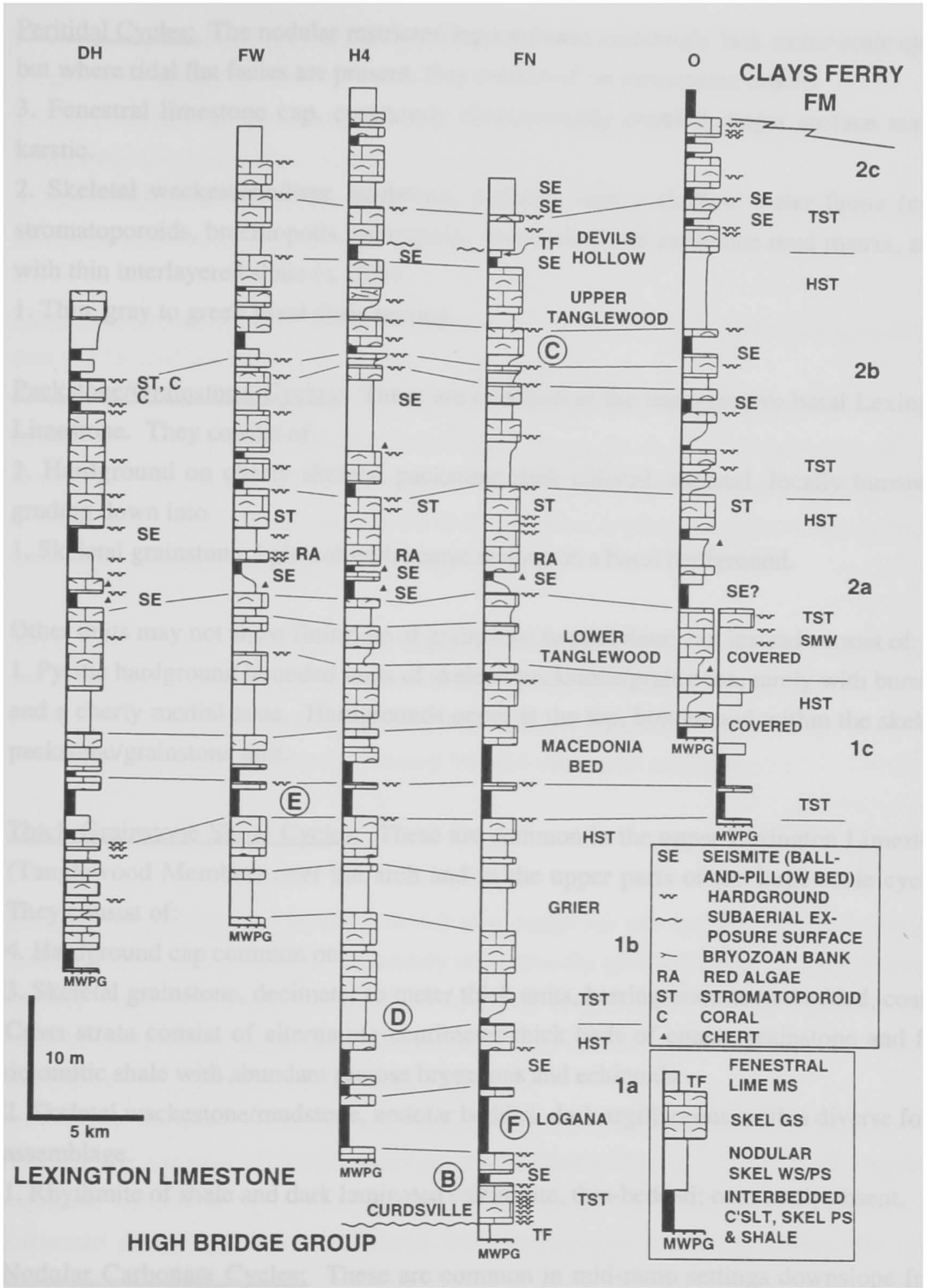

Figure 10. South to north stratigraphic cross-section of large outcrops near Frankfort, showing members and correlations of some meter-scale cycles. Macedonia Bed and Devil's Hollow Member are local units traceable on Jessamine Dome (Cressman, 1973).

Peritidal Cycles: The nodular restricted lagoon facies commonly lack meter-scale cycles, but where tidal flat facies are present, they consist of (in descending order):

3. Fenestral limestone cap, commonly diagenetically mottled; upper surface may be karstic.

2. Skeletal wackestone/lime mudstone, nodular, with a shallow water fauna (coral, stromatoporoids, brachiopods, gastropods, ostracodes) and carbonate mud matrix, along with thin interlayered shale (< 25%).

1. Thin, gray to green basal shale parting.

Packstone/Grainstone Cycles: These are common in the transgressive basal Lexington Limestone. They consist of:

2. Hardground on cherty skeletal packstone dark colored, skeletal, locally burrowed, grading down into

1. Skeletal grainstone, light colored, coarse resting on a basal hardground.

Other units may not show fining-up of grainstone to packstone, but instead consist of:

1. Pyritic hardground bounded units of skeletal packstone/grainstone, rarely with burrows and a cherty medial zone. Hardgrounds occur at the top, bottom and within the skeletal packstone/grainstone unit.

Thick-Grainstone Shoal Cycles: These are common in the upper Lexington Limestone (Tanglewood Member) over the arch and in the upper parts of the large-scale cycles. They consist of:

4. Hardground cap common on

3. Skeletal grainstone, decimeter to meter thick units, herring-bone cross-bedded, coarse. Cross strata consist of alternating centimeter thick beds of coarse grainstone and fine dolomitic shale with abundant ramose bryozoans and echinoids.

2. Skeletal wackestone/mudstone, nodular bedded, dark argillaceous, with a diverse fossil assemblage.

1. Rhythmite of shale and dark laminated calcisiltite, thin-bedded; commonly absent.

Nodular Carbonate Cycles: These are common in mid-ramp settings downslope from peritidal and shoal units. They consist of :

3. Skeletal grainstone, thin coarse-grained; rarely cross-bedded; may show a rippled top or hardground cap.
2. Shaly skeletal packstone/wackestone, nodular bedded with open marine biotas; some storm beds are present, but typically burrowed.
1. Rhythmite (rare). In symmetrical cycles, the rhythmites may grade down into nodular limestone and then thin grainstone.

Shale-Limestone Cycles: These occur in deeper ramp positions in shale-rich sections and near the base of the large-scale cycles. They consist of:
3. Thin skeletal grainstone or packstone that is rarely tidally cross-bedded.
2. Skeletal packstone/wackestone; contain interlayered storm-graded beds and up to 50% shale beds. Limestones tend to thin and fine downward with increasing shale content.
1. Rhythmite (rare). May grade down in symmetrical cycles into shaly wackestone that rests on an underlying thin grainstone cap.

Rhythmite Cycles: These typically occur in the bases of the 3rd-order sequences; more commonly they are non-cyclic. However, the rare cyclic units consist of:
2. Thin grainstone/packstone that varies from massive to laminated.
1. Thick (up to 8 m thick) units of evenly bedded calcisiltite and shale.

INTERPRETATION

Duration of Cycles: Given the 3 to 4.8 m.y. range for the duration of the Lexington Limestone, it is not possible to accurately determine the periodicities of the cycles, except broadly. Sequences 1 and 2 are about 2 to 3 m.y. long and are 3rd-order. Smaller-scale sequences (1a-c and 2a, b) are estimated to be approximately 0.6 to 1 m.y. in duration. Thus, these also appear to be 3rd-order sequences.

The duration of small-scale cycles in a subtidal section can be obtained by dividing the duration of the sequence by the number of cycles. The lack of long-term exposure surfaces in these sections allow us to neglect subaerial hiatuses, however, the uncertain amount of time associated with hardground formation makes the cycle estimates only a rough approximation. Frankfort North, the best exposed, most complete outcrop of the Lexington Limestone contains 76 cycles with average thickness of 1.1 m (range 0.2 to 5.8 m), whose calculated cycle duration is 3 to 4.8 m.y. divided by 76cycles

equals ~ 39 to 63 k.y. per cycle. This range is within the range of Milankovitch periodicities. Precessional cycles are not well preserved given the range of durations for the Lexington Limestone cycles, the lack of precessional cycles and dominance of obliquity or eccentricity signals would be compatible with glacially driven eustasy associated with continental ice-sheets (Goldhammer et al., 1990).

Tectonic Controls on 3rd-Order Cycle Distribution: The facies within the small-scale sequences is controlled by local and regional tectonics. Shallow water, carbonate-dominated deposition of the Lexington Limestone occurred along the Cincinnati Arch only because it was uplifted while the remainder of the Appalachian Basin and the Sebree trough were deeper basins dominated by shaley turbidites or storm deposits.

The regionally developed tidal flat facies (Salvisa Bed-Perryville Member) prograded along the apex of the Cincinnati Arch indicating they were structurally controlled (Mackey, 1972). The distribution of the shaly calcisiltite (Brannon Member) above the regional tidal flat facies was also structurally controlled along the edge of the Jessamine Dome (Kulp, 1995). If the Jessamine Dome is fault-bounded, as suggested by Borella and Osborne (1978), then the Brannon Member rhythmites (Fig. 4) may be filling in a topographic low on a downthrown block adjacent to the uplifted Jessamine Dome. The abundant seismites in shaly facies above the regional shallowing of Sequence 1 (Salvisa Bed-Perryville Member and correlative grainstone) supports a tectonic control for formation of the Jessamine Dome. Similarly, the abundance of tidally influenced skeletal grainstones over the Jessamine Dome while correlative rocks to the south are shale-dominated deeper water calcisiltites, skeletal packstones and shale with rare skeletal grainstones and restricted facies indicate this dome was topographically high during deposition of the upper Lexington Limestone. Thus, tectonics controlled much of the facies distribution on this ramp.

Magnitude of High-Frequency Sea Level Changes

The maximum magnitude of the high-frequency sea level changes may be estimated from distinctive meter-scale cycles which show juxtaposition of deep water facies (rhythmites), with overlying shallow tidally-deposited (grainstone) facies. Such cycles are common in the TST's of small-scale sequences in the Lexington Limestone. This would suggest sea levels were raised a maximum of 20 to 50 m to deposit the rhythmites, and then fell to form the tidally cross-bedded grainstone. Little of the

shallowing could have been due to sedimentation which would only have filled in a few meters of accommodation space.

Most meter-scale cycles throughout the Lexington Limestone do not show such a juxtapositon of rhythmite and grainstone facies, but instead are composed of interbedded shale-limestone or nodular limestone/shale overlain by skeletal grainstone or peritidal limestone caps (Fig.6). These suggest sea level fluctuations of 10 to perhaps 30 m. Substantial changes in sea level also are suggested by the pyritized hardgrounds on drowning surfaces on grainstone beds. These pyrite encrusted hardgrounds could have developed near or below the pycnocline, or they also could have developed in restricted shallow water settings, beneath a "microbial soup" covering a stagnant bottom between banks. In either case the deposition of synsedimentary pyrite would require a quiet, stratified water mass.

Large amplitude sea-level oscillations (>20 m) cannot be driven solely by changes in groundwater, lake, or heating/cooling of global sea temperatures (Jacobs and Sahagian, 1993) Gondwana glaciation was probably occurring during deposition of the Lexington Limestone and was the most likely mechanism that formed the meter-scale cycles. If so, then this suggests glaciation in the Ordovician began by 454 Ma and may have lasted at least 9 m.y., which is contrary to recent isotopic data (Brenchley et al., 1994).

High-frequency sea level fluctuations of 10 to 30 m which apparently occurred during deposition of the HST's of the Lexington 3rd-order sequences, should have left some record in the peritidal sections updip. The only major disconformity developed is on the Perryville tidal flat facies, which is a 3rd-order sequence boundary. In contrast, sea level drop at the tops of other meter-scale peritidal cycles is only evidenced by lighter (oxidized) colors near cycle tops, mottling of the caps due to oxidizing groundwaters migrating down through the section via fenestral and burrow passageways, and thin gray-green shale layers separating cycles; such light-colored shale layers are common on other high-frequency cycles, and may be primitive paleosols, or fine siliciclastic muds carried into supratidal areas during exceptional storm flooding (Walls and Burrowes, 1985). Because the peritidal sections formed during high-frequency highstands, they should have felt the full effect of any sea level fall, however, because they lack intercalated deep water facies, we suggest that sea level fluctuations during 3rd-order HST deposition may have been were reduced relative to those in the TST's. Also, lack of land plants at this time would allow carbonate sediments to be exposed without undergoing the intense soil formation, karsting and caliche formation observed today. The relatively wet climate and

lack of land plants, may have inhibited soil and caliche formation, helping to maintain relatively high groundwaters beneath emergent flats, and limiting depth of vadose alteration. The dominantly calcitic mineralogy of the offshore "carbonate factory" (brachiopods and bryozoans) also may have resulted in relatively stable calcitic mineralogies in the peritidal facies, which would tend to have inhibited dissolution and vadose/phreatic diagenesis.

EVIDENCE FOR COOL WATER DURING LEXINGTON LIMESTONE DEPOSITION

Paleogeographic Evidence: Paleogeographic reconstructions of North America based on paleomagnetism (Van der Voo, 1988; Scotese and McKerrow, 1990; Webby, 1993) and paleoclimatic indicators (Witzke, 1990) place Kentucky at 20 to 30° south latitude during the Middle to Late Ordovician (Fig. 11) suggesting a temperate climatic setting. The climate appears to have been humid because the sediments lack evaporites or ooids, or well-preserved algal laminites which are most common on arid tropical ramps (Read, 1985). Also, the tidal flat facies contain abundant fenestrae that show iron-stained (oxidative) "ground-water mottling" and indicative of humid, wet climates.

Isotopic Evidence: Isotopic studies of brachiopods in the Lexington equivalent, the Trenton Group of New York suggest near-surface and mid-shelf waters were cool (13-19°C), had low-salinities, and became progessively warmer and more saline with depth (Railsback et al., 1990). The low surface salinities are probably due to the humid climatic setting in a semi-restricted basin. Oxygen isotopes from brachiopods in North American Ordovician strata show an ~2 per mil positive shift at the beginning of the Caradocian that may indicating a cooling of ocean waters (Popp et al., 1986). However, the limited data set and lack of high-resolution dating used to accurately time this shift obscures how and why this shift occurred.

Faunal Evidence: The dominance of brachiopods and bryozoans in the Lexington Limestone has some similarities to modern bryomol assemblages (Lees and Buller, 1972; Lees, 1975; Nelson, 1988). The brachiopods and bryozoans are highly diverse with numerous genera (Cressman, 1973; Fig. 6). However, the species diversity, especially of corals, stromatoporoids (Hudson, 1984), and red algae is low with respect to tropical carbonates (Nelson, 1988). Monoplacopherans (molluscs) in the subtidal facies (Fig. 5) may indicate cool ocean waters, since modern-day monoplacopherans are restricted to

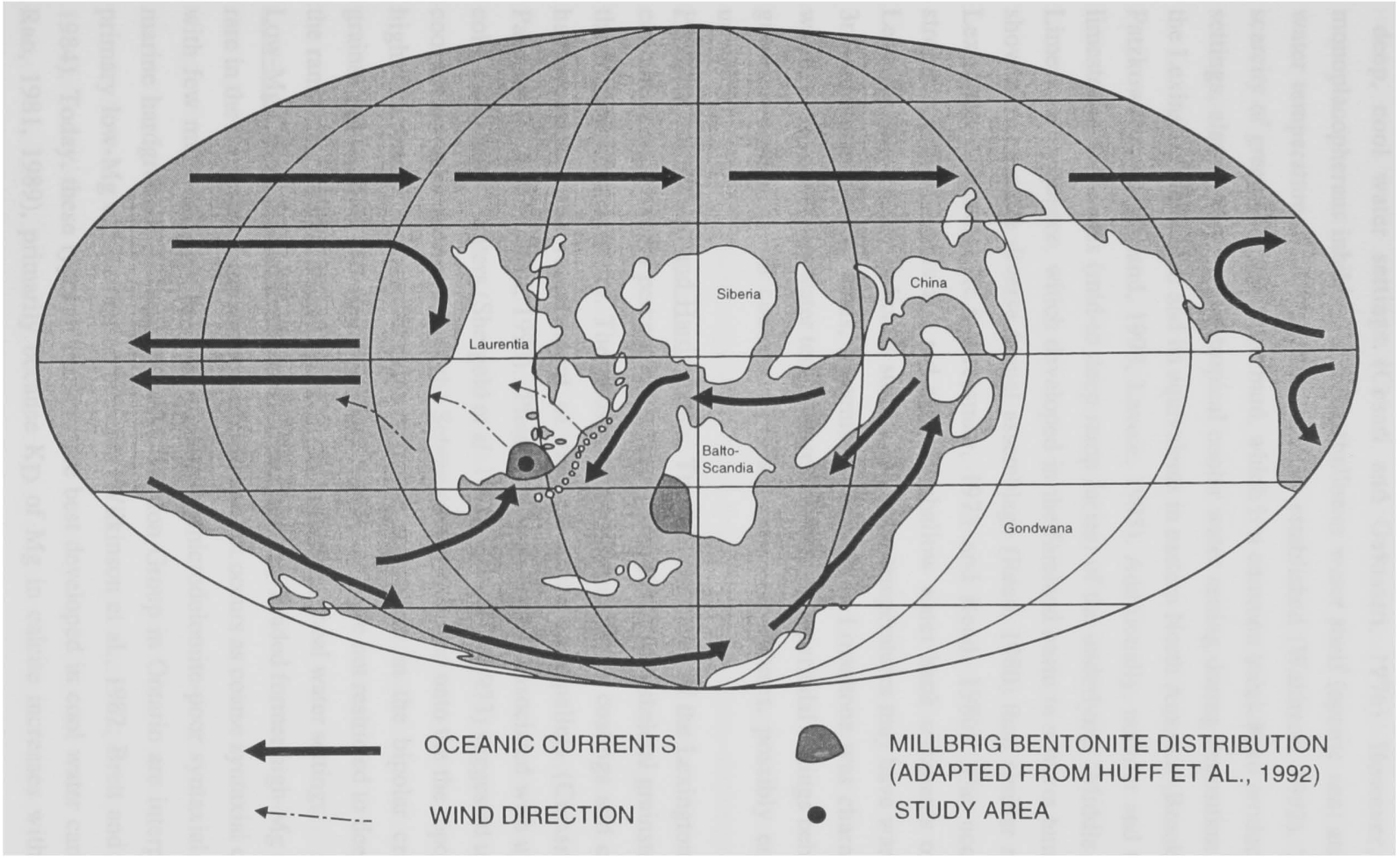

Figure 11. Proposed paleogeographic reconstruction during the late Middle Ordovician (from Scotese and McKerrow, 1990), the study area is shown by a solid black dot. Oceanic currents are modified from Wilde (1991). Note the cool current flowing from the southwest to the northeast onto the southern portion of Laurentia, and possible blockage of warm, equatorial currents by the Taconic magmatic arc.

deep, cool water settings (Cesari and Guidastri, 1976). However, Ordovician monoplacopherans inhibited a much shallower water shelf (epeiric sea) and their cool water temperature affinities have not been established (Wahlman, 1992). The relative scarcity of green algae and lime mud, which is a common breakdown product in tropical settings, also supports a non-tropical cooler water setting during deposition of much of the Lexington Limestone and its equivalents in eastern North America (Brookfield, 1988; Patzkowsky and Holland, 1993; Lavoie, 1995). Additionally, nodular and thin-bedded limestones and shales (mid-to deep ramp facies) of the underlying "Middle Ordovician Limestone" sequence, which developed in the foreland basin in a warm humid climate, show a much more diverse faunal assemblage (Read, 1980) than similar rocks in the Lexington Limestone (c.f. Cressman, 1973 and Read, 1980). The occurrence of stromatoporoids, corals and red algae in shallow water bank sediments of the upper Lexington Limestone, indicates surface sea water temperatures may have warmed during 3rd-order highstands. Thus, it seems the Lexington Limestone was characterized by warm, near surface sea water temperatures, especially in peritidal settings behind skeletal grainstone shoals, and cooler deeper subtidal temperatures, possibly enhanced by upwelling.

Phosphatized Grains and Hardgrounds: The subtidal facies of the Lexington Limestone contain 0.8-2.4 weight percent P_2O_5 (Cressman, 1973) with skeletal grainstones having the highest concentration. The phosphate usually occurs as coatings and crusts along hardgrounds or as replacement of skeletal grains and pellets (Cressman, 1973; Patzkowsky and Holland, 1993). Phosphate is commonly associated with upwelling of cold, nutrient-rich waters (Shergold et al. 1991). Cressman (1973) suggested upwelling of cool deep waters occurred from the Sebree trough eastward onto the the topographically high Cincinnati Arch. The abundance of phosphate in the bipolar cross-bedded grainstones indicate that cool phosphate-rich waters were not restricted to deeper parts of the ramp but extended into shallow, tidally influenced shoal water settings.

Low-Mg Calcite Marine Cements and Hardgrounds: Bladed former high-Mg cements are rare in the Lexington Limestone, and most cement occurs as coarse syntaxial overgrowths with few microdolomite inclusions . Similar microdolomite-poor syntaxial cements in marine hardgrounds of the correlative Trenton Group in Ontario are interpreted to be primary low-Mg calcite marine cements (Wilkinson et al., 1982; Brett and Brookfield, 1984). Today, these types of cements are best developed in cool water carbonates (cf. Rao, 1981, 1989), primarily because K_D of Mg in calcite increases with increasing

temperature (Hardie and Fuchtbauer, 1976), though many other factors may also be important in development of these cements (Givens and Wilkinson, 1986). Given that Ontario was closer to the equator than Kentucky (Scotese and Mckerrow, 1990) it is likely that the Lexington carbonates formed in even cooler waters than the Trenton Group of Ontario (Brookfield, 1988), although the data from the marine cements is equivocal.

The Lexington Limestone hardgrounds and the associated meter-scale cycles are similar to hardgrounds and meter-scale cycles in Oligocene-Miocene cool water carbonates of southern Australia (James and Bone, 1992, 1994). Similarities include:

1. pyritic staining and coatings on regionally developed hardgrounds,
2. bioerosion and corrosion evident on hardground surfaces,
3. coarse, clean grainstone overlies hardgrounds, and grades upward into burrowed and muddier sediment.

These types of hardgrounds commonly develop on high-energy shelves with cool, upwelling waters and slow sedimentation rates typical of the modern-day cool water carbonates of southern Australia (James et al., 1992; Boreen et al., 1993).

Sedimentation Rate: On most tropical platforms, which are punctuated by numerous subaerial disconformities, calculations of sedimentation rates from thickness divided by time generally give "accomodation rate". Because there are few subaerial disconformities in this dominantly subtidal section, sedimentation rates for the Lexington Limestone can be estimated from the formation thickness divided by time. Based on the 91 m thick section and 3 to 3.8 m.y. duration, sedimentation rates for the Lexington Limestone are about 2 to 3 cm/kyr . These low rates are compatible with modern cool water carbonate rates (< 10 cm/kyr, Nelson, 1988) although the deep ramp setting of much of the Lexington Limestone would tend to keep rates low, as would the high turbidity induced by the abundant, fine clastic influx, indicated by the widespread shale stringers and interbeds. Nevertheless, these low sedimentation rates prevented the bulk of the ramp from building up rapidly to sea level, during high-frequency high stands, and thus limited subaerial exposure to updip peritidal sections of the ramp during sea level falls. Consequently there is little evidence for subaerial disconformities in offshore facies, even though the basin apparently was subjected to numerous high-frequency eustatic fluctuations. In contrast, the tropical Late Cambrian-Early Ordovician platform in the Appalachians rapidly built back to sea level following incipient drowning events and the resulting section is dominated by meter-scale peritidal cycles with cycle-capping disconformities, reflecting deposition on avery shallow, flat topped, aggraded shelf (Bova

and Read, 1987; Koerschner and Read, 1989; Montanez and Read, 1992). Similarly, the early Mohawkian High Bridge Group in Kentucky and Middle Ordovician Limestone in Viginia (Fig. 6) are dominated by 1 to 10 m scale peritidal cycles with cycle capping disconformities and karstic surfaces (Grover and Read, 1977; Read and Grover, 1980) reflecting higher sedimentation rates on the shallow ramp and/or smaller high-frequency sea level oscillations, which allowed peritidal facies to keep up with subsidence of the ramp.

The Lexington Ramp Compared to Modern Cool Water Ramps: The Lexington Limestone is comparable to modern cool water shelf deposits of Australia (Table 3) (Collins, 1988; James et al., 1992; Boreen et al., 1993). Similarities include: bryomol faunas, low-Mg calcite cements, phosphatic encrusted hardgrounds, evidence of upwelling, scarcity of tidal flat capped regional cycles, and abundance of hardground-bounded cycles. However, there are some fundamental differences between these settings. The Lexington Limestone was deposited at non-tropical latitudes (20-30^{o} S) whereas the Australian sediments are being deposited at higher latitudes (32-40^{o} S). Also, the Australian sediments are forming on a passive margin with a steep continental slope, under the influence of intense swells generated by the large fetches of the deep, open ocean (James et al., 1992; Boreen et al., 1993), whereas the Lexington Limestone deposition was dominated by tidal and storm processes on a large, shallow epeiric sea ramp peripheral to a foreland basin. Swell wave base on the Australian margin is commonly 50 to 130 m (Collins, 1988; James et al., 1992), whereas storm wave base in a setting such as the Ordovician epeiric sea of North America likely was on the order of a few tens of meters. Additionally, many of the hardgrounds capped cycles of southern Australia were subaerially exposed and calichified prior to subsequent drowning and formation of the hardgrounds (Collins, 1988), however, these features are not discernible in the Lexington Limestone hardgrounds; perhaps reflecting the lack or scarcity of Ordovician land plants, in contrast to the extensive vegetation on exposed carbonate platforms today.. The tidal flat and restricted muddy (lagoonal) facies of the Lexington Limestone have no correlatives in the modern-day settings where high-energy beach facies pass landward into eolianites and restricted ponds or lakes (Lowry, 1970).

Table 3. Comparison of characteristics of a modern-day temperate carbonate shelf off southern Australia and the late Middle Ordovician Lexington Limestone

	Modern-day southwest Australia	Lexington Limestone
Tectonic Setting	Swell Dominated Passive Margin	Tidal, Storm Dominated Ramp Peripheral to Foreland Basin
Water Temperature	< 18°C	13-19°C (Railsback et al., 1990)
Fauna	Bryozoan dominated offshore; mollusc and coralline algae dominated nearshore	Bryozoan-brachiopod-echinoderm dominated
Cement	Low-Mg -calcite and aragonite in shallow water, low -Mg-calcite mid-shelf to slope	Low Mg-calcite and high-Mg calcite in
Hardgrounds/ Disconformities	Caliches drowned and encrusted with pyrite; colonized by red algae.	Pyritic and phosphatic, relief from less than 1 cm to more than 20 cm; overlain by pyritic shales
Latitude	32-40° S	20-30° S
Shallow Shelf Sediments	Algal pavements, quartzose bivalve bryozoan gravels, bivalve lithoclast gravel; abundant hardgrounds	Fenestral lime mudstone, nodular skeletal wackestone and packstone, cross-bedded skeletal grainstone, abundant hardgrounds
Water depths	< 70m	< 10 m
Mid Shelf-Intermediate Ramp Sediments	Cross-bedded bryozoan gravel, laminated graded bioclastic sand, poorly sorted mollusc sand	Laminated skeletal grainstone, nodular skeletal wackestone/packstone and shale
Water depths	60-130 m	10-30 m
Deep Shelf or Ramp Sediments (Above storm wave base)	Fine grained bioclastic sand, delicate branching bryozoan muddy sand	Interbedded irregular beds of skeletal packstone, calcisiltite, and shale
Water depths	130-250 m	30-50 m
Upper Slope/Basinal Sediments (Below storm wave-base)	Robust branching bryozoan muddy sand, coral mollusc, brachiopod mudstone, pelletal skeletal mud	Evenly bedded calcisiltite and calcareous shale
Water depths	250-500 m	> 50 m

ORIGIN OF COOL WATERS DURING LEXINGTON LIMESTONE DEPOSITION

The Lexington Limestone and time-equivalent units further north were deposited in latitudes from 15 to 30° S (Scotese and McKerrow, 1990). Today waters along many coastlines at these latitudes might be somewhat warmer than those proposed for the Ordovician, thus we need to examine if there is evidence for overall cooler waters regionally in the later Ordovician and why cool surface waters might have migrated equatorward. Patzkowsky and Holland (1993) suggested the Lexington Limestone formed as a result of local deepening associated with thrust loading, that caused upwelling of cooler, less saline intermediate waters, leading to nutrient-poisoning and increased turbidity, which favored cool water faunas at the expense of warm water faunas. Given the paleogeographic location of eastern North America in the Late Middle Ordovician, prevailing wind currents at 20 to 30° S latitude should have moved from the southeast toward the northwest, causing offshore currents that would promote upwelling onto the Cincinnati Arch region (Fig. 11).

Global rise in sea level may have caused cooler, deeper, marine waters to flood the continent, leading to a generally deeper subtidal depositional setting because sea levels were at near-record high levels (Vail et al., 1977; Hallam, 1984). If bottom waters in the Taconic foredeep in New York were warm and saline (Railsback et al., 1990) then upwelling waters from here could not have caused cool bottom conditions on the ramp. Thus the cooler bottom waters may have come from the southern passive margin.

Gradual southward movement of North America (Laurentia) from 10° S in the Early Ordovician to 20 to 30° S in the Late Ordovician (Scotese and McKerrow, 1990) could have aided cooling of the epeiric sea. However, a simple southward migration still does not explain why the northern Appalachian Basin was undergoing cool water deposition in the Middle Ordovician. Also, the transition from warm water tidal flats of the underlying High Bridge Group up into cool water, subtidal-dominated ramp facies of the Lexington Limestone is a sharp boundary with little evidence of prolonged exposure (less than 1 m.y. according to Patzkowsky and Holland, 1993). This suggests there was a rapid shift in temperature and water depth across the Early to Later Middle Ordovician, which cannot be related simply to plate motion.

Global cooling of the oceanic surface waters resulting in cooler water, epeiric sea-deposition, may have been associated with the onset of continental glaciation of Gondwana, which may have begun during the Caradocian (Frakes et al., 1992) (Fig. 12).

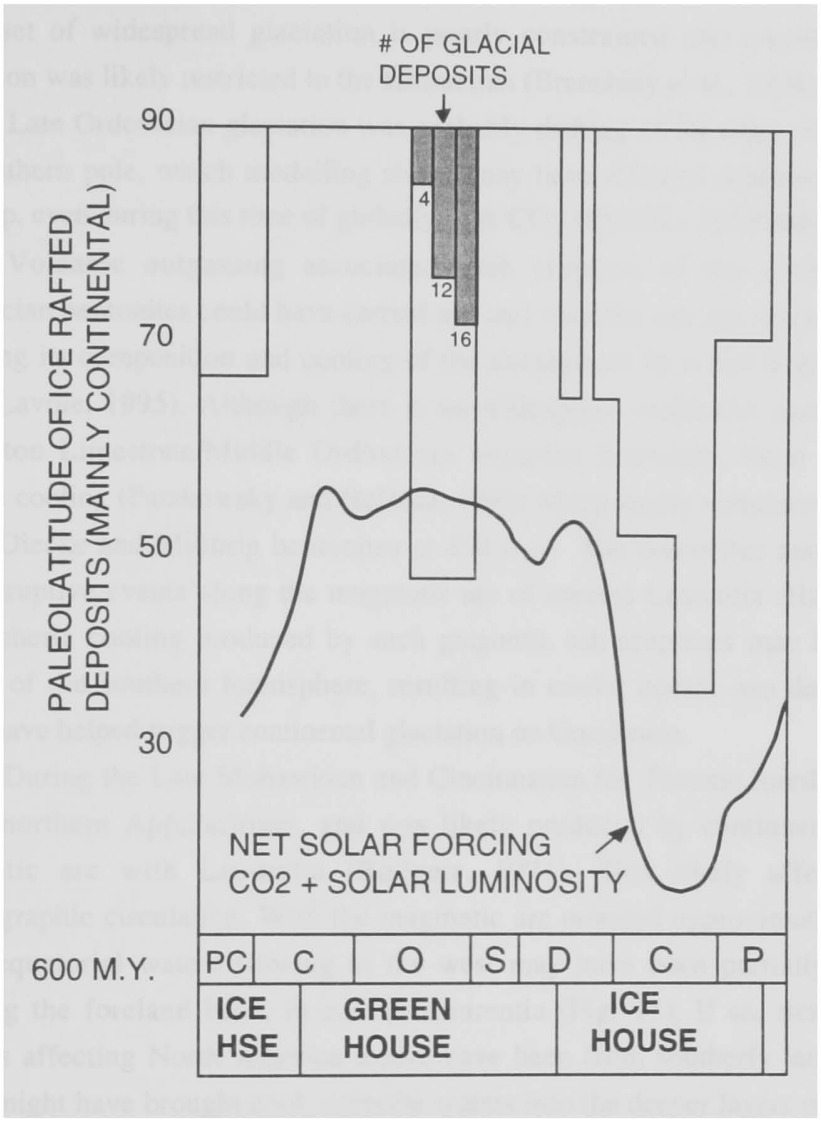

Figure 12. Diagram showing global climate setting during the Late Proterozoic through Paleozoic (adapted from Frakes et al., 1992).

The moderate amplitude sea level flucuations evident in the meter-scale cycles of the Lexington Limestone, suggest glacio-eustasy was occurring at this time. However, timing the onset of widespread glaciation is poorly constrained and maximum continental glaciation was likely restricted to the Hirnantian (Brenchley et al., 1994). A major trigger for the Late Ordovician glaciation was probably drifting of the edge of Gondwana over the southern pole, which modelling shows may have allowed continental ice sheets to build up, even during this time of globally high CO_2 (Crowley and Baum, 1991).

Volcanic outgassing associated with eruption of the widespread Middle Ordovician bentonites could have carried ash and volatiles into the stratosphere, possibly changing its composition and cooling of the atmosphere by a few degrees (Huff et al., 1993, Lavoie, 1995). Although there is no widespread extinction associated with the Lexington Limestone/Middle Ordovician sequence boundary, there is evidence for oceanic cooling (Patzkowsky and Holland, 1993) which nearly coincides with deposition of the Diecke and Millbrig bentonites at 454 m.y. The bentonites may be just one of many eruptive events along the magmatic arc of eastern Laurentia (Huff et al., 1992). Atmospheric cooling produced by such giagantic ash eruptions may have cooled the oceans of the southern hemisphere, resulting in cooler epeiric sea deposition, which might have helped trigger continental glaciation on Gondwana.

During the Late Mohawkian and Cincinnatian the Taconic foredeep was located in the northern Appalachians, and was likely produced by continued collision of a magmatic arc with Laurentia (Rodgers, 1971). This likely affected the local oceanographic circulation. With the magmatic arc oriented approximately north-south, warm equatorial waters flowing to the west may have been partially blocked from reaching the foreland basin in eastern Laurentia (Fig. 11). If so, most of the ocean currents affecting North America would have been from southerly latitudes (Fig. 11) which might have brought cool, subpolar waters into the deeper layers of the epeiric sea (Wilde, 1991).

CONCLUSIONS

1. The late Middle Ordovician (Late Mohawkian) Lexington Limestone in Kentucky is a cool water, mixed carbonate-siliciclastic unit that formed on a pericratonic ramp peripheral to the Taconic Appalachian foredeep. Evidence for cool water includes:

bryomol fauna, abundant phosphatized grainstones and hardground surfaces, and lack of warm water carbonates such as oolites and algal laminites.

2. The Lexington Limestone is the TST of an approximately 9 to 14 m.y. supersequence. The supersequences formed on a carbonate ramp that deepened to the north, west and east. During the 2nd-order late highstand/lowstand it shallowed to the south into tidal flat facies. Tectonics controlled the location of the foredeep to the northeast, and the narrow Sebree trough to the west, and the distribution of shoal water facies over the Cincinnati Arch.

3. The Lexington sequence 1 contains 3 smaller scale, 3rd-order depositional sequences and sequence 2 contains 2 small-scale sequences (5 to 25 m thick). Each small-scale depositional sequence contains well-defined flooding events and upward shallowing HST.

4. The third-order depositional sequences contain numerous high-frequency cycles (1 to 8 m thick), which are asymmetric shallowing upward cycles or symmetrical transgressive-regressive cycles. In TST's, these meter-scale cycles contain deep water rhythmites up into nodular carbonates and grainstone caps. They reflect moderate amplitude high frequency sea level changes of up to 30 m or more, and periodicities of 39 to 63 k.y. There is little evidence of precessional cyclicity. In HST's, meter-scale cycles are of nodular carbonate up into grainstone on the mid-ramp, and reflect lower amplitude sea level changes (10 to 30 m) with little evidence of exposure. In HST's on the inner ramp, peritidal cycles show some ground-water mottling in caps, but little major karsting except at the second-order sequence boundary (top of Salvisa Bed-Perryville Member).

5. The Ordovician cool water carbonates may reflect cooling due to southward drift of Laurentia, high sea levels on the craton (causing deeper water, cooler conditions, and depressed sedimentation rates), northward marine currents carrying cool southern waters northward into the epeiric sea, explosive volcanism triggering global cooling, and drift of Gondwana near the South Pole. The Taconic arc may have acted as a sill or barrier to southward moving currents, thus preventing warm, tropical waters from reaching the Appalachian foreland basin and allowing cool subpolar currents from the south to inundate the ramp.

REFERENCES

Aigner, T., 1985, Storm Depositional Systems: Lecture notes in Earth Sciences, v. 3, Springer-Verlag, Berlin, 174 p.

Bergstrom, S.M., and Sweet, W.C., 1966, Conodonts from the Lexington Limestone (Middle Ordovician) of Kentucky and its lateral equivalents in Ohio and Indiana: Bulletin of American Paleontology, v. 50, p. 271-441.

Berner, R.A., 1990, Atmospheric carbon dioxide levels over Phaneozoic time: Science, v. 249, p. 1382-1386.

Berner, R.A., 1992, Palaeo-CO_2 and climate: Nature, v. 358, p. 114.

Black, D.F.B., and Haney, D.C., 1975, Selected structural features and associated dolostone occurrences in the vicinity of the Kentucky River Fault System: Annual Field Conference, Geological Society of Kentucky, Kentucky Geological Survey, Lexington, Ky, p. 6-43.

Boreen , T., James, N.P., Wilson, C., and Heggie, D.,.1993, Surficial cool-water carbonate sediments on the Otway continental margin, southeastern Australia: Marine Geology, v. 112, p. 35-56.

Borella, P.E., and Osborne, R.H., 1978, Late Middle and early Late Ordovician history of the Cincinnati arch Province, central Kentucky to central Tennessee: Geological Society of America Bulletin, v. 89, p. 1559-1573.

Bova, J.A., and Read, J.F., 1987, Incipiently drowned facies within a cyclic peritidal continental ramp sequence, Chepultepec interval, Virginia Appalachians: Geological Society of America Bulletin, v. 98, p. 714-727.

Brenchley, P.J., Marshall, J.D., Carden, G.A.F., Robertson, D.B.R., Meidla, T., Hints, L., and Anderson, T.F., 1994, Bathymetric and isotopic evidence for short-lived Late Ordovician glaciation in a greenhouse period: Geology, v. 22, p. 295-298.

Brett, C.E., and Brookfield, M.E., 1984, Morphology, faunas and genesis of Ordovician hardgrounds from southern Ontario, Canada: Palaeogeography, Palaeoclimatology, Palaeoecology, v. 46, p. 233-290.

Brookfield, M.E., 1988, A mid-Ordovician temperate carbonate shelf-The Black River and Trenton Limestone Groups of southern Ontario, Canada: Sedimentary Geology, v. 60, p. 137-154.

Cable, M.S., and Beardsley, R.W., 1984, Structural control on Late Cambrian and Early Ordovician carbonate sedimentation in eastern Kentucky: American Journal of Science, v. 284, p. 797-823.

Caputo, M.V., and Crowell, J.C., 1985, Migration of glacial centers across Gondwana during Paleozoic Era: Geological Society of America Bulletin, v. 96, p. 1020-1036.

Cesari, P., and Guidastri, R., 1976, Contributo alla conoscenza dei Monoplacophori recenti: Conchliglie, v. 12, p. 223-250.

Collins, L.B., 1988, Sediments and history of the Rottnest Shelf, southwest Australia: a swell-dominated, non-tropical carbonate margin: Sedimentary Geology, v. 60, p. 15-49.

Cressman, E.R., 1973, Lithostratigraphy and depositional environments of the Lexington Limestone (Ordovician) of central Kentucky: United States Geological Survey Professional Paper 768, 61 pp.

Cressman, E.R., and Noger, M.C., 1976, Tidal-flat carbonate environments in the High Bridge Group (Middle Ordovician) of central Kentucky: Kentucky Geological Survey, Series 10, Report of Investigations 18, 15 pp.

Crowley, T.J., and Baum, S.K., 1991, Toward reconciliation of Late Ordovician (~440 Ma) glaciation with very high CO_2 levels: Journal of Geophysical Research, v. 96, p. 22,597-22,610.

Drake, A.A., Sinha, A.K., Laird, J., and Guy, R.E., 1989, The Taconic orogin in the Appalachian Oauchita orogen in the U.S.: *in* Hatcher, R. D., Thomas, W. A., and Viele, G.W. (eds), Geological Society of America, Boulder, CO, v. F-2, p. 101-178.

Elrick, M., Read, J.F., and Coruh, C., 1991, Short-term paleoclimatic fluctuations expressed in lower Mississippian ramp-slope deposits, southwestern Montana: Geology, v. 19, p. 799-802.

Ettensohn, F.R. (ed.), 1992, Changing interpretations of Kentucky geology--layer-cake, facies, flexure, and eustacy: State of Ohio, Department of Natural Resources, Miscellaneous Report No. 5, 184 p.

Rast, N., and Ettensohn, F.R., 1995, Effects of seismic disturbance on epicontinental depositional systems in the Ordovician and Devonian rocks of central Kentucky: Geological Society of America Annual Meeting Program with Abstracts, v. 27, p. A 381.

Frakes, L.A., Francis, J.E., and Syktus, J.I., 1992, Climatic modes of the Phanerozoic: Cambridge University Press, Cambridge, UK, 274 pp.

Goldhammer, R.K., Dunn, P.A., and Hardie, L.A., 1990, Depostiional cycles, composite sea level changes, cycle stacking patterns, and thehierarchy of stratigraphic forcing: examples from platform carbonates of the Alpine Triassic: Geological Society of America Bulletin, v. 102, p. 535-562.

Grossnickle, E.A., 1985, Tempestites and depositional interpretations of the Middle Ordovician Curdsville Limestone of central Kentucky: (unpub. M.S. thesis) University of Kentucky, Lexington, KY, 107 p.

Grover, G., Jr., and Read, J.F., 1978, Fenestral and associated vadose diagenetic fabrics of tidal flat carbonates, Middle Ordovician New Market limestone, southwestern Virginia: Journal of Sedimentary Geology, v. 48, p. 453-473.

Hallam, A., 1984, Pre-Quaternary sea-level changes: Annual Review of Earth and Planetary Sciences, v. 12, p. 205-243.

Hambrey, M.J., 1985, The Late Ordovician-Early Silurian glacial period: Palaeogeography, Palaeoclimatology, Palaeoecology, v. 51, p. 273-289.

Hardie, L.A., and Fuchtbauer, H., 1976, Experimentally determined homogenous distribution for precipitated magnesian calcites; applications to marine carbonate cements: Geological Society of America Annual Meeting Program with Abstracts, v. 8, p. 877.

Haq, B.U., Hardenbol, J., and Vail, P.R., 1987, Chronology of fluctuating sea level since the Triassic: Science, v. 235, p. 1156-1167.

Harland, W.B., Armstrong, R.L., Cox, A.V., Craig, L.E., Smith, A.G., and Smith, D.G., 1990, A geologic time scale, 1989: Cambridge University Press, Cambridge, UK, 261 pp.

Haynes, J.T., 1994, The Ordovician Deicke and Millbrig K-Bentonite beds of the Cincinnati Arch and the southern Valley and Ridge Province: Geological Society of America Special Paper 290, 80 p.

Hrabar, S.V., Cressman, E.R., and P.E. Potter, 1971, Crossbedding of the Tanglewood Limestone Member of the Lexington Limestone (Ordovician) of the Blue Grass region of Kentucky: Brigham Young University Geology Studies, v. 18, p. 99-114.

Hudson, T.W., 1984, Depositional environment, diagenesis, and stromatoporoid paleoecology of Labrechia Huronensis (Billings) beds in the Tanglewood Limestone and Stamping Ground Members of the Lexington Limestone (Ordovician) central Kentucky: (Unpubl. M.S. thesis) University of Cincinnati, Cincinnati, OH, 299 p.

Huff, W.D., Bergstrom, S.M., and Kolata, D.R., 1992, Gigantic Ordovician volcanic ash fall in North America and Europe: Biological, tectonomagmatic, and event-stratigraphic significance: Geology, v. 20, p. 875-878.

Huff W.D., Kolata, D.R., and Bergstrom, S.M., 1993, Possible climatic impact of the Middle Ordovician Millbrig-Big Bentonite ultraplinian volcanic eruption: Geological Society of America, Northeastern Section, Abstracts with Programs, v. 25, p. 25.

Jacobi, R.D., 1981, Peripheral bulge-a causal mechanism for the Lower/Middle Ordovician disconformity along the western margin of the northern Appalachians: Earth and Planetary Science Letters, v. 56, p. 245-251.

Jacobs, D., and Sahagian, D., 1993, Climate induced fluctuations in sea level during non-glacial times: Nature, v. 361, p. 710-712.

James, N.P., and Bone, Y., 1991, Origin of a cool-water, Oligo-Miocene deep shelf limestone, Eucla Platform, southern Australia: Sedimentology, v. 38, p. 323-341.

James, N.P., and Bone, Y., 1992, Synsedimentary cemented calcarenite layers in Oligo-Miocene cool water shelf limestones, Eucla Platform, southern Australia: Journal of Sedimentary Geology, v. 62, p. 860-872.

James, N.P., Bone, Y., Von der Borch, C.C., and Gostin, V.A., 1992, Modern carbonate and terrigeneous clastic sediments on a cool-water, high-energy, mid-latitude shelf: Lacepede, southern Australia: Sedimentology, v. 39, p. 877-903.

James, N.P., and Bone, Y., 1994, Paleoecology of cool-water, subtidal cycles in Mid-Cenozoic limestones, Eucla Platform, southern Australia: Palaios, v. 9, p. 457-476.

Jennette, D.C., and Pryor, W.A, 1993, Cyclic alternation of proximal and distal storm facies: Kope and Fairview Formations (Upper Ordovician), Ohio and Kentucky: Journal of Sedimentary Petrology, v. 63, p. 183-203.

Keith, B.D., 1989, Regional facies of Upper Ordovician Series of eastern North America: *in* B.D. Keith (ed.), The Trenton Group (Upper Ordovician Series) of eastern North America, American Association of Petroleum Geologists, Tulsa, OK, Studies in Geology #29, p. 1-16.

Koerschener, W.F, III, and Read, J.F., 1989, Field and modelling studies of Cambrian carbonate cycles, Virginia Appalachians: Journal of Sedimentary Petrology, v. 51, 823-848.

Kreisa, R.D., 1981, Storm-generated sedimentary structures in subtidal marine facies with examples from the Middle and Upper Ordovician of southwestern Virginia: Journal of Sedimentary Petrology, v. 51, p. 823-848.

Kreisa, R.D., Dorobek, S.L., Accorti, P.J., and Ginger, E.P., 1981, Recognition of storm-generated deposits in the Cincinnatian Series, Ohio: Geological Society of America Program with Abstracts, v. 13, p. 285.

Kulp, M., 1995, Paleoenvironmental interpretation of the Brannon Member, Middle-Upper Ordovician Lexington Limestone, central Bluegrass region of Kentucky: Unpublished master's thesis, University of Kentucky, Lexington, Kentucky, 222 p.

Lash, G.G., 1989, Middle and Late Ordovician shelf activation and foredeep evolution, central Appalachian Orogen: *in* B.D. Keith (ed.), The Trenton Group (Upper Ordovician Series) of eastern North America, American Association of Petroleum Geologists, Tulsa, OK, Studies in Geology #29, p. 37-53.

Lavoie, D., 1995, A Late Ordovician high-energy temperate-water carbonate ramp, southern Quebec, Canada: implications for Late Ordovician oceanography: Sedimentology, v. 42, p. 95-116.

Lees, A., 1975, Possible influence of salinity and temperature on modern shelf carbonate sedimentation: Marine Geology, v. 19, p. 159-198.

Lees, A., and Buller, 1972, Modern temperate-water and warm-water shelf carbonate sediments contrasted: Marine Geology, v. 13, p. M67-M73.

Lowry, D.C., 1970, Geology of the Western Australia part of the Eucla Basin: Geological Survey of Western Australia Bulletin, v. 122, 201 p.

Mackey, R.T., 1972, Lithostratigraphy and depositional environment of the Perryville Limestone and related members of the Lower Lexington Limestone (Ordovician) of south-central Kentucky: (Unpubl. M.S. thesis) University of Kentucky, Lexington, KY, 76 p.

Mitchell, , R.W., 1985, Comparative sedimentology of shelf carbonates of the Middle Ordovician St. Paul Group, central Appalachians: Sedimentary Geology, v. 43, p. 1-41.

Montanez, I., and Read, J.F., 1992, Eustatic control on early dolomitization of cyclic peritidal carbonates; evidence from the Early Ordovician upper Knox Group, Appalachians: Geological Society of America Bulletin, v. 104, p. 872-886.

Mussman, W.J., and Read, J.F., 1986, Sedimentology and development of a passive- to convergent-margin unconformity: Middle Ordovician Knox unconformity, Virginia Appalachians: Geological Society of America Bulletin, v. 97, p. 282-295.

Nelson, C.S., 1988, An introductory perspective on non-tropical shelf carbonates: Sedimentary Geology, v. 60, p. 3-12.

Palmer, P., Decade of North American geology, 1983 geological time scale: Geology, v. 9, p. 503-504.

Patzkowsky, M.E., and Holland, S.M., 1993, Biotic response to a Middle Ordovician paleoceanographic event in eastern North America: Geology, v. 21, p. 619-622.

Pope, M. C., and Read, J. F., 1992, Possible Middle Cambrian to Late Ordovician Seismites from Extensional to Compressional Regimes, Geological Society of America Abstracts with Programs, v. 24, p. A 186.

Pope, M.C., and Read, J.F., 1994, Characteristics of depositional sequences, ststems tracts and bounding surfaces in Early Ordovician greehouse passive margin carbonates to Late Ordovician glacio-eustatic

influenced foreland basin facies: Southeastern section of Geological Society of America Program with Abstracts, v. 26, p. 58.

Popp, B.N., Anderson, T.F., and Sandberg, P.A., 1986, Brachiopods as indicators of original isotopic compositions in some Paleozoic limestones: Geological Society of America Bulletin, v. 97, p. 1262-1269.

Purser, B.H., and Seibold, E., 1973, The principal environmental factors influencing Holocene sedimentation and diagenesis in the Persian Gulf: *in* Purser, B.H., (ed), The Persian Gulf, Springer-Verlag, New York, p. 1-10.

Railsback, L.B., Ackerly, S.C., Anderson, T.F., and Cisne, J.L., 1990, Paleontological and isotope evidence for warm saline deep waters in Ordovician oceans: Nature, v. 343, p. 156-159.

Rao, C.P., 1981, Cementation in cold-water bryozoan sand, Tasmania: Marine Geology, v. 40, p. M23-M33.

Rao, C.P., 1991, Geochemical differences between subtropical (Ordovician) cool-temperate (Recent and Pleistocene) and subpolar carbonates, Tasmania, Australia: Carbonates and Evaporites, v. 6, p. 83-106.

Read, J.F., 1980, Carbonate ramp-to-basin transitions and foreland basin evolution, Middle Ordovician, Virginia Appalachians: American Association of Petroleum Geologists Bulletin, v. 64, p. 1575-1612.

Read, J.F., 1989, Controls on evolution of Cambrian-Ordovician passive margin, U.S. Appalachians: *in* Crevello, P.D., Wilson, J.L., Sarg, J.F., and Read, J.F. (eds), Controls on carbonate platform and basin development, Society of Economic Paleontologists and Mineralogists Special Publication No. 44, p. 147-165.

Read, J.F., and Grover, G., Jr., 1977, Scalloped and planar erosion surfaces, Middle Ordovician limestones, Virginia: Analogues of Holocene exposed karst or tidal rock platforms: Journal of Sedimentary Petrology, v. 47, p. 956-972.

Rodgers, J., 1971, The Taconic orogeny: Geological Society of America Bulletin, v. 82, p. 1141-1178.

Scotese, C.R., and McKerrow, W.S., 1990, Revised world maps and introduction: *in* McKerrow, W.S., and Scotese, C.R., (eds.), Palaeozoic palaeogeography and biogeography, Geological Society of London Memoir 12, p. 1-21.

Sweet, W. D., 1979, Conodonts and conodont stratigraphy of post-Tyrone Ordovician rocks of the Cincinnati Region: United States Geological Survey Professional Paper 1066-G, 26 p.

Tucker, R.D., Krogh, T.E., Ross, R.J. Jr., and Williams, S.H., 1990, Time-scale calibration by high-precision U-Pb zircon dating of interstratified volcanic ashes in the Ordovician and Silurian stratotypes of Britain: Earth and Plantary Science Letters, v. 100, p. 51-58.

Tucker, R.D., and McKerrow, W.S., 1995, Early Paleozoic chronology: a review in light of new U-Pb zircon ages from New Foundland and Britain: Canadian Journal of Earth Sciences, v. 32, p. 368-379.

Vail, P.R., Mitchum R.M., and Thompson, S., 1977, Seismic stratigraphy and global changes in sea level: *in* Seismic stratigraphy: Application to hydrocarbon exploration, American Association of Petroleum Geologists Memoir 26, p. 83-97.

Van der Voo, R., 1988, Paleozoic paleogeography of North America, Gondwana, and intervening displaced terranes: Comparison of paleomagnetism with paleoclimatology and biogeographical patterns: Geological Society of America Bulletin, v. 100, p. 311-324.

Wahlman, G.P., 1992, Middle and Upper Ordovician symmetrical univalved mollusks (Monoplacophora and Bellerophontina) of the Cincinnati Arch region: United States Geological Survey Professional Paper 1066-O, 194 p.

Webby, B.D., 1992, Global biogeography of Ordovician corals and stromatoporoids: in Webby, B.D., and Laurie, J.R., (eds.), Balkema, Rotterdam, p. 261-276.

Wilde, P., 1991, Oceanography in the Ordovician: *in* Advances in Ordovician Geology, C.R. Barnes and S.H. Williams (eds.), Geological Survey of Canada, Paper 90-9, p. 283-298.

Wilkinson, B.H., Janecke, S.U., and Brett, C.E., 1982, Low-magnesian calcite marine cement in Middle Ordovician hardgrounds from Kirkfield, Ontario: Journal of Sedimentary Petrology, v. 52, p. 47-57.

Wilkinson, B.H., and Given, R.K., 1986, Secular variation in abiotic marine carbonates, constaints on Phanerozoic atmospheric carbon dioxide contents and oceanic Mg/Ca ratios: Journal of Geology, v. 94, p. 321-333.

Witzke, 1990, Palaeoclimatic constraints for Paleozoic palaeolatitudes of Laurentia and Euramerica: in McKerrow, W.S., and Scotese, C.R., (eds.), Palaeozoic palaeogeography and biogeography, Geological Society of London Memoir 12, p. 57-74.

Weir, G.W., Peterson, W.L., and Swadley, W.C., 1984, Lithostratigraphy of Upper Ordovician strata exposed in Kentucky: United States Geological Survey Professional Paper 1151-E, 121 pp.

Chapter 4: Late Middle to Late Ordovician Seismites of Kentucky, Southwest Ohio and Virginia: Sedimentary Recorders of Earthquakes in the Appalachian Basin

ABSTRACT

Synsedimentary ball-and-pillow beds, breccias and faults in late Middle to Late Ordovician foreland basin rocks of Kentucky, southwest Ohio and Virginia indicate broad zones of seismicity near the Cincinnati Arch and Taconic orogenic front during deposition. Earthquake-induced liquefaction formed ball-and-pillow beds and rare sedimentary breccias (seismites) that are correlative over large areas (100's to 1000's km^2). Comparison with liquefaction-induced sedimentary features and their areal distribution in Holocene sediments indicate the Ordovician seismites were probably generated by earthquakes with moment magnitudes (M_O) of 6.2 to 7.7. These seismites provide information about seismicity (e.g., magnitude epicenter, magnitude recurrence interval) in the Ordovician foreland basin. Some of the seismites are due to basement faulting in the foreland and accretionary prism. However, outcrops and a core in the Jeptha Knob cryptoexplosive structure contain horizons of re-sedimented cataclastic breccias which appear to correlate with several ball-and-pillow beds on Jessamine Dome to the east, along the Cincinnati Arch, suggesting that some of the seismites may be genetically related to the Jeptha Knob cryptoexplosive structure.

INTRODUCTION

Syn- or early post-depositional deformation structures in the form of ball-and-pillow structures and convolute bedding are common features in some sedimentary sequences. Such structures can originate as "soft sediment" deformation caused by loading or slumping (Mills, 1983) or as seismically-induced structures called "seismites" (Seilacher, 1969; 1984). Two types of seismites are distinguished: primary seismites are sediments deformed in-situ by a seismic event and include features such as sand blows, neptunian dikes, and ball-and-pillow structures (Hempton and Dewey, 1983; Obermeier et al., 1991; Clague et al., 1992); secondary seismites are the depositional products of a seismic event whose record may be obscured, and include re-sedimented facies such as some turbidites (Kastens, 1984; Mutti et al., 1984; Klevekaar, 1987; Adams, 1990; Karlin and Abella, 1992), submarine slumps and debris beds (Helwig, 1970; Maltman,

1981; Kastens, 1984), tsunami deposits (Kastens and Cita, 1981; Atwater, 1987; Minoura et al., 1991, 1994; Atwater and Moore, 1992) and tectonically homogenized beds (Heike, 1984; Cita et al., 1984).

Probable primary and secondary seismites in the late Middle to Late Ordovician strata of Kentucky, southwest Ohio, and Virginia were encountered during a larger study on sequence stratigraphy and greenhouse to ice-house transitions of the Ordovician in this foreland basin. In this paper, we document the stratigraphic occurrence of the seismites, their potential significance and possible overall relationships to basement faults and nearby cryptoexplosive structures.

STRUCTURAL AND STRATIGRAPHIC SETTING OF SEISMITE BEARING BEDS

The seismites occur in Ordovician foreland basin deposits of the Appalachian Basin (Figures 1 to 3). This foreland basin was formed by the collision of a magmatic arc with the Cambrian-Early Ordovician passive margin which produced the regional Knox unconformity (Jacobi, 1981; Mussman and Read, 1986; Lash, 1988). The foreland basin extends from Alabama to Newfoundland (Rodgers, 1971) and was bordered on the east by tectonic highlands, and on the west by a shallow carbonate ramp. Major structural elements on the ramp were the Nashville and Jessamine domes on the Cincinnati Arch and the Sebree Trough west of the arch (Figure 1).

The foreland basin developed in two phases (Rodgers, 1971). The first was the "Blountian phase" (Llanvirn to Early Caradoc) when the "Middle Ordovician Limestone" sequence was deposited on the ramp in Virginia peripheral to the rapidly subsiding Sevier Basin of Alabama, Tennessee, and Virginia (Shanmugam and Walker, 1983). Its updip equivalent, the High Bridge Group, formed in Kentucky on the shallow ramp.

The second orogenic phase was the "Taconic" phase or late Middle to Late Ordovician (Late Caradoc to Ashgill), during which time the seismites described in this paper developed (Figure 2). Martinsburg Formation turbidites were deposited during this phase in northern Virginia, Maryland, and Pennsylvania in a foredeep further northeast of the earlier Sevier Basin (Read, 1989; Lash, 1988). In Kentucky and Virginia, a predominantly deeper subtidal shallow ramp developed, which sloped gently northeastward from the Cincinnati Arch into the turbiditic Appalachian Basin, and passed westward across an abrupt margin into the narrow, shaly, Sebree Trough (Cressman, 1973; Keith, 1988).

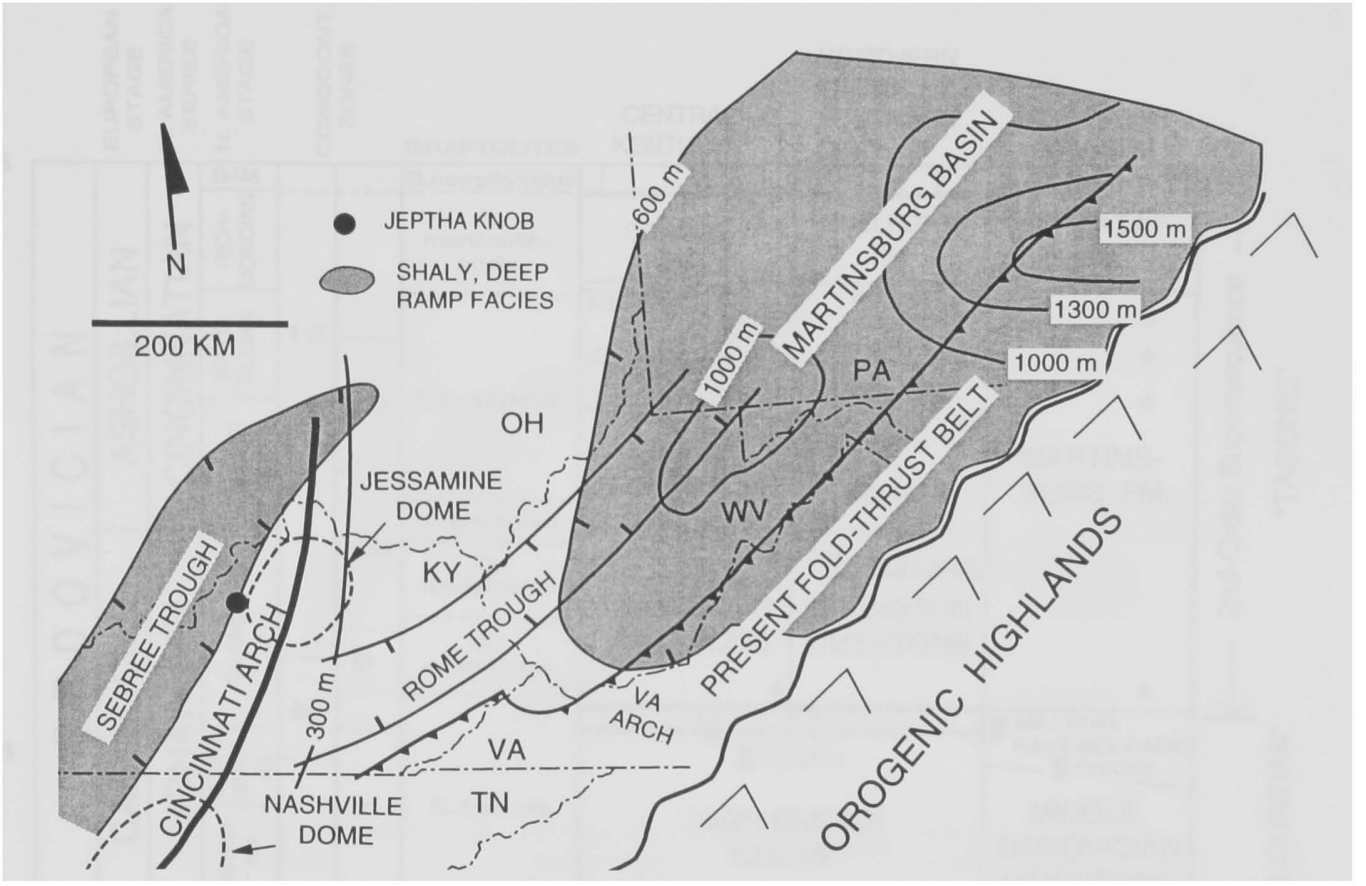

Figure 1. Generalized map of the Appalachian Basin, eastern U.S.A. showing structural features active during the late Middle to Late Ordovician. The barbed fault line delineates the present western limit of the fold-thrust belt. The contour intervals are thicknesses of late Middle to Late Ordovician strata.

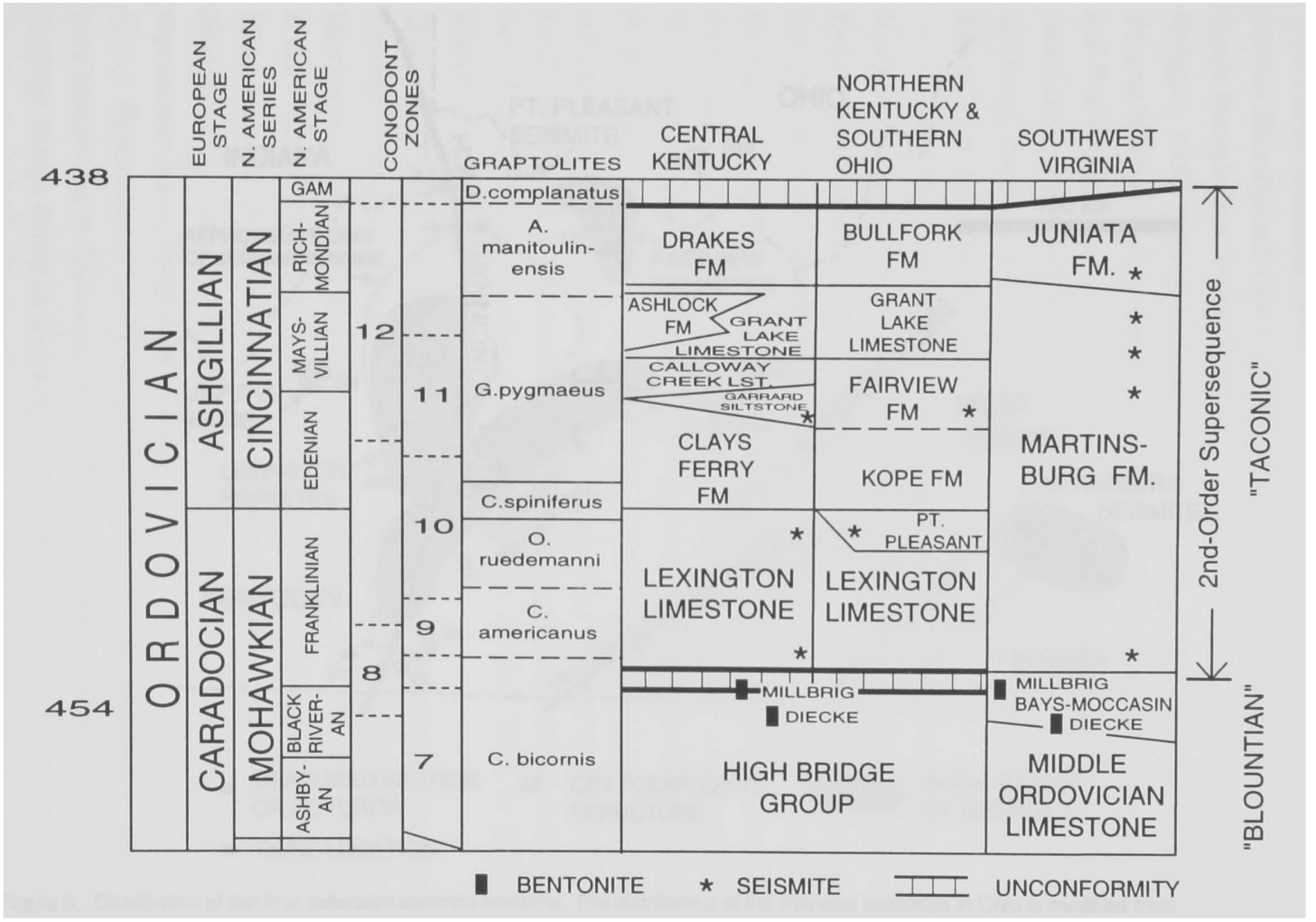

Figure 2. Chronostratigraphic chart of Middle to Late Ordovician rocks in Kentucky, southwest Ohio, and Virginia

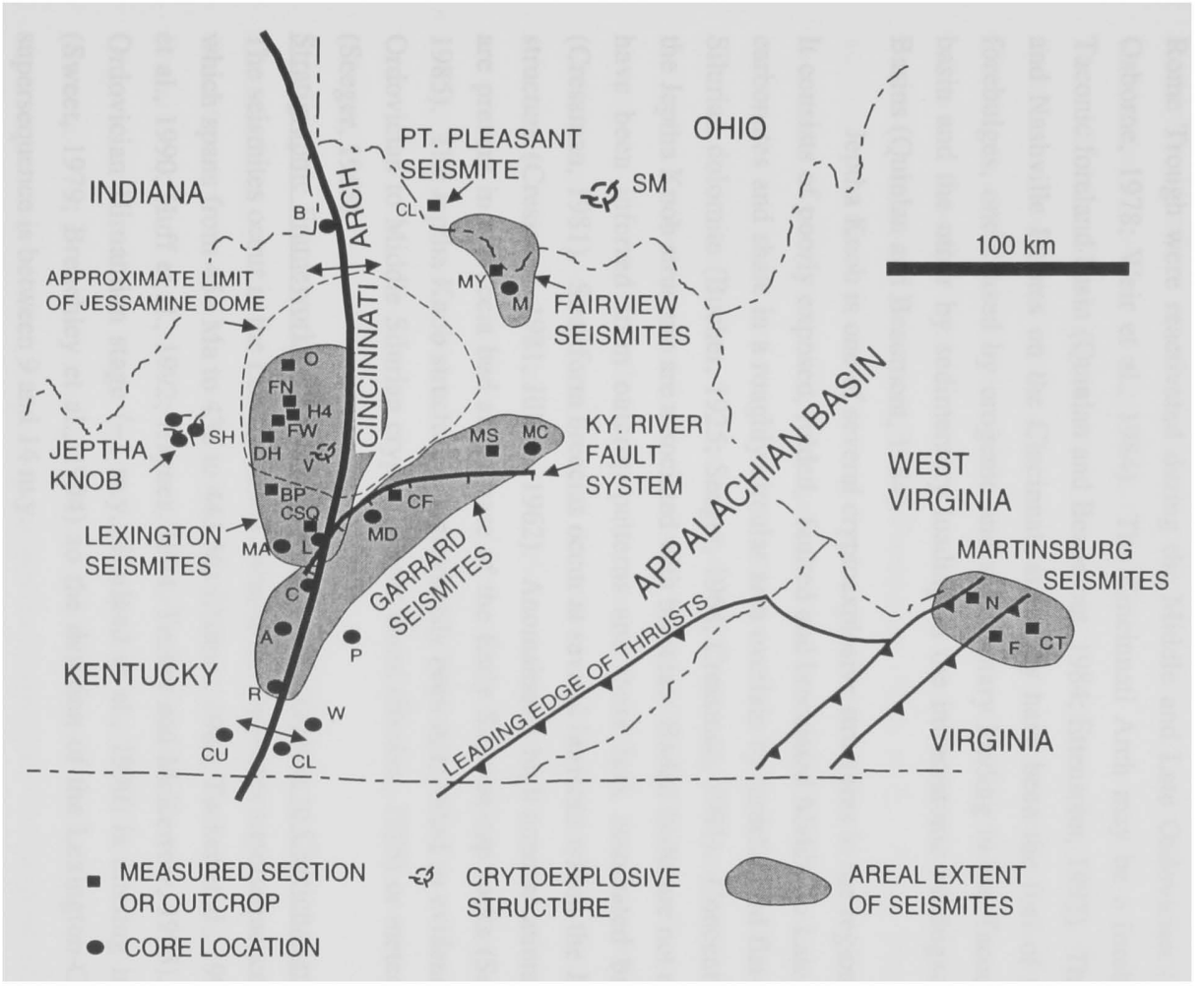

Figure 3. Distribution of the four extensive seismite horizons. The distribution of the Fairview seismites in Ohio is modified from Schumacher (1992). Cryptoexplosion structures in the area that affect Middle to Late Ordovician rocks are Jeptha Knob, Versailles (V), and Serpent Mound (SM). Location of outcrops and cores are given in Appendix 1.

The Cincinnati Arch (Figures 1 and 3) was an active positive feature resisting subsidence during the Late Middle Ordovician (Borella and Osborne, 1978). It was cross-cut by east-west trending faults which produced a series of uplifted domes and saddles (Borella and Osborne, 1978; Mackey, 1972). Border faults of the Cambrian Rome Trough were reactivated during the Middle and Late Ordovician (Borella and Osborne, 1978; Weir et al., 1984). The Cincinnati Arch may be a forebulge of the Taconic foreland basin (Quinlan and Beaumont, 1984; Ettensohn, 1992). The Jessamine and Nashville Domes on the Cincinnati arch may have been the foci of overlapping forebulges, one caused by orogenic and sedimentary loading in the Taconic foreland basin and the other by sedimentary loading in the intracratonic Michigan or Illinois Basins (Quinlan and Beaumont, 1984).

Jeptha Knob is one of several cryptoexplosive structures in the region (Figure 3). It consists of poorly exposed, folded, faulted and brecciated Middle to Late Ordovician carbonates and shale in a roughly circular area overlain by undeformed flat-lying Early Silurian dolomite (Bucher, 1925; Seeger, 1968; Cressman, 1981). Concentric faults in the Jeptha Knob structure are associated with breccias. Radial faults are not exposed and have been inferred from outcrop patterns and these lack associated breccia beds (Cressman, 1981). Stratiform breccias occur at several horizons within the Jeptha Knob structure (Cressman, 1981; Jillson, 1962). Anomalously high concentrations of iridium are present in a breccia bed at the base of the Early Silurian cap rocks (Seeger et al., 1985). The Jeptha Knob structure has previously been interpreted as evidence of a Late Ordovician to Middle Silurian cryptovolcanic event (Bucher, 1925) or meteorite impact (Seeger, 1968).

Stratigraphic Framework of the Seismite Beds of Lexington to Cincinnatian Sequence:

The seismites occur in the Lexington to Cincinnatian 2nd-order supersequence (Figure 2), which spans from 454 Ma to 438 to 443 Ma (Palmer, 1982; Tucker et al., 1990; Harland et al., 1990; Huff et al., 1992; Haynes, 1994; Tucker and McKerrow, 1995). The latest Ordovician Hirnantian stage (~2 m.y.; Harland et al., 1990) is missing in Kentucky (Sweet, 1979; Brenchley et al., 1994) so the duration of the Lexington-Cincinnatian supersequence is between 9 and 14 m.y.

The Lexington Limestone (Late Caradocian) is the transgressive lower part of the Late Mohawkian to Cincinnatian 2nd-order supersequence and rests disconformably on the High Bridge Group in Kentucky (Cressman, 1973) and southern Ohio (Figure 2). It consists dominantly of subtidal cool-water skeletal limestone and shale (Patzkowsky and

Holland, 1993; Pope and Read, 1993; in press; Holland and Patzkowsky, in press). Downdip in Virginia, time-equivalent lower Martinsburg Formation sediments conformably overlie red mudrocks of the Moccasin and Eggleston Formations or coarse clastics of the Bays Formation, which represent a coastal plain/tidal flat complex derived from the southeast that prograded longitudinally into the basin over the Middle Ordovician Limestone sequence (Read, 1980).

The Lexington Limestone is overlain by the deeper water Clays Ferry and Kope Formations, composed of thin interbedded limestone and shale with abundant storm beds (Kreisa et al., 1981; Ettensohn, 1992; Jennette and Pryor, 1993) which passes upward into calcareous siltstone nodular limestone, and rare grainstone, capped by peritidal silty dolomites of the Ashlock and Drake Formations (Weir et al., 1984). These are time-equivalent to the upper Martinsburg Formation, overlying Juniata and basal Tuscarora Formations in Virginia. The Martinsburg Formation in the study area is composed of interbedded subtidal skeletal limestone, siltstone, fine sandstone and shale storm beds (Kreisa, 1980) and is more like the Reedsville Formation than the turbiditic Martinsburg Formation of the Appalachian Basin further north (McBride, 1962). The succession is capped by the regional Ordovician-Silurian unconformity, which is believed to be synchronous with a worldwide oceanic drawdown caused by latest Ordovician glaciation (Hambrey, 1985; Caputo and Crowell, 1985), though multiple unconformities may be present in the Appalachian Basin where proximal tectonics probably influenced sedimentation more than eustatic fluctuations (Dorsch et al., 1994).

DESCRIPTION OF PRIMARY SEISMITES

Host Sediments: The inferred primary seismites occur in the Lexington Limestone, the Point Pleasant Tongue of the Clays Ferry Formation, the Garrard Siltstone, the Fairview Formation, and their eastern equivalents, the Martinsburg and Juniata Formations (Figures 2 to 5). These in-situ synsedimentary deformational structures most commonly occur in interbedded skeletal packstone, calcisiltite and shale, rarely in fine-grained skeletal grainstone with shale partings or interbeds, and rarely in fine-grained sandstone.

Ball-and-Pillow Structures (Contorted Laminations): Ball-and pillow structures occur in single beds or multiple horizons in the Lexington to Cincinnatian sequence in Kentucky (MacQuown et al., 1981; Jacobs, 1986; Potter et al., 1991; Pope and Read, 1992; Schumacher, 1992; Kulp, 1995; Ettensohn and Rast, 1995), and in the Martinsburg and

Juniata Formations in Virginia (Kreisa, 1980) (Figures 2 and 3). Some of these horizons are traceable over hundreds of square kilometers (c.f., Schumacher, 1992). The four most widely traceable horizons in Kentucky occur in the Logana Member near the base of the Lexington Limestone, in interbedded skeletal grainstones and shales in the upper Lexington Limestone (Tanglewood and Brannon Members, Figures 2, 4 and 5), within the Garrard Siltstone and in the Fairview Formation (Figures 2 and 3). The seismites of the Point Pleasant tongue of the Clays Ferry Formation and Fairview Formations also outcrop in southern Ohio. In Virginia, regionally extensive horizons are found near the base and top of the Martinsburg Formation and at the base of the Juniata Formation (Figures 2 and 3).

The ball-and-pillow beds (Figures 6 and 7) are 2 cm to 6 m thick and generally can be traced across outcrops for over 100 m horizontally. Some pinch out laterally but may then reappear at the same horizon further along the outcrop. The deformed units are overlain and underlain by undeformed beds (Figures 6A, B, C and D). Most commonly, siltstone, calcisiltite and less commonly fine skeletal grainstone forms "balls" and "pillows" surrounded by a shaly matrix (Figure 6). Ball-and-pillow beds also occur in clean, well-sorted sandstone near the base of the Juniata Formation (Figure 2). Here, the sandstone is highly contorted in the lower half of a 1 m thick bed, but shales above and below the deformed bed are undeformed and the sands in the upper half of the bed are structureless. Primary laminations in siltstone, calcisiltite and skeletal grainstone are highly contorted and convoluted but generally are traceable laterally. Most underlying shales are unlaminated, structureless, homogenized or chaotic, but some have faint laminations which parallel the "balls" and "pillows". Shaly matrix enclosing balls and pillows rarely contains brecciated fragments of interbedded calcisiltites. The distorted beds and surrounding matrix are usually abruptly overlain by flat-laminated shale (Figure 7). Some ball-and-pillow beds contain abundant chert (Kuhnhenn and Haney, 1986) (Figure .

Large circular, polygonal to irregularly shaped blocks with upturned, rounded edges occur in bedding plane exposures of ball-and-pillow beds in the grain-rich units of the Point Pleasant Tongue of the Clays Ferry Formation near Clermontville, Ohio (Figure 8). Matrix between the blocks is limestone breccia. Limestone breccia also occurs locally above the grain- rich blocks, primarily in the depressions enclosed by the upturned edges.

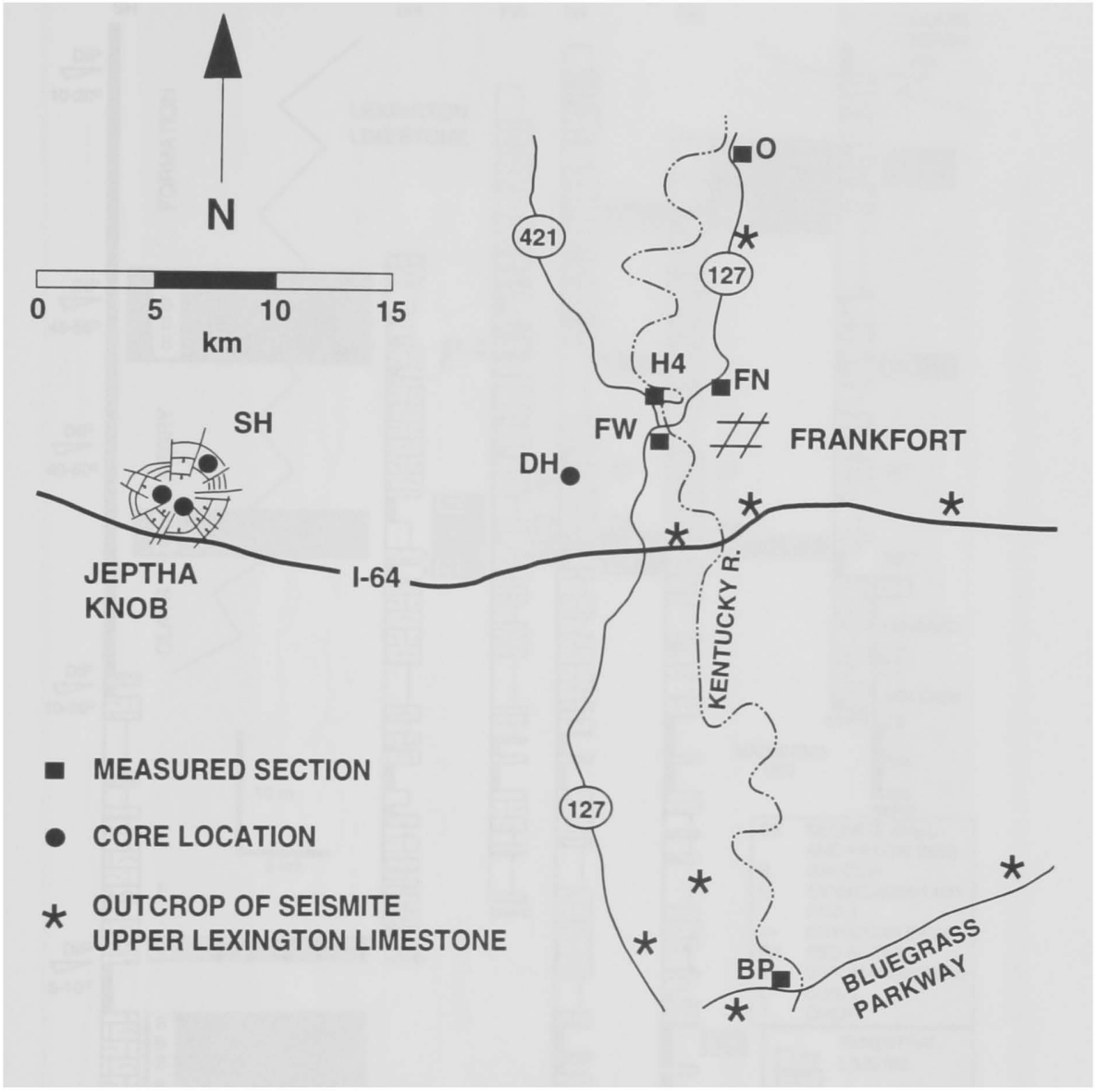

Figure 4. Sketch map showing location of large (> 60 m high) outcrops and cores of Lexington Limestone and Clays Ferry Formation on the west side of Jessamine Dome near Frankfort, Kentucky. Small outcrop of seismites are shown by an asterisk (*).

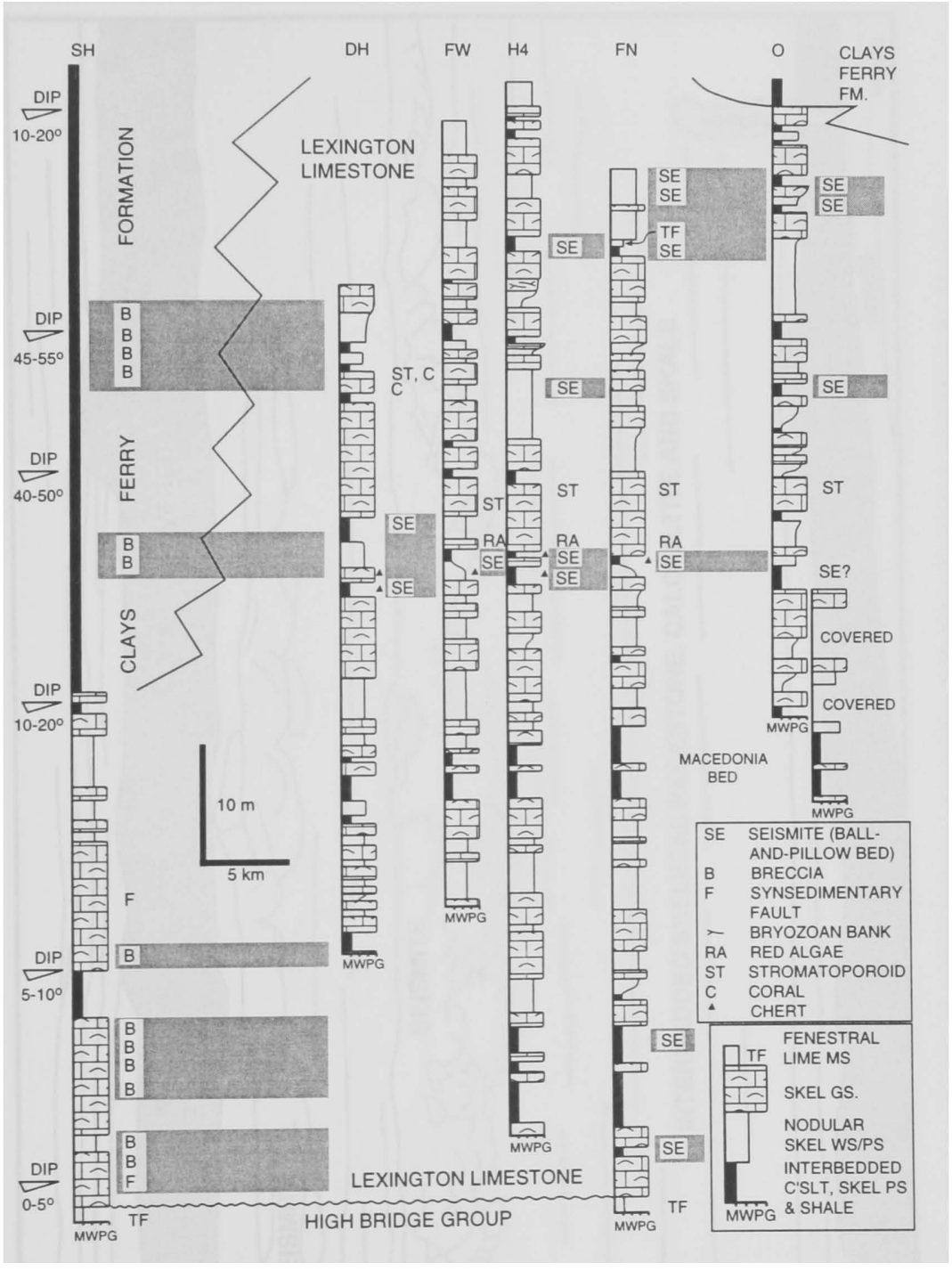

Figure 5. Southwest to northeast cross-section from a core in the Jeptha Knob structure, Shelby County (JK 78-1) to the Owenton composite section. Zones of correlative seismites are shaded light gray. The sections are hung on the medial bed of the Macedonia Bed, a widespread marker over the Jessamine Dome (Cressman, 1973).

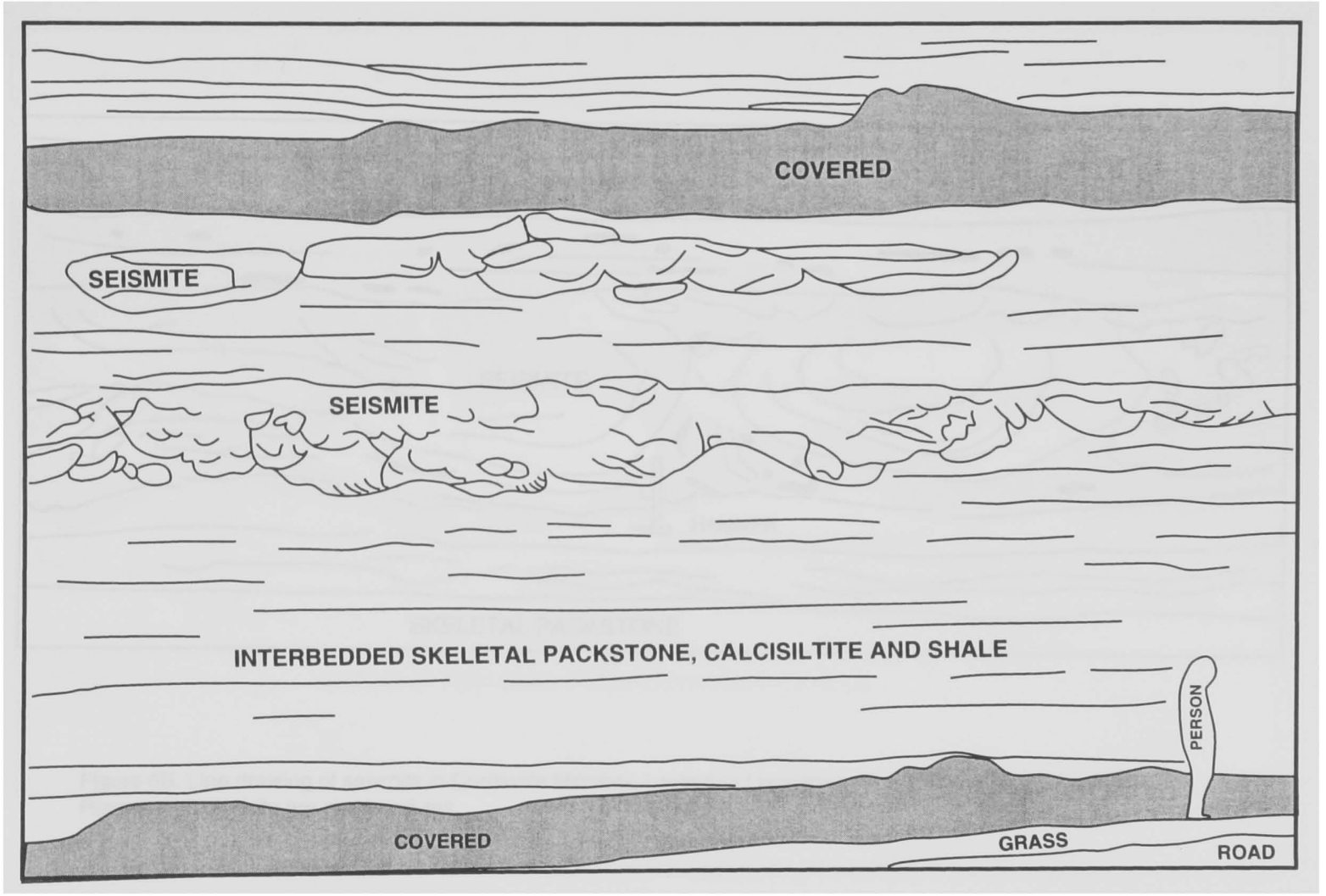

Figure 6A. Line drawing of multiple horizons of seismites, in Fairview Formation, near Maysville, Kentucky.

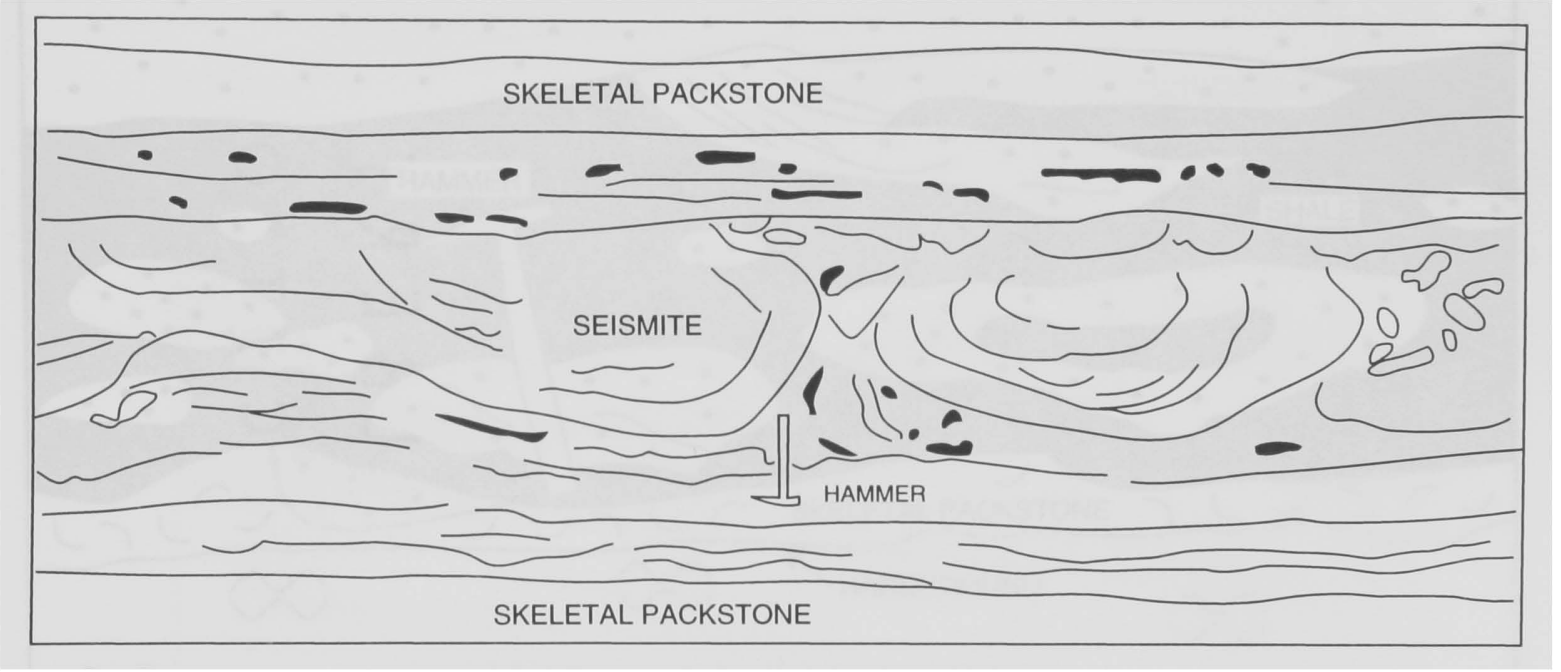

Figure 6B. Line drawing of seismite in Curdsville Member, Lexington Limestone, near Camp Nelson, Kentucky. Rounded black units are chert nodules.

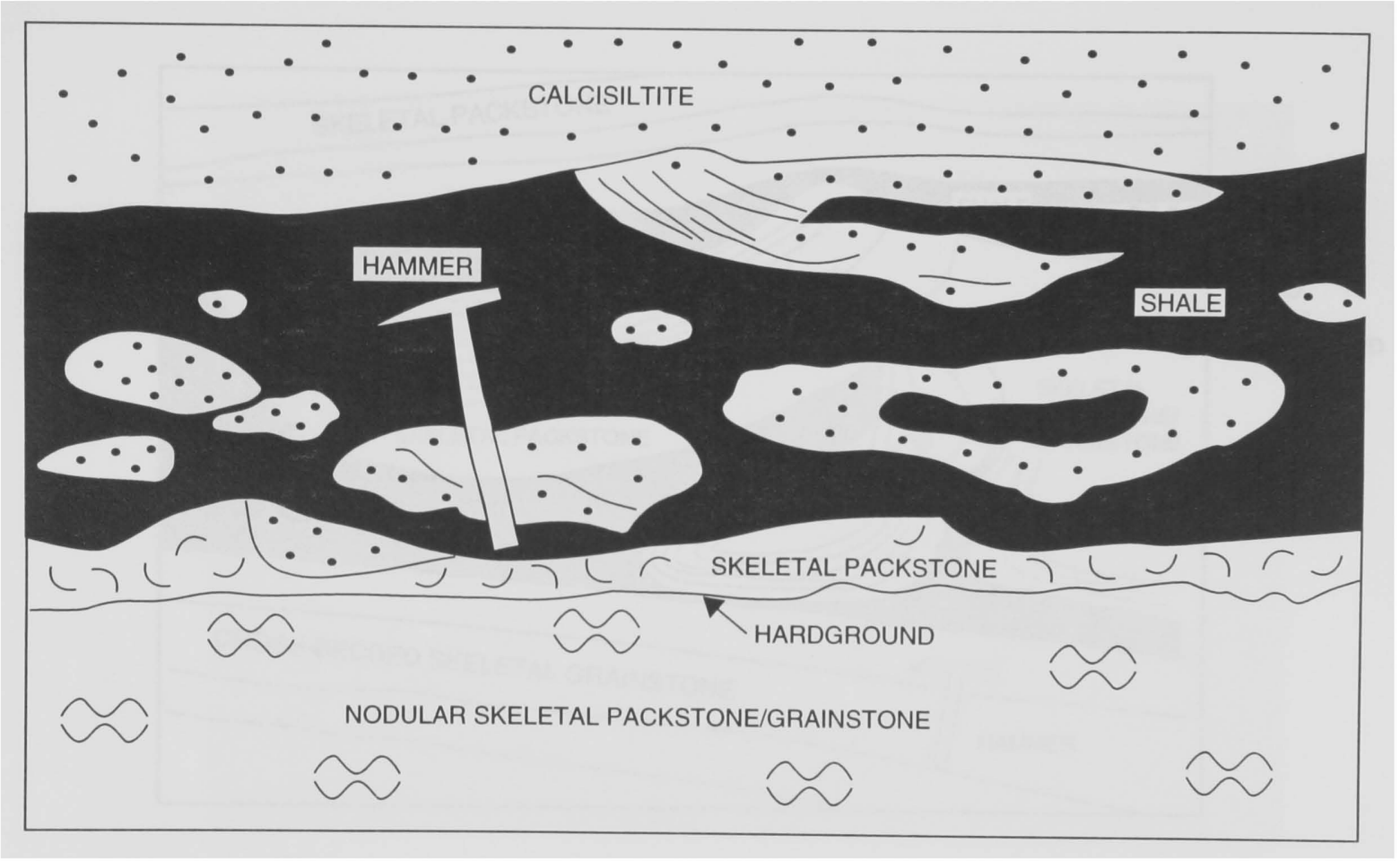

Figure 6C. Line drawing of seismite in Logana Member, Lexington Limestone, near Frankfort, Kentucky.

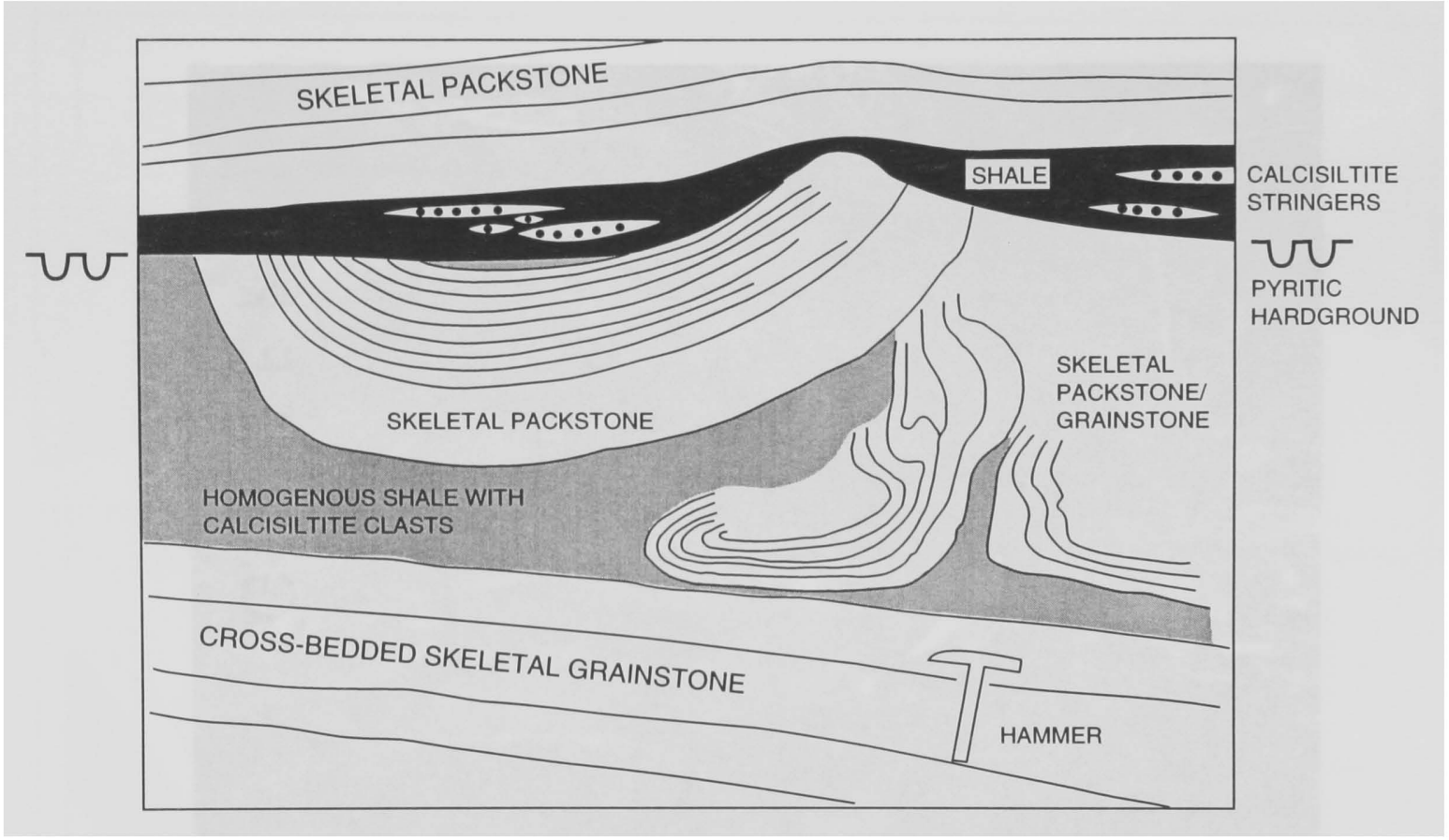

Figure 6D. Line drawing of hardground-capped seismite in Tanglewood Member, Lexington Limestone, near Owenton. The material immediately below the hardground in the depression above the "ball" and below the shale is similar to the shaly matrix material below.

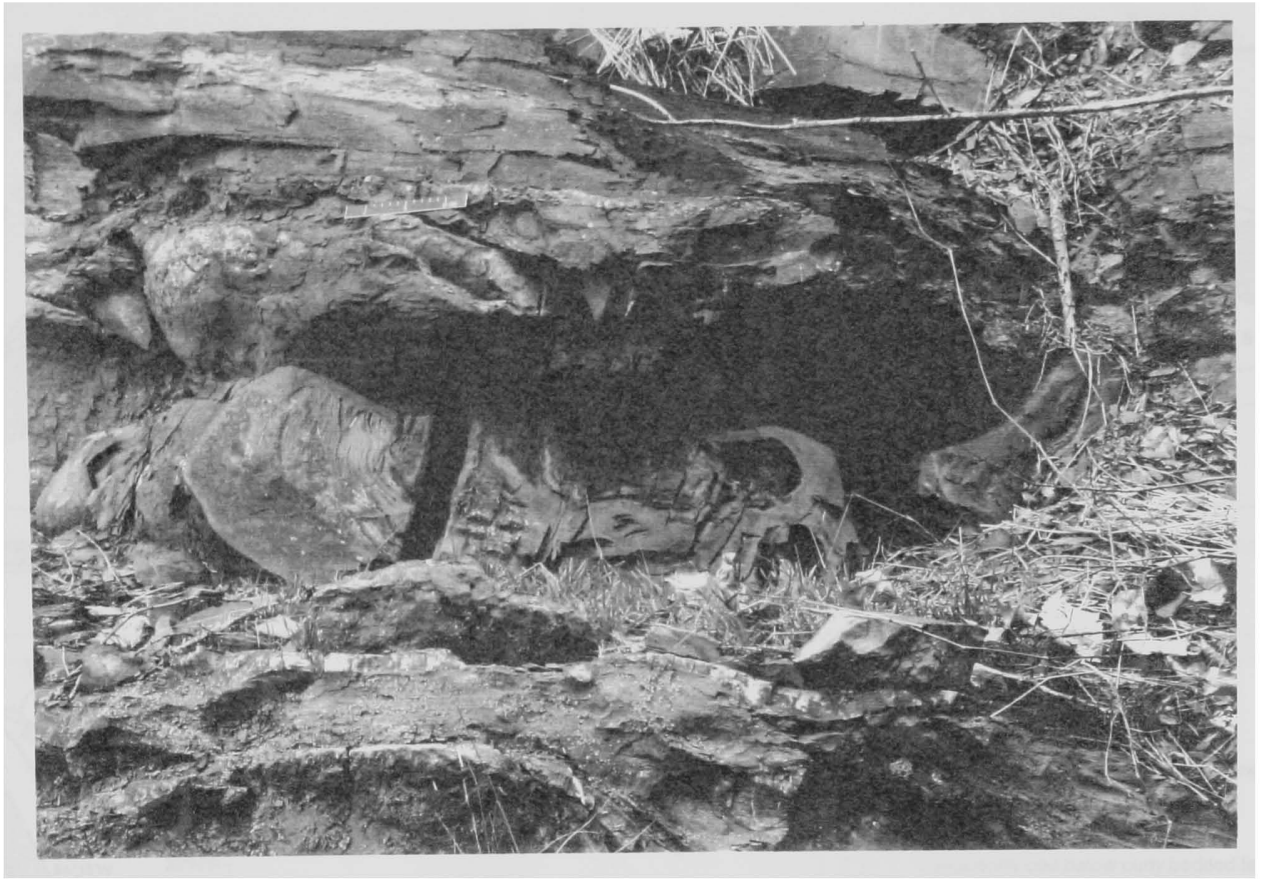

Figure 7. Photograph of multiple seismites (ball-and-pillow beds) in upper Martinsburg Formation, Narrows, Virginia.

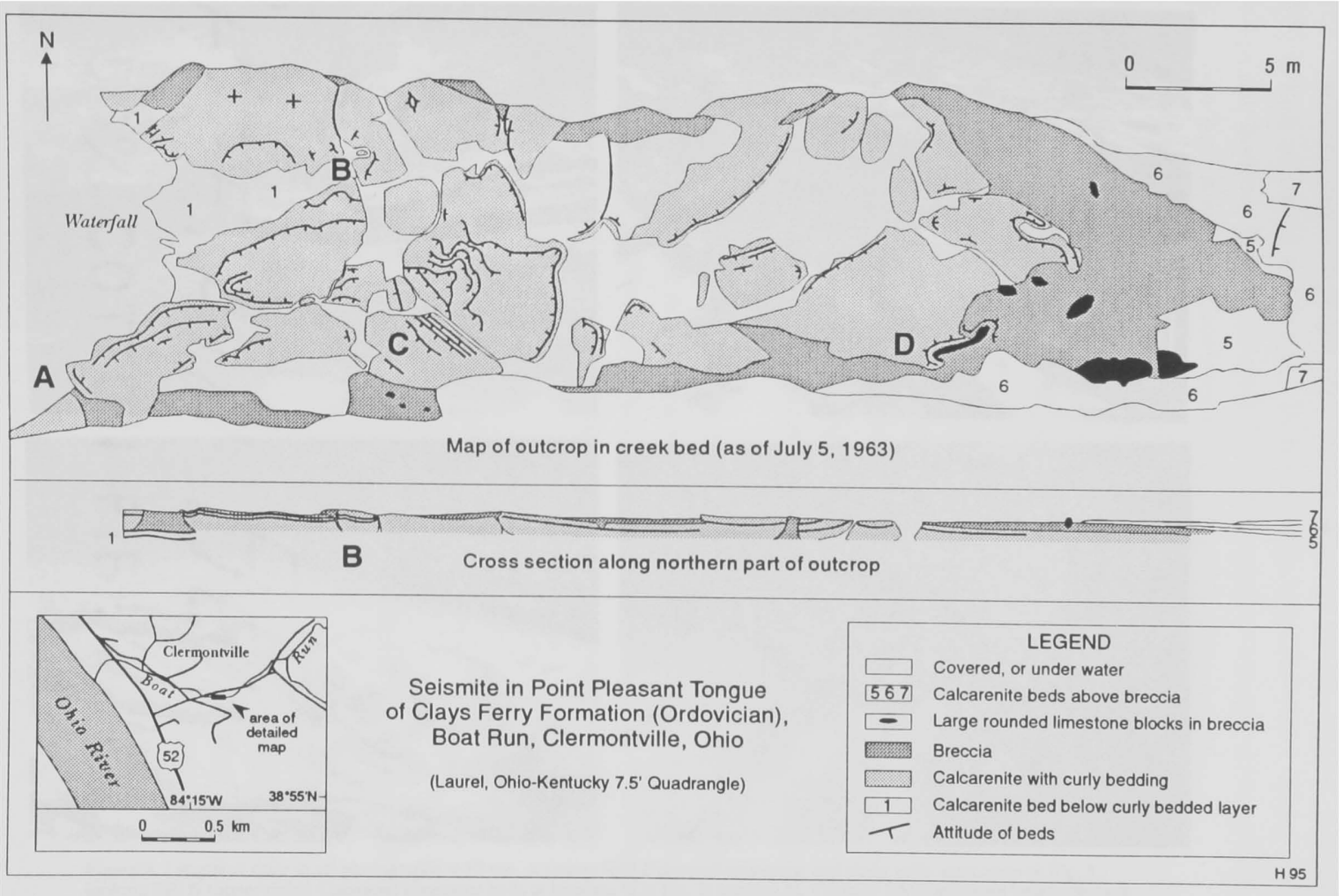
N
0
5 m
Waterfall
A
B
C
D
1
5
6
7
Map of outcrop in creek bed (as of July 5, 1963)
B
Cross section along northern part of outcrop
Clermontville
Boat Run
Ohio River
area of detailed map
52
84°15'W
38°55'N
0
0.5 km
Seismite in Point Pleasant Tongue of Clays Ferry Formation (Ordovician), Boat Run, Clermontville, Ohio
(Laurel, Ohio-Kentucky 7.5' Quadrangle)
LEGEND
Covered, or under water
5 6 7 Calcarenite beds above breccia
Large rounded limestone blocks in breccia
Breccia
Calcarenite with curly bedding
1 Calcarenite bed below curly bedded layer
Attitude of beds
H 95

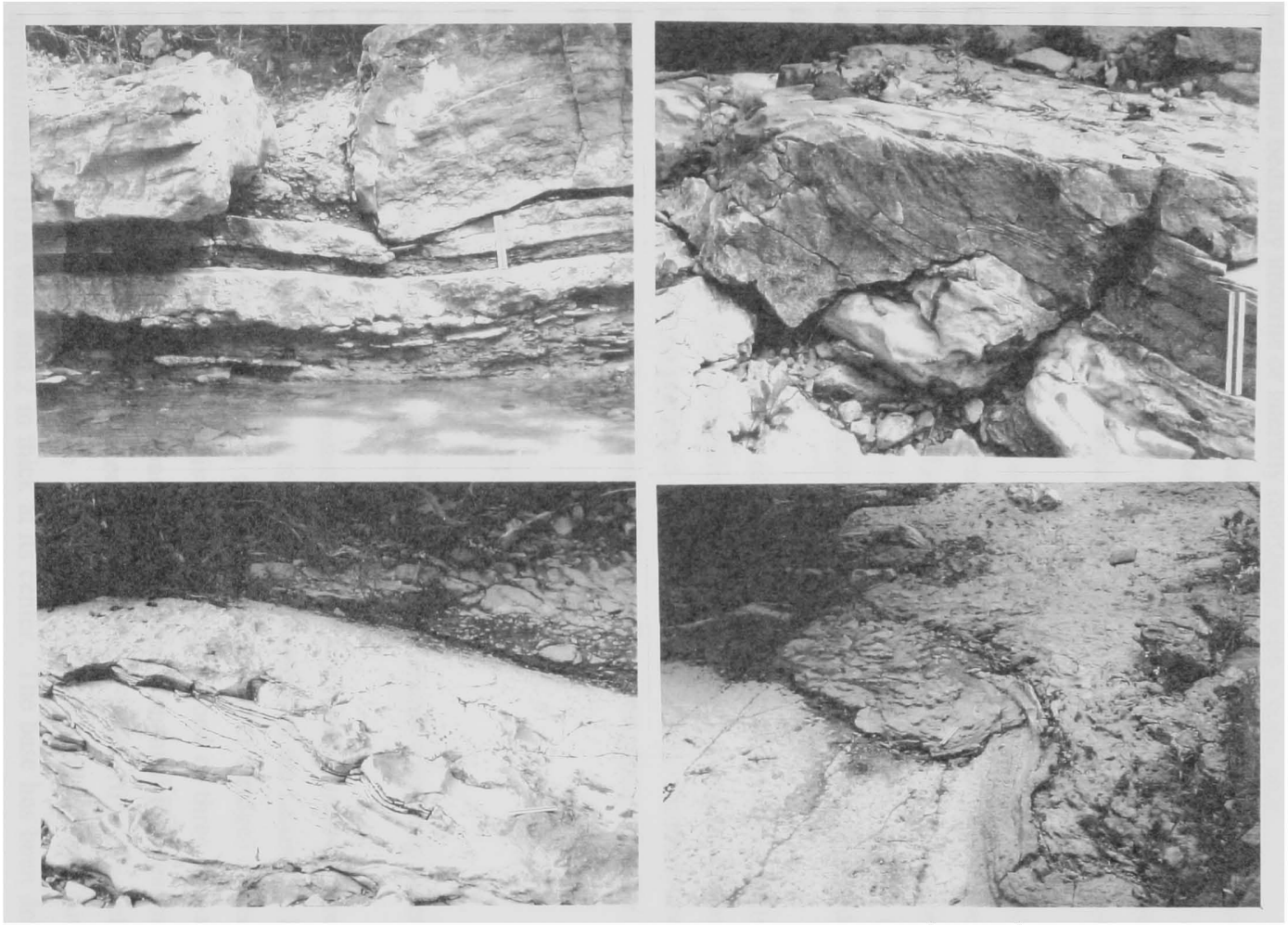

Figure 8. Length of ruler in all photographs = 15 cm. A (upper left) Disrupted limestone and shaly beds at location in Fig. 8, looking SE; B (upper right) Contorted limestone beds at location B in Fig. 8, looking N; C(lower left) Deformed limestone beds and overlying breccia at location C in Fig. 8, looking SSE; D. (lower right) Sigmoidally deformed piece of limestone and enveloping breccia at location D in Fig. 8, looking ENE.

In cores, ball-and-pillow beds are identified by steeply dipping laminae (up to 90°) in beds underlain and overlain by horizontally laminated shale. Many of the ball-and-pillow horizons in the Lexington Limestone contain irregular chert nodules. Ball-and-pillow beds may underlie or laterally interfinger with breccia beds.

Pyritic marine hardgrounds cap some deformed beds and are overlain by horizontally laminated shales (Figure 6D). The matrix may be chaotic and brecciated, and some fills topographic lows on the contorted "balls" beneath the hardgrounds. The hardground surface locally may be arched upward, broken and the overlying shales may be slightly distorted (Figure 6D).

Regional gradients in thickness of ball-and-pillow beds are observed in the Garrard Siltstone and Martinsburg Formation. The Garrard ball-and-pillow beds thin to the south and east. One of the upper Martinsburg Formation ball-and-pillow beds, shows an east to west (basinward) thinning from 2.5 m to 1.0 m over 65 km. Fossils in this bed change from a nearshore (Lingula- dominated) to an offshore (Rafinesquina-dominated) faunal assemblage.

Strike and dip measurements of over 200 axial planar surfaces defined by 3-dimensional exposures of ball-and-pillow beds in the upper Lexington Limestone near Lexington, Kentucky show no preferred orientation (Kulp, 1995). Similarly, twenty four measurements from a single bed along I-64 near Frankfort, Kentucky are randomly oriented (Figure 9).

DESCRIPTION OF SECONDARY SEISMITES

Secondary seismites are the depositional product of a seismic triggering event that may be obscured.

Deformed Channel-Fill: Irregular masses (or "blocks") of bedded grainstone occur along a stratigraphic horizon near the top of the Brannon Member of the Lexington Limestone (along the Bluegrass Parkway, south of the Kentucky River Bridge) (Cressman and Karklins, 1970). The horizon is equivalent to the upper bed of three ball-and-pillow horizons. At least one of the grainstone masses retains a channel-form geometry, even though it has undergone soft-sediment deformation (Figure 10). The channel-fill truncates the horizontal layering in the subjacent thin bedded rhythmite, and is approximately 10 m wide and 2 m thick at its center. The base has been deformed by injection of a plug of shaly limestone from below. Layering within the channel-fill

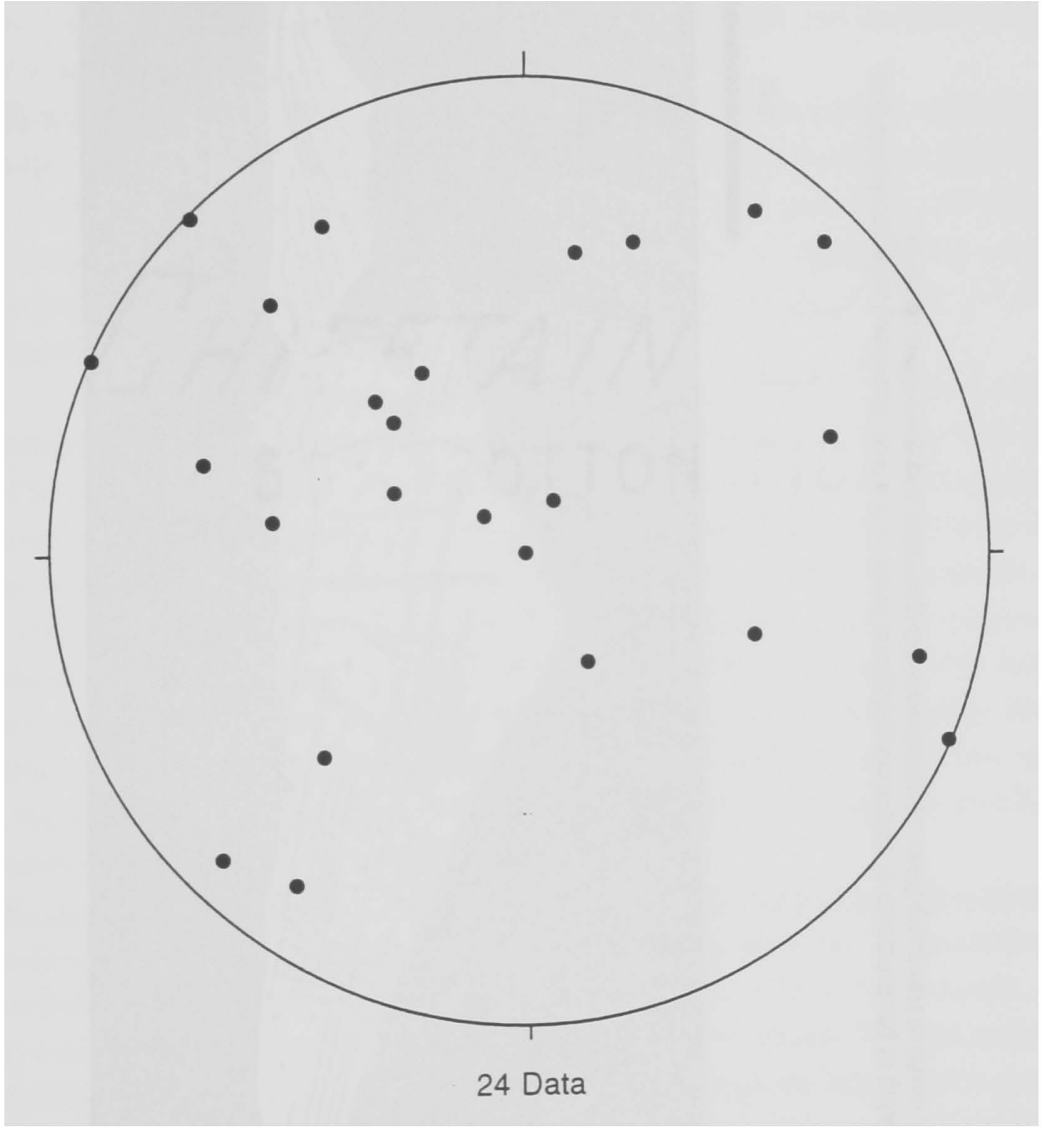

Figure 9. Poles to axial planar surfaces defined by contorted bedding, Lexington Limestone, Interstate 64, approximately 2 miles east of junction with Highway 127, near Frankfort, Kentucky. All measurements taken on northern side of eastbound traffic lane.

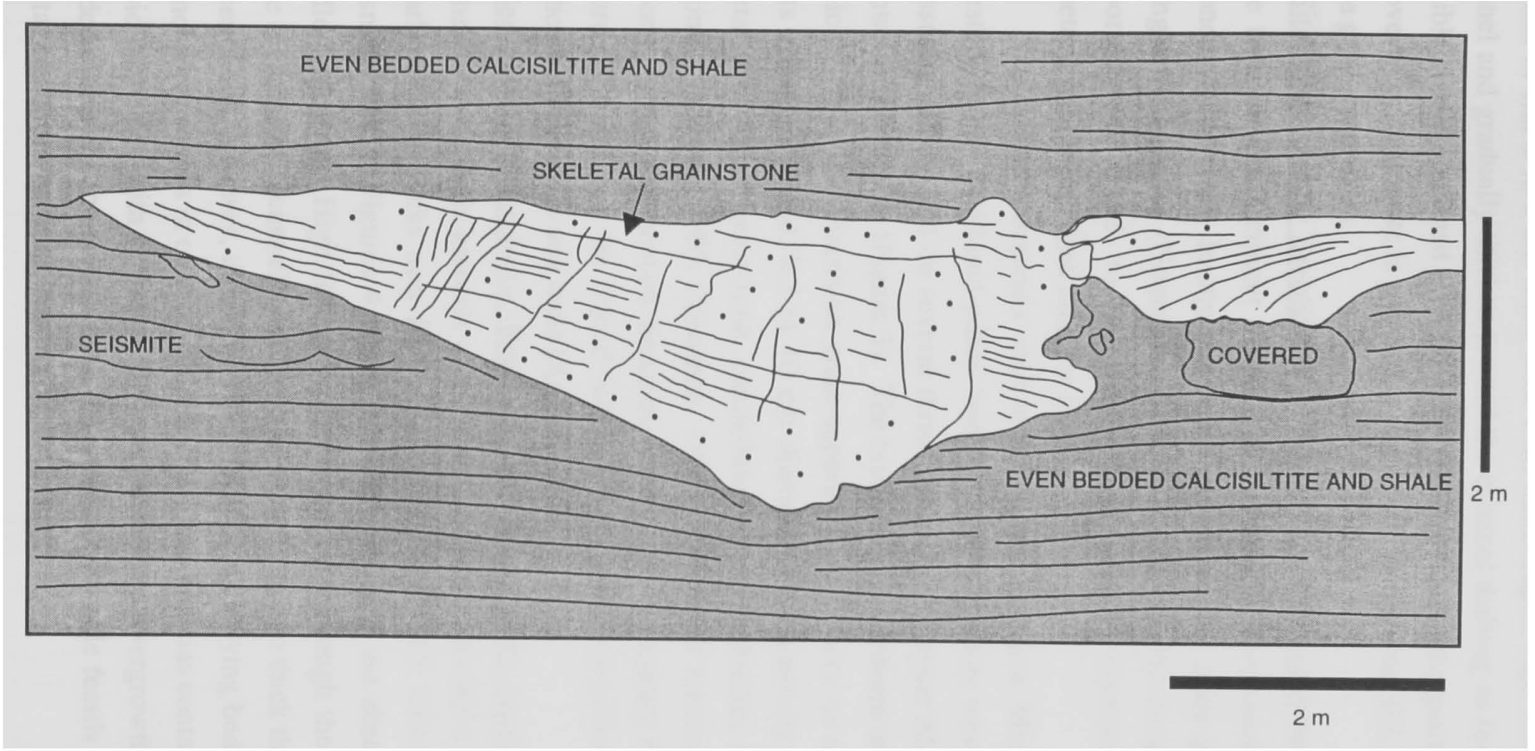

Figure 10. Line drawing of photomosaic of deformed grainstone block in Brannon Member, Lexington Limestone, Bluegrass Parkway, south of Kentucky River. Note channel-like geometry and correlative seismite.

consists of flat 2 to 5 cm thick beds with mud draped caps that parallel the base of the channel and gradually thicken toward the channel thalweg to form wedge-shaped layers. Possible slightly inclined soft-sediment faults cross-cut the grainstone mass. Bedding in the overlying rhythmite is parallel to the top of the channel fill, and drapes the one edge of the grainstone mass.

"In-Situ" Sedimentary Breccia Beds: Stratiform sedimentary breccias in the Ordovician range from in-situ incipient breccias to completely brecciated and re-mobilized beds (secondary seismites). In-situ incipient breccias occur in some grain-rich intervals of the Lexington Limestone (Noger and Kepferle, 1985) . The incipient breccias are clast-supported with fitted- to rounded skeletal grainstone/packstone clasts (to 20 cm diameter), with stylolitized margins (Figure 11).

Sedimentary breccias also occur in the Brannon Member of the Lexington Limestone below a ball-and-pillow bed (Bluegrass Parkway west of the Kentucky River) (Cressman, 1973); and on several thrust sheets in the upper Martinsburg Formation in southwestern Virginia (Figure 3). The breccias are stratiform units from 5 cm to over 5 m thick, generally matrix-to grain-supported, and occur as single or multiple beds. Clasts are subrounded, 0.5 to 10 cm diameter, and generally polymict composed of skeletal packstone/ grainstone, calcisiltite, or whole fossils, however, rare beds are monomict (Kreisa, 1980; Cressman, 1981). Matrix of breccias is generally shale or siltstone. Some sedimentary breccias (as in the Martinsburg Formation) fine upward (Figure 12) and can be traced laterally into ball-and-pillow beds or undeformed interbedded limestone and shale (Kreisa, 1980).

Re-Sedimented Cataclastic Breccias Associated with Jepth Knob Structure: Re-sedimented cataclastic breccias occur in surface exposures and a core of Late Ordovician to Early Silurian rocks near Jeptha Knob (Bucher, 1925; Jillson, 1962; Seeger, 1968; Cressman, 1981) (Figures 4, 5 and 13, 14). Breccias are absent from the underlying Middle Ordovician High Bridge Group in the core through the Jeptha Knob structure. These breccias are generally stratiform in beds up to 2 m thick that are conformable with adjacent beds, however, they may erode into the underlying beds and show mounded to channel form shapes in outcrop (Figure 15a). The breccias contain very angular clasts of crinoid fragments with syntaxial, clear calcite-cement overgrowths, along with angular to rounded clasts of cemented skeletal limestones and whole fossils in either an argillaceous skeletal packstone or shale matrix (Figure 14).

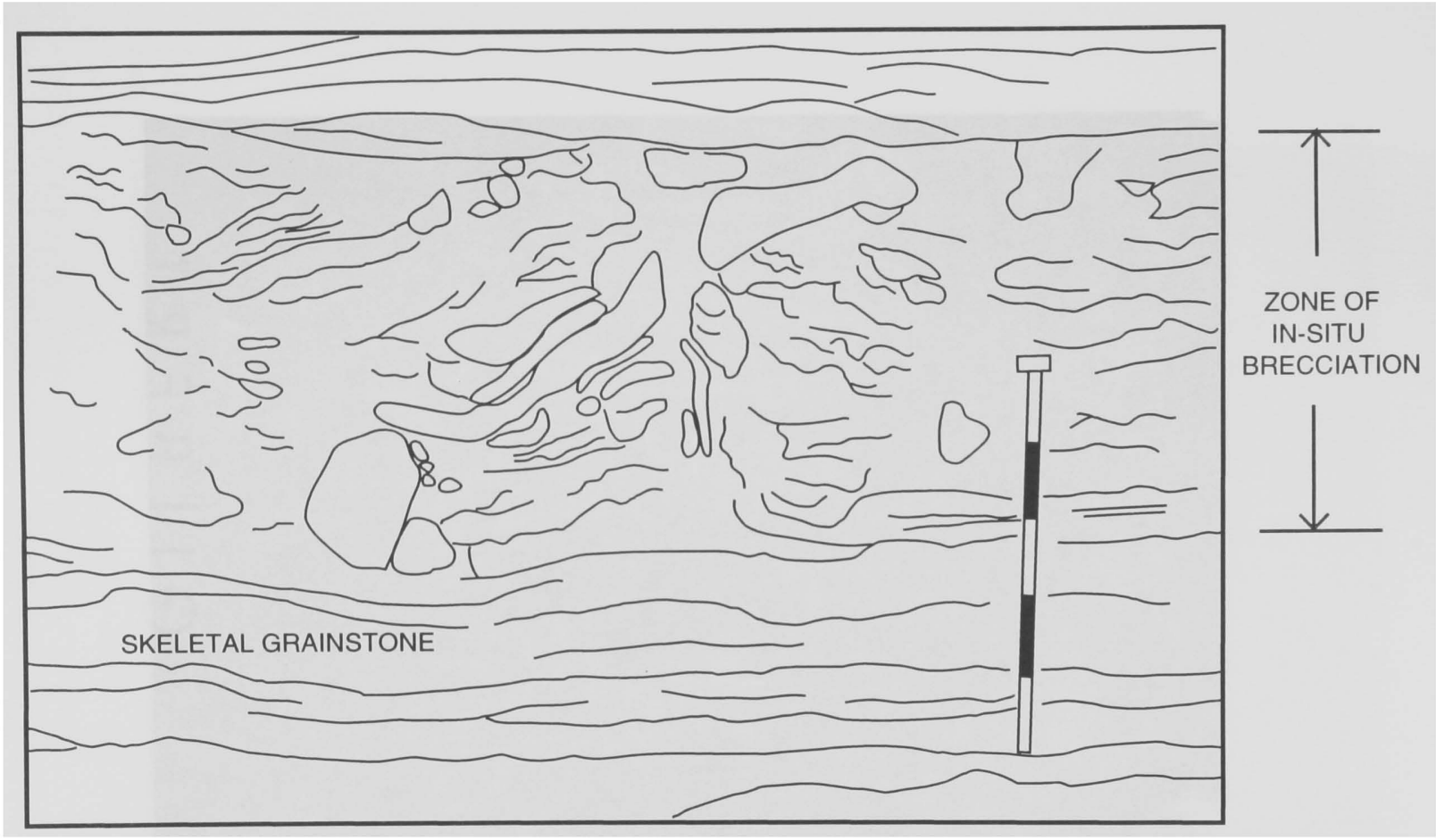

Figure 11. Line drawing of incipient brecciation in skeletal grainstone of Tanglewood Member, Lexington Limestone, Bluegrass Parkway, north of Kentucky River.

Figure 12. Normal graded breccia bed in upper Martinsburg Formation, Narrows, Virginia.

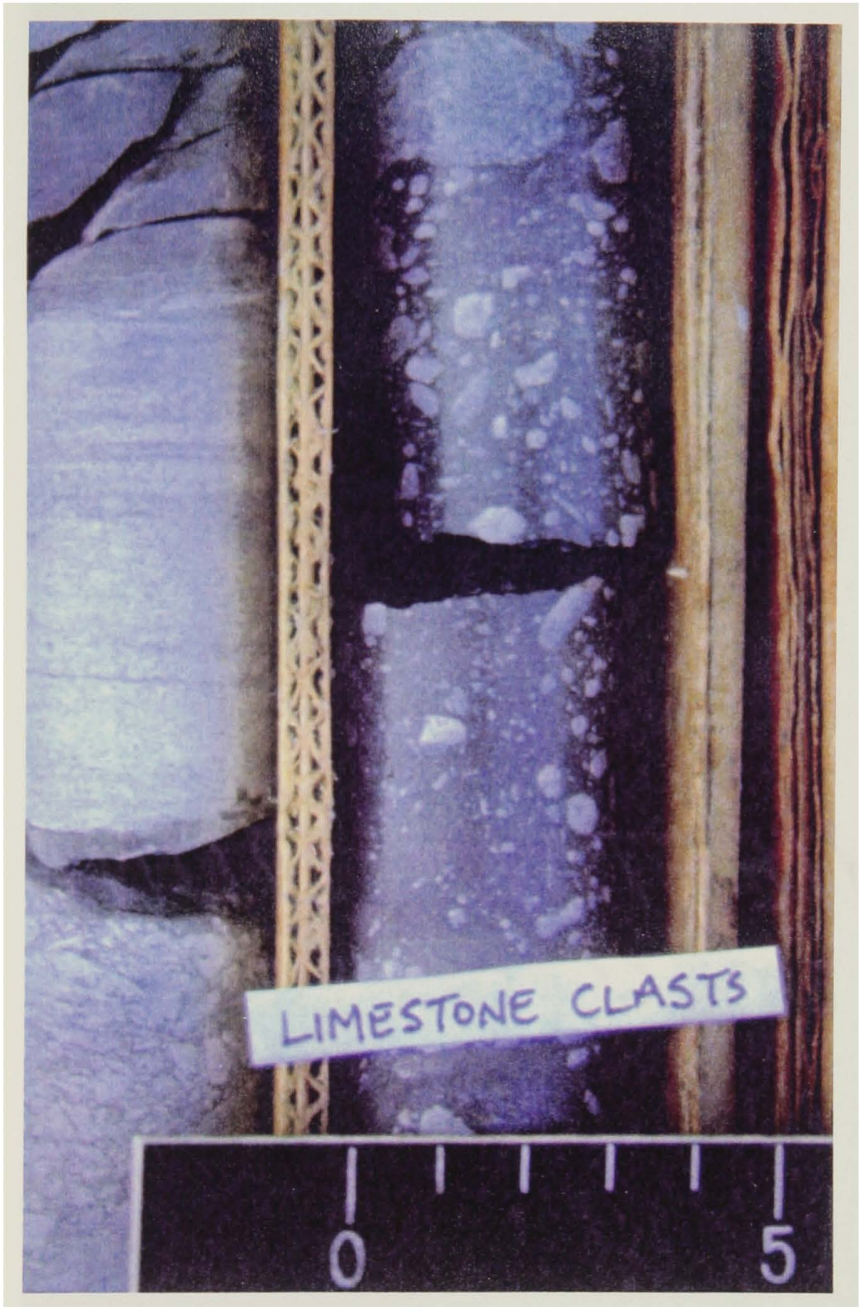

Figure 13A. Resedimented cataclastic breccia in Shelby Co. (JK 78-2) core. Subangular clasts of skeletal packstone in shaly matrix.

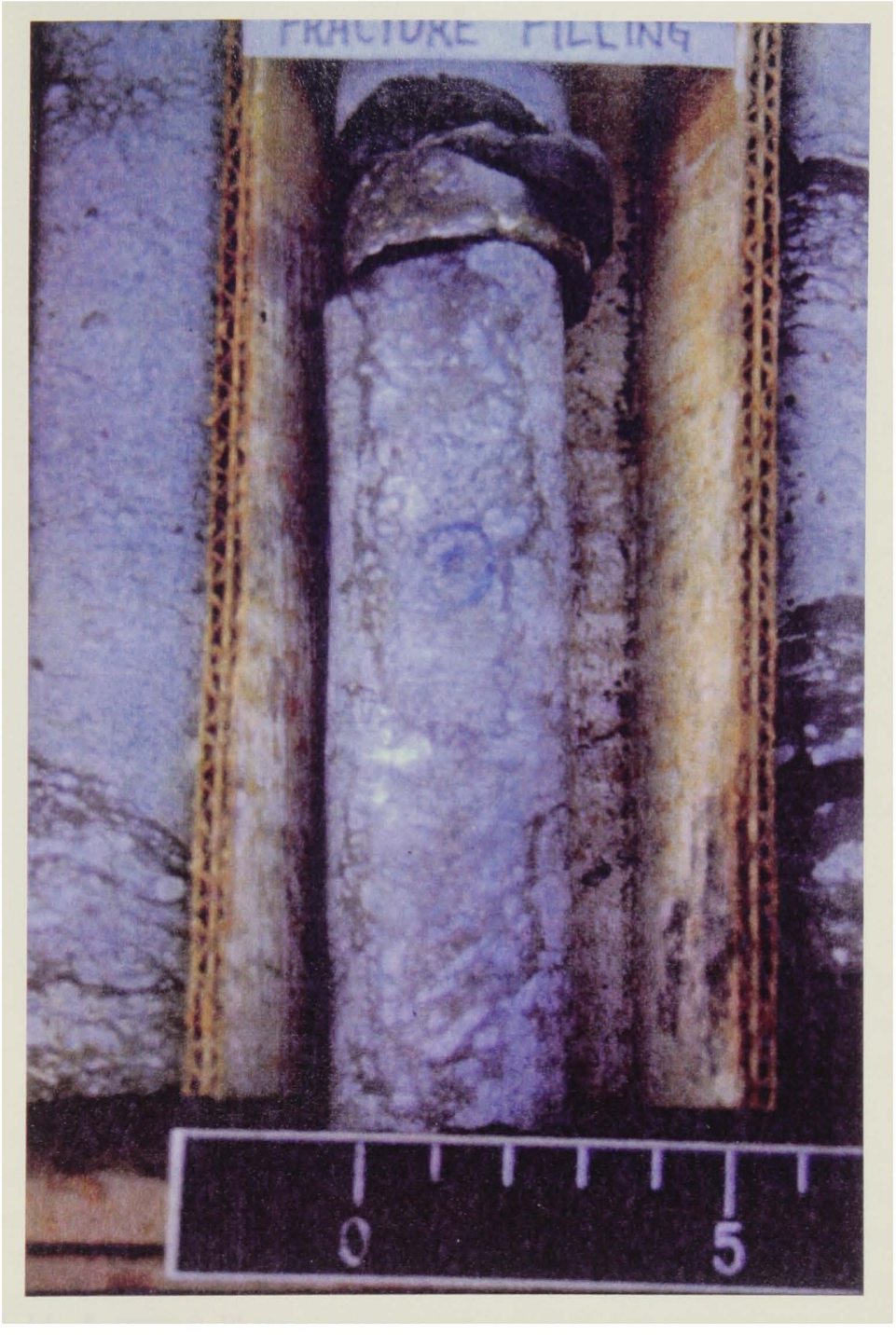

Figure 13B. Re-sedimented cataclastic breccia in Shelby Co. (JK 78-2) core. Subangular to angular clasts in shaly matrix, capped by pyritic hardground.

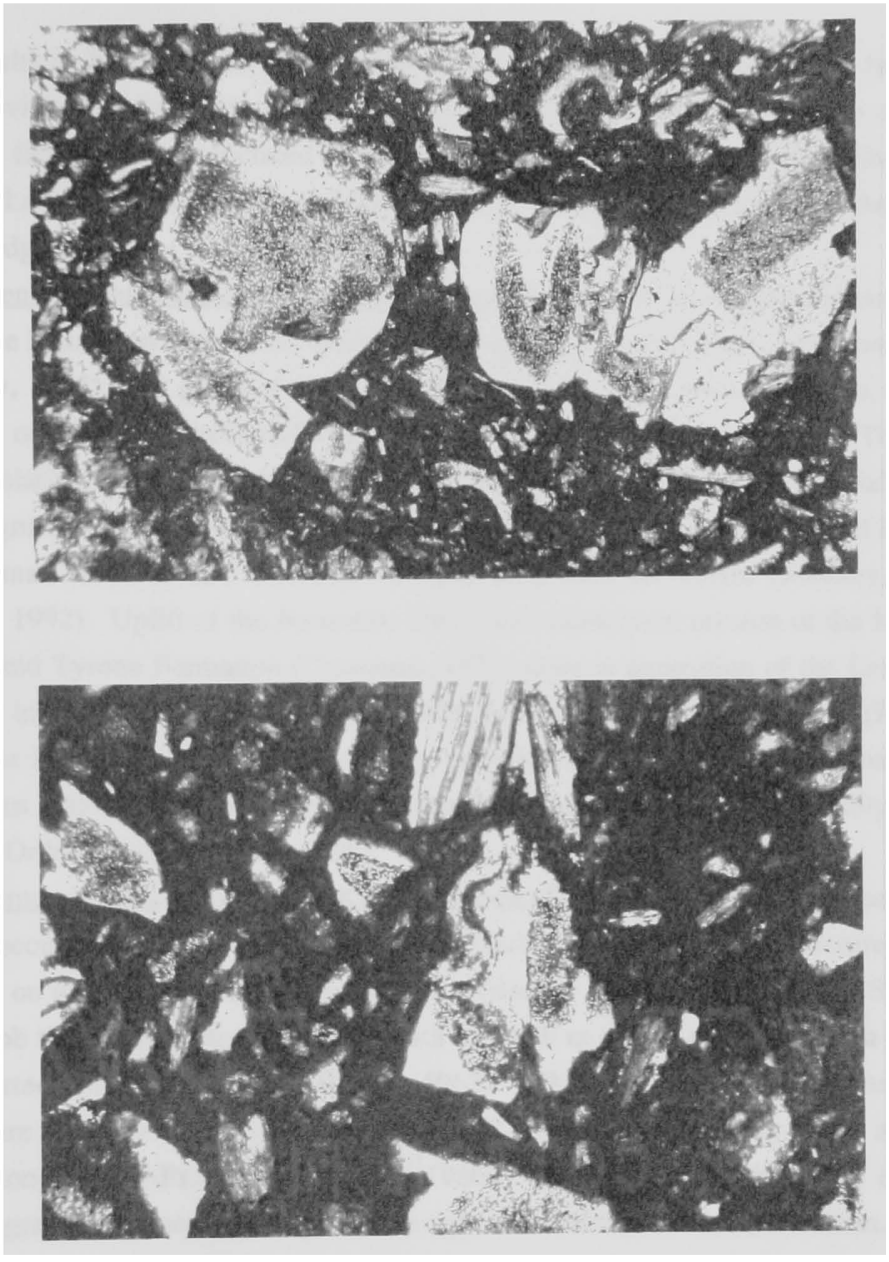

Figure 14. A (upper) Photomicrograph of euhedral terminations on echinoderm overgrowths, Shelby Co. (JK 78-2) core. Field of view is ~ 4 mm; B (lower) Photomicrograph of euhedral termination on echinoderm overgrowths, and as fragments in shaly matrix, Shelby Co. (JK 78-2) core. Field of view is ~ 2 mm.

SYNSEDIMENTARY FAULTS AND FAULT BRECCIAS

Faults in the Cincinnati Arch region are synsedimentary because: 1) the faults cut only Ordovician strata, some restricted to single beds; 2) bedding thickness changes across the fault; 3) the associated fault breccias contain only subrounded-subangular Middle to Late Ordovician clasts and fossils; and 4) truncation of at least one fault by a marine hardground.

Synsedimentary Faults adjacent to the Cincinnati Arch: Numerous synsedimentary faults occur in the Lexington Limestone in the central Kentucky region, near Lexington (Black and Haney, 1975), and south of Owenton. These faults offset beds over 2 m, die out within the outcrop and show bedding thickness variations across the fault. The fault walls are relatively undeformed and the fault gouge matrix is argillaceous and friable.

Segmentation of shallow water carbonates into fault controlled highs and lows on the Cincinnati Arch is also evidence of synsedimentary tectonism (Mackey, 1972; Ettensohn, 1992). Uplift of the Jessamine Dome and subsequent erosion of the Millbrig bentonite and Tyrone Formation (Cressman, 1973) prior to deposition of the Lexington Limestone indicates this was a positive feature during the Middle Ordovician (Haynes, 1994). The Kentucky River Fault zone is a complex system of faults that bounds the southeastern side of Jessamine Dome (Tanglewood Buildup) and was probably active during the Ordovician (Ettensohn, 1992).

Synsedimentary Faults in the Jeptha Knob Structure: Concentric normal faults and fault breccias occur associated with the Jeptha Knob cryptoexplosive structure, most commonly on the southeast side of the structure (Bucher, 1925; Seeger, 1968). South of Jeptha Knob there are extensional faults, with up to 30 m offset, associated with breccia and contorted limestone blocks (Jillson, 1962). The outcrops of the Jeptha Knob structure are poor (Seeger, 1968; Cressman, 1981) and the concentric faults are best exposed along I-64 (Jillson, 1962; Seeger, 1986). Other concentric faults are inferred from stratigraphic relationships, sparse outcrops and brecciated float (Cressman, 1981). The radial faults in the Jeptha Knob area are not exposed, lack associated breccias and are inferred from stratigraphic relationships (Cressman, 1981), though Bucher (1925) stressed the lack of any evidence for radial faults. Similar, concentric and radial faults and their fault breccias are associated with other cryptoexplosive structures in the region.

In a core through the Jeptha Knob structure, dips in the upper and lower part of the Lexington Limestone to Cincinnatian sequence are horizontal, and from 20° to 50°

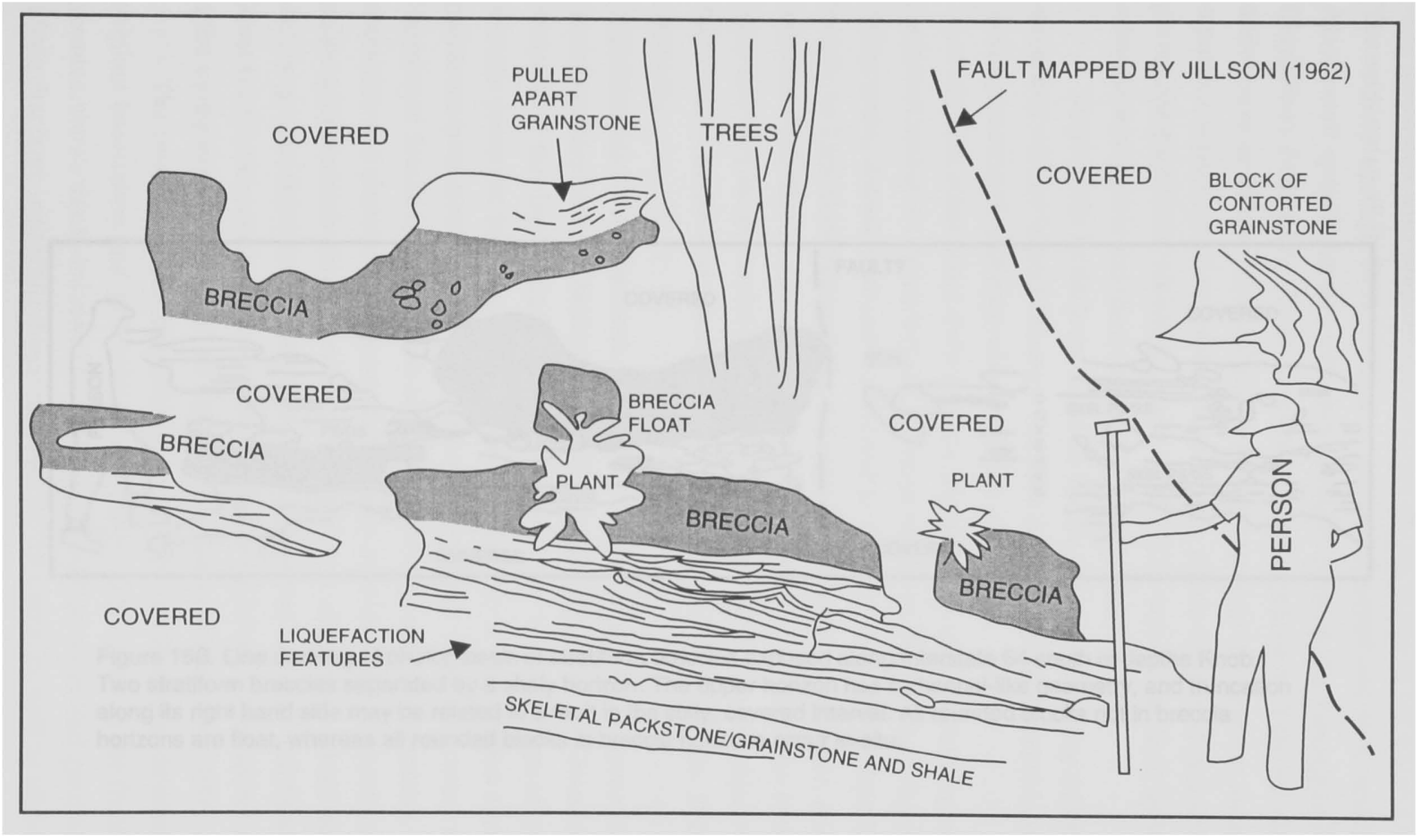

Figure 15A. Line drawing of photomosaics of stratiform breccias along Interstate 64, south of Jeptha Knob. Stratiform breccia horizon overlies deformed skeletal packstone and shale, and is overlain by pulled-apart grainstone. East of the fault mapped by Jillson (1962) is a large block of contorted grainstone unearthed during highway construction in the early 1960's.

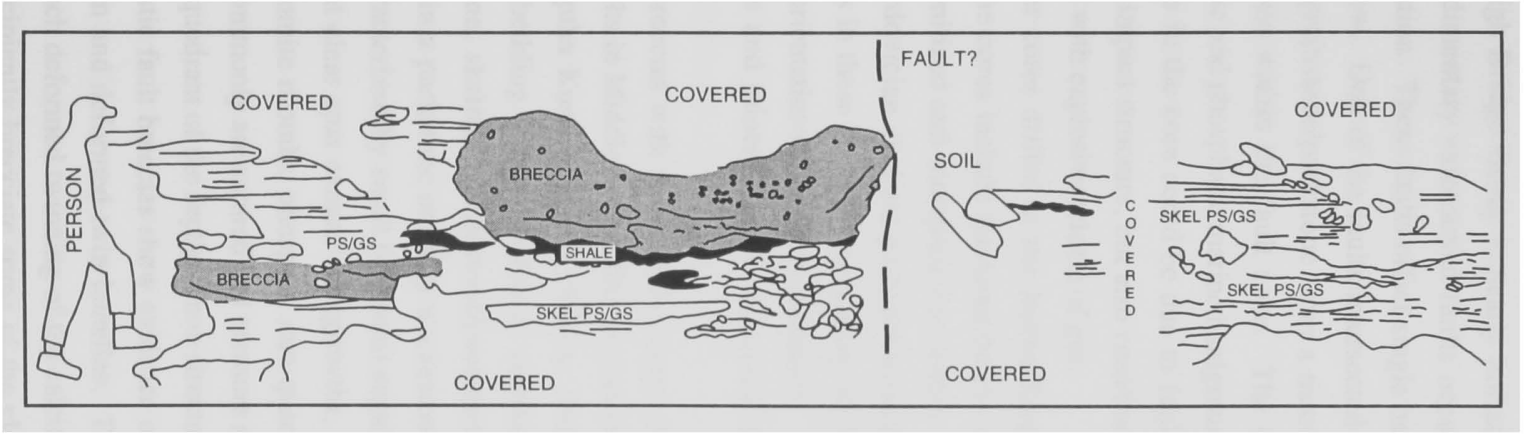

Figure 15B. Line drawing of photomosaic of stratiform breccias exposed along Interstate 64 south of Jeptha Knob. Two stratiform breccias separated by a shaly horizon. The upper horizon has a channel-like geometry, and truncation along its right hand side may be related to a fault in the soily, covered interval. All rounded blocks not in breccia horizons are float, whereas all rounded blocks in breccia horizons occur in-situ.

and associated with abundant slickensides on the shales in the Clays Ferry Formation. The underlying High Bridge Group is nearly horizontal and lacks stratiform breccias. Also, small synsedimentary extensional faults occur in the Lexington Limestone and Clays Ferry Formation. These faults offset single beds up to 3 cm but do not affect the beds above or below. One of the faults intersected in the core has sharp margins and separates skeletal grainstone/packstone from a matrix-supported incipiently brecciated grainstone/packstone within the fault zone. The top of the fault is truncated by a subhorizontal pyritic and phosphatic marine hardground.

Varying dip in the core could be due to faulting, slumping and/or bed rotation associated with an impact structure, but also could be due to repeated basement faulting possibly associated with explosive release of gas.

In two other cores drilled in the Jeptha Knob area no coherent stratigraphy is preserved, rather the cores include fractured blocks of Middle Ordovician High Bridge Group rocks, dolomitized and transported to within 4 m of the surface, brecciated late Middle to Late Ordovician skeletal packstone/grainstone and shale, and argillaceous dolomite. The dips in these cores are very steep 45-90^{o} and contacts between units are sharp and vary in orientations over short distances. There are abundant vugs and later diagenetic cements and mineralization, including dolomite, pyrite, chalcopyrite and marcasite.

Fault Breccias: Breccias with variably developed cataclastic textures occur along the synsedimentary faults in Middle to Late Ordovician rocks south of Owenton and along I-64 south of the Jeptha Knob structure (Jillson, 1962). Most fault-related cataclastic breccias cross-cut bedding. They consist of angular to subrounded clasts of skeletal grainstone/packstone, skeletal wackestone/packstone, lime mudstone, and whole or fragmented fossils in a packstone or shaly wackestone/mudstone matrix. The matrix is distinctive and characterized by small (< 2 mm) angular clasts composed of echinoderm grains with remnant clear spar cement overgrowths, along with whole and fragmented skeletal grains, dolomite rhombs, phospate, rare quartz silt, clay and framboidal pyrite. Grain boundaries commonly are sutured and pressure solved. Breccias are most common in the southeastern quadrant of the Jeptha Knob structure (Cressman, 1981).

The cataclastic fault breccias show evidence of subsequent deformation, such as incipient brecciation and deformed twin lamellae. The clasts in the fault breccia from Owenton shows much deformed twinning of the calcite and several generations of cross-cutting fractures incipiently brecciate some of the clasts, as well as skeletal fragments

(Figures 14). Similar deformed twin lamellae and "flow" textures in carbonate grains from cements in a fault breccia near were also described from fault breccias in the Jeptha Knob structure (Seeger, 1968; Cressman, 1981). These textures are not present in samples from the fault breccias along I-64 collected during this study suggesting these fabrics may have been caused by later faulting.

INTERPRETATION OF PRIMARY SEISMITE FEATURES

The bulk of the features interpreted as seismites are preserved in sub-storm wave base, deep ramp facies, although some occur in shallow, tidally influenced ramp facies. All of these features occur in tectonically active areas on the foreland, on or near the Jessamine Dome on the Cincinnati Arch, in the Jeptha Knob area, and in the foreland basin on thrust sheets proximal to the Taconic orogenic front (Figure 3). The interbedded skeletal packstone, calcisiltite and shale were deposited in deep ramp settings within storm wave base but below the level of intensive bioturbation (Cressman, 1973; Jennette and Pryor, 1993). The fine-grained skeletal grainstone with shale interbeds and fine-grained sandstone were deposited in shallow marine settings, with tidal currents affecting the interbedded skeletal grainstone and shale (Hrabar et al., 1976).

Synsedimentary Origin of Ball-and-Pillow Beds (Contorted Lamination): The ball-and-pillow beds developed early as indicated by the following: 1) they occur in beds that are bounded above and below by undeformed beds; 2) the horizontal tops of ball-and-pillow beds suggests they formed at or near the sediment/water interface which formed the tops of these features; and 3) the marine hardgrounds on top of some ball-and-pillow horizons indicates these horizons formed at the sediment/water interface, prior to hardground formation. The contorted laminations in the carbonate and clastic beds suggests that they were coherent before deformation and that they deformed hydroplastically (Visher and Cunningham, 1981). The contorted laminations and ball-and-pillow structures likely were produced by liquefaction soon after deposition, when the slight density contrast between the silts and clays made them susceptible to liquefaction (c.f. Lowe and LoPiccolo, 1974; Visher and Cunningham, 1981). Homogenization of the underlying shales probably occurred during the dewatering phase of liquefaction. Because the contorted beds commonly developed in calcisilts and shales, coarse sediment was not available to be deposited above the sediment-surface as in modern-day sand-blows (cf., Obermeier et al., 1990). The Ordovician deformation features formed subaqueously, thus

mobilized sediment at the sediment-water interface tended to fill in topographic lows, as at the ball-and-pillow horizon south of Owenton, Kentucky (Figure 6D) and near Clermontville, Ohio (Figure 8), and shown experimentally by Anketell et al. (1970).

Mechanisms Forming Ball-and-Pillow Beds

The characteristics of processes capable of producing submarine liquefaction features are given in Table 1.

Loading-Induced Liquefaction: Depositional loading of coarser, denser materials over finer, less dense materials can form loading features (i.e. ball-and-pillow beds and convolute laminations). This is because rapid deposition above water-saturated clays leads to increased pore fluid pressures, which may exceed the shear strength and lead to failure (Dzulynski and Walton, 1965; Allen, 1982; Brodzikowski et al., 1987; Obermeier, 1995). Montmorillonitic clays are most susceptible to liquefaction clay because of their ability to absorb water and remain soft (Obermeier, 1995). Clays in the Lexington Limestone and Clays Ferry Formation now are illitic to chloritic (Cressman, 1973), and have not undergone much burial that would have converted a montmorillonite precursor. Most of the ball-and-pillow beds occur in deep-water facies where long term accumulation rates are probably even lower than the average accumulation rate of 2 to 3 cm/kyr (Pope and Read, in press), which might argue against rapid depositional loading. There could have been rapid storm or tsunami deposition on the seafloor, but the relatively thin, coarse grained storm beds are of insufficient thickness to produce the thick ball-and-pillow beds in the Ordovician strata.

The tabular bedding and planar laminations of many of the calcisiltites could form from uniform settling through the water column, which has been shown experimentally to produce overcompaction of underlying beds, but not contorted bedding (McKee and Goldberg, 1969). Loading can cause contorted bedding if the load is unevenly applied (McKee and Goldberg, 1969) and experiments have shown that rapid, uneven depositional loading produces deformed laminations but does not produce isolated pillows (Weaver and Jeffcoat, 1978). Thus, density or viscosity differences between beds may make the load distribution beneath the bed unstable and cause overcompaction, but without an applied shock the bedding should not be much deformed. Because most of the sediment in these deep water facies settles through the water column or is locally derived during large storms, there is no point source such as a delta or fan for the sediments, and so little or no rapid loading from a point source, hence there is no mechanism to cause widespread differential loading. Thus, the deep ramp setting, the lack of depositional

Table 1. Characteristics of features capable of producing submarine liquefaction (i.e., ball-and-pillow bedding, breccia beds, foundered blocks)

	Depositional Loading	Storms/	Tides	Slumping	Tsunamis	Earthquake-Induced Deformation Structures
Slope	N/A	N/A	N/A	$>2^{o}$	N/A	N/A
Areal extent	100's to 1000's km^2	100's to 1000's km^2 (rare)	< 10 km^2	100's km^2	100's to 1000's km^2	100's to 1000's km^2
Bedding	Thick slugs of coarser sediment overlying finer sediment	Large ripple and dune bedforms; local mobilzation of in-situ sediment, thick mud layers in otherwise coarse deposits	Deformed foresets, avalanche faces	Complexly deformed, may have scarp at upper surface, down dip bed thickening, brecciation, basal glide plane	Thin marine layers within terrestrial sediments onshore. Offshore, coarse, often chaotic beds in finer grained facies.	Brecciation, sand blows, sand dikes, ball-and-pillow bedding, distorted bedding
Water Depths	0-50 m or more	0-40 m or more	0-10 m	All depths	All depths	All depths
Depositional Setting	Delta Fronts	Shallow to Deep Ramp	Shallow Ramp	Shallow to Deep Ramp	N/A	N/A
Latitudinal Constraints	None	Most common 0-30^{o} N or S of equator	None	None	None	None
Sediment Accumulation Rate	High	Low to High	Low to High	N/A	N/A	N/A
Orientation of deformed bedding	Preferred orientation of deformed beds downslope or upslope	Unidirectional in direction most prevalent during storm	Random???	Unidirectional downslope	Bidirectional onshore and offshore	Randomly oriented

point sources, and slow sedimentation rates argues against loading-induced liquefaction for the ball-and-pillow structures.

Storm- and Tide-Induced Liquefaction: Although many of the contorted beds are in alternating shale and calcisiltite or siltstone deposited near storm wave base but below the level of intense bioturbation, and most show storm-generated sedimentary features (e.g., graded bedding, hummocky cross stratification, aligned shell beds), only a few beds are deformed. Theoretically, large hurricanes are capable of creating areas of liquefaction over 100 km^2, because they can produce intense bottom currents in water depths of 10 to 30 m (Herbich, 1977) that greatly exceed the shear velocity necessary for liquefaction and/or fluidization (Lowe, 1976). However, studies of hurricane-induced sedimentation on clastic and carbonate shelves do not show any soft-sediment deformation (cf., Vaughan et al., 1987; Morton, 1988; Boss and Neumann, 1993; Shinn et al., 1993). Also, the random orientation of the axial planar traces from the ball-and-pillow horizons contrast with the preferred orientations expected from large unidirectional storm waves (Prentice, 1960; Dzulynski and Smith, 1963).

Shear drag associated with tidal fluctuations may produce contorted bedding in very shallow water settings, but these are of limited areal extent (Dalrymple, 1979). Repeated pounding by shallow tide-waves may produce overcompaction in modern-marine sediments (Bjerrum, 1973; Lee and Focht, 1975) and this could decrease the potential for liquefaction in sediments (Dalrymple, 1979). Although most of the Ordovician deformation features did not form under the influence of shallow storm waves, this mechanism may have caused some deformed bedding in tidally influenced grainstones of the Tanglewood Bank. The storm beds in the Martinsburg/Kope/Clays Ferry Formations are generally 5-30 cm thick, but the thickness of the ball-and-pillow horizons is usually much thicker 1 to >5 m so it is unlikely these features were produced by single storms. Moreover, the wide lateral extent of the ball and pillow features suggests a different mechanism.

Slumping: Downslope slumping of sediment can produce contorted laminations and distorted bedding (Elliott and Williams, 1988). Slumped and contorted beds are most common on steep, unstable continental slopes or delta fronts (Morton, 1988). The Ordovician ramp slope in Kentucky, southwest Ohio and Virginia was probably less than 0.1 degrees (2 m/km) which is too low for most gravity-induced slumping, which require slopes of 2 to 4^o or more (Lowe, 1975). However, seismically triggered slumping may occur on seafloors with as little as 0.25^o slope during magnitude 6 to 7 earthquakes (Field

et al., 1982). The Ordovician rocks show no glide planes or master surfaces on which slumps moved, instead beds deformed in-situ, with little evident downslope movement. Slumping usually produces downslope thickening and bed rotation, as well as marked symmetry in the axial planar traces of the contorted beds in a downslope direction (Prentice, 1960; Brenchley and Newall, 1977; Seilacher, 1984). The random axial planar traces and lack of downslope thickening in the Ordovician units rules out a slump origin. Furthermore, the gradational bases of beds, the lack of evidence of horizontal movement, and the lateral interfingering with undisturbed beds, suggests that the ball-and-pillow structures were not caused by slumping (Kreisa, 1980).

Seismically-Induced Liquefaction: Seismically-induced liquefaction produces seismites by releasing pore-pressure instabilities between sedimentary layers. These pressure instabilities can be caused by a reverse density gradient produced by sedimentation or seismic shaking, and the subsequent loss of load-bearing capacity of the underlying bed (Hempton and Dewey, 1983; Seilacher, 1984). The seismic shock induces dewatering of sediment, liquefaction, and water-escape structures which release the pore-pressure instability and distort original layering (Kuenen, 1958; Lowe, 1975; Seilacher, 1984). Most primary seismites occur at or within 10 to 15 m of the sediment-water interface (Obermeier et al., 1991), though some may be produced even 50 m below the sediment-water interface (Scott and Price, 1988).

Experiments that mechanically shocked alternating beds of siliciclastic or carbonate sand and mud in flumes or fish tanks produced contorted and convoluted bedding similar to that seen in the field (Kuenen, 1958; Anketell et al., 1970; Weaver and Jeffcoat, 1978). A continuum of structures, from slightly undulated bases on beds to isolated sand balls encased in shale are formed experimentally as the strength and duration of shaking increases (Kuenen, 1958; Weaver and Jeffcoat, 1978; Visher and Cunningham, 1981). The experimentally deformed sediments show wide synclinal areas defined by upturned laminations in the overlying bed, separated by narrow anticlines, with material injected upward from the lower bed.

Anticlinal axes of these deformed beds generally are randomly oriented with a predominant vertical component due to the upward movement of overpressured fluids during the loss of bearing capacity. However, seismites may show rare asymmetry of anticlinal axes in outcrop (Sims, 1973) and in experiments (Kuenen, 1958; Anketell et al., 1970; Weaver and Jeffcoat, 1978).

The experimental deformation affected a uniform depth below the sediment surface, but the deformation structures may die out laterally, indicating that excess pore-pressure was not released uniformly, but through many small areas between larger passively deformed areas that sank into the underlying sediment (see Weaver and Jeffcoat, 1978; Figure 4). These liquefaction features probably are similar to sand-blows that form after large earthquakes (Obermeier et al., 1990; 1991). Undeformed sediments occur below the deformed zone, because each temblor only effects sediments near the sediment-water interface (Kuenen, 1958).

The contorted Ordovician beds in Kentucky, southwest Ohio and Virginia are interpreted to have formed mainly by seismically-induced liquefaction because: 1) they are similar to structures produced in the laboratory; 2) there is no preferred orientation in the axial planar traces, contrary to what would be expected from large shallowing storm-waves, or slumping; 3) the large area and lateral extent of these deposits seems to rule out storm-waves; 4) the sloping ramp was not conducive to slumping without a tectonic trigger; 5) the slow sedimentation rate and lack of a point source tend to rule out load-induced liquefaction; and 6) the area was tectonically active along the Cincinnati Arch in Kentucky and the thrust front in Virginia during the Middle to Late Ordovician (Mackey, 1972; Borella and Osborne, 1978; Glover et al., 1983; Weir et al., 1984; Pope and Read, 1992).

However, if the structures were produced by seismic shock, the tsunamis generated by this may also have played a role in liquefaction. Tsunamis produce large shear stresses on the seafloor as the waves move into shallow waters. These may induce liquefaction, although unequivocal submarine deposits produced by tsunamis are few. The tsunami-induced "homogenite" bed shed from steep slopes of islands in the Mediterranean Sea is a single normally graded bed up to 7 m thick but lacks any other sedimentary structures and shows no evidence of liquefaction (Kastens and Cita, 1981). Thus it seems likely that tsunamis may have accentuated the effects on any seismically induced liquefaction on the Ordovician sea-floor, but deciphering those events from these seismites is presently indeterminable.

ORIGIN OF SECONDARY SEISMITES

Foundered Channel Fills: The asymmetrical cross-section, the internal layering of mud draped carbonate sands, which thicken into the axis of the fill, truncation of finer host

sediments by the basal contact all suggest this feature was originally a channel fill formed by tidal currents, and perhaps by storm currents. Subsequent seismic shaking modified the original form, faulting the grainstone fill, diapirically intruding a shaly limestone plug into the fill, and forming ball-and-pillow structures in the adjacent bed(s). The well preserved bedding in the grainstone channel and the abrupt truncation of bedding on the thickest part of the channel suggests the wedge was coherent or competent prior to shaking. The density and rigidity of the channel fill allowed it to sink into the underlying muds during seismic shaking. The underlying muds were still soft during shaking because they have lost their original layering adjacent to the channel fill. The lateral continuity of skeletal grainstone channel-fill, other grainstone masses and ball-and-pillow beds indicate these structures were caused by a similar mechanism.

Non-Cataclastic Carbonate Breccia Beds: The rare non-cataclastic sedimentary breccia beds in the Martinsburg Formation in Virginia and Brannon Member in Kentucky probably formed by seismically induced liquefaction, fragmentation and in-situ re-mobilization of semi-plastic carbonate units, which is indicated by the close association of the breccia beds-and-ball and pillow horizons (Black and Haney, 1975; Kreisa, 1980). Rare occurrence of grading, as in the Martinsburg bed, may indicate some downslope transport on the underlying ball-and-pillow layer. Clasts in these breccias are locally derived from within the horizon and upward movement of fluid probably rotated and rounded the soft but coherent clasts. Ball-and-pillow beds developed below and adjacent to some of these breccias suggest that both were produced by similar, if not the same, events.

Cataclastic Breccias in Jeptha Knob: The stratiform cataclastic breccias in the Jeptha Knob area appear to be re-sedimented cataclastic units because they are interstratified with shales and limestones, show massive grain-flow and debris flow fabrics (cf. Lowe, 1976) and contain highly fragmented clasts of previously cemented limestone. The clasts commonly have original porosity around their grain boundaries which are filled by the matrix suggesting that some of the clasts had high original porosity with cements only rimming grains. This is further indicated by the euhedral calcite terminations on echinoderm grains which developed into open pores prior to fragmentation. Given that the previous mapping suggests that these features are closely associated with the Jeptha Knob cryptoexplosive structure and apparently do not occur away from the structure (Bucher, 1925; Seeger, 1968; Cressman, 1981) this suggests that the stratiform breccias are genetically related to the cryptoexplosive structure. The early cemented grainstone

clasts within some of the breccias, along with numerous re-worked angular fragments of echinoderm overgrown with cement, suggests that early cemented beds were explosively fragmented and re-sedimented as breccia beds which punctuated the normal background shale and skeletal limestone accumulation in the region. We propose that these breccias were shed into lows from seismically active topographic highs and fault scarps over the cryptoexplosive structure. Tsunamis or debris flows generated by faulting and/or gas explosion may have re-sedimented the fragmental material on the surface of the structure to form the individual breccia beds. The numerous horizons of breccia suggest that this was not a single seismic or impact event, but involved repeated events, perhaps related to basement faulting in conjunction with explosive release of gas from below.

DISCUSSION OF PRIMARY SEISMITES

Epicenter Location and Magnitudes: Seismically-induced sedimentary dikes and their decreasing size with distance from the epicenter have been used to define epicenter location of past quakes in Holocene sediments (Obermeier et al., 1991; Munson et al., 1995). In a similar manner, seismically-induced liquefaction features in marine sediments (e.g. ball-and-pillow beds, contorted laminations) may help broadly define epicenters in ancient settings. The distribution of seismites in Kentucky, southwest Ohio and Virginia is poorly constrained beyond the outcrop belt and cored areas. Thus, the distribution of the seismites shown of Figure 3 provides only a minimum estimate of their areal extent.

Since magnitude 5 earthquakes produce little or no liquefaction features, whereas earthquakes of magnitude 6 or above produce abundant liquefaction features (Kuribayashi and Tatsuoka, 1975; Youd, 1977), earthquakes of moment magnitudes of 5.8 ± 0.4 are considered necessary to form widespread liquefaction features (Obermeier et al., 1991).

For shallow focus earthquakes (< 50 km depth), the radius of the area containing liquefaction features such as sand blows and clastic dikes is related to Moment Magnitude (M_O) (Ambraseys, 1988). The magnitude of the earthquakes that formed the Ordovician seismites may be quantitatively estimated by determining the maximum epicentral radius of the observed features and comparing that radius with the plot for the Holocene structures (Ambraseys, 1988; Figure 16). Allen (1986) used the empirical

Table 2. Proposed Moment Magnitude of earthquakes that formed seismite horizons in late Middle and Late Ordovician rocks of Kentucky, Ohio, and Virginia.

FORMATION AND LOCATION	MAXIMUM EPICENTRAL DISTANCE (KM)	MOMENT MAGNITUDE (M_0)	
		ALLEN (1986)	AMBRASAYS (1988)
LEXINGTON LIMESTONE KENTUCKY	35	6.9	6.2-6.9
LEXINGTON LIMESTONE (WESTERLY SOURCE)	65	7.3	6.7-7.4
LEXINGTON LIMESTONE & PT. PLEASANT COMBINED	75	7.3	6.7-7.4
GARRARD SILTSTONE KENTUCKY	100	7.5	6.9-7.7
FAIRVIEW FM KENTUCKY & OHIO	35	6.9	6.2-6.9
MARTINS-BURG FM VIRGINIA	65	7.3	6.7-7.4

relationships of sedimentary response from Kuribayashi and Tatsuoka (1975) and Youd (1977) to derive the following relationship.

$$M = 0.499 \ln (X/3.162 \times 10^{-5}) \quad (1)$$

where M is Moment Magnitude and X is the maximum epicentral radius in km. This equation consistently gives values on the high end of the estimates from observed data (Ambrasays, 1988) (Table 2 and Figure 16).

Caution must be used when extrapolating data from Recent continental depositional settings to ancient continental and marine settings because such features as water table elevation, the effects of an overlying water column, length of seismic shock, compaction and saturation of the sediment at the time of the earthquake, and depth of earthquake foci are difficult to determine in ancient sediments, but may profoundly affect the sediment response (Amick and Gelinas, 1991), thus these values must be viewed as crude estimates. Similarly, we do not know if liquefaction features that formed in the Ordovician marine sediments obey the same relationship as liquefaction features in Holocene terrestrial environments. Further, experimental work has focused on interbedded sand and shale, so we know little about the seismic response of quartz-carbonate silt and shale of this study. The density difference between silt and shale layers should be less than the sand and shale, and the increased plasticity and lower permeability might make silt and shale more difficult to liquefy than sand and shale. Consequently, the following estimates of paleoseismicity should be viewed as preliminary.

Although the Lexington Limestone seismites show no systematic variation in size, their increased abundance on the western margin of the Jessamine Dome suggest that epicenters may have been located west of the dome. Furthermore, the increasing number of seismites upward in the Lexington Limestone suggests that the Jessamine Dome became more tectonically active during upper Lexington Limestone deposition. Epicentral radius (half the map distance) for the Lexington Limestone seismites is about 35 km, suggesting M_O=6.2 to 6.9 earthquakes. However, if the seismites in the Lexington Limestone were induced from earthquakes further west the epicentral radii for these features may be closer to 65 km, indicating a M_O= 6.7 to 7.4.

Additionally, if the Point Pleasant Tongue of the Clays Ferry in southern Ohio correlates with the upper Lexington Limestone, as suggested by Sweet, 1979, then the epicentral radii for these seismites may be more than 80 km indicating a M_O = 6.8 to 7.5.

The concentration of Garrard seismites south and east of the Jessamine Dome and near the Kentucky River Fault system suggests that epicenters for these may have been

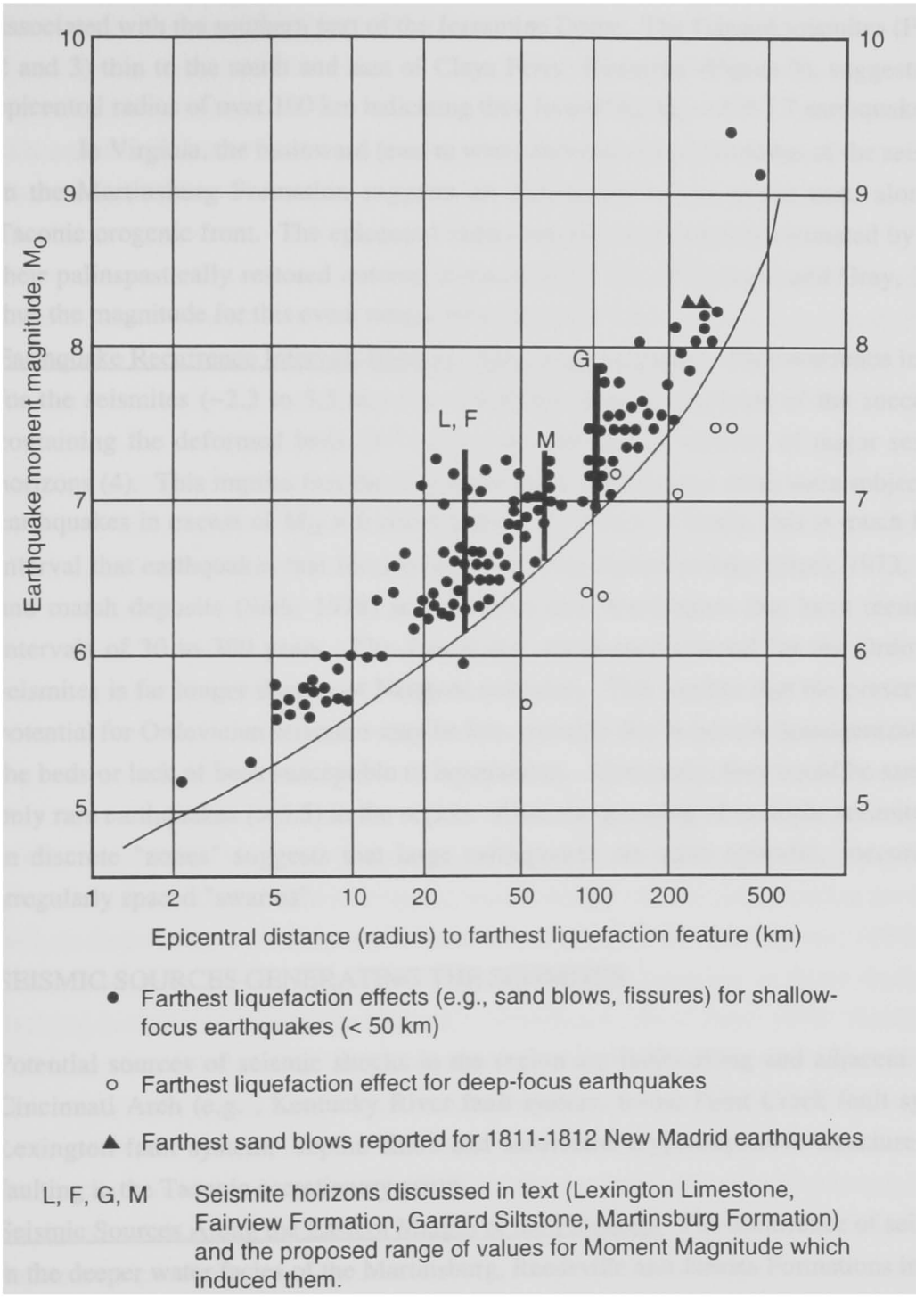

Figure 16. Diagram showing the relationship between Moment Magnitude and epicentral radius (modified from Ambrasays, 1988). The range of Moment Magnitudes for the epicentral radii of seismites discussed in text indicated by vertical black bars.

associated with the southern part of the Jessamine Dome. The Garrard seismites (Figures 2 and 3) thin to the south and east of Clays Ferry, Kentucky (Figure 3), suggesting an epicentral radius of over 100 km indicating they formed by M_O = 6.9-7.7 earthquakes.

In Virginia, the basinward (east to west) decrease in bed thickness of the seismites in the Martinsburg Formation suggests an earthquake source to the east, along the Taconic orogenic front. The epicentral radius can be conservatively estimated by using their palinspastically restored outcrop distance of 65 km (Woodward and Gray, 1985), thus the magnitude for this event ranges from M_O= 6.7-7.4.

Earthquake Recurrence Intervals from the Ordovician Seismites: The recurrence interval for the seismites (~2.3 to 3.5 m.y.) is calculated from the duration of the succession containing the deformed beds (9-14 m.y.) divided by the number of major seismite horizons (4). This implies that the Cincinnati Arch and Virginia areas were subjected to earthquakes in excess of M_O = 6 about every 2 to 4 m.y. Clearly, this is much longer interval that earthquakes that formed seismites from Holocene lake (Sims, 1973, 1975) and marsh deposits (Sieh, 1978) in California and Washington that have recurrence intervals of 30 to 300 years. The 2 to 4 m.y. recurrence interval for the Ordovician seismites is far longer than most Neogene seismites. This implies that the preservation potential for Ordovician seismites may be low, possibly due to burrow homogenization of the beds or lack of beds susceptible to liquefaction. Alternately, they could be sampling only rare earthquakes (> 5.5) in the region. Also, the grouping of multiple seismite beds in discrete "zones" suggests that large earthquakes are quite episodic, occuring in irregularly spaced "swarms".

SEISMIC SOURCES GENERATING THE SEISMITES

Potential sources of seismic shocks in the region are faults along and adjacent to the Cincinnati Arch (e.g. , Kentucky River fault system, Irvine Paint Creek fault system, Lexington fault system, Jeptha Knob and associated cryptoexplosive structures, and faulting in the Taconic accretionary prism.

Seismic Sources Along the Eastern Margin of the Foredeep: The occurrence of seismites in the deeper water facies of the Martinsburg, Reedsville and Juniata Formations indicate seismic activity was prevalent in the Late Ordovician foredeep. The seismites described from these rocks are most likely caused by earthquakes related to the faulting and overthrusting along the Taconic orogenic front. Evidence for active tectonism during

development of the Taconic foreland basin includes: 1) the increasing abundance of deeper water facies (Sevier, Blockhouse, Liberty Hall, Martinsburg and Reedsville Formations) on the eastern side of the foreland basin indicate more rapid subsidence in this area as a result of easterly derived thrust loading on the plate margin; 2) the Middle Ordovician Fincastle and Avens Bridge conglomerates cannibalizing uplifted Early Cambrian to Ordovician sediments from the rising accretionary prism (Lowry, 1974); 3) slump structures in the Middle Ordovician foredeep sediments (Read, 1979) may have been triggered by earthquakes in this area; 4) synsedimentary down-to-basement faulting produced much of the Taconic foredeep in New York (Bradley and Kidd, 1991); abundant ash beds and volcanism at this time indicate subduction and seismicity along the eastern foreland margin (Samson et al., 1989).

Faulting and Seismicity Associated with the Cincinnati Arch: All of the seismites in Kentucky and southwest Ohio occur the late Middle to Late Ordovician strata along the Cincinnati Arch indicating it may have been a focus of paleoseismicity throughout this time. If the Cincinnati Arch was a forebulge (Quinlan and Beaumont, 1984; Ettensohn, 1991), then it appears to have responded repeatedly to plate stress loading along the craton margin, possibly along reactivated basement structures. Uplift of blocks by reactivation on older structures corresponds well with exposures of Trenton rocks in the Appalachian Basin in New York and Pennsylvania that show down-to-the-basin block faulting as the main mechanism for foreland basin development in this area (Cisne et al., 1982; Lash, 1985; Hay and Cisne, 1988; Mehrtens, 1988a, b). This may explain the presence of several discrete forebulges (synsedimentary positive areas) during the Middle to Late Ordovician sedimentation in the foreland (c.f., Borella and Osborne, 1978; Read, 1980; Diecchio, 1993; Goggin and Haynes, 1995). Cambrian to Early Ordovician faulting is well-documented in Kentucky (Woodward, 1961; Heyl, 1972; Webb, 1980; Cable and Beardsley, 1984). However, the first evidence of uplift on the Cincinnati Arch is in the Middle Ordovician, which is manifested by removal of the Millbrig bentonite over the Jessamine Dome at the disconformity between the High Bridge Group and Lexington Limestone (Haynes, 1994). Evidence for uplift along the Cincinnati Arch in the Middle to Late Ordovician is the restriction of tidal flats (Mackey, 1972) and tidally influenced grainstone shoals (Hrabar et al., 1971) of the Lexington Limestone to the Jessamine Dome.

Synsedimentary faulting during the Middle to Late Ordovician allowed the Cincinnati Arch to remain a positive element while the Sebree Trough and Appalachian

Basins were subsiding more rapidly as shown by the restriction of shallow water facies to the Arch during this time (Mackey, 1972; Borella and Osborne, 1978). The segmentation of these shallow water facies into alternating highs and intervening lows on the Arch reflect cross-cutting structures (Mackey, 1972). The development of a structurally controlled shale basin on the Cincinnati Arch during the Late Middle Ordovician (Kulp, 1995) also indicates the influence of synsedimentary structures. Similarly, the development of the shallow water Jessamine and Nashville Domes while the remainder of the area was relatively deep water suggests local tectonics differentiated the Arch into numerous small blocks that moved independently of one another (Borella and Osborne, 1978). The seismites described from Kentucky and southern Ohio are likely related to earthquakes originating along basement faults along the Cincinnati Arch which kept it a positive element resisting subsidence during this phase of basin development.

Seismic Sources Associated with the Jeptha Knob Structure: The Jeptha Knob cryptoexplosive structure has been ascribed to a meteorite impact based on folded and faulted beds of Late Ordovician rocks outcropping in a semi-circular map pattern in this area, and a 1 to 1.2 mgal gravity anomaly associated with this feature (Seeger, 1968). Decreasing evidence of faulting (Bucher, 1925; Seeger, 1968) and brecciation (Cressman, 1981) to the west and north indicate deformation in the Jeptha Knob structure was most intense in its southeastern quadrant. Additionally an anomalously high iridium content in the basal Early Silurian breccia beds overlying the faulted and folded Ordovician rocks is also interpreted to result from this impact (Seeger et al., 1985). However, the lack of impact features (e.g., shatter cones or other shocked minerals) and the poor outcrops lead Cressman (1981) to conclude that the origin of this feature is enigmatic, but not directly traceable to a meteorite impact.

If the Jeptha Knob cryptoexplosive structure was formed by a meteorite (Seeger, 1968), we would expect to see a single breccia zone at the surface of the impact site, rather than the multiple stratiform breccias evident on the surface (Jillson, 1962; Seeger, 1968; Cressman, 1981; Seeger, 1986) and in the core. The multiple stratiform re-sedimented cataclastic breccias in the Shelby County core and in outcrops surrounding Jeptha Knob cannot be related to a single impact but instead require several events involving local earthquakes and slumping at the sediment-water interface. Furthermore, the multiple re-sedimented cataclastic breccia bed horizons may correlate with ball-and-pillow beds near Frankfort, Kentucky, 25 km from the Jeptha Knob structure (Figure 5). One stratiform breccia lies directly on a ball and pillow bed along I-64 (Figure 15) and

may be related to a nearby fault. Also, these breccias require a local source for high-energy grainstone clasts or they would have to have come from far to the east on the arch, which is unlikely given the low depositional slopes and localized occurrence.

It is possible the earthquakes generated from the Jeptha Knob cryptoexplosive structure and other such structures in the area could form the re-sedimented cataclastic breccias in the local area, as well as some of the seismites elsewhere. If the Jeptha Knob structure was formed by periodic earthquakes associated with explosive release of gas then hydro-fracturing of the overlying partly cemented, but very permeable carbonate beds might produce some of the stratiform cataclastic breccias while simultaneously forming the seismites in the Lexington area. The interpretation of the Jeptha Knob as a structure resulting from seismicity and explosive release of gas at depth can explain the concentric and radial faulting in this area, and the plug of Logana Member sediments mapped the center of this structure (Cressman, 1981), the Middle Ordovician High Bridge Group blocks within 4 m of the present-day surface in the cores, and the repeated stratiform re-sedimented cataclastic breccias in the core and on the surface.

MARINE SEISMITES, HIGH-FREQUENCY CYCLES AND TIME-MARKERS

These seismically-induced liquefaction features are unique because they provide in-situ evidence of earthquakes in a marine subtidal setting. In a sense they are shallow, epicontinental analogs to the broken telephone lines in the Atlantic Ocean which recorded the 1929 Grand Banks earthquake and slumping (Heezen and Ewing, 1952). These marine seismites differ from terrestrial examples because: 1) the liquefied layer is shale and silt, rather than sand, and the capping layer is coarser than the underlying beds; 2) they rarely show preserved expelled sediment above the overlying confining bed; and 3) they are difficult to sample in modern settings which may account for the paucity of descriptions of these features.

In the Late Mohawkian to Cincinnatian supersequence, which is composed of >100 shallowing upward meter-scale cycles (Pope and Read, in press), the presence of only four extensive seismite horizons, spaced about 2 to 4 m.y. apart, might argue against earthquakes as a major cause of the Ordovician high-frequency carbonate cycles that are common throughout the succession. However, because observations of Holocene seismically-induced liquefaction features require >5 magnitude earthquakes, then most smaller events would not leave a seismite record. The Richter-Gutenberg law of

earthquake recurrence indicates there is a ten-fold decrease in frequency of occurrence of earthquakes with each integer increase in moment Magnitude. For example if a M_O=7 earthquake affected an area every 3 m.y., then 10 M_O=6 earthquakes should affect the same area (~1 every 300,000 years) and 100 M_O=5 earthquakes. This suggests that the study area likely was subjected to many earthquakes, which could have caused local subsidence and small-scale cycle formation locally. However the sedimentary record of these earthquakes is not preserved in the Ordovician strata.

Earthquakes associated with jerky subsidence have been cited as a cause for the formation of carbonate cycles (Cisne, 1986; Hardie et al., 1990). Multiple seismites in peritidal carbonates of the Middle Proterozoic Belt Supergroup were shown to indicate that earthquakes did not form the shallowing upward cycles (Pratt, 1994). Clearly, the seismite data from the Ordovician does not provide a test for a tectonic vs eustatic origin for the cycles, because the seismites only record the large events.

Seismites are synchronous, regional time-markers that are useful in correlating stratigraphy within a region (Sims, 1973; Sieh, 1978; Cojan and Thiry, 1992). Seismites in the Ordovician beds form excellent markers where few other distinctive markers are present and also appear to correlate with some of re-sedimented cataclastic breccia beds in the Jeptha Knob structure (Figure 5). These seismite beds may provide high-resolution time markers if they formed over a sufficiently large area. For instance, ball-and-pillow horizons in the Logana Member in Kentucky may be correlative to similar features at the same stratigraphic position on the Nashville Dome, and these types of horizons may help us determine when specific structures became active. Additionally, if ball-and-pillow beds, slump beds and breccia beds were formed by earthquakes, then they could be used to make intrabasinal correlations with similar features in time-equivalent rocks in the Appalachian Basin further to the north (Pickering, 1987; Mehrtens, 1988a, b; Lash, 1988; Blewett, 1991). However, the limited areal extent of the seismites and the intermittent outcrop exposures and cores would require several discrete horizons to be useful.

CONCLUSIONS

1. Regionally mappable ball-and-pillow structures in Middle to Late Ordovician rocks in Kentucky, southwest Ohio and Virginia appear to be seismites (earthquake generated sedimentary structures). Besides ball-and pillow features, there are deformed channel-fills, sedimentary breccias, cataclastic breccias and re-sedimented cataclastic breccias, and synsedimentary faults, associated with regional structures and local cryptoexplosive structures.

2. These features indicate active tectonism along the Cincinnati Arch during deposition of Late Middle to Late Ordovician strata.

3. The seismites are used to define earthquake epicenters, magnitudes, and recurrence intervals for the Ordovician rocks. However, because the seismites appear to record only the larger events, they provide little information of higher frequency earthquakes that affected the region, and thus cannot be used to assess the role of tectonics in high-frequency carbonate cycle formation.

4. The apparent correlation of the seismites with fault- and re-sedimented cataclastic breccias in the Jeptha Knob cryptoexplosive structure suggests that at least some of the seismites may relate to repeated earthquakes, and the explosive release of gas from depth possibly associated with formation of this structure. They cannot relate to a single meteorite impact, since they occur in multiple horizons, both on the Cincinnati Arch, and in the Jeptha Knob cryptoexplosive structure. More work is need to separate seismites related to regional basement fault structures from those possibly generated by cryptoexplosive structures.

REFERENCES

Adams, J., 1990, Paleoseismicity of the Cascadia subduction zone: Evidence from turbidites off the Oregon-Washington margin: Tectonics, v. 9, p. 569-583.

Allen, J.R.L., 1982, Sedimentary structures, volume II, Amsterdam, Elsevier, 663 p.

Allen, J.R.L., 1986, Earthquake magnitude-frequency, epicentral distance, and soft-sediment deformation in sedimentary basins: Sedimentary Geology, v. 46, p. 67-75.

Ambrasays, N.N., 1988, Engineering Seismology: Journal of the Internaltional Association of Earthquake Engineering, V. 17, p. 1-105.

Amick, D., and Gelinas, R., 1991, The search for evidence of large prehistoric earthquakes along the Atlantic Seaboard: Science, v. 251, p. 655-658

Anketell, J.M., Cegla, J., and Dzulynski, S., 1970, On the deformational structures in systems with reversed density gradients: Annual Society of Geology Poland, v. 40, p. 3-30.

Atwater, B.F., 1987, Evidence for great Holocene earthquakes along the outer coast of Washington State:Science, v. 236, p. 942-944.

Atwater, B.F., and Moore, A.L., 1992, A tsunami about 1000 years ago in Puget Sound, Washington: Science, v. 258, p. 1614-1617.

Bjerrum, J., 1973, Geotechnical problems involved in foundations of stuctures in the North Sea: Geotechnique, v. 23, p. 319-358.

Black, D.F.B., and Haney, D.C., 1975, Selected structural features and associated dolostone occurrences in the vicinity of the Kentucky River Fault System: Annual Field Conference, Geological Society of Kentucky, Kentucky Geological Survey, Lexington, Ky, p. 6-43.

Blewett, R.S., 1991, Slump folds and early structures, northeastern Newfoundland Appalachians: Re-examined: Journal of Geology, v. 99, p. 547-557.

Borella, P.E., and Osborne, R.H., 1978, Late Middle and early Late Ordovician history of the Cincinnati Arch Province, central Kentucky to central Tennessee: Geological Society of America Bulletin, v. 89, p. 1559-1573.

Boss, S.K., and Neumann, A.C., 1993, Impacts of Hurricane Andrew on carbonate platform environments, northern Great Bahama Bank: Geology, v. 21, p. 897-900.

Bradley, D.C., and Kidd, W.S.F., 1991, Flexural extension of the upper continental crust in collisional foredeeps: Geological Society of America Bulletin, v. 103, p. 1416-1438.

Brodzikowski, K., Haluszczak, A., Krzszkowski, D., and Van Loon, A.J., 1987, Genesis and diagnostic value of large-scale gravity-induced pencontemporaneous deformation horizons in Quaternary sediments of the Kleszczow Graben (central Poland): *in* M.E. Jones, and R.M.F. Preston, eds., Deformation of Sediments and Sedimentary Rocks, Geological Society Special Publication no. 29, p. 287-298.

Brenchley, P.J., Marshall, J.D., Carden, G.A.F., Robertson, D.B.R., Meidla, T., Hints, L., and Anderson, T.F., 1994, Bathymetric and isotopic evidence for short-lived Late Ordovician glaciation in a greenhouse period: Geology, v. 22, p. 295-298.

Brenchley, P.J., and Newall, G., 1977, The significance of contorted bedding in Upper Ordovician sediments of the Oslo region, Norway: Journal of Sedimentary Petrology, v. 47, p. 819-833.

Bucher, W.H., 1925, The goelogy of Jeptha Knob: Kentucky Geological Survey, Series 6, v. 21, p. 193-237.

Cable, M.S., and Beardsley, R.W., 1984, Structural control on Lae Cambrian and Early Ordovician carbonate sedimentation in eastern Kentucky: American Journal of Science, v. 284, p. 797-823.

Caputo, M.V., and Crowell, J.C., 1985, Migration of glacial centers across Gondwana during Paleozoic Era: Geological Soxiety of America Bulltein, v. 96, p. 1020-1036.

Cisne, J.L., 1986, Earthquakes recorded stratigraphically on carbonate platforms: Nature, v. 323, p. 320-322.

Cisne, J.L., Karig, D.E., Rabe, B.D., and Hay, B.J., 1982, Topography and tectonics of the Taconic outer trench shelf slope as revealed through gradient analysis of fossil assemblages: Lethaia, v. 15, p. 230-246.

Cita, M.B., Camerlenghi, A., Kastens, K.A., and McCoy, F.W., 1984, New findings of Bronze Age homogenites in the Ionian Sea: geodynamic implications for the Mediterranean: Marine Geology, v. 55, p. 47-62.

Clague, J.J., and Bobrowsky, P.T., 1994, Tsunami deposits beneath tidal marshes on Vancouver Island, British Columbia: Geological Society of America Bulletin, v. 106, p. 1293-1303.

Cojan, I., and Thiry, M., 1992, Seismically induced deformation structures in Oligocene shallow-marine and aeolian coastal sands (Paris Basin): Tectonophysics, v. 206, p. 79-89.

Cressman, E.R., 1973, Lithostratigraphy and depositional environments of the Lexington Limestone (Ordovician) of central Kentucky: United States Geological Survey Professional Paper 768, 61 pp.

Cressman, E.R., 1981, Surface geology of the Jeptha Knob cryptoexplosion structure, Shelby County, Kentucky: United States Geological Survey Professional Paper 1151-B, 16 p.

Cressman, E.R., and Karklins, D.L., 1970, Lithology and fauna of the Lexington Limestone (Ordovician) of central Kentucky: Guidebook for Field Trips, Geological Society of America, Southeastern Section, Kentucky Geological Survey, Lexington, Kentucky, p. 17-28.

Dalrymple, R.W., 1979, Wave-induced liquefaction: a modern example from the Bay of Fundy: Sedimentology, v. 26, p. 835-844.

Diecchio, R.J., 1993, Stratigraphic interpretation of the Ordovician of the Appalachian Basin and implications for Taconian flexural modeling: Tectonics, v. 12, p. 1410-1419.

Dorsch, J., Bambach, R.K., and Driese, S.G., 1994, Basin-rebound origin for the "Tuscarora unconformity" in southwestern Virginia and its bearing on the nature of the Taconic orogeny: American Journal of Science, v. 294, p. 237-255.

Dzulynski, S., and Smith, A.J., 1963, Convolute lamination, its origin, preservation and directional significance: Journal of Sedimentary Petrology v. 33, p. 616-627.

Dzulynski, S., and Walton, E.K., 1965, Sedimentary features of flysch and greywackes: Developments in sedimentology, v.7, Elsevier, 274 p.

Elliott, C.G., and Williams, P.F., 1988, Sediment slump structures: a review of diagnostic criteria and application to an example from Newfoundland: Journal of Structural Geology, v. 10, p. 171-182.

Ettensohn, F.R., 1991, Flexural interpretation of relationships between Ordovician tectonism and stratigraphic sequences, central and southern Appalachians, U.S.A.: *in* Barnes, C.R., and Williams, S.H., eds., Advances in Ordovician geology: Geological Survey of Canada Paper 90-9, p. 213-224.

Ettensohn, F.R. (ed.), 1992, Changing interpretations of Kentucky geology--layer-cake, facies, flexure, and eustacy: State of Ohio, Department of Natural Resources, Miscellaneous Report No. 5, 184 p.

Ettensohn, F.R., Pashin, J.C., and Jacobs, G.W., 1986, Characteristics of shallow-water, marine shelf silts and sands: Two Paleozoic examples from eastern Kentucky: Spring Program, Appalachian Basin Industrial Associates, v. 10, p. 197-207.

Field, M.E., Gardner, J.V., Jennings, A.E., and Edwards, B.D., 1982, Earthquake induced sediment failures on a 0.25^{o} slope, Klamath River Delta, California: Geology, v. 10, p. 542-546.

Glover, L., III, Speer, J.A., Russell, G.S., and Farrar, S.S., 1983, Ages of metamorphism and ductile deformation in the central and southern Appalachians: Lithos, v. 16, p. 223-245.

Goggin, K.E., and Haynes, J.T., 1995, Mohawkian clastic wedges in the central and southern Appalachians: early signatures of the Taconic orogeny: Geological Society of America, Southeastern Section, Abstracts with Programs, v. 27, p. 56-57.

Goodmann, P.T., and Rast, N., 1995, The Cincinnati Arch: An isostatically buoyant structure: Geological Society of America, Southeastern Section, Abstracts with Programs, v. 27, p. 56-57.

Hambrey, M.J., 1985, The Late Ordovician-Early Silurian glacial period: Palaeogeography, Palaeoclimatology, Palaeoecology, v. 51, p. 273-289.

Hardie, L.A., Dunn, P.A., and Goldhammer, R.K., 1991, Field and modelling studies of Cambrian carbonate cycles, Virginia Appalachians-Discussion: Journal of Sedimentary Petrology, v. 61, p. 636-646.

Harland, W.B., Armstrong, R.L., Cox, A.V., Craig, L.E., Smith, A.G., and Smith, D.G., 1990, A geologic time scale, 1989: Cambridge University Press, Cambridge, UK, 261 pp.

Hay, B.J., and Cisne, J.L., 1988, Deposition in the oxygen-deficient Taconic foreland basin, Late Ordovician: in B.D. Keith (ed.), The Trenton Group (Upper Ordovician Series) of eastern North America, American Association of Petroleum Geologists, Tulsa, OK, Studies in Geology #29, p. 113-134.

Haynes, J.T., 1994, The Ordovician Deicke and Millbrig K-Bentonite beds of the Cincinnati Arch and the southern Valley and Ridge Province: Geological Society of America Special Paper 290, 80 pp.

Heezen, B.C., and Ewing, M., 1952, Turbidity currents and submarine slumps, and the 1929 Grand Banks earthquake: American Journal of Science, v. 250, p. 849-873.

Heike, W., 1984, A thick Holocene homogenite from the Ionian Abyssal Plain (eastern Mediterranean): Marine Geology, v. 55, p. 63-78.

Helwig, J., 1970, Slump folds and early structures, northwestern Newfoundland, Appalachians: Journal of Geology, v. 78, p. 172-187.

Hempton, M.R., and Dewey, J.F., 1983, Earthquake-induced deformational structures in young lacustrine sediments, East Anatolian Fault, southeast Turkey: Tectonophysics, v. 98, p. T7-T14.

Herbich, J.B., 1977, Wave-induced scour around offshore pipelines: Offshore Technology Conference, v. 4, p. 79-90.

Heyl, A.V., 1972, The 38th parallel lineament and its relationship to ore deposits: Economic Geology, v. 67, p. 879-894.

Holland, S., and Patzkowsky, M.E., in press, Sequence stratigraphy and long-term paleoceanographic change in the Middle and Upper Ordovician of the eastern United States: *in* Witzke, B.J., Ludvigsen, G.A., and Day, J.E., (eds.), Paleozoic Sequence Stratigraphy: Views from the North American craton, Geological Society of America Special Publication 306, Boulder, CO.

Hrabar, S.V., Cressman, E.R., and P.E. Potter, 1971, Crossbedding of the Tanglewood Limestone Member of the Lexington Limestone (Ordovician) of the Blue Grass region of Kentucky: Brigham Young University Geology Studies, v. 18, p. 99-114.

Huff, W.D., Bergstrom, S.M., and Kolata, D.R., 1992, Gigantic Ordovician volcanic ash fall in North America and Europe: Biological, tectonomagmatic, and event- stratigraphic significance: Geology, v. 20, p. 875-878., 1991

Jacobi, R.D., 1981, Peripheral bulge-a causal mechanism for the Lower/Middle Ordovician disconformity along the western margin of the northern Appalachians: Earth and Planetary Science Letters, v. 56, p. 245-251.

Jacobs, G.W., 1986, Mixed siliciclastic-carbonate storm deposits in the Upper Ordovician of central Kentucky: Geological Society of America Annual Meeting Program with Abstratcts, p. 268.

Jennette, D.C., and Pryor, W.A, 1993, Cyclic alternation of proximal and distal storm facies: Kope and Fairview Formations (Upper Ordovician), Ohio and Kentucky: Journal of Sedimentary Petrology, v. 63, p. 183-203.

Jillson, W.R., 1962, Geology of a recently discovered faulted area south of Jeptha Knob in Shelby Couny, Kentucky: Roberts Printing Company, Frankfort, Kentucky, 23 p.

Karlin, R.E., and Abella, S.E.B., 1992, Paleoearthquakes in the Puget Sound region recorded in sediments from Lake Washington, U.S.A.: Science, v. 258, p. 1617-1620.

Kastens, K.A., 1984, Earthquakes as a triggering mechanism for debris flows and turbidites on the Calabrian Ridge: Marine Geology, v. 55, p. 13-34.

Kastens, K.A., and Cita, M.B., 1981, Tsunami-induced sediment transport in the abyssal Mediterranean Sea: Geological Society of America Bulletin, v. 92, p. 845-857.

Keith, B.D., 1988, Regional facies of Upper Ordovician Series of eastern North America: in B.D. Keith (ed.), The Trenton Group (Upper Ordovician Series) of eastern North America, American Association of Petroleum Geologists, Tulsa, OK, Studies in Geology #29, p. 1-16.

Klevekaar, K., 1987, Gordo Megabed: A possible seismite in a Tortonian submarine fan, Tabernas Basin, Province Almeria, southeast Spain: Sedimentary Geology, v. 51, p. 165-180.

Kreisa, R.D., 1980, The Martinsburg Formation (Middle and Upper Ordovician) and related facies in southwestern Virginia: unpublished Ph.D. dissertation, Virginia Polytechnic Institute and State University, Blacksburg, Virginia, 358 p.

Kreisa, R.D., Dorobek, S.L., Accorti, P.J., and Ginger, E.P., 1981, Recognition of storm-generated deposits in the Cincinnatian Series, Ohio: Geological Society of America Program with Abstracts, v. 13, p. 285.

Kuenen, P.H.H., 1958, Experiments in Geology: Transactions of the Geological Society of Glasgow, v. 23, p. 1-28.

Kuhnhenn, G.L., and Haney, D.C., 1986, Middle Ordovician High Bridge Group and Kentucky River fault system in central Kentucky: *in* Neathery, T.L., ed., Southeastern Section of the Geological Society of America: Geological Society of America Centennial Field Guide, v. 6, p. 25-29.

Kulp, M., 1995, Paleoenvironmental interpretation of the Brannon Member, Middle-Upper Ordovician Lexington Limestone, central Bluegrass region of Kentucky: Unpublished master's thesis, University of Kentucky, Lexington, Kentucky, 222 p.

Kuribayashi, E., and Tatsuoka, F., 1975, Brief review of liquefaction during earthquakes in Japan: Soils Foundation, v. 15, p. 81-92.

Lash, G.G., 1988, Middle and Late Ordovician shelf activation and foredeep evolution, central Appalachian Orogen: in B.D. Keith (ed.), The Trenton Group (Upper Ordovician Series) of eastern North America, American Association of Petroleum Geologists, Tulsa, OK, Studies in Geology #29, p. 37-53.

Lee, K.L., and Focht, J.A., 1975, Liquefaction potential at Ekofisk Tank in North Sea: Journal of Geotechnical Engineering Division of American Society of Civil Engineers, v. 101, p. 1-18.

Lowe, D.R., 1975, Water escape structures in coarse-grained sediments: Sedimentology, v. 22, p. 157-204.

Lowe, D.R., 1976, Subaqueous liquefied and fluidized sediment flows and their deposits: Sedimentology, v. 23, pl. 285-308.

Lowe, D.R., and LoPiccolo, R.D., 1974, The characteristics and origins of dish and pillar structures: Journal of Sedimentary Petrology, v. 44, p. 484-501.

Lowry, W.D., 1974, North American geosynclines, a test of continental-drift theory: American Association of Petroleum Geologists Bulletin, v. 58, p. 575-620.

Mackey, R.T., 1972, Lithostratigraphy and depositional environment of the Perryville Limestone and related members of the Lower Lexington Limestone (Ordovician) of south-central Kentucky: (unpubl. masters thesis) University of Kentucky, Lexington, KY, 76 p.

MacQuown, W.C., Kuhnhenn, G.L., Sheperd, R.G., and Gooding, P.J., 1984, Lithostratigraphy and depositional environments of the Middle Ordovician limestones in central Kentucky: *in* Fieldtrip guides for Geological Society of America Southeastern and North central sections, Rast, N., and Hay, H.B., eds., p. 66-82.

Maltman, A.J., 1981, Primary bedding-parallel fabrics in structural geology: Journal of the Geological Society of London, v. 138, p. 475-483.

McBride, E. F., 1962, Flysch and associated beds of the Martinsburg Formation (Ordovician), Central Appalachians: Journal of Sedimentary Petrology, v. 32, p. 39-91.

McKee, E.D., and Goldberg, M., 1969, Experiments on formation of contorted structures in mud: Geological Society of America Bulletin, v. 80, p. 231-244.

Mehrtens, C.J., 1988a, Bioclastic turbidites in the Trenton Limestone: Significance and criteria for recognition: *in* B.D. Keith (ed.), The Trenton Group (Upper Ordovician Series) of eastern North America, American Association of Petroleum Geologists, Tulsa, OK, Studies in Geology #29, p. 87-112.

Mehrtens, C.J., 1988b, Comparison of foreland basin sequences: The Trenton Group in southern Quebec and central New York: *in* B.D. Keith (ed.), The Trenton Group (Upper Ordovician Series) of eastern North America, American Association of Petroleum Geologists, Tulsa, OK, Studies in Geology #29, p. 139-157.

Mills, P.C., 1983, Genesis and diagnostic value of soft-sediment deformation structures-a review: Sedimentary Geology, v. 35, p. 83-104.

Minoura, K., and Nakaya, S., 1991, Traces of tsunami preseved in inter-tidal lacustrine and marsh deposits: Some examples from northeast Japan: Journal of Geology, v. 99, p. 265-287.

Minoura, K., Nakaya, S. and Uchida, M., 1994, Tsunami deposits in a lacustrine sequence of the Sanriku coast, northeast Japan: Sedimentary Geology, v. 89, p. 25-31.

Montgomery, D.R., 1990, Effects of the Loma Prieta earthquake, October17, 1989: California Geology, v. 43, p. 8-13, 23-24.

Morton, R.A., 1988, Nearshore responses to great storms: *in* H.E. Clifton, ed., Sedimentary consequences of convulsive geologic events, Geological Society of America Special Paper 229, p. 7-22.

Munson, P.J., Munson, C.A., and Pond, E.C., 1995, Paleoliquefaction evidence for a strong Holocene earthquake in south-central Indiana: Geology, v. 26, p. 325-328.

Mussman, W.J., and Read, J.F., 1986, Sedimentology and development of a passive- to convergent-margin unconformity: Middle Ordovician Knox unconformity, Virginia Appalachians: Geological Society of America Bulletin, v. 97, p. 282-295.

Mutti, E., Ricci-Lucchi, F., Seguret, M., and Zanzucchi, G., 1984, Seismoturbidites: a new group of resedimented deposits: Marine Geology, v. 55, p. 103-116.

Noger, M.C., and Kepferle, R.C., 1985, Stratigraphy along and adjacent to the Bluegrass Parkway: Field Guidebook for Annual Field Conference of the Geological Society of Kentucky, Kentucky Geological Survey, Lexington, Kentucky, 24 p.

Obermeier, S.F., Jacobsen, R.B., Smoot, J.P., Weems, R.E., Gohn, G.S., Monroe, J.E., and Powars, D.S., 1990, Earthquake-induced liquefaction features in the coastal setting of South Carolina and in the fluvial setting of the New Madrid Seismic zone: United State Geological Survey Professional Paper 1504, 44 pp.

Obermeier, S.F., Bleuer, N.R., Munson, C.A., Munson, P.J., Martin, W.S., McWilliams, K.M., Tabaczynski, D.A., Odum, J.K., Rubin, M., and Eggert, D.L., 1991, Evidence of Strong Earthquake shaking in the Lower Wabash Valley from Prehistoric Liquefaction Features: Science, v. 251, p. 1061-1063.

Obermeier, S.F., 1995, Using liquefaction-induced features for paleoseismic analysis: *in* S.F. Obermeier and R.W. Jibson, eds., Using ground-failure features for paleoseismic Analysis, United States Geological Survey Open-File Report 94-663, p. 1-60

Palmer, P., 1983, Decade of North American geology, 1983 geological time scale: Geology, v. 9, p. 503-504.

Patzkowsky, M.E., and Holland, S.M., 1993, Biotic response to a Middle Ordovician paleoceanographic event in eastern North America: Geology, v. 21, p. 619-622.

Pickering, K.T., 1987, Wet-sediment deformation in the Upper Ordovician Point Leamington Formation: an active thrust-imbricate system during sedimentation, Notre Dame Bay, north-central Newfoundland: *in* M.E. Jones, and R.M.F. Preston, eds., Deformation of Sediments and Sedimentary Rocks, Geological Society Special Publication no. 29, p. 213-239.

Pope, M. C., and Read, J. F., 1992, Possible Middle Cambrian to Late Ordovician Seismites from Extensional to Compressional Regimes, GSA Abstracts with Programs, p. A 186.

Pope, M.C., and Read, J.F., 1993, Evidence for large high-frequency glacio-eustatic sea level fluctuations in Late Middle Ordovician cool water carbonates, Kentucky, Geological Society of America Programs with Abstracts, p 267.

Pope, M.C., and Read, J.F., (in press), High-frequency cyclicity of the Lexington Limestone (Middle Ordovician), a cool-water carbonate clastic ramp in an active foreland basin: Society of Economic Paleontologists and Mineralogists Special Publication.

Potter, P.E., Ausich, W.I., Klee, J., Krissek, L.A., Mason, C.E., Schumacher, G.A., Wilson, T.R., and Wright, E.M., 1991, Geology of the Alexandria-Ashland Highway (Kentucky Highway 546), Maysville to Garrison, Joint Field Conference, Geological Society of Kentucky and Ohio Geological Society: Kentucky Geological Survey, Lexington, Kentucky, 64 p.

Pratt, B.R., 1994, Seismites in the Mesoproterozoic Altyn Formation (Belt Supergroup), Montana: A test for tectonic control of peritidal carbonate cyclicity: Geology, v. 22, p. 1091-1094.

Prentice, J.E., 1960, Flow structures in sedimentary rocks: Journal of Geology, v. 68, p. 217-221.

Quinlan, G.M., and Beaumont, C., 1984, Appalachian thrusting, lithospheric flexure, and the Paleozoic stratigraphy of the eastern interior of North America: Canadian Journal of Earth Science, v. 21, p. 973-996.

Read, J.F., 1980, Carbonate ramp-to-basin transitions and foreland basin evolution, Middle Ordovician, Virginia Appalachians: American Association of Petroleum Geologists Bulletin, v. 64, p. 1575-1612.

Read, J.F., 1989, Controls on evolution of Cambrian-Ordovician passive margin, U.S. Appalachians: in (eds), Controls on carbonate platform and basin deveolopment, Society of Economic Paleontologists and Mineralogists Special Publication No. 44, p. 147-165.

Rodgers, J., 1971, The Taconic orogeny: Geological Society of America Bulletin, v. 82, p. 1141-1178.

Samson, S.D., Patchett, P.J., Roddick, J.C., and Parrish, R.R., 1989, Origin an tectonic setting of Ordovician bentonites in North America: Isotopic and age constraints: Geological Society of America Bulletin, v. 101, p. 1175-1181.

Schumacher, G.A., 1992, Lithostratigraphy, cyclic sedimentation, and event stratigraphy of the Maysville, Kentucky, Area: *in* Ettensohn, F.R., ed., Changing interpretations of Kentucky geology--layer-cake, facies, flexure, and eustacy: State of Ohio, Department of Natural Resources, Miscellaneous Report No. 5, p. 165-172.

Scott, B., and Price, S., 1988, Earthquake-induced structures in young sediments: Tectonophysics, v. 147, p. 165-170.

Seeger, C.R., 1968, Origin of the Jeptha Knob structure Kentucky: American Journal of Science, v. 266, p. 630-660.

Seeger, C.R., 1986, The Jeptha Knob cryptoexplosion structure, Kentucky: Geological Society of America Centennial Field Guide-Southeastern Section, Geological Society of America, Boulder, Colorado, p. 17-20.

Seeger, C.R., Asaro, F., Michel, H., Alvarez, W., and Alvarez, L., 1985, Iridium discovery at the Jeptha Knob cryptoexplosion structure, Kentucky: Eos, v. 69, p. 1293.

Seilacher, A., 1969, Fault graded beds interpreted as seismites: Sedimentology, v. 13, p. 155-159.

Seilacher, A., 1984, Sedimentary structures tentatively attributed to seismic events: Marine Geology, v. 55, p. 1-12.

Shanmugam, G., and Walker, K., 1980, Sedimentation, subsidence and evolution of a foredeep basin in the Middle Ordovician, southern Appalachians: American Journal of Science, v. 280, p. 479-496.

Shinn, E.A., Steinen, R.P., Dill, R.F., and Major, R., 1993, Lime-mud layers in high-energy tidal channels: A record of hurricane deposition: Geology, v. 21, p. 603-606.

Sieh, K.E., 1978, Prehistoric large earthquakes produced by slip on the San Andreas Fault at Pallett Creek, California: Journal of Geophysical Research, v. 83, p. 3907-3939.

Sims, J.D., 1973, Earthquake-induced structures in sediments of Van Norman Lake, San Fernando, California, Science, v. 182, p. 161-163.

Sims, J.D., 1975, Determining recurrence intervals from deformational structures in young lacustrine sediments: Tectonophysics, v. 29, p. 141-152.

Sweet, W.C., 1979, Conodonts and conodont stratigraphy of post-Tyrone Ordovician rocks of the Cincinnati region: U. S. Geological Survey Professional Paper 1066-G, 26 p.

Tucker, R.D., Krogh, T.E., Ross, R.J. Jr., and Williams, S.H., 1990, Time-scale calibration by high-precision U-Pb zircon dating of interstratified volcanic ashes in the Ordovician and Silurian stratotypes of Britain: Earth and Plantary Science Letters, v. 100, p. 51-58.

Tucker, R.D., and McKerrow, W.S., 1995, Early Paleozoic chronology: a review in light of new U-Pb zircon ages from New Foundland and Britain: Canadian Journal of Earth Sciences, v. 32, p. 368-379.

Vaughan, N.D., Johnson, T.C., Mearns, D.L., Hine, A.C., Kerby-Smith, W.W., Ostach, J.F., and Riggs, S.R., 1987, The impact of Hurricane Diana on the North Carolina continental shelf: Marine Geology, v. 76, p. 169-176.

Visher, G.S., and Cunningham, R.D., 1981, Convolute laminations - A theoretical analysis: example of a Pennsylvanian sandstone: Sedimentary Geology, v. 28, p. 175-188.

Weaver, J.D., and Jeffcoat, R.E., 1978, Carbonate ball and pillow structures: Geological Magazine, v. 115, p. 245-253.

Webb, E.J., 1980, Cambrian sedimentation and structural evolution of the Rome Trough in Kentucky: unpubl. Ph.D. thesis, Cincinnati, Ohio, University of Cincinnati, 115 p.

Weir, G.W., Peterson, W.L., and Swadley, W.C., 1984, Lithostratigraphy of Upper Ordovician strata exposed in Kentucky: United States Geological Survey Professional Paper 1151-E, 121 p.

Woodward, H.P., 1961, Preliminary subsurface study of south-eastern Appalachian Interior Plateau: American Association of Petroleum Geologists Bulletin, v. 45, p. 1634-1655.

Woodward, N.B., and Gray, D.R., 1985, Chap. III Southwest Virginia, Tennessee and northern Georgia sections: *in* Woodward, N.B., ed., Valley and Ridge Thrust Belt: Balanced Structural Sections, Pennsylvania to Alabama, Appalachian Basin Industrial Associates, University of Tennessee, Department of Geological Sciences Studies in Geology #12, p. 40-53.

Youd, T.L., 1977, Discussion of "Brief review of liquefaction during earthquakes in Japan" by E. Kuribayashi and F. Tatsuoka: Soils Foundation, v. 17, p. 82-85.

Chapter 5: Meter-Scale Cycles of Ordovician Rocks in Kentucky and Virginia: Implications for Climate and Eustatic Fluctuations in the central Appalachian Basin during the Ordovician

ABSTRACT

Meter-scale shallowing-upward cycles in Ordovician carbonates of the central Appalachian Basin record climate and eustatic fluctuations during a transition from Early Ordovician global greenhouse to Late Ordovician glacial conditions. Climatic indicators in peritidal cycles and the increasing abundance of shale through time suggest a long-term trend toward more humid conditions through the early Late Ordovician followed by more semi-arid conditions in the Late Ordovician. Longterm fluctuations in this trend were likely produced by tectonic processes (plateau uplift and erosion), and the amount of water covering the shelf. Facies within peritidal cycles indicate that high- frequency eustatic fluctuations were of low amplitude throughout most of the Ordovician. However, facies in late Middle to Late Ordovician subtidal cycles, and an increase in compartmentalization of buildups in the Late Ordovician suggest moderate amplitude (> 20 m) fluctuations during this time. The change in amplitude of eustatic fluctuations likely represents the onset of Gondwana glaciation in the Late Ordovician.

INTRODUCTION

Ordovician carbonate rocks of Kentucky and Virginia were deposited during a transition from global greenhouse (Early Ordovician) to glacial conditions (Latest Ordovician). These rocks can be separated into three large, 2nd-order (10 to 30 m.y. duration), unconformity-bounded, transgressive-regressive depositional supersequences (Vail et al., 1991; Weber et al., 1995), composed of 3rd-order (1 to 10 m.y. duration) depositional sequences, which are, in turn made up of stacked meter-scale, shallowing-upward cycles. Each supersequence contains a distinctive set of meter-scale cycles whose sedimentary characteristics preserve some record of the climate setting and amplitude of eustatic fluctuations during its deposition. We present a brief synopsis of the common meter-scale cycle types and sedimentary characteristics and discuss their implications for eustatic fluctuations and regional climate during the Ordovician.

STRUCTURAL FRAMEWORK

The Early Ordovician Upper Knox Group (Figure 1) carbonates developed on an aggraded shallow water ramp on a several hundred kilometer wide passive margin (Reinhardt, 1974; Read, 1989), which formed following Late Proterozoic rifting of Laurentia (Bond et al., 1984). Cambrian to Early Ordovician passive margin deposition ended with collision between Laurentia and a magmatic arc (Rodgers, 1971). Onset of collision was marked by development of the Knox unconformity (approximately 10 million years duration), followed by development of a foreland basin, extending from Alabama to Newfoundland (Rodgers, 1971; Jacobi, 1983; Mussman and Read, 1986; Lash, 1988). The deep foreland basin in the Virginia-Kentucky study area was bordered on the east by tectonic highlands, and on the west by a shallow carbonate ramp. The Nashville and Jessamine Domes on the Cincinnati Arch, the Rome Trough and the Sebree Trough were periodically active structural features in the foreland (Borella and Osborne, 1978; Cable and Beardsley, 1984; Ettensohn, 1992).

The foreland basin was initiated during the "Blountian phase" (Chazyan to Blackriveran) (Rodgers, 1971) when the St. Paul and Chambersburg limestones of Maryland and Pennsylvania, the "Middle Ordovician Limestone" in Virginia (Read, 1980), and the updip High Bridge Group, Kentucky (Cressman and Noger, 1976) (Figure 1), formed peripheral to the deep Sevier Basin (Shanmugam and Walker, 1983).

During the "Taconic phase" (Late Mohawkian to Cincinnatian) Martinsburg turbidites were deposited in the Taconic foredeep in northern Virginia, Maryland, and Pennsylvania (McBride, 1962; Rodgers, 1971; Lash, 1988; Read, 1989) (Figure 2). In Kentucky and southwest Virginia, a subtidal ramp sloped gently northeastward from the Cincinnati Arch into the Taconic foredeep, and passed westward into the narrow, shaly, Sebree Trough (Cressman, 1973; Weir et al., 1984; Keith, 1988).

STRATIGRAPHY

Characteristic facies, cycles and climatic indicators of each supersequence are given in Table 1.

Early Ordovician (Canadian): The Early Ordovician Upper Knox Group is a large 2nd-order supersequence, approximately 25 m.y. in duration and 200 to 1200 m thick (Read, 1990). It is composed of approximately six 3rd-order sequences from 10's of meters to

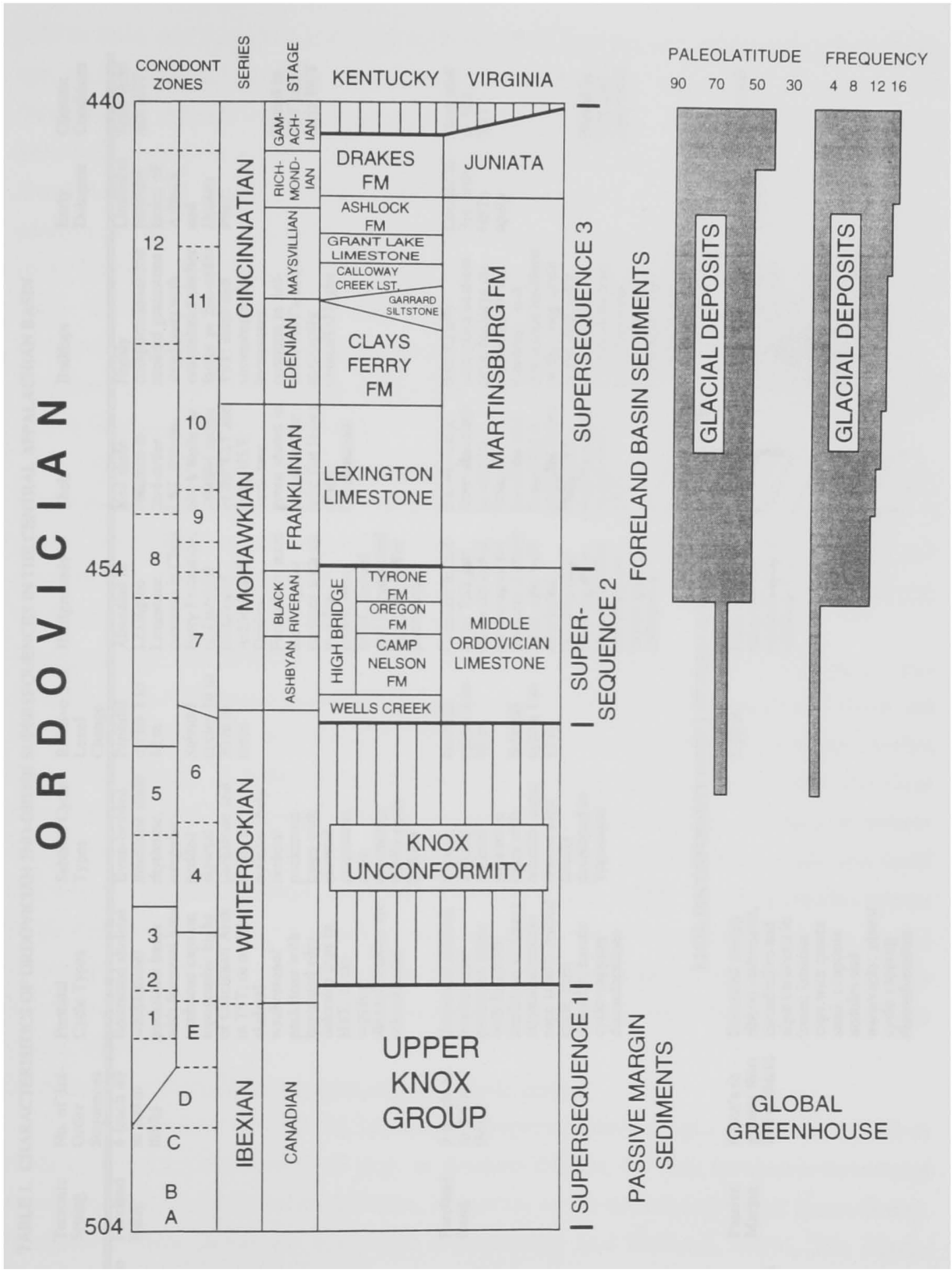

Figure 1. Chronostratigraphic chart of Ordovician rocks in Kentucky and Virginia. Data on glacial deposits is adapted from Frakes et al. (1992).

TABLE 1. CHARACTERISITICS OF ORDOVICIAN 2ND-ORDER SUPERSEQUENCES IN THE CENTRAL APPALACHIAN BASIN

	Tectonic Setting	No. of 3rd-Order Sequences	Peritidal Cycle Types	Subtidal Cycle Types	Relative Sea Level Change	Hardgrounds	Shale	Buildups	Early Dolomite	Climatic Conditions
Late Middle to Late Ordovician (Lexington Limestone-Clays Ferry/ Kope-Ashlock-Drakes-Martinsburg Formations)	Foreland Basin	4 (each 40 to 100 m thick)	Restricted skeletal wackestone/ packstone bases with fenestral lime mudstone caps on topographic highs of Cincinnati Arch in TST; or nodular skeletal wackestone/ packstone with laminated silty dolomite caps in HST; cycle-capping disconformities are microkarstic	Even-bedded limestone shale rhythmite, irregular-bedded skeletal packstone and shale, or nodular shaly skeletal packstone bases with skeletal grainstone caps, commonly tidally cross-bedded	Peritidal cycles 1 to 10 m Subtidal cycles 10 to 30 m or more	Abundant in Lexington Limestone, common in Clays Ferry Formation, and subtidal portions of Ashlock and Drakes Formations; most are irregular surfaces with up to a few centimeters relief, stained and impregnated by pyrite and/or phosphate	Red shale common in 2nd-order LST; Brown-black shale in subtidal facies of the TST and early HST; very rare green shales in silty dolomitic tidal flat facies of the Cincinnatian	Highly compartmentalized skeletal grainstone shoal units with intercalated shalier facies in 2nd-order TST; coral and stromatoporoid biostromes common in 3rd-order HST's and on structually controlled highs	Limited to peritidal facies of Ashlock and Drakes Fms.	Semi-Arid late HST Humid in TST and early HST
Middle Ordovician (High Bridge Group and Middle Ordovician Limestone; St. Paul Group)	Foreland Basin	3 (each 30 to 200 m thick)	Burrowed skeletal wackestone/ packstone bases with fenestral mudstone or (rare) cryptalgalaminite caps (rare); redbed cycle caps downdip; karstic cycle-capping disconformities	Cherty, nodular skeletal packstone bases with oncolitic caps; Oolitic caps locally developed in Tennessee	Peritidal cycles 1 to 10 m Subtidal cycles 1 to 15 m	Common in 2nd-order TST just below the initial drowning of the platform (Liberty Hall), also well-developed between slope buildups; most have little relief and many are coated with collophane	Brown-black shale abundant in subtidal facies in foredeep and as partings in peritidal facies updip; red shales common in 3rd-order LST's	Structurally-controlled shallow ramp buildups on the margin of the foredeep, and downslope buildups on the ramp slope in the 2nd-order TST, banks composed of lime mudstone with stromatctis and bryozoans; not compartmentalized	Limited to 3rd-order HST's updip	Semi-arid in late HST Humid in TST and early HST
KNOX UNCONFORMITY (ONSET OF FORELAND BASIN DEFORMATION)										
Early Ordovician (Upper Knox Group)	Passive Margin	6 (ten's to greater than 200 m thick)	Burrowed muddy ribbon carbonates, thrombolites and algal bioherms in bases; laminite caps with quartz sand, evaporite nodules and mudcracks; planar cycle capping disconformities		1-10 m	Rare, occur as sharp-planar surfaces with no staining	Green shale common in cycle caps	Common along the aggraded platform margin, these are Renalcid and Epiphyton biostromes (< 5 m thick); not compartmentalized	Very abundant	Semi-arid

200 m thick and 2 to 5 m.y. duration (Read and Goldhammer, 1989). These sequences are composed of 1 to 12 m thick, peritidal meter-scale cycles with biohermal and thrombolitic skeletal wackestone, or oolitic grainstone bases and extensive, mudcracked microbial laminite caps containing silicified evaporite nodules (Hardie and Shinn, 1986; Bova and Read, 1987; Hardie, 1989; Montanez and Read, 1992). In general, inner platform cycles are completely dolomitized whereas outer platform cycles tend to contain more limestone in lower parts of cycles (Figure 2). Third-order LST's have sandy cycle caps. TST's have relatively thicker cycles with limestone-rich bases, and on the outer platform, biohermal complexes are common along with thick subtidal ribbon carbonates; laminites are relatively minor. HST's are dominated by thin, completely dolomitized cycles (Montanez and Read, 1992).

Planar hardgrounds cemented by micritic or fibrous marine cement are common. Some outer ramp bioherms have scalloped and planar erosion surfaces marking tops of cycles. Buildups along the aggraded platform margin include microbial stromatolites and thrombolites (Bova and Read, 1987) and thin (< 10 m thick) Renalcis and Epiphyton bioherms and skeletal sands (Goldhammer et al., 1984).

Interpretation: The abundance of early dolomite, ooids, evaporite nodules and mudcracks indicate these rocks were deposited under arid to semi-arid climatic conditions (Bova and Read, 1987; Montanez and Read, 1993). An abundance of semi-arid indicators across Laurentia (Figure 3) indicates a very uniform, possibly azonal climate was prevalent during this period. Regional tidal flat laminites capping the cycles, and lack of deeper water facies in lower parts of cycles suggest that they formed under small sea level fluctuations (Bova and Read, 1987; Montanez and Read, 1992). Cycle durations appear to be 4th-order (~100 k.y.) which in part reflects the very low subsidence rates on the mature passive margin just prior to collision. However, higher frequency cycles likely were preserved in the more rapidly subsiding Pennsylvania and Tennessee depocenters (Read, 1989).

Middle Ordovician (Whiterockian to Early Mohawkian)

The "Middle Ordovician Limestone" supersequence ranges from 200 to 500 m thick and was approximately 15 m.y. in duration (Figure 4). This limestone-dominated supersequence generally lacks dolomite, in contrast to the underlying Upper Knox Group. It contains three 3rd-order sequences (Patzkowsky and Holland, 1993). The Knox-Beekmantown unconformity (approximately 10 m.y. duration) is well developed in the

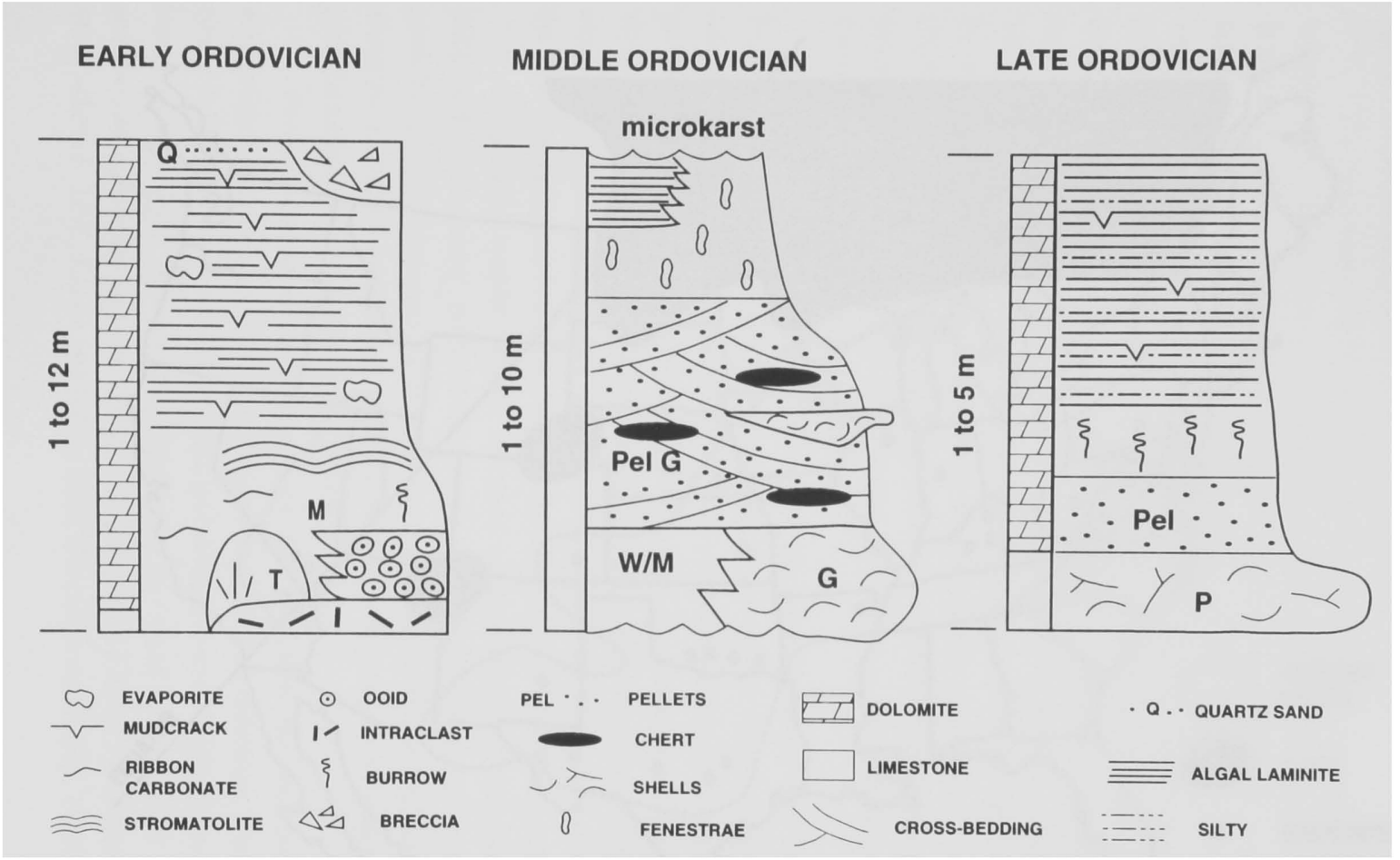

Figure 2. Representative peritidal meter-scale cycles of Ordovician strata in the Kentucky and Virginia.

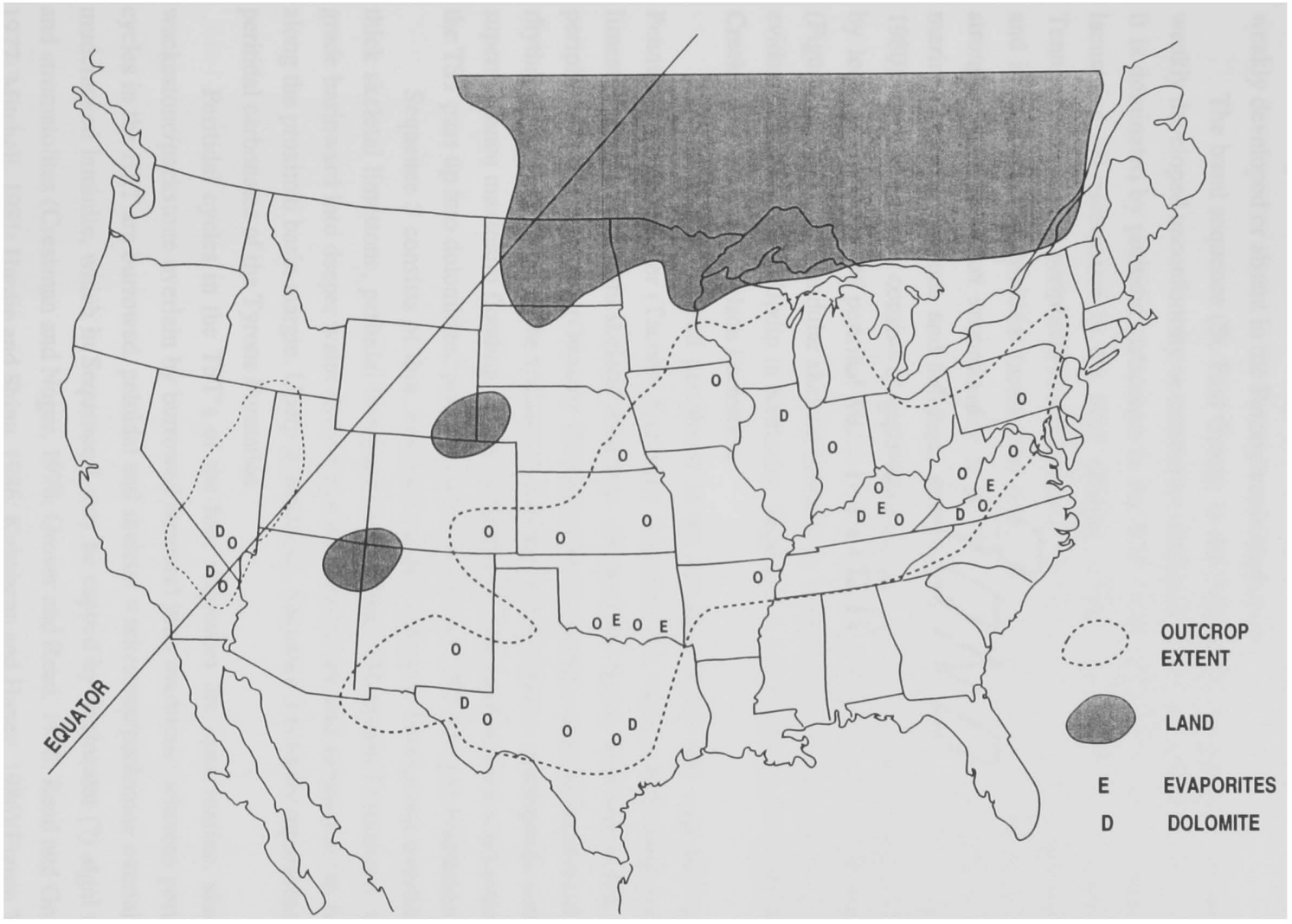

Figure 3. U.S. map showing paleoclimatic indicators of the Early Ordovician. The position of the equator is from Witzke (1990).

Tennessee depocenter, over the Virginia Arch, and onto the foreland, however, it is only weakly developed or absent in the Pennsylvania depocenter.

The basal sequence (St. Paul Group) in the Pennsylvania depocenter overlies the weakly developed unconformity or correlative conformity (Mitchell, 1981; Hardie, 1988). It is dominated by peritidal carbonates in the TST which are progressively overlain by lacustrine (?) carbonates in the HST (Hardie, 1989). Sequence 1 in Virginia and Tennessee developed peripheral to a foredeep in the Tennesse depocenter (Sevier Basin) and is dominated by peritidal facies over much of the foreland basin. Peritidal cycles strongly onlap the Knox unconformity in the TST progressively are overlain by open marine skeletal limestone and buildups, and then thick rhythmite successions (Read, 1980). The HST mainly consists of aggradational cycles and the late HST may be marked by local progradation of peritidal facies (Peery Member) above the Rockdell buildup (Figure 4). Downramp nodular skeletal limestones, buildups and rhythmites show little evidence of shallowing. Updip in Kentucky, Sequence 1 is peritidal cycles of the Wells Creek and lower Camp Nelson Formation.

Sequence 2 developed peripheral to the foredeep which had migrated to the Pennsylvania depocenter (Taconic foredeep). Sequence 2 is mainly deep ramp nodular limestones grading up into skeletal limestone and peritidal facies, with rare oolitic bars peripheral to the foredeep (Ottoseee Formation in Tennessee); passing basinward into rhythmites and black shale. The maximum flooding in this sequence corresponds with the supersequence maximum flooding. Updip in Kentucky, burrowed skeletal wackestone of the TST pass up into dolomitized peritidal facies in the Late HST (Oregon Formation).

Sequence 3 consists of thin, lowstand red beds (Bowen Formation) overlain by thick skeletal limestone, peritidal limestones and redbeds (Moccasin Formation), these grade basinward into deeper water shaly limestone, rhythmites, and submarine fan facies along the proximal basin margin. Updip in Kentucky, Sequence 3 is likely represented by peritidal carbonates of the Tyrone Formation.

Peritidal cycles in the TST's of the four sequences are open marine, skeletal wackestone/packstone overlain by burrowed fenestral lime mudstone; whereas peritidal cycles in the HST are burrowed, peloidal and skeletal wackestone/packstone overlain by mudcracked laminite, which in Sequence 1 may be capped by freshwater (?) algal tufas and stromatolites (Cressman and Noger, 1976; Grover and Read, 1978; Read and Grover, 1977; Mitchell, 1981; Hardie and Shinn, 1986; Kuhnhenn and Haney, 1986)(Figure 3).

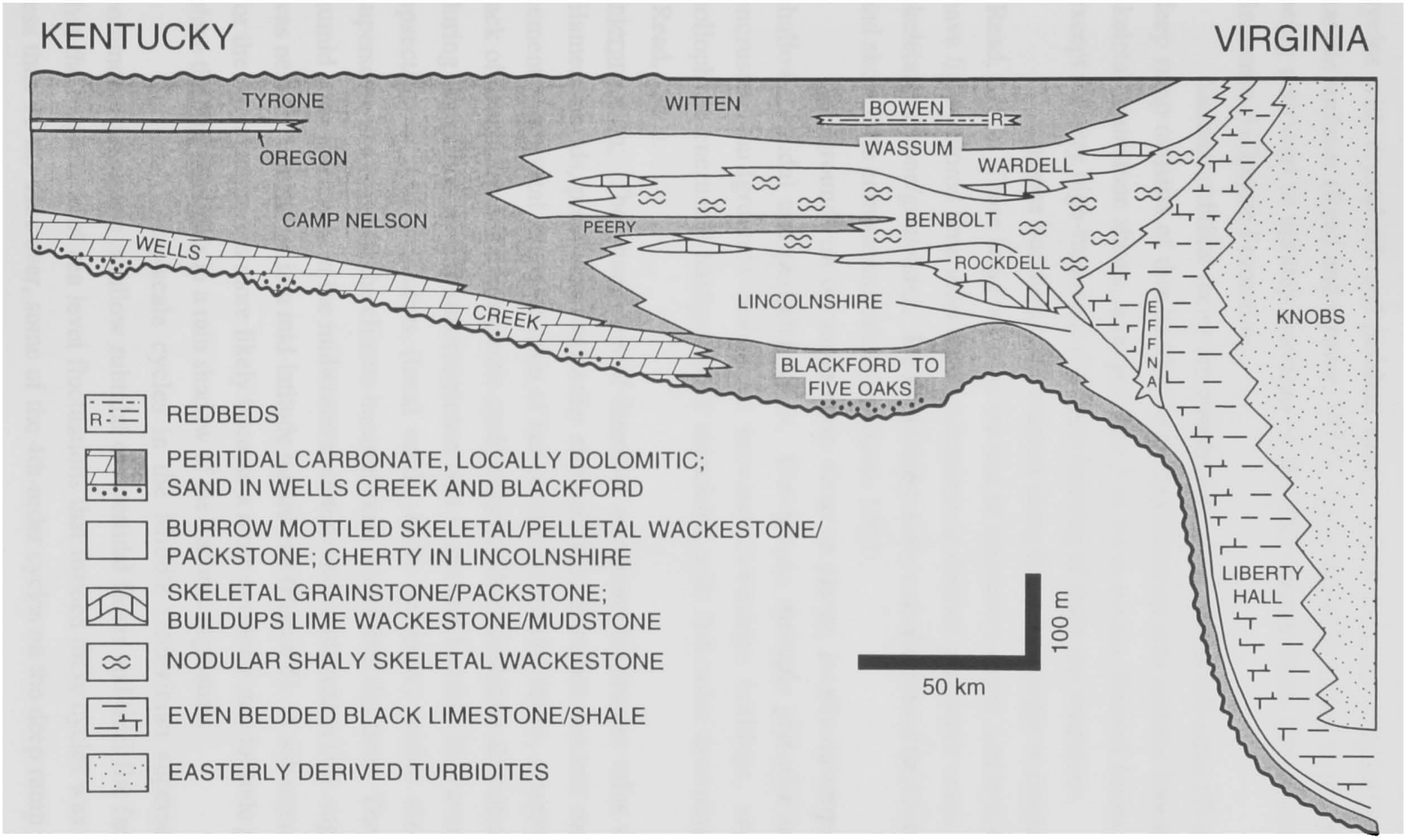

Figure 4. Generalized cross-section of Middle Ordovician supersequence in Kentucky and Virginia.

Tidal flat facies show much evidence of meteoric diagenesis and emergence, and cycles with crystal silt and pendant sparry calcite cements commonly are capped by karstic surfaces (Read and Grover, 1977). Early dolomite is rare in this supersequence, being restricted to upramp positions in the TST (Wells Creek Formation) and HST of Sequence 3 (Oregon Formation).

Skeletal subtidal facies are mainly non-cyclic. Weak 4th-order (?) cyclicity in the deep ramp consists of thin-bedded shaly limestone up into nodular limestone then into skeletal grainstone sheets, arranged into 3 to 10 m cycles. Basinal facies lack cyclicity except for very high-frequency rhythmic layering of shale and limestone.

Downslope buildups are common along the ramp margin in deeper water facies (Read, 1982). These large buildups are tens of kilometers across, and tens to 250 m high, have light-colored lime mudstone/wackestone or skeletal grainstone cores, with flanking skeletal pacstone/grainstone. These buildups rarely contain intercalated deep water facies and show little compartmentalization (Read, 1982).

Hardgrounds on the inner ramp occur as planar, locally-developed surfaces in shallow subtidal and peritidal facies. Downramp, multiple phosphorite and sulfide-encrusted hardgrounds developed between downslope buildups, and a regional collophane-encrusted hardground is associated with 2nd-order drowning of the ramp (Read, 1982).

Interpretation: The abundance of fenestral mudstone, freshwater tufas with abundant filament molds, presumed freshwater stromatolites, abundant pendant meteoric calcite cement and crystal silt, restriction of laminites to supratidal facies, scarcity of dolomite, lack of evaporites and microkarstic cycle-capping disconformities all indicate the climate during deposition of this supersequence was warm and humid. However, the increase upsection in arid indicators (local ooids, early dolomite) within the HST of the supersequence suggests the climate became more arid during this time. The abundance of humid zone indicators in the midwestern, eastern and southeastern U.S. suggests this belt was near the equator or in a mid-latitude humid belt (Figure 5). A sub-equatorial position for the Appalachians is more likely because a more northerly mid-latitude position might place the Appalachians in a rain shadow of the Taconic highlands.

Peritidal meter-scale cycles in the Middle Ordovician supersequence most commonly juxtapose shallow subtidal or intertidal facies and tidal flat facies indicating that the magnitude of sea level fluctuations that formed these cycles was low, probably less than 10 m. However, some of the 4th-order cycles on the deep ramp juxtapose thin

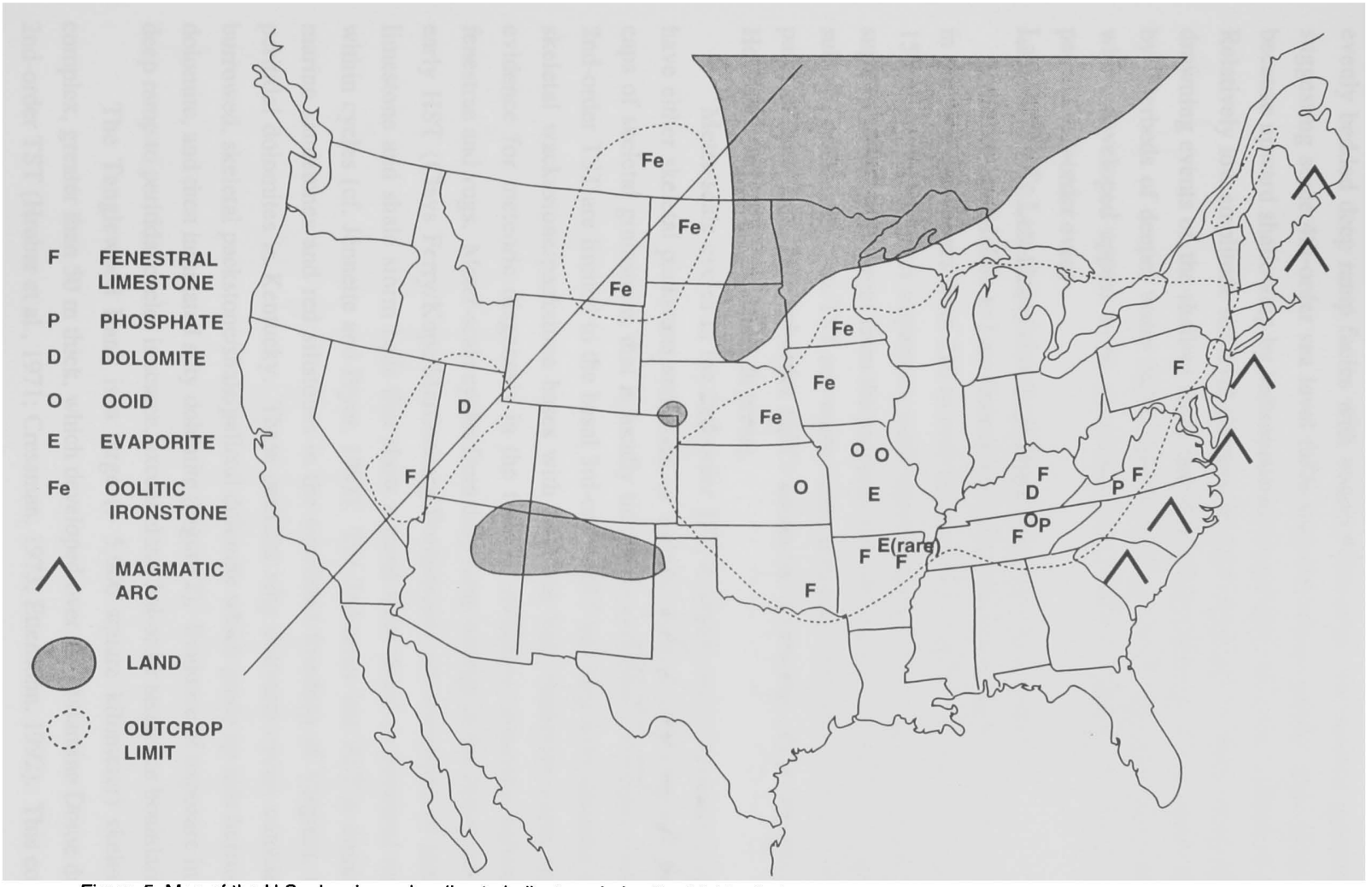

Figure 5. Map of the U.S. showing paleoclimate indicators during the Middle Ordovician (Mohawkian). Equator from Witzke (1990)

evenly bedded deep ramp facies with nodular limestone and skeletal grainstone caps, suggesting some 4th-order sea level fallls may have been greater than 10 m at times, because upward shallowing by sedimentation would only fill a few meters of the space. Relatively low amplitude sea level changes also are suggested by the scarcity of incipient drowning events on the shallow ramp and downslope buildups which would be marked by interbeds of deeper water facies within buildups. Such incipient drowning events, where developed appear to be associated with aborted regional drowning events, or perhaps 4th-order events.

Late Middle To Late Ordovician (Late Mohawkian to Cincinnatian)

The Late Middle to Late Ordovician supersequence is approximately 9 to 14 m.y. in duration and ranges from 210 to over 500 m thick (Fig. 6). It contains 4 large (30 to 150 m thick) 3rd-order sequences, each approximately 3 m.y. duration. This 2nd-order supersequence is different from the previous two because it is dominated by cool water, subtidal carbonates in its TST and warm water, peritidal carbonates restricted to its upper parts of both 2nd- and 3rd-order HST's along the Cincinnati Arch (Patzkowsky and Holland, 1993; Pope and Read, in press).

Meter-scale cycles in the 2nd-order TST in updip areas (Lexington Limestone) have either skeletal packstone and shale, or nodular skeletal packstone and shale, with caps of skeletal grainstone, that is locally tidally cross-bedded. Peritidal cycles in the 2nd-order TST are limited to the basal 3rd-order HST and they have faunally restricted skeletal wackestone/packstone bases with fenestral lime mudstone caps; and minor evidence for meteoric diagenesis in the form of oxidation-reduction haloes around fenestrae and vugs. Meter-scale cycles from deep ramp settings in the 2nd-order TST and early HST (Clays Ferry/Kope/Martinsburg Formations) are composed of interbedded limestone and shale storm beds that show a trend from distal to proximal conditions within cycles (cf. Jennette and Pryor, 1993). The 2nd-order late HST is dominated by marine sandstones and red siltstones in the overfilled foredeep of Virginia, and silty peritidal dolomites in Kentucky. These peritidal silty dolomite cycles consist of thin, burrowed, skeletal packstone/shale/pelletal dolomite which grade up into burrowed silty dolomite, and then laminated silty dolomite (Figure 2). Evidence of exposure in both the deep ramp to peritidal cycles is scarce, except along 3rd-order sequence boundaries.

The Tanglewood Bank is a large (> 5,000 square kilometer) skeletal shoal complex, greater than 50 m thick, which developed over the Jessamine Dome during the 2nd-order TST (Hrabar et al., 1971; Cressman, 1973; Ettensohn, 1992). This complex is

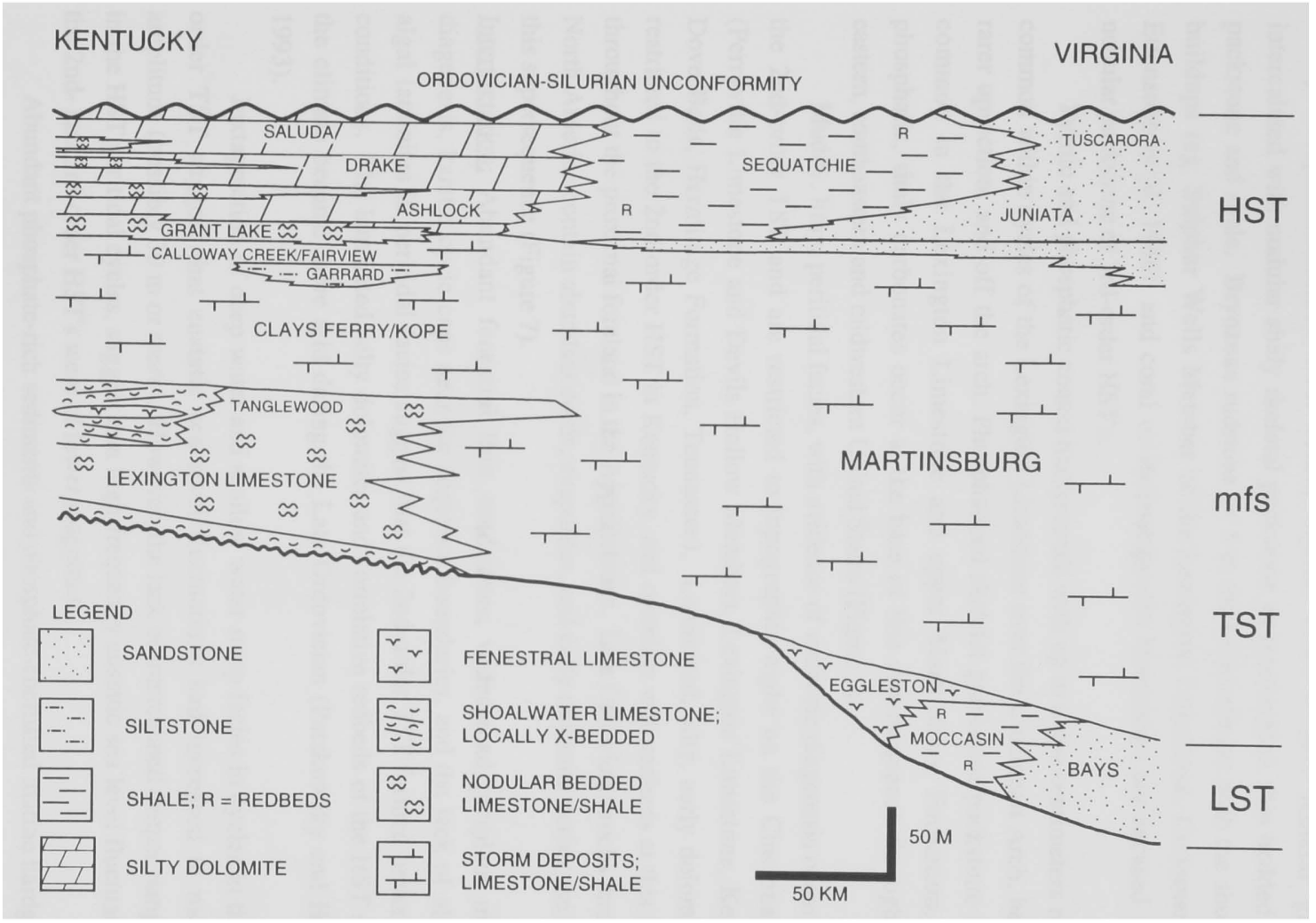

Figure 6. Generalized cross-section of late Middle to Late Ordovician rocks in Kentucky and Virginia.

very compartmentalized with clean, bipolar cross-bedded skeletal grainstone, intercalated with nodular shaly skeletal packstone or interbedded, thin bedded skeletal packstone and shale. Bryozoan rudstone (< 5 m thick) interfinger with the shoal water buildups (eg. Sulphur Wells Member of the Lexington Limestone, Cressman, 1973; Ettensohn et al. 1986), and coral or stromatoporoid biostromes are encased in shaly nodular packstone of 3rd-order HST's.

Pyritic and phosphatic coated hardgrounds with up to a few centimeters relief are common within cycles of the Lexington Limestone over the Cincinnati Arch, becoming rarer upsection, and off the arch. Phosphatized skeletal grainstone/packstone also are common in the Lexington Limestone and upper Martinsburg Formation. Such phosphatic, shaly carbonates occur at the base of this supersequence throughout the eastern, southeastern and midwestern United States (Figure 7).

Muddy, limy, peritidal facies, with evidence of meteoric diagenesis occur only in the 2nd-order TST and are restricted to topographic highs on the Cincinnati Arch (Perryville Limestone and Devils Hollow Members, Lexington Limestone, Kentucky; Dove Beds, Hermitage Formation, Tennessee). Laminated, silty, early dolomites are restricted to the 2nd-order HST in Kentucky, and correlate with redbeds at this horizon throughout the proximal foreland in the Appalachians. Late Ordovician rocks throughout North America contain abundant ooids, evaporites, and early dolomite during the HST of this supersequence (Figure 7).

Interpretation: Abundant fenestral lime mudstones, widespread incipient meteoric diagenesis, karstic cycle caps near the sequence boundaries, and the lack of abundant algal laminites in peritidal facies suggest that the 2nd-order TST formed under humid conditions. The laminated, silty dolomites and correlative redbeds of the HST suggest the climate became more arid during the Late Ordovician (Patzkowsky and Holland, 1993).

Juxtaposition of deep water and shallow water ramp facies in cycles in the 2nd-order TST suggest that eustatic sea level fluctuations had increased to moderate amplitude (possibly 30 m or more). However, the lack of intercalated deeper ramp facies in the HST peritidal cycles, suggest that high-frequency eustatic sea level fluctuations in the 2nd- and 3rd-order HST's were of lower magnitude.

Abundant phosphate-rich sediments and phosphate-encrusted marine hardgrounds in the 2nd-order TST may indicate intense upwelling of deep, phosphate-rich waters onto the craton during this time. The upwelling probably was from the south, because

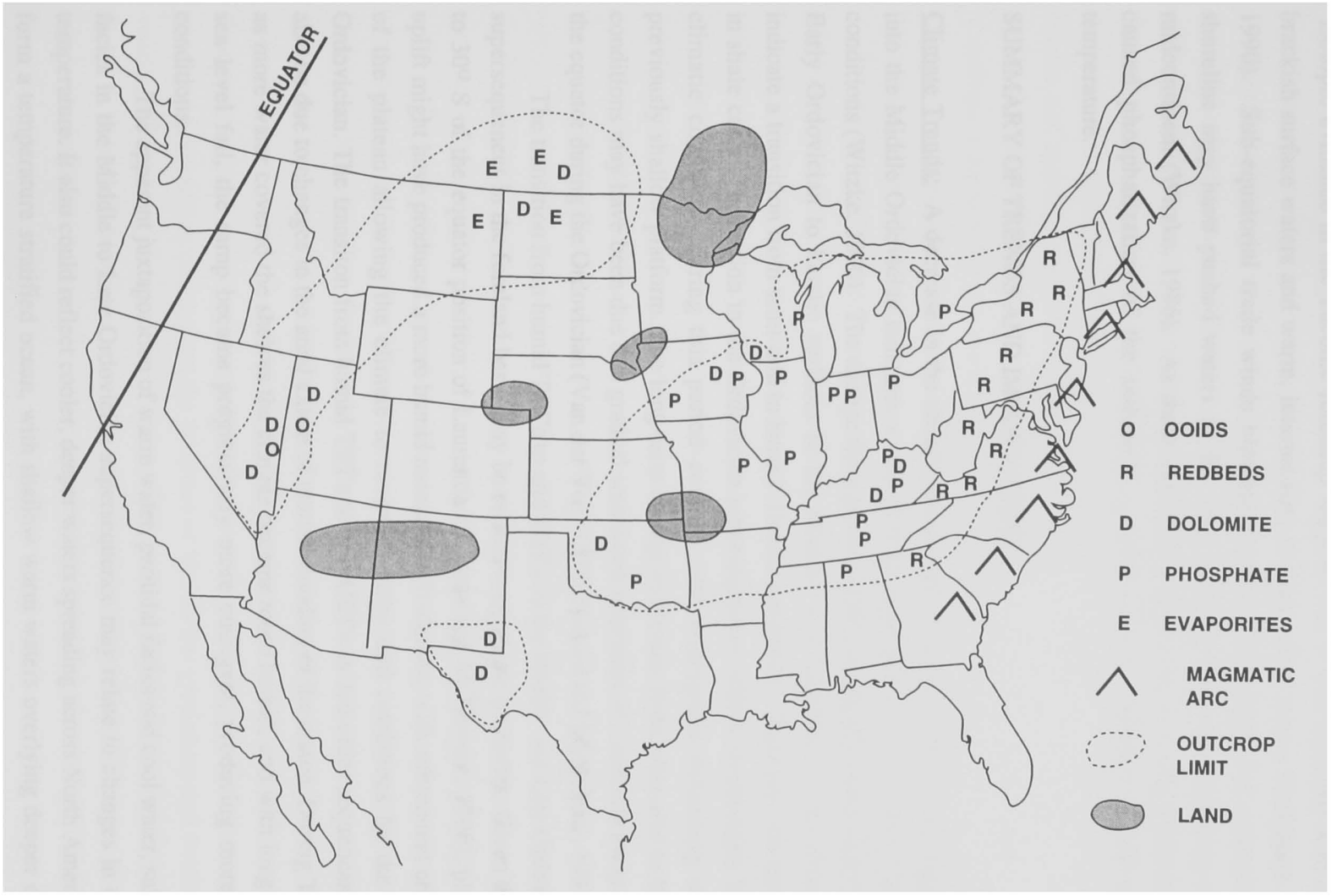

Figure 7. Map of U.S. showing paleoclimatic indicators for late Middle and Late Ordovician. Equator from Witzke (1990).

isotopic evidence in the Taconic foredeep suggests that it was stratified with cooler, brackish surface waters and warm, intermediate to deep saline waters (Railsback et al., 1990). Sub-equatorial trade winds blowing from the east along the midcontinent shoreline may have pushed waters to the west, causing intensive upwelling in the midcontinent (Witzke, 1986). As these upwelling waters rose onto the platform they caused phosphatization of the sediments, perhaps due to changes in pH and/or temperature.

SUMMARY OF TRENDS AND IMPLICATIONS

Climate Trends: A decrease in the abundance of early dolomite, ooids, and evaporites into the Middle Ordovician indicates a change from semi-arid to more humid climatic conditions (Witzke, 1990). The change from planar cycle-capping disconformities in the Early Ordovician to karstic surfaces in the Middle- and Late Ordovician also may indicate a transition from semi-arid to humid climatic conditions. Similarly, the increase in shale content upsection in the Ordovician supersequences reflect increasingly humid climatic conditions during this period coupled with widespread deepening of the previously shallow platform. The long-term change in climate from semi-arid to humid conditions may have been due to a gradual southward migration of Laurentia away from the equator during the Ordovician (Van der Voo, 1988; Scotese and McKerrow, 1991).

The transition from humid TST's to arid HST's in the Middle and Late Ordovician supersequences in the foreland basin may be related to orogenic processes. Given the 15 to 30° S of the equator position of Laurentia (Scotese and McKerrow, 1990), plateau uplift might have produced a more humid monsoonal(?) climate, with subsequent erosion of the plateau allowing the climate to revert to more arid conditions by the Late Ordovician. The transiton from humid TST's to arid HST's in 3rd-order sequences may also be due to changes in the areal extent of marine flooding of the craton. During TST's, as more water covered the shelves the climate became more humid, and with long-term sea level fall, the ramp became progressively more emergent, producing more arid conditions.

The apparent juxtaposition of warm water, peritidal facies and cool water, subtidal facies in the Middle to Late Ordovician supersequence may relate to changes in ocean temperature. It also could reflect cooler, deeper waters spreading across North America to form a temperature stratified ocean, with shallow warm waters overlying deeper cooler

waters (c.f., Martindale and Boreen, 1995). The cool-water carbonates at the base of the Late Ordovician supersequence were likely produced by a global drop in ocean temperature. Widespread bentonites deposited near the boundary between the two foreland supersequences (Haynes, 1994) may have helped trigger oceanic cooling reflected in the cool water, subtidal carbonates (Lavoie, 1995).

Eustasy: In Supersequence 1 (Early Ordovician), meter-scale cycles with regional tidal flat caps that extend over much of the platform, predominance of very shallow water facies, and aggraded nature of the platform all point to only small 4th- and 5th(?)-order sea level fluctuations comparable with greenhouse setting continuing from a Late Cambrian, relatively ice-free earth (Frakes et al., 1992). High-frequency, low-amplitude eustasy and semi-arid climate favored regional early dolomitization of the platform (Montanez and Read, 1992).

By Middle Ordovician (Chazy-Blackriver; Ordovician Supersequence 2) time, high- frequency sea level oscillations were still small, but suggestions of a slight increase from the Early Ordovician is the presence of thin 4th-order subtidal cycles on the deep ramp juxtaposing skeletal grainstone and dysaerobic (?) sub-storm wave base facies. However, peritidal cycles updip commonly are capped by tidal flat facies (fenestral limestone, minor laminites) and micro-karsting of cycle tops, along with much meteoric sparry cementation and crystal silt infilling fenestrae and vugs which probably reflects humid climate, atlthough it could in part be due to increased explosure of the inner platform and lowered ground water tables. Buildups on the platform were little affected by the relatively small high-frequency sea level fluctuations which rarely exposed them, or even caused incipient drowning except during major longer term flooding events.

The late Middle to Late Ordovician time (Supersequence 3), meter-scale subtidal ramp cycles in the 2nd-order TST show juxtaposition of deeper water facies (thin-bedded limestone and shale or rhythmites) with nodular limestone and shale or skeletal grainstone caps, indicating high-frequency sea level fluctuations of at least some tens of meters. These sea level events caused numerous inipient drowning events of the Tanglewood Bank, resulting in much compartmentalization. These moderate amplitude sea level fluctuations may record the initiation of Gondwana glaciation, and waxing and waning of ice sheets (Jacobs and Sahagian, 1993). Meter-scale cyclicity in peritidal facies tends to be poorly developed compared with the Early Ordovician. However, given the moderate amplitude eustasy, the relative paucity of erosional surfaces on peritidal cycles

is puzzling; such surfaces only appear to be developed near major 3rd-order sequence boundaries.

Evidence of moderate amplitude eustasy in the Supersequence 3 HST is scarce, suggesting that sea level fluctuations may have decreased by this time, prior to the onset of the less than 2 m.y. peak glaciation of the Hirnantian stage (Brenchley et al., 1994), which is represented by the regional Ordovician-Silurian unconformity in the study area.

CONCLUSIONS

1. Meter-scale cycles in the three Ordovician supersequences in Kentucky and Virginia may record the transition from Early Ordovician greenhouse to later Ordovician glaciation of Gondwana.

2. Early and Late Ordovician cycles appear to have formed from relatively small, high-frequency fluctuations of sea level, in contrast to the late Middle Ordovician cycles, which on the subtidal ramp show juxtaposition of deeper and shallower water facies, requiring tens of meter sea level changes. These also caused frequent incipient drowning of Late Mohawkian carbonate banks.

3. The evidence of moderate amplitude high-frequency eustasy in the late Middle Ordovician appears to coincide with a major cooling of the waters flooding the deeper platform. It was apparently followed by decreasing amplitude sea level fluctuations, warming, and increased aridity prior to major glaciation, glacio-eustatic drawdown and platform exposure.

REFERENCES

Bond, G.C., Nickeson, P.A., and Kominz, M.A., 1984, Breakup of a supercontinent between 625 Ma and 555 Ma, new evidence and implications for continental histories: Earth and Planetary Science Letters, v. 10, p. 325-345.

Borella, P.E., and Osborne, R.H., 1978, Late Middle and early Late Ordovician history of the Cincinnati arch Province, central Kentucky to central Tennessee: Geological Society of America Bulletin, v. 89, p. 1559-1573.

Bova, J.A., and Read, J.F., 1987, Incipiently drowned facies within a cyclic peritidal continental ramp sequence, Chepultepec interval, Virginia Appalachians: Geological Society of America Bulletin, v. 98, p. 714-727.

Brenchley, P.J., Marshall, J.D., Carden, G.A.F., Robertson, D.B.R., Meidla, T., Hints, L., and Anderson, T.F., 1994, Bathymetric and isotopic evidence for short-lived Late Ordovician glaciation in a greenhouse period: Geology, v. 22, p. 295-298.

Cable, M.S., and Beardsley, R.W., 1984, Structural control on Late Cambrian and Early Ordovician carbonate sedimentation in eastern Kentucky: American Journal of Science, v. 284, p. 797-823.

Cressman, E.R., 1973, Lithostratigraphy and depositional environments of the Lexington Limestone (Ordovician) of central Kentucky: United States Geological Survey Professional Paper 768, 61 pp.

Cressman, E.R., and Noger, M.C., 1976, Tidal-flat carbonate environments in the High Bridge Group (Middle Ordovician) of central Kentucky: Kentucky Geological Survey, Series 10, Report of Investigations 18, 15 pp.

Ettensohn, F.R. (ed.), 1992, Changing interpretations of Kentucky geology--layer-cake, facies, flexure, and eustacy: State of Ohio, Department of Natural Resources, Miscellaneous Report No. 5, 184 p.

Ettensohn, F.R., Amig, B.C., Pashin, J.C., Greb, S.F., Harris, M.Q., Black, J.C., Cantrell, D.J., Smith, C.A., McMahan, T.M., Axon, A.G., and McHargue, G.J., 1986, Paleoecology and paleoenvironments of the bryozoan-rich Sulphur Well Member, Lexington Limestone (Middle Ordovician), central Kentucky: Southeastern Geology, v. 26, p. 199-219.

Frakes, L.A., Francis, J.E., and Syktus, J.I., 1992, Climatic modes of the Phanerozoic: Cambridge University Press, Cambridge, UK, 274 pp.

Goldhammer, R.K., Lehmann, P.J., and Dunn, P.A., 1993, The origin of high-frequency platform carbonate cycles and third-order sequences (Lower Ordovician El Paso Gp, west Texas): constraints from outcrop data and stratigraphic modeling: Journal of Sedimentary Petrology, v. 63, p. 318-359.

Grover, G., Jr., and Read, J.F., 1978, Fenestral and associated vadose diagenetic fabrics of tidal flat carbonates, Middle Ordovician New Market limestone, southwestern Virginia: Journal of Sedimentary Geology, v. 48, p. 453-473.

Hardie, L.A., 1989, Cyclic platform carbonates in the Cambro-Ordovician of the central Appalachians: *in* Fieldtrip T161:Cambro-Ordovician carbonate banks and siliciclastic basins of the United States Appalachians, in Sedimentation and Stratigraphy of Carbonate Rock Sequences, American Geophysical Union, Washington, D.C., v. 1, p. T161:51-88.

Hardie, L.A., and Shinn, E.A., 1986, Carbo ate depostional environments; Part 3: Tidal flats: Colorado School of Mines Quarterly, v. 81, p. 59-74.

Haynes, J.T., 1994, The Ordovician Deicke and Millbrig K-Bentonite beds of the Cincinnati Arch and the southern Valley and Ridge Province: Geological Society of America Special Paper 290, 80 p.

Hrabar, S.V., Cressman, E.R., and P.E. Potter, 1971, Crossbedding of the Tanglewood Limestone Member of the Lexington Limestone (Ordovician) of the Blue Grass region of Kentucky: Brigham Young University Geology Studies, v. 18, p. 99-114.

Jacobi, R.D., 1981, Peripheral bulge-a causal mechanism for the Lower/Middle Ordovician disconformity along the western margin of the northern Appalachians: Earth and Planetary Science Letters, v. 56, p. 245-251.

Jacobs, D., and Sahagian, D., 1993, Climate induced fluctuations in sea level during non-glacial times: Nature, v. 361, p. 710-712.

Jennette, D.C., and Pryor, W.A, 1993, Cyclic alternation of proximal and distal storm facies: Kope and Fairview Formations (Upper Ordovician), Ohio and Kentucky: Journal of Sedimentary Petrology, v. 63, p. 183-203.

Keith, B.D., 1988, Regional facies of Upper Ordovician Series of eastern North America: *in* B.D. Keith (ed.), The Trenton Group (Upper Ordovician Series) of eastern North America, American Association of Petroleum Geologists, Tulsa, OK, Studies in Geology #29, p. 1-16.

Kreisa, R.D., 1980, The Martinsburg Formation (Middle and Upper Ordovician) and related facies in southwestern Virginia: unpublished Ph.D. dissertation, Virginia Polytechnic Institute and State University, Blacksburg, Virginia, 358 p.

Kuhnhenn, G.L., and Haney, D.C., 1986, Middle Ordovician High Bridge Group and Kentucky River fault system in central Kentucky: *in* Neathery, T.L., ed., Southeastern Section of the Geological Society of America: Geological Society of America Centennial Field Guide, v. 6., p. 25-29.

Lash, G.G., 1981, Middle and Late Ordovician shelf activation and foredeep evolution, central Appalachian Orogen: *in* B.D. Keith (ed.), The Trenton Group (Upper Ordovician Series) of eastern North America, American Association of Petroleum Geologists, Tulsa, OK, Studies in Geology #29, p. 37-53.

Lavoie, D., 1995, A Late Ordovician high-energy temperate-water carbonate ramp, southern Quebec, Canada: implications for Late Ordovician oceanography: Sedimentology, v. 42, p. 95-116.

McBride, E. F., 1962, Flysch and associated beds of the Martinsburg Formation (Ordovician), Central Appalachians: Journal of Sedimentary Petrology, v. 32, p. 39-91.

Mitchell, , R.W., 1985, Comparative sedimentology of shelf carbonates of the Middle Ordovician St. Paul Group, central Appalachians: Sedimentary Geology, v. 43, p. 1-41.

Montanez, I., and Read, J.F., 1992, Eustatic control on early dolomitization of cyclic peritidal carbonates; evidence from the Early Ordovician upper Knox Group, Appalachians: Geological Society of America Bulletin, v. 104, p. 872-886.

Mussman, W.J., and Read, J.F., 1986, Sedimentology and development of a passive- to convergent-margin unconformity: Middle Ordovician Knox unconformity, Virginia Appalachians: Geological Society of America Bulletin, v. 97, p. 282-295.

Patzkowsky, M.E., and Holland, S.M., 1993, Biotic response to a Middle Ordovician paleoceanographic event in eastern North America: Geology, v. 21, p. 619-622.

Pope, M.C., and Read, J.F., (in press), High-frequency cyclicity of the Lexington Limestone (Middle Ordovician), a cool-water carbonate clastic ramp in an active foreland basin: Society of Economic Paleontologists and Mineralogists Special Publication on Cool Water Carbonates.

Railsback, L.B., Ackerly, S.C., Anderson, T.F., and Cisne, J.L., 1990, Paleontological and isotope evidence for warm saline deep waters in Ordovician oceans: Nature, v. 343, p. 156-159.

Reinhardt, J.W., 1974, Stratigraphy, sedimentology and Cambro-Ordovician paleogeography of the Frederick Valley, Maryland: Maryland Geologic Survey Report of Investigations no. 23, 74 p.

Read, J.F., 1980, Carbonate ramp-to-basin transitions and foreland basin evolution, Middle Ordovician, Virginia Appalachians: American Association of Petroleum Geologists Bulletin, v. 64, p. 1575-1612.

Read, J.F., 1982, Geometry, facies, and development of Middle Ordovician carbonate buildups, Virginia Appalachians: American Association of Petroleum Geologists Bulletin, v. 66, p. 189-209.

Read, J.F., 1989, Controls on evolution of Cambrian-Ordovician passive margin, U.S. Appalachians: *in* Crevello, P.D., Wilson, J.L., Sarg, J.F., and Read, J.F. (eds), Controls on carbonate platform and basin development, Society of Economic Paleontologists and Mineralogists Special Publication No. 44, p. 147-165.

Read, J.F., and Grover, G., Jr., 1977, Scalloped and planar erosion surfaces, Middle Ordovician limestones, Virginia: Analogues of Holocene exposed karst or tidal rock platforms: Journal of Sedimentary Petrology, v. 47, p. 956-972.

Read, J.F., and Goldhammer, 1988, Use of Fischer plots to define third-order sea-level curves in Ordovician peritidal cyclic carbonates: Geology, v. 16, p. 895-899.

Rodgers, J., 1971, The Taconic orogeny: Geological Society of America Bulletin, v. 82, p. 1141-1178.

Scotese, C.R., and McKerrow, W.S., 1990, Revised world maps and introduction: *in* McKerrow, W.S., and Scotese, C.R., (eds.), Palaeozoic palaeogeography and biogeography, Geological Society of London Memoir 12, p. 1-21.

Shanmugam, G., and Walker, K., 1980, Sedimentation, subsidence and evolution of a foredeep basin in the Middle Ordovician, southern Appalachians: American Journal of Science, v. 280, p. 479-496.

Vail, P.R., Audemard, F., Bowman, S.A., Eisner, P.N., and Perez-Cruz, C., 1991; The stratigraphic signatures of tectonics, eustacy, and sedimentology-an overview: *in* Einsele, G., Ricken, W., and Seilacher, A., (eds), Cycles and Events in Stratigraphy, Springer-Verlag, New York, p. 617-659.

Van der Voo, R., 1988, Paleozoic paleogeography of North America, Gondwana, and intervening displaced terranes: Comparison of paleomagnetism with paleoclimatology and biogeographical patterns: Geological Society of America Bulletin, v. 100, p. 311-324.

Weber, L.J., Sarg, J.F., and Wright, F.M., 1995, Part 3, Sequence stratigraphy and reservoir delineation of the Middle Pennsylvanian (Desmoinesian), Paradox Basin and Aneth Field, southwestern U.S.A: *in* Read, J.F., Kerans, C., Weber, L.J., Sarg, J.F., and Wright, F.M., (eds), Milankovitch sea-level changes, cycles, and reservoirs on carbonate platforms in Greenhouse and Ice-free worlds, Society of Economic Paleontologists and Mineralogists, Short Course Notes No. 35, Tulsa, p. 1-81.

Witxke, B.J., 1986, Models for circulation patterns in epicontinental seas applied to Paleozoic facies of North American craton: Paleooceanography, v. 2, p. 229-248.

Witzke, 1990, Palaeoclimatic constraints for Paleozoic palaeolatitudes of Laurentia and Euramerica: in McKerrow, W.S., and Scotese, C.R., (eds.), Palaeozoic palaeogeography and biogeography, Geological Society of London Memoir 12, p. 57-74.

Weir, G.W., Peterson, W.L., and Swadley, W.C., 1984, Lithostratigraphy of Upper Ordovician strata exposed in Kentucky: United States Geological Survey Professional Paper 1151-E, 121 pp.

Appendix 1A: CORES USED IN THIS STUDY

COUNTY	LOCATION	OPERATOR	FARM	WELL NO	KGS CALL NO.
ADAIR	24-I-54	Exxon Minerals	Tabernacle School	Du-2	C-276
BOONE	19-CC-57	Dravo Lime	Patriot	BB73-1	C-1272
CASEY	14-K-57	Humble Oil	Patterson	Ch-3	C-113
CLINTON	24-D-53	Exxon Minerals	Staton	AA-3	C-509
CUMBERLAND	10-D-50	Cominco American	Bonher	Ca-210	C-757
FAYETTE	24-S-61	KGS-USGS	Glenn	Lex-E1	C-199
JESSAMINE	1-Q-58	ASARCO	Owens	Ack-5	C-193
LINCOLN	23-N-58	Humble Oil	Feldman	CH-5	C-115
MADISON	9-0-61	ASARCO	Taylor &Tussey	Ack-6	C-194
MARION	17-N-54	Humble Oil	Lanham	CH-4	C-114
MASON	11-Y-70	Cominco American	Cooper	Ca-37	C-211
MONTGOMERY	8-R-67	Cominco American	Martin Burchell	Ca-35	C-209
NICHOLAS	19-W-67	KGS-USGS	Cox	1	C-169
PULASKI	24-H-60	Cominco American	Edwards	Ca-295	C-324
RUSSEL	1-E-53	Murray Drilling	Story	1	C-505
SHELBY				JK 78-1	
SHELBY	19-U-53		Newton	JK 78-2	
SHELBY	23-U-53		Schmidt	JK 78-3	
WAYNE	25-E-56	Cominco American	Savage	Ca 303	C-493

Appendix 1B: LARGE OUTCROPS/ROADCUTS IN THIS STUDY

NAME (ABBREVIATION)	LOCATION	UNIT(S) DESCRIBED
BOONESBORO	Bridge Abutment, Ky. Hwy. 627 crossing over Kentucky River, east side	High Bridge Group, Basal Lexington Limestone
BLUEGRASS PARKWAY (BP)	Buegrass Parkway immediately south of Kentucky River crossing	Lexington Limestone
BURKESVILLE (BU)	Ky. State Hwy. 61, ~ 1 mi. south of Burkesville	Upper Cincinnatian, Chattanooga
CALDWELL STONE QUARRY (CSQ)	Quarry south of Danville, Ky; near Hwy. 127	Lexington Limestone, Clays Ferry
CAMP NELSON (CN)	Hwy. 27 ~ 5 miles south of Nicholasville	High Bridge Group
CLAYS FERRY(CF)	Frontage road below I-75 bridge and outcrops immediately south of bridge on I-75	Top of Lexington Limestone Clays Ferry Fm., Garrard Siltstone
DEVILS HOLLOW ROAD(DH)	Devils Hollow Road, ~ 4 miles from junction with Hwy. 127	Lexington Limestone
DIX DAM (DD)	Dix Dam Spillway; off Ky. Hwy. 68	Camp Nelson Fm.
FRANKFORT WEST (FW)	Hwy. 127 ~ 2 miles SE of downtown Frankfort	Lexington Limestone
FRANKFORT NORTH (FN)	Hwy. 127 ~ 3 miles N of downtown	Tyrone Fm., Lexington Limestone
FREDERICKTOWN (F)	Hwy. 150 ~4 miles east of junction with Bluegrass Parkway	Cincinnatian
HIGHWAY 421 (H4)	Hwy. 421 immediately west of its junction with Hwy. 127, ~ 1 mi west of downtown Frankfort	Lexington Limestone
MAYSVILLE (MYO)	Hwy. 11 immediately north of junction with KY 546	Cincinnatian
MT. STERLING	~3 miles east of Mt. Sterling exit, south side of Interstate 64	Cincinnatian
OWENTON (O)	Hwy. 127 ~ 10 mi. north of Frankfort	Lexington Limestone, Clays Ferry Fm.

Appendix 1C: Gamma Ray logs used in this study

A-A'

County	Location	Well name
CUMBERLAND	7-C-50	#3 VOLUNTEER DRILLING
CUMBERLAND	7-D-50	BARTON THRASHER #3
CLINTON	5-C-52	EDWARD RIDDLE #1
WAYNE	20-D-54	PETRO-HUNT #1
RUSSELL	4-E-53	JAMES WOOLRIDGE #1
ADAIR	21-G-51	JIMMY BRUMMETT #254
ADAIR	6-G-53	FORMULA DALTON#1
PULASKI	22-I-59	CLYDE JASPER #1
CASEY	7-I-57	CITIES GARRETT #1
CASEY	15-K-57	LULU SHORT #1
ROCKCASTLE	9-K-61	FRANK BRADLEY ET AL. #1
MADISON	23-N-62	RICHARDSON ET AL., #1
ESTILL	2-N-66	VANHOOSE/POTTER/FRANK3
MONTGOMERY	10-R-67	RUSSELL TRIMBLE #1
BATH	20-V-68	QUASAR VICE #1
FLEMING	2-W-70	LEONARD SPENCER #1
MASON	15-Y-71	WILSON RAWLINGS #9061-T

B-B'

MCCREARY	8-B-62	ANNE MARY CREEKMORE #1
WHITLEY	12-E-64	EDWIN JASPER #3
WHITLEY	12-C-63	OVA MANNING #1
WHITLEY	21-D-63	WILLIAM SMITH #1
WHITLEY	1-E-64	JFE FIELD #7
LAUREL	15-H-67	O & E WILKERSON #1
CLAY	1-H-67	WALTER BRUNER #1
LAUREL	23-I-67	CRIT BOWLING #1
JACKSON	10-K-67	ISAACS #1
JACKSON	12-L-67	STANLEY, NEELEY #1
WOLFE	20-O-73	EARL WHITE #2
LEE	21-N-71	WALLACE BRANSON
WOLFE	13-O-74	ORVILLE BANKS #1
WOLFE	23-P-73	H.C. CHAMBERS #1
MORGAN	23-R-73	BURCHELL, BLANTON #1
MENIFEE	21-S-72	FRANK BROWN 9380-T
MORGAN	14-S-75	LEE CLAY PRODUCTS #1
ROWAN	25-U-75	FANNIE MAY #1
CARTER	25-W-77	TAYLOR DUNCAN #547
LEWIS	13-Y-77	ASHLAND WOLFE #1

Appendix 1C (continued)

C-C'

MADISON	23-N-62	RICHARDSON ET AL., #1
ESTILL	3-O-68	MCKINNEY 1-G
LEE	3-N-69	P Y DRAKE HEIRS #1
LEE	21-0-69	ASHLAND GROSS #1
LEE	25-N-72	VIRGIL COMBS #1
WOLFE	13-O-74	ORVILLE BANKS #1
BREATHITT	13-M-75	UNITED FUEL GAS CO.
FLOYD	1-L-81	HALL #1
PIKE	8-L-85	HENRY STRATTON #1

D-D'

JEFFERSON	11-U-44	DUPONT DE NEMOURS #2
BULLITT	10-S-45	T.H. FROMAN #1
HENRY	21-X-53	EARL HOLMES #1
BATH	20-V-68	QUASAR VICE #1
MONTGOMERY	10-R-67	RUSSELL TRIMBLE #1
MENIFEE	21-S-72	FRANK BROWN 9380-T
MORGAN	14-S-75	LEE CLAY PRODUCTS
MORGAN	8-R-78	LENA BROWN #1
JOHNSON	16-Q-79	ASHLAND OIL #20537-T
JOHNSON	11-P-81	DOLLARHIDE #14
PIKE	4-N-87	ROGERS BROTHERS TRUST #6

Appendix 2: Duration of High-Frequency Cyclicity

The duration of high-frequency cycles in the Late Mohawkian to Cincinnatian sequence can be estimated two ways: 1) dividing the duration for the Late Mohawkian to Cincinnatian interval (9 to 14 m.y.) by the total number of cycles (110 Wayne Co. core; >147 Mason Co. core); or 2) using the peaks from the "time"(depth) series and the average sedimentation rate for each data set to calculate the duration of cycles of variable thickness. Both methods are have very large error bars, due mainly to the uncertainty in dating of the Ordovician-Silurian boundary (438-443 m.y.).

The first method gives durations for the meter-scale cycles of 75 to 200 k.y. These values are similar to an estimate (57 k.y.) of the duration of meter-scale deep ramp cycles in the Kope and Fairview Formations using a similar method of calculation (Tobin, 1982).

Spectral Analysis-Methods: Amplitude spectra of three gamma ray logs through, and two large cores and two large outcrops within the Late Mohawkian to Cincinnatian supersequence were generated using a Macintosh application (Coruh, in prep) that utilizes spectral analysis of evenly and unevenly sampled data (Press et al., 1992). In this application the number of different cycles (wavenumber per 1000 feet) to output is controlled by the user. The maximum cycles are limited by the Nyquist frequency defined by the even or smallest sample interval to avoid aliased information about any signal components at cycles greater than the Nyquist frequency. In order to increase graphing resolution, the evenly sampled input data series was debiased before spectral analysis was performed. Debiasing was intended to remove "white" noise from spectral analysis; this also nearly eliminates the zero frequency or DC component. In this study the maximum cycles per 1000 feet was limited to 350 on the gamma ray logs, and 1000 on the cores and outcrops.

"Time" series used in the analysis are actually amplitude vs. depth plots, because stratigraphic distance is used as a proxy for "time" (Swarzacher and Hass, 1986). Data in this paper are from detailed bed-by-bed logs made of continuous diamond drill core through the Late Mohawkian to Cincinnatian carbonates and clastics in Adair County (Exxon Du-2). The lithologic "time series" were generated from the bed-by-bed log by digitizing the log with a sample interval of 0.5 feet. Similar analyses were performed on portions of detailed logs of large Martinsburg Formation outcrops near Narrows, Virginia.

A lithologic "time series" was generated from the largest outcrop of Lexington Limestone near Frankfort, Kentucky, by using a rock type index (1=shale or fenestral lime mudstone, 2=cross-bedded skeletal grainstone, 3=nodular skeletal wackestone/packstone, and 4=interbedded skeltal packstone, calcisiltite, and shale) with a sampling interval of 0.5 feet.

Depth ("time") series were also generated from three gamma ray logs of wells used in the gamma ray correlation diagrams (Adair, Floyd, Pike Counties). These logs were sampled at 1.0, 0. 5, and 0.5 feet, respectively. The gamma ray values of the entire Late Mohawkian to Cincinnatian interval were analyzed then this data was subdivided into two parts (Lexington Limestone and Clays Ferry/Kope/Cincinnatian) which were then analyzed separately.

A Lomb Normalized Periodogram (LNP) was used to generate the amplitude spectrum of each time series (Press, 1992). A probablility function (Coruh, in prep) was used to determine the probability that each spectral peak represented a unique value above the background noise. For this study, only values of greater than 0.85 probability are reported.

Durations of each significant peak were calculated using the sedimentation rate at each site determined by dividing the interval thickness by the estimated time of each subdivision 3.9 m.y. for the Lexington Limestone and 7.7 m.y for Clays Ferry/Kope/Cincinnatian. The derived values have an error of $\pm$ 22% due to the uncertainty of the Late Ordovician-Silurian boundary.

Spectral mapping of the gamma ray time series was performed using a program written by Peavy (in prep) that is based on the Short-Time Fourier Transform (SFTF) of Nawab and Quatieri (1988). In this method the data are sampled within a sliding window and the Fourier amplitude spectrum is calculated separately for each window in turn. A Hamming window is used to sample the data instead of a rectangular window, as this reduces possible side-lobe "ringing " in the amplitude spectra. The resulting map provides information on the variability of amplitude spectra with depth. Parameters for window length and depth-step were chosen to optimize both frequency and depth resolution and were iterated until the reconstructed logs were nearly identical to the original logs.

Spectral Analysis Results:

Depth ("time") series analysis of the Late Mohawkian (Lexington Limestone) interval indicate numerous peaks from 0.9 to 91.3 m corresponding to durations from 55

k.y. to 3.9 m.y.(Table 1). Durations from the Lexington Limestone interval group at 890 to 894 k.y., 523 to 529 k.y., 213 to 252 k.y., 105 to 108 k.y., 75 to 77 k.y., and 55 to 56 k.y (Table 2). The average cycle thickness from the Frankfort North outcrop is 1.2 m and corresponds to a duration of 52 k.y. The ratio of the duration of spectral peaks from this analysis is 1: 1.4 : 1.9 : 4.1: 9.5: 16.2.

Depth (time") series analysis of the Cincinnatian interval has a wide range of spectral peaks from 0.3 to 122 m and corresponding durations from 5 k.y. to 6.78 m.y. (Table 3). Durations of the spectral peaks group at 1.27 to 1.41 m.y., 563 to 570 k.y, 314 to 432 k.y., 170 to 192 k.y., 104 to 112 k.y., 81 to 94 k.y., 18 to 30 k.y. and 6 k.y. The ratio of the durations for these spectral peaks is 1:4:14.5: 18: 30:62: 94:221 using 6 k.y. and 1:3.6:4.5:7.5:15.5:23.6::55.8: using 24 k.y. as a base.

Interpretations of Depth ("Time") Series:

The spectral peaks likely represent to the numerous superimposed scales of depositional sequences and meter-scale cycles in the Late Mohawkian to Cincinnatian supersequence described previously in this paper. The low frequency peaks probably represent 3rd-order sequences and the higher frequency peaks probably correspond to the meter-scale cycles. The spectral maps indicate the basal, shalier part of the two subdivisions is the best area to differentiate the higher frequency signal. The durations of the high-frequency spectral peaks and the spectral ratios are similar to Milankovitch orbital parameters suggesting the corresponding meter-scale cycles and depositional sequences were at least, in part, produced by eustatic sea level fluctuations resulting from the interactions of these orbital parameters. The abundance of durations in the 80 to 110 k.y range in both data sets indicate the eccentricity signal is very strong while the obliquity signal may be present in the Lexington Limestone data (55 to 56 k.y.) but the precessional signal may only be recorded in the deep ramp Martinsburg Fm. The lack of a strong precession signal may be a characteristic of the moderate amplitude eustatic sea level changes produced by orbital forcing.

Table 1 Spectra of Cycle Thickness and Possible Durations, Late Mohawkian to Cincinnatian Supersequence (**Note: All values have errors of ± 22%**)

	>1 m.y.	0.5-1 m.y.	200-500 k.y.	100-200 k.y.	< 100 k.y.
ADAIR CO CORE Accumulation rate= 210 m/11.5 m.y. =0.018 m/ky	6.32 m.y. (113.8 m) 2.46 m.y. (44.2 m)	616 k.y. (11.1m)	250 k.y. (4.5 m) 222 k.y. (4.0 m)	189 k.y. (3.4 m) 150 k.y. (2.7 m) 106 k.y. (1.9 m)	83 k.y. (1.5 m)
ADAIR CO. GAMMA RAY Accumulation rate=0.019 m/ky	6.17 m.y (117.3 m) 3.27 m.y. (62.2 m) 2.06 m.y. (39.1 m) 1.27 m.y. (24.2 m)	658 k.y. (12.5 m)	489 k.y. (9.3 m) 321 k.y. (6.1 m) 300 k.y. (5.7 m)	142 k.y. (2.7 m) 137 k.y. (2.6 m)	
FLOYD CO. GAMMA RAY Accumulation rate=0.034 m/ky	2.42 m.y. (82.4 m) 1.45 m.y. (49.2 m) 1.09 m.y. (37.2 m)	671 k.y. (22.8 m)	341 k.y. (11.6 m) 265 k.y. (9.0 m)	188 k.y. (6.4 m) 156 k.y. (5.3 m) 132 k.y. (4.5 m) 103 k.y. (3.5 m)	74 k.y. (2.5 m) 65 k.y. (2.2 m) 61 k.y. (2.1 m) 55 k.y. (1.9 m)
PIKE CO. GAMMA RAY Accumulation rate=0.042 m/ky	5.26 m.y. (220.9 m) 1.29 m.y. (44 m) 1.05 m.y. (44.2 m)	879 k.y. (36.9 m) 805 k.y. (33.8 m) 567 k.y. (23.8 m)	405 k.y. (17.0 m) 340 k.y. (14.3 m) 229 k.y. (9.6 m)		76 k.y. (3.2 m) 71 k.y. (3.0 m) 55 k.y. (2.3 m) 43 k.y. (1.9 m)

Table 2 Spectra of Cycle Thicknesses and Possible Durations, Lexington Limestone (**Note: All values have errors of ± 22%**)

	> 1 m.y.	0.5 to 1 m.y.	200 to 500 k.y.	100 to 200 k.y.	< 100 k.y.
ADAIR CO. CORE Accumulation Rate=60 m/ 3.9 m.y. = 0.016 m/k.y.	2.11 m.y. (33.8 m)	894 k.y. (14.3 m)	213 k.y. (3.4 m)		75 k.y. (1.2 m) 56 k.y. (0.9 m)
FRANKFORT N- OUTCROP Acc. rate = 0.023 m/k.y.	1.24 m.y. (28.5 m)		422 k.y. (9.7 m) 252 k.y. (5.8 m) 230 k.y. (5.3 m)	178 k.y. (4.1 m) 130 k.y. (3.0 m)	
ADAIR CO. GAMMA RAY Acc.rate = 0.024 m/k.y.	3.9 m.y. (91.3 m) 1.05 m.y. (25.3 m)	529 k.y. (12.7 m)		180 k.y. (4.3 m) 108 k.y. (2.6 m)	
PIKE CO. GAMMA RAY Acc. rate = 0.039 m/k.y.		782 k.y. (30.5 m)	331 k.y. (12.9 m)	105 k.y. (4.1 m)	77 k.y. (3.0 m)
FLOYD CO. GAMMA RAY Acc. rate = 0.047 m/k.y.		890 k.y. (41.8 m) 523 k.y. (31.4 m)	245 k.y. (11.5 m)	192 k.y. (9.0 m) 136 k.y. (6.4 m)	96 k.y. (4.5 m) 81 k.y. (3.8 m) 75 k.y. (3.5 m) 55 k.y. (2.6 m)

Table 3. Spectra of Cycle Thicknesses and Possible Durations, Cincinnatian Interval
(**Note: All values have errors of ± 22%**)

	>1 m.y.	500 k.y- 1 m.y.	200- 500 k.y.	100 - 200 k.y.	< 100 k.y.
ADAIR CO CORE Accumulation rate= 150 m/7.7 m.y. =0.018 m/ky	6.78 m.y. (122 m) 2.87 m.y. (51.6 m)	628 k.y. (11.3 m)	256 k.y. (4.6 m)	161 k.y. (2.9 m) 126 k.y. (2.4 m) 106 k.y. (1.9 m)	83 k.y. (1.5 m)
ADAIR CO. GAMMA RAY Accumulation rate=0.019 m/ky	2.10 m.y. (39.8 m) 1.37 m.y. (26.1 m)	563 k.y. (10.7 m)	321 k.y. (6.1 m)		
FLOYD CO. GAMMA RAY Accumulation rate=0.027 m/ky	3.04 m.y. (82 m) 1.41 m.y. (38 m)	826 k.y. (22.3 m) 570 k.y (15.4 m)		170 k.y. (4.6 m) 104 k.y. (2.8 m)	93 k.y. (2.5 m) 81 k.y. (2.2 m)
PIKE CO. GAMMA RAY Accumulation rate=0.042 m/ky	1.27 m.y. (53.5 m) 1.05 m.y. (44 m)	886 k.y. (37.2 m) 569 k.y. (23.9 m)	407 k.y. (17.1 m) 342 k.y. (14.4 m) 229 k.y. (9.6 m)	186 k.y. (7.8 m)	
MARTINSBURG OUTCROP Upper A Accumulation rate=402 m/6.2 m.y. = 0.066 m/ky			373 k.y.-avg. 314-432 k.y. (20.7-28.5 m)	183 k.y.-avg. 173-192 k.y. (11.4-12.7 m) 112 k.y. (7.4 m)	30 k.y. (2.0 m) 26 k.y. (1.7 m) 14 k.y. (0.9 m) 6 k.y. (0.4 m)

Table 3 (continued)

MARTINSBURG OUTCROP Upper B	1.03-1.85 m.y. (68-122 m)		286 k.y. (18.9 m)		92-94 k.y. (6.1-6.2 m) 40 k.y. (2.6 m) 30 k.y. (2.0 m) 20 k.y. (1.3 m) 6 k.y. (0.4 m) 5 k.y. (0.3 m)
MARTINSBURG OUTCROP Lower			378 k.y.-avg. 360-395 k.y. (23.7-26.1 m)	109 k.y.-avg. 106-112 k.y. (7.0-7.4 m)	89 k.y. (5.9 m) 65 k.y. (4.3 m) 59 k.y. (3.9 m) 21 k.y. (1.4 m) 18 k.y. (1.2 m) 14 k.y. 0.9 8 k.y. (0.5 m) 6 k.y. (0.4 m)

Appendix 3. Measured Sections.

Copies of the measured sections used to construct the cross-sections are provided in pockets of this thesis.

Sheet 1. Lexington Limestone, Clinton to Marion Counties; Datum is Salvisa Bed of Perryville Member

Sheet 2. Lexington Limestone, Lincoln to Mason Counties; Datum is Basal Unconformity.

Sheet 3. Lexington Limestone, Shelby County to Owenton Composite Section; Datum is Macedonia Bed.

Sheet 4. Cincinnatian Units, Clinton to Fredericktown; Datum is Top of Tidal Flat Facies (Tate Member) Ashlock Formation.

Sheet 5. Cincinnatian Units, Montgomery to Maysville, Datum is base of tidal flats and nodular skeletal packstone near base of Fairview Formation.

VITA

Mike Pope was born July 6th, 1961 in San Diego. He received a B.S. in Earth Sciences from UCLA in June 1985. He worked for two years in San Diego as an engineering geologist, then returned to school in 1987, receiving a M.S. in Geology from the University of Montana in 1989. Mike was married to Pauline Esquibel in 1990. After two more years working as an engineering geologist and part-time teacher at Sacramento State University in Sacramento, Mike entered the Ph.D. program at Virginia Tech in the fall of 1991. Following completion of his doctoral studies Mike will be employed as a post-doctoral research associate at MIT.